UiT The Arctic University of Norway

Faculty of Health Sciences

Department of Pharmacy

The development journey of an artificial intestinal model predicting oral drug absorption: the mucus-PVPA model

Margherita Falavigna

A dissertation for the degree of Philosophiae Doctor - February 2021

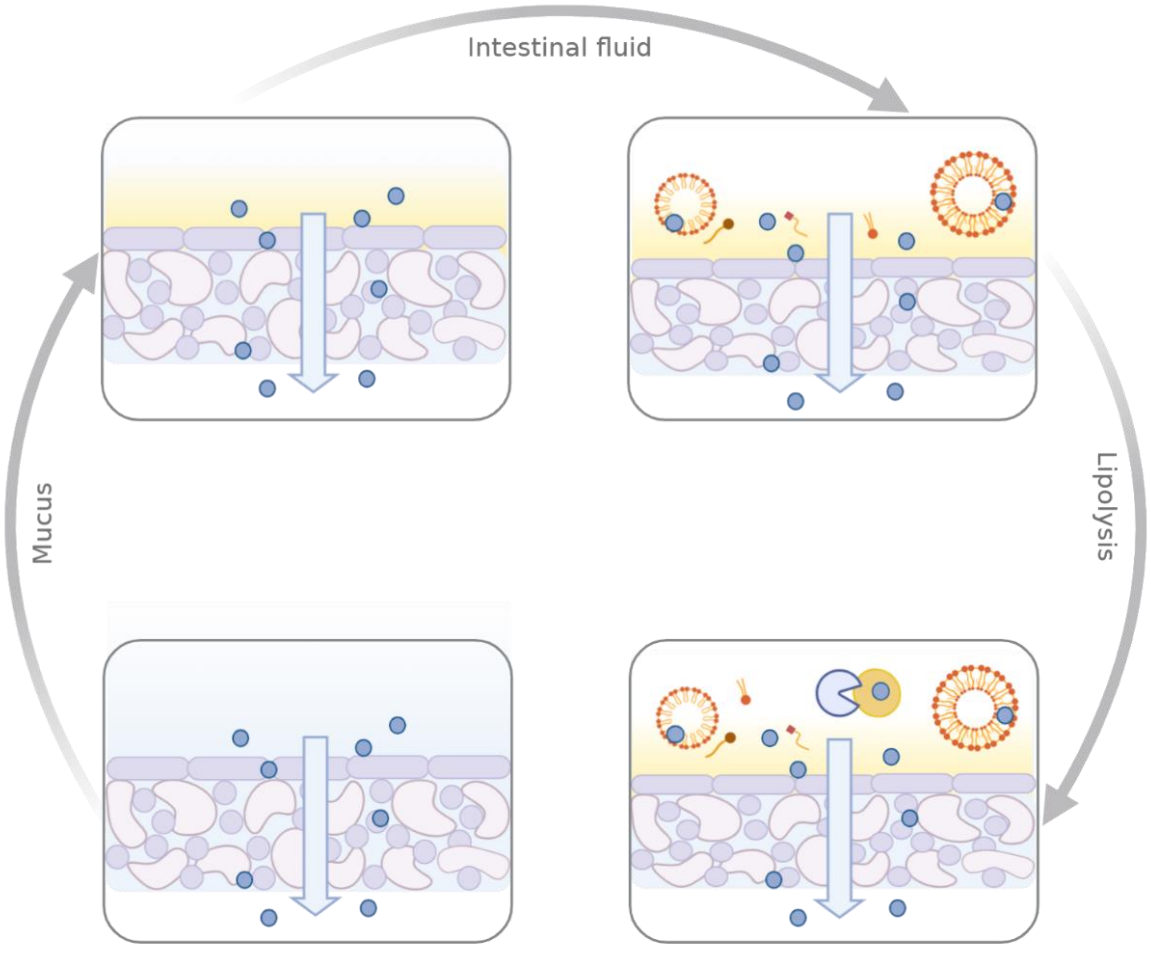

A dissertation for the degree of Philosophiae Doctor

The development journey of an artificial intestinal model predicting oral drug absorption: the mucus-PVPA model

Margherita Falavigna

Tromsø - February 2021

Drug Transport and Delivery Research Group

Department of Pharmacy

Faculty of Health Sciences

UiT The Arctic University of Norway

Norway

Front page content: pictorial illustration of the development of the mucus-PVPA model

All illustrations in this thesis were created with the use of BioRender.com by Margherita Falavigna

To understand

the intricate and dynamic dance between all the bodily parts is

To recognize

the inevitable connection of all physical things

To my pillars: the family that I was born in

and the one that I have created all around the globe

Acknowledgements

The work presented in this thesis was carried out at the Drug Transport and Delivery Research Group, Department of Pharmacy, UiT The Arctic University of Norway from January 2017 to February 2021. Throughout these years I have been lucky enough to receive the help and support of many people, to whom I would like to express my deepest gratitude.

Firstly, I would like to thank my supervisors, Professor Gøril Eide Flaten and Professor Natasa Škalko-Basnet, who have given me great guidance during these years. Gøril and Natasa, I am really grateful for your encouragement during the PhD and for giving me the freedom to express my scientific creativity. Gøril, I am beyond grateful for the opportunities that you gave me, which allowed me to travel, expand my network and grow as a more complete scientist. I am grateful for the many travelling memories together, and I thank you for being a great companion in the many conferences and meetings we attended together. Natasa, thank you for always being present, for being the compass of the DTD group and for always showing your support both professionally and personally.

This thesis is also a result of the hard work of the master students and co-authors that I have been lucky to work with and to whom I am very thankful. Mette, Richard, Martina and Sunniva, thank you for sharing your time and efforts with me. In particular, Mette, thank you so much for the great scientific (and musicals) discussions, for making me feel at home in Copenhagen, for the heartfelt and inspiring talks, and for making this your part-time PhD.

I am grateful for the whole DTD group, that through the years has changed and evolved so much, and that now makes coming to work even more enjoyable. In particular, thanks to Laura, Lisa, Jennifer, Sybil, Martin and Eirik. Our (1-meter distance) lunch breaks together have been one of the things I was looking forward to the most during the strange corona times. Thanks to my former and current office mates, Jennifer, Barbara, Iren and Selenia. You have all taught me how crucial and vital respect, balance and freedom are, and I have learnt much more than I could have ever imagined because of you.

This whole PhD adventure would not have happened without the help and support of the person who has brought me to Tromsø in the first place, Associate Professor Massimiliano Pio di Cagno. Max, thank you so much for your guidance and continuous encouragement.

During these past four years, I have been lucky enough to be surrounded by great friends, which have made this experience as special as it could be. To my Norwegian 'family', Chris, Alex, Jonina, Joao, Antal, Jennifer, thank you so much for the great memories together, all the parties, the hikes, trips, the dinners and the feeling of togetherness. I am also grateful for the nice time spent together with Giacomo, Pietro, Juncal, Joseph, Fabrizio.

I have had the blessing of starting and continuing this adventure in the Arctic with Chris, and the past five years have been filled with so many great memories together. From when we were wild and free Erasmus students to when we felt more like grownups (but always crying during Disney movies), you have always been there for me, through thick and thin, and our friendship has flourished and become one of the things that I cherish the most. I am forever grateful for the time spent together and I am looking forward to the next chapter.

I have also been fortunate enough to be able to count on the friends that have known me since I was the little girl that did not even know about the existence of Tromsø. To Angela, Manuela, Giulia, Saya and Alessia, I am so grateful for the fact that our friendships have proven to be able to withstand the distance that separates Italy from Norway, and I am so proud of what we have built together through many years.

Being here in Tromsø, doing a PhD, is not something random. It all started when my curiosity regarding what was beyond what I knew started to grow, and when my hunger for new experiences started to show up. No matter what (and where), I have been fortunate enough of always being able to count on the love and support of my amazing parents. Mom, dad, it really is true that 'the stronger the bow (family) the furthest the arrow (the child) will land'. Dad, thank you for your excitement and support regarding the work in academia, and for always making sure I knew how proud you are of me. Mom, thank you for always offering the emotional and physical support I was seeking in the moments of doubt, and for being the rock that I needed in moments of need. Thanks also to my grandma, who is a great example of toughness, curiosity and endless love for life, and to my brother and his family, that have enabled me to feel the joy of being an aunt.

To Michaela and Petter, thank you so much for making me feel part of your family, for the great dinners, wine tasting, skiing tours, trips and academic mentoring and discussions.

Last, but definitely not least, Garri(bieri). I have been lucky enough to meet you in the middle of the PhD. Since then, you have always encouraged me in all the projects that I wanted to pursue, inspired me in chasing more and better things for my life, made me laugh when I needed to get out of my 'robo(tto)' mood and made me feel protected and cared for. Thank you for bringing to life the vision of a relationship where, hand in hand, two people look in the same direction, and I cannot wait to see what the future will bring us. 'Let them bloom'.

Tromsø, February 2021

Table of Contents

Abstract I

List of abbreviations III

List of publications discussed in the thesis V

Other publications VI

Authors' contributions VI

1 Introduction 1

1.1 Oral drug administration 1

1.1.1 Gastrointestinal tract anatomy, physiology and contents 1

1.1.2 The fate of the drug through the GI tract 5

1.1.3 Factors affecting oral drug absorption 6

1.1.4 Oral delivery of PWSDs and related formulation strategies 11

1.2 *In vitro* assessment of drug absorption and formulation performance 15

1.2.1 Simulated intestinal fluids 16

1.2.2 *In vitro* lipolysis models 18

1.2.3 Cell free *in vitro* permeation tools 20

1.2.4 Mucus models and sources 24

1.2.5 Combined lipolysis – permeation *in vitro* models 25

2 Aims of the thesis 29

3 Summary of papers 31

3.1 Paper I 31

3.2 Paper II 33

3.3 Paper III 35

3.4 Paper IV 37

4 Results and discussion 39

4.1 From a naked to a mucus-covered *in vitro* permeation barrier – simulation of the intestinal mucosa (Paper I-II) 39

4.1.1 Simulation of the intestinal mucus 39

4.1.2 PVPA barrier integrity in the presence of mucus 41

4.1.3 Selection of the mucus model used for permeability studies 43

4.2 Use of the mucus-PVPA barriers to distinguish between different drugs and formulations (Paper I and II) 45

4.2.1 Assessment of drug permeability from solutions (Paper I and II) 45

4.2.2 Assessment of drug permeability from liposomal formulations (Paper I) ... 47
4.3 Simulation of the intestinal environment on top of the mucus-PVPA barriers (Paper II) ... 50
4.3.1 Solubility-permeability interplay in the presence and absence of mucus ... 50
4.3.2 Use of fasted and fed state SIFs with the mucus-PVPA barriers ... 52
4.4 Combination of *in vitro* intestinal lipolysis with *in vitro* drug permeation (Paper III) 57
4.4.1 Mucus-PVPA barrier integrity in the presence of a digesting environment 58
4.4.2 *In vitro* intestinal lipolysis of fenofibrate-loaded SNEDDSs ... 61
4.4.3 Permeation of fenofibrate using the mucus-PVPA barriers ... 64
4.4.4 Correlation of *in vivo* absorption with *in vitro* permeation data ... 66
4.5 Simultaneous *in vitro* lipolysis-permeation (Paper IV) ... 68
4.5.1 Functionality of the HTP *in vitro* intestinal lipolysis model ... 69
4.5.2 Effect of lipolysis on drug permeation and prediction of *in vivo* drug absorption ... 72
5 Conclusions ... 77
6 Perspectives ... 79
References ... 81

Abstract

The most convenient strategy to systemically deliver drugs is to utilize the oral route of administration due to its non-invasiveness, cost-effectiveness and high patient compliance. However, when a drug is orally administered it will be exposed to the different physiological processes and environments found along the gastrointestinal (GI) tract, which will determine its ability of being absorbed and reach the systemic circulation. For this reason, a close evaluation of the impact of the GI physiology on drug absorption should be carried out when new drugs and formulations are being developed. As a result of this, the need for reliable *in vitro* models able to mimic both the GI processes and environment has become ever so evident. In fact, such models have the potential of being utilized in the early stages of drug discovery and formulation development and can aid in the reduction of the cost-, time- and ethical- related issues usually associated with animal testing.

To answer the above-mentioned need, this work focused on the development of an *in vitro* model that could be employed to study drug permeation in the presence of an intestinally relevant environment. The construction of this model was stepwise. Firstly, the already established *in vitro* PVPA (Phospholipid Vesicle-based Permeation Assay) barriers were implemented with the addition of a mucus layer to simulate the intestinal mucosa, leading to the development of the mucus-PVPA barriers. The mucus-PVPA model demonstrated the ability to distinguish between the permeabilities of drugs characterized by different physicochemical properties and between different liposomal formulations. Secondly, intestinally relevant pH conditions were added to the mucus-PVPA model to account for their impact on drug absorption, and a pH-dependent trend was observed regarding the permeability and solubility of ionizable drugs. Additionally, commercially available simulated intestinal fluids were added to the mucus-PVPA barriers, to increase the biorelevance of the model during permeation studies. Further, the assessment of drug permeation was coupled with *in vitro* lipolysis to produce a combined model capable of mimicking this intestinal process and to unravel the impact of lipid digestion on the permeation of drugs contained in lipid-based formulations. Finally, the combined model was modified to permit *in vitro* lipolysis and permeation to occur simultaneously. Both the combined and simultaneous *in vitro* lipolysis-permeation models demonstrated to predict *in vivo* drug absorption in rats for three fenofibrate-loaded SNEDDSs (Self Nano-Emulsifying Drug Delivery Systems), underlining their potential use in the assessment of the performance of novel drugs and formulations.

List of abbreviations

AMI	Artificial Membrane Insert
ATN	Atenolol
AUC	Area Under the Curve
BCS	Biopharmaceutics Classification System
BM	Biosimilar Mucus
BS	Bile Salt
Caco-2	Human colorectal adenocarcinoma cell line
CAL	Calcein
CH	Cholesterol
CLSM	Confocal Laser Scanning Microscopy
DG	Diglycerides
(F)FA	(Free) Fatty Acid
FaHIF	Fasted Human Intestinal Fluids
FaSSIF	Fasted State Simulated Intestinal Fluid
FeHIF	Fed Human Intestinal Fluids
FeSSIF	Fed State Simulated Intestinal Fluid
GI	Gastrointestinal
HTP	High Throughput
IBP	Ibuprofen
IND	Indomethacin
IVIVC	*In Vivo-In Vitro* Correlation
LBF	Lipid-Based Formulation
LFCS	Lipid Formulation Classification System
LP	Lipoprotein

MG	Monoglycerides
MTP	Metoprolol
MTR	Metronidazole
NaOH	Sodium Hydroxide
NPR	Naproxen
PAMPA	Parallel Artificial Membrane Permeation Assay
P_{app}	Apparent Permeability
PC	Phosphatidylcholine
PL	Phospholipid
PVPA	Phospholipid Vesicle-based Permeation Assay
PWSD	Poorly Water-Soluble Drug
SIF	Simulated intestinal fluid
SNEDDSs	Self Nano-Emulsifying Drug Delivery Systems
TG	Triglycerides

List of publications discussed in the thesis

Paper I:

M. Falavigna, M. Klitgaard, C. Brase, S. Ternullo, N. Škalko-Basnet, G.E. Flaten, Mucus-PVPA (mucus phospholipid vesicle-based permeation assay): an artificial permeability tool for drug screening and formulation development, *Int. J. Pharm.* 537 (**2018**), 213–222.

Paper II:

M. Falavigna, M. Klitgaard, E. Steene, G.E. Flaten, Mimicking regional and fasted/fed state conditions in the intestine with the mucus-PVPA *in vitro* model: The impact of pH and simulated intestinal fluids on drug permeability, *Eur. J. Pharm. Sci.* 132 (**2019**), 44-54.

Paper III:

M. Falavigna, M. Klitgaard, R. Berthelsen, A. Müllertz, G.E. Flaten, Predicting oral absorption of fenofibrate in lipid-based drug delivery systems by combining *in vitro* lipolysis with the mucus-PVPA permeability model, *J. Pharm. Sci.* 110 (**2021**), 208-216.

Paper IV:

M. Falavigna, S. Brurok, M. Klitgaard, G.E. Flaten, Simultaneous assessment of *in vitro* lipolysis and permeation in the mucus-PVPA model to predict oral absorption of a poorly water soluble drug in SNEDDSs, *Int. J. Pharm.* 596 (**2021**), 120258.

Other publications

A

M. Falavigna, P.C. Stein, G.E. Flaten, M.P. Di Cagno, Impact of mucin on drug diffusion: development of a straightforward *in vitro* method for the determination of drug diffusivity in the presence of mucin, *Pharmaceutics* 12 (2) 168 (**2020**), 1-13.

B

M. Falavigna, M. Pattacini, R. Wibel, F. Sonvico, N. Škalko-Basnet, G.E. Flaten, The vaginal-PVPA: A vaginal mucosa-mimicking *in vitro* permeation tool for evaluation of mucoadhesive formulations, *Pharmaceutics* 12 (6) 568 (**2020**), 1-15.

Authors' contributions

Publication	Experimental design	Execution of experiments	Data analysis	Original draft preparation	Visualization	Reviewing and editing
Paper I	MF; MK; GEF; NSB	MF; MK; CB; ST	MF; MK; ST	MF	MF	MF; MK; ST; NSB; GEF
Paper II	MF; MK; ES; GEF	MF; MK	MF; MK	MF	MF	MF; MK; ES; GEF
Paper III	MF; MK; AM; GEF	MF	MF	MF	MF	MF; MK; RB; AM; GEF
Paper IV	MF; MK; GEF	SB; MF	MF	MF	MF	MF; MK; GEF
A	MF; PCS; MPDC; GEF	MF	MF; PCS	MF	MF; PCS	MF; PCS; MPDC; GEF
B	MF; NSB; GEF	MF; MP; RW	MF	MF	MF	MF; RW; FS; NSB; GEF

Authors: Margherita Falavigna (MF); Mette Klitgaard (MK; master student supervised by MF); Christina Brase (CB); Selenia Ternullo (ST); Natasa Škalko-Basnet (NSB); Gøril Eide Flaten (GEF); Erik Steene (ES); Ragna Berthelsen (RB); Anette Müllertz (AM); Sunniva Brurok (SB; master student supervised by MF); Paul C Stein (PCS); Massimiliano Pio Di Cagno (MPDC); Martina Pattacini (MP; master student supervised by MF); Richard Wibel (RW; master student supervised by MF); Fabio Sonvico (FS).

1 Introduction

1.1 Oral drug administration

The administration of drugs *via* the oral route is regarded as the most convenient strategy to systemically deliver drugs, due to its non-invasiveness, low cost and high patient compliance [1]. However, the physiological complexity and structure of the gastrointestinal (GI) tract can greatly influence the ability of a drug to exert its effect [2]. In particular, the impact that the GI tract anatomy and physiology have on drug absorption need to be carefully understood and taken into consideration when new drugs or formulations are being developed and studied.

1.1.1 Gastrointestinal tract anatomy, physiology and contents

The GI tract comprises a series of connected compartments that go from the mouth to the anus, it is linked to organs such as the liver, gallbladder and pancreas; its overall function is the one of mediating the interaction between the environment and the body, with the aim of maintaining homeostasis [1]. The three main sections of the GI tract are the stomach, small intestine and large intestine (Figure 1.1). The stomach serves as a storage for the content ingested through the mouth, and has the function of mixing, grinding and digesting this content thanks to its muscular layers, its highly acidic pH (pH 1.7-3.3) and enzymatic secretions [3]. The composition of the content found in the stomach determines the gastric emptying time, which is slower in the case of a high-caloric meal [4, 5]. The stomach gradually

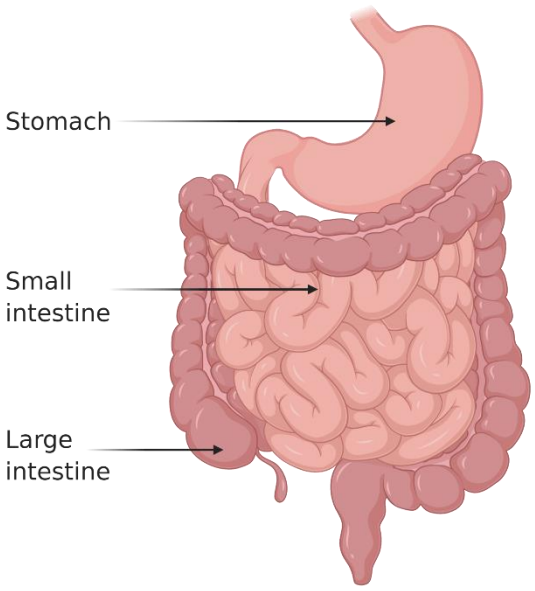

Figure 1.1: The three main portions of the GI tract: stomach, small intestine and large intestine

empties its content through the pylorus into the small intestine, which has the main function of digesting and absorbing nutrients and drugs [3]. In particular, the duodenum, the first portion of the small intestine, receives bile, phospholipids and cholesterol from the gallbladder, and pancreatic fluids containing lipase and proteases from the pancreas [6]. These secretions play a key role in the digestion process. The second section of the small intestine, the jejunum, has the primary function of absorbing what has been made available after digestion, while the last section (*i.e.* the ileum) has the role of absorbing lipid degradation products and bile salts [3]. The large intestine, also referred to as colon, is the distal part of the GI tract, and has the function of absorbing water, vitamins and electrolytes, while being able to ferment undigested fibers and collect fecal content [1, 7].

1.1.1.1 The gastrointestinal mucosa

The mucosal structure present through the whole GI tract is a barrier that separates the GI luminal content from the blood circulation. The structure of the GI mucosa differs according to the specific GI compartment (*i.e.* stomach, small intestine, colon), leading to region-dependent properties (Figure 1.2). As the focus of this work revolves around drug absorption, the following discussion will mainly be centered on the characteristics and processes taking place in the portion where absorption is most abundant, *i.e.* the small intestine. The small intestine mucosa is composed of four layers: the epithelium covered by a mucus layer, the basal membrane, the *lamina propria* and the *muscularis mucosa* which provides support and nutrition to the epithelium [8]. The absorbing function of the small intestine is made efficient by the specific conformation of the enterocytes present

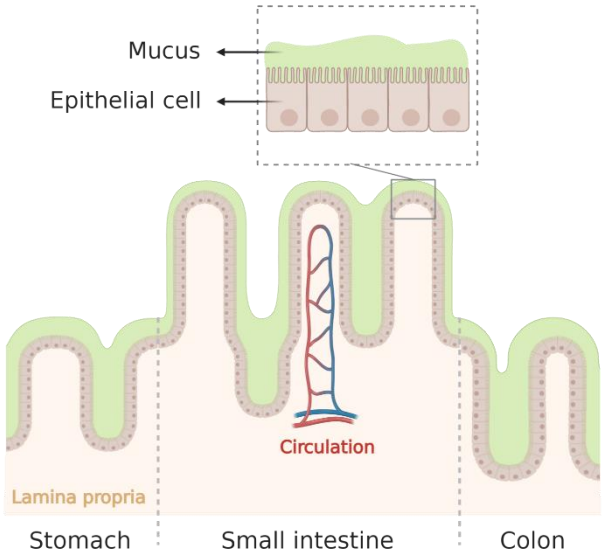

Figure 1.2: The mucosa of the stomach, small intestine and colon, composed of epithelial cells and covered by a mucus layer.

in the epithelium. In fact, the enterocytes in the small intestine are characterized by the presence of numerous protrusions called villi, which extend the absorptive surface area of the small intestine [9]. Other than the enterocytes, cells such as mucus-secreting goblet cells, M-cells and Paneth cells are also present in the intestinal epithelium (Figure 1.3) [9]. All these cells are linked together in a monolayer through tight junctions, which prevent leakage of unwanted material between the luminal and the basal side of the intestinal mucosa while allowing the absorption of essential nutrients from the intestinal contents [10].

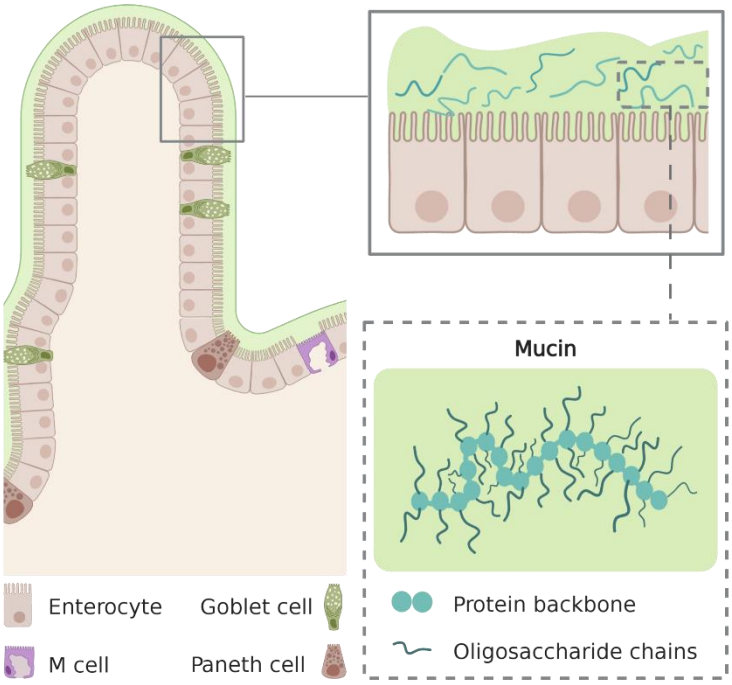

Figure 1.3: The intestinal mucosa, its epithelial cells, the mucus layer and the mucin glycoprotein contained in mucus.

The mucus layer present on top of the intestinal mucosa represents the first barrier for absorption, and it is able to selectively prevent unwanted molecules from being absorbed by trapping and moving them towards the colon with the help of the migrating motor complex [11, 12]. While both the stomach and colon are characterized by an evident double-layered mucus (*i.e.* inner strongly adherent layer plus loosely adherent layer), the small intestine mainly presents a single-layered and loosely bound mucus [13]. For instance, in the small intestine of rats, the strongly adherent layer can range from 16 to 29 µm, whereas the loosely adherent one can be 123 to 480 µm thick [14]. In general, the mucus layer is composed of water (≈ 90% w/w), glycoproteins (*i.e.* mucins ≈ 0.2-5% w/v; MUC2 prevails in the GI tract), proteins (≈ 0.5% w/v), salts (≈ 0.5-1% w/w), lipids (≈ 1-2% w/w), DNA, cells, and cellular debris, and represents both a steric and physicochemical barrier to the absorption of unwanted molecules [11, 15]. Currently, 19 mucin genes (MUC) have been discovered, and it has been found that MUC2 is mainly secreted in the

intestine, while MUC5 and MUC6 are usually found in the stomach [16]. Mucins play a key role in the barrier function of mucus, as their structure (bottle-brush composed of a protein backbone to which numerous oligosaccharide attach to) contributes to structuring the mucus network, and the glycan domains in the mucin generate its gel-like properties [9, 10, 17-19] (Figure 1.3). Furthermore, the highly glycosylated mucin regions, which account for 80% of the dry weight of mucins [20, 21], give mucus an overall hydrophilic behavior, with a distinctive negative charge caused by the prevalence of sialic acid (pKa ≈ 2.6) in the oligosaccharide chain [22]. The sections of the protein backbone that are not associated to oligosaccharide chains are characterized by cysteine-rich regions, which lead to the establishment of inter-mucin disulfide bonds that create the mesh-like network of mucus [23]. The mucus mesh-like structure acts as a size-exclusion filter, which leads to steric hindrance to the diffusion of pathogens, while its overall hydrophilicity and negative charge produces a physicochemical barrier to molecules that are not compatible with such environment [15, 24]. Moreover, the pH of mucus along the GI tract changes according to the specific GI compartment, and it has been shown that the viscosity of mucus increases at more acidic pH due to a pH-dependent sol-gel transition and varies with temperature and salt concentration [25-27]. This pH-dependent behavior leads to increased protective properties for the mucus found in the stomach, compared to the more permeable mucus found in the small intestine [16, 17].

1.1.1.2 The gastrointestinal fluids

The characteristics and composition of the fluids found throughout the GI tract depend on the GI compartment (*i.e.* stomach, small intestine or colon) and on the prandial state (*i.e.* fasted or fed state) [28, 29]. For instance, the stomach is characterized by an acidic pH (1.7-3.3), the small intestine pH ranges between 6 and 8 (*i.e.* 5.6- 7.0 in the duodenum; 6.5-7.8 in the jejunum), while the pH of the fluids found in the colon is highly variable [5, 8, 28, 30, 31]. Moreover, after meal intake an increased concentration of bile salts, phospholipids, cholesterol, free fatty acids, mono, di and tri-acylglycerides can be observed in the small intestine (Table 1.1) [32, 33], together with higher enzymatic activity, resulting from increased gallbladder and pancreatic secretions [8]. The change in fluid

composition occurring in the fed state determines the formation of various structures, such as (mixed) micelles, vesicles of different sizes and lipid droplets, which add a lipophilic microenvironment to the fed intestinal fluid that is not found in fasted one [34].

Table 1.1: Fasted human intestinal fluids (FaHIF) and fed human intestinal fluids (FeHIF) composition, including bile salts (BS), phospholipids (PL), cholesterol (CH), free fatty acids (FFA), monoglycerides (MG), diglycerides (DG) and triglycerides (TG) [33, 35].

	BS (mM)	**PL (mM)**	**CH (mM)**	**FFA (mg/mL)**	**MG (mg/mL)**	**DG (mg/mL)**	**TG (mg/mL)**
FaHIF	4.4	0.9	0.08	0.64	0.14	-	-
FeHIF	12.1	4.1	0.71	6.72	2.82	1.04	0.87

1.1.2 The fate of the drug through the GI tract

Once a drug is orally administered, it will be exposed to the different GI compartments and fluids before being absorbed and eventually reach the systemic circulation. In particular, when an oral drug formulation is being swallowed, it will first need to disassemble and provide the dissolution of the drug in the GI fluids [36, 37]. The specific characteristics of the formulation and of the drug itself, together with their interaction with the GI compartments and related fluids, will determine the extent of drug dissolution (as discussed in Section 1.1.3). As soon as the drug is freely dissolved, it will be available for absorption and it will cross the small intestine epithelium *via* transport mechanisms such as passive transcellular diffusion, passive paracellular diffusion, carrier-mediated influx transport, active efflux transport and transcytosis (Figure 1.4) [38]. Passive transcellular diffusion and carrier-mediated transport occur across the enterocytes, whereas passive paracellular diffusion takes place between the enterocytes (Figure 1.4) [39].

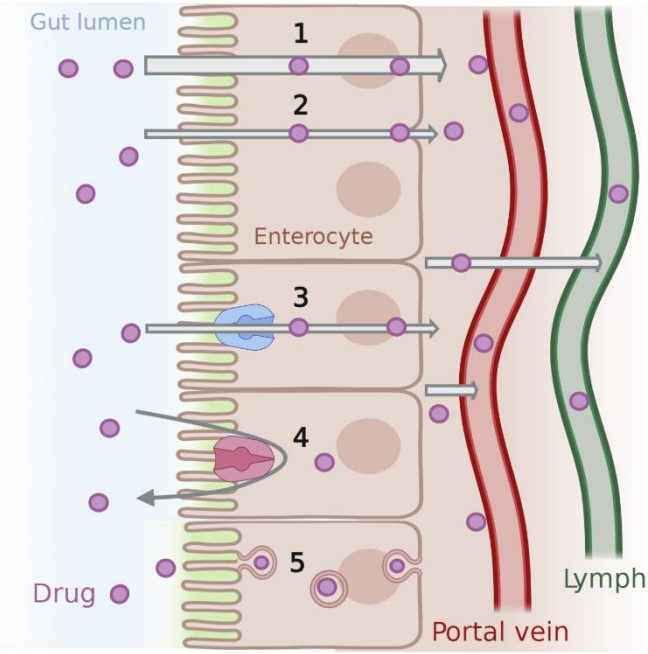

Figure 1.4: Intestinal drug transport mechanisms, including 1) passive transcellular diffusion, 2) passive paracellular diffusion, 3) carrier-mediated influx transport, 4) efflux transport and 5) transcytosis.

On the other hand, efflux transport and transcytosis depend on active transporters and on the incorporation of the drug into vesicles from the enterocyte membrane, respectively (Figure 1.4) [40, 41]. Out of these five drug transport mechanisms, passive transcellular diffusion is regarded as the predominant one, especially for lipophilic drugs [38], whereas passive paracellular diffusion is the preferred transport route of small hydrophilic drugs [42, 43]. However, because of the limited surface area available for paracellular diffusion (*i.e.* 0.01 % of the overall absorptive intestinal surface area) drug absorption resulting from this transport mechanism is limited [44]. Following transport, the fraction of drug absorbed (F_a) in the intestinal epithelium is either able to reach the portal vein or the lymph, depending on the physicochemical characteristics of the drug (Figure 1.4). A percentage of the drug arriving to the liver through the portal vein will be metabolized by the hepatic enzymes before being transported to the systemic circulation, whereas the amount of drug absorbed in the lymphatic circulation is directly able to reach the systemic blood circulation (Figure 1.4) [45]. Once in the systemic circulation, the drug will be distributed to the tissues where it will exert its effect.

1.1.3 Factors affecting oral drug absorption

As previously mentioned, the extent to which a drug is able to reach the systemic circulation depends on various factors. Such factors include both the characteristics of the drug and of the formulation in which the drug is loaded (drug and formulation

characteristics) as well as the GI physiology (physiological factors) [1]. More specifically, oral drug absorption is driven by the interaction between the characteristics of the drug and formulation and the physiological GI environment. To achieve high drug absorption, this interaction should lead to high dissolution (solubility) of the drug in the GI fluids together with high drug permeation across the intestinal epithelium.

1.1.3.1 The impact of drug and formulation characteristics on drug absorption

The impact of the drug physicochemical characteristics in attaining high drug absorption has been highlighted by the 'rule of five' introduced by Lipinski [46] and by the Biopharmaceutics Classification System (BCS), introduced by Amidon and colleagues [47]. The 'rule of five' states that that high absorption is occurring when: hydrogen bond acceptors are less than 10, hydrogen bond donor are less than 5, the drug molecular weight is lower than 500 Da, and the lipophilicity (described by the logP) is lower than 5 [46]. On the other hand, the BCS categorizes drugs into four classes (Figure 1.5): class I (high solubility and permeability), class II (high permeability but low solubility), class III (high solubility but low permeability) and class IV (low solubility and permeability) [47]. For highly soluble drugs the highest given dose is soluble in a 250 mL aqueous medium (pH 1-7.5), whereas for highly permeable drugs 90% or more of the administered drug dose is absorbed from the GI tract to the blood stream. Both solubility and permeability are tightly connected to the physicochemical characteristics of the drugs, such as the dissociation constant pKa, logP, logD and melting point (Figure 1.6). More specifically, the

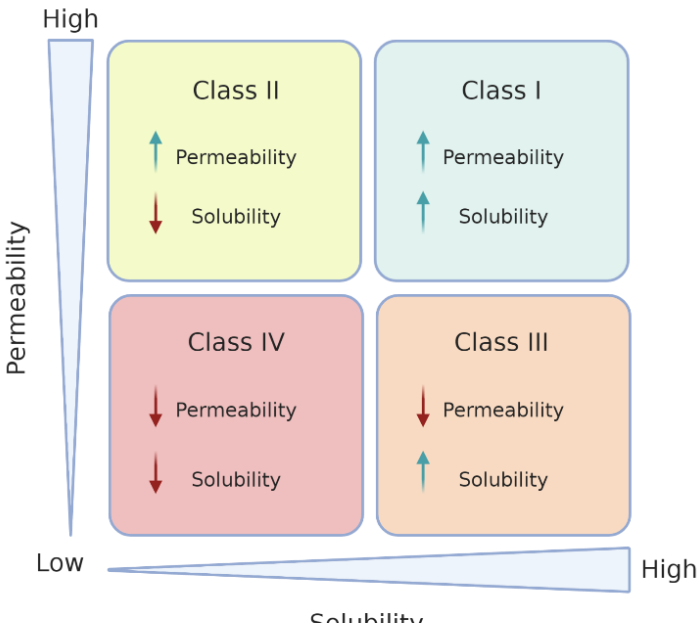

Figure 1.5: Biopharmaceutics Classification System (BCS).

pKa determines the charge of an ionizable compound in a specific pH environment. The ionized state of the compound will have a positive effect on its solubility, while having a negative effect on its passive permeability [48, 49]. This concept has been summarized in the pH partitioning theory [50, 51]. Consequently, weak bases are highly soluble at the acidic pH of the stomach (*i.e.* drug ionization > 50%) and their transfer into the small intestine, characterized by a more neutral pH, can cause their precipitation [52, 53]. The opposite is true for weak acids, which are less soluble in the stomach compared to the small intestine [54]. For such ionizable compounds, solubility and permeability display opposite trends. In fact, high drug ionization (> 50%) causes high solubility and low permeability, whereas low drug ionization (< 50%) leads to the opposite effect [48]. Instead, logP (*i.e.* affinity of the neutral drug form for a water-immiscible organic phase compared to an aqueous one) is directly proportional to passive permeability and inversely proportional to drug solubility [55], and it is a parameter that makes it possible to assess the affinity of a drug for biological membranes. On the other hand, logD (*i.e.* affinity of the charged drug form for a water-immiscible organic phase compared to an aqueous one) determines the distribution of ionizable drugs at a specific pH, and it is thus directly related to the pKa of the drug [55]. Drugs with logD > 3 are referred to as 'grease ball' compounds, and they are characterized by a solvation-limited solubility caused by their high lipophilicity [56, 57]. Differently, 'brick dust' compounds are drugs with high melting point (T_m > 200 °C) and their dissolution is energy-limited, as high energy is needed to dissociate these molecules from their solid form [36, 49].

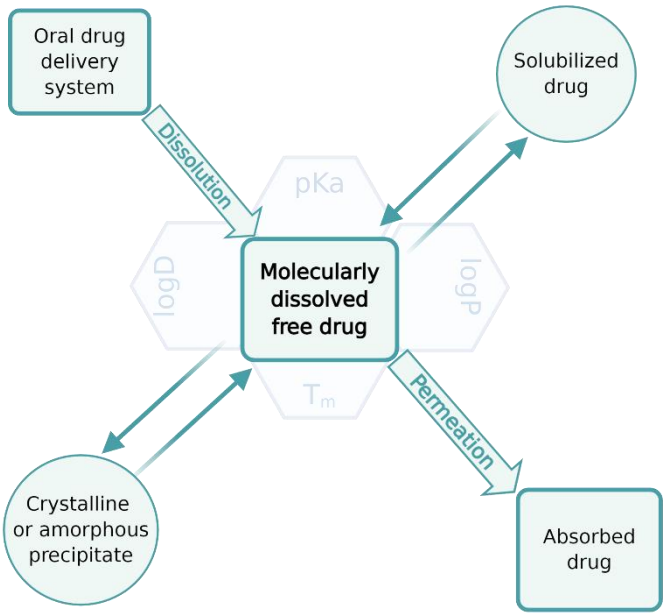

Figure 1.6: From dissolution to drug absorption.

As drug dissolution is the first limiting step contributing to drug absorption, it is important to highlight than only the molecularly dissolved free drug is able to permeate the intestinal walls. This solubility is not only connected to the physicochemical characteristics of the drug, but also to the excipients of the formulation in which the drug is loaded and to the GI fluids composition and characteristics [36]. For this reason, the definition of drug solubilization has been introduced, referring to the amount of drug solubilized by formulation excipients, digestion products and endogenous bile salts and phospholipids present in the intestine. The solubilized drug is not molecularly and freely dissolved, as it is associated with the colloidal structures present in the GI fluids, and it is therefore not able to be directly absorbed (Figure 1.6). However, the solubilized drug can serve as a drug reservoir for further drug dissolution, thus being able to directly enhance drug absorption [58]. Several techniques have been used to enhance the solubility of poorly water-soluble drugs (PWSDs) like the ones in BCS class II, and this has led to the development of enabling formulations such as lipid-based formulations (LBFs) [36]. The use of LBFs to enhance drug dissolution and drug absorption will be discussed in Section 1.1.4.

1.1.3.2 The impact of physiological factors on drug absorption

The physicochemical characteristics described above determine how the drug is able to interact with the contents found in the GI tract and with its physiological barriers, and this interaction determines the extent of drug absorption. The GI factors that can either aid or hamper drug absorption going from a luminal-to-basal direction are i) the dissolution properties of the luminal fluids, ii) the interaction and size filtering properties of the mucus layer, iii) the permeation pathways of the intestinal epithelium and iv) the distribution mechanisms of the drugs to the systemic circulation. Dissolution in the luminal fluids is particularly central for PWSDs, as their low aqueous solubility can lead to precipitation and thus low absorption [8]. However, for PWSD such as the ones classified as BCS class II compounds (*i.e.* drugs with high permeability but low solubility) the increase in the presence of solubilizing agents found in the fed intestinal fluids leads to higher drug dissolution and absorption [8]. The composition of the fed intestinal fluids primarily

affects drug solubilization and dissolution for neutral compounds, whereas for weak acid and bases the pH is the major driver of drug dissolution [55, 59, 60]. Moreover, the composition of the ingested meal can lead to negative, positive or neutral food effects, depending on the specific drug and its interaction with the food components [8, 61-63].

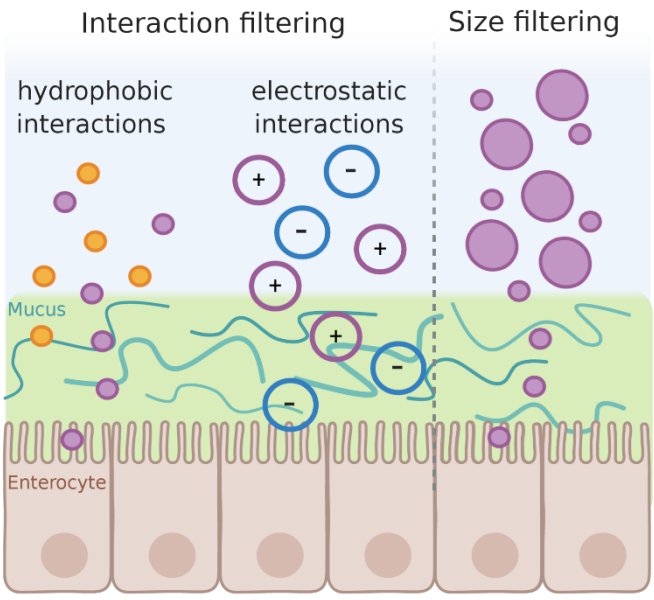

Figure 1.7: Interaction and size filtering processes working against the diffusion of drugs across the mucus layer.

Proceeding towards the intestinal membrane, the likelihood that a drug is able to reach the epithelial absorption site depends on its interaction with the mucus layer [19]. In fact, this layer acts as a barrier for the diffusion of drugs through two main mechanisms: interaction and size filtering [24]. The first mechanism takes into account a decrease in the diffusion of drugs due to electrostatic or hydrophobic interactions, hydrogen bonds and selective binding interactions (Figure 1.7) [15, 21]. For instance, lipophilic drugs have affinity for the non-glycosylated regions of mucins (*i.e.* protein backbone, Figure 1.3), thus their diffusion through the mucus layer is slowed down more than hydrophilic ones [64-66]. On the other hand, positively charged drugs can electrostatically bind the negatively charged mucins, and this interaction can cause their retention in the mucus layer and slow down their diffusion through it (Figure 1.7) [25, 67]. However, even though the absorption of lipophilic drugs is negatively affected by the mucus layer, their nature makes them more likely to passively cross the intestinal epithelium because of their high affinity for biological membranes [55, 68]. Additionally, gel-forming mucins are capable of forming a mesh-like structure that is able to impede the diffusion of large molecules (Figure 1.7) [69], while the overall high viscosity of mucus layer can retard drug diffusion [27]. The active and passive permeation pathways described in Section 1.1.2 can also determine the extent of drug absorption, and they can vary across the GI tract [8].

Finally, drug lipophilicity can determine the way by which the drug will reach the systemic circulation. In fact, drugs with logP higher than 5 are assembled into triglyceride-rich lipoproteins inside the enterocyte (Figure 1.8) [45, 70]. This drug-lipoprotein aggregate is able to reach the mesenteric lymphatic system, which is connected to the systemic circulation. Instead, drugs with logP lower than 5 reach the systemic circulation through uptake into the portal vein, thus having to be exposed to the first-pass metabolism of the liver before reaching the systemic blood stream (Figure 1.8) [45, 70].

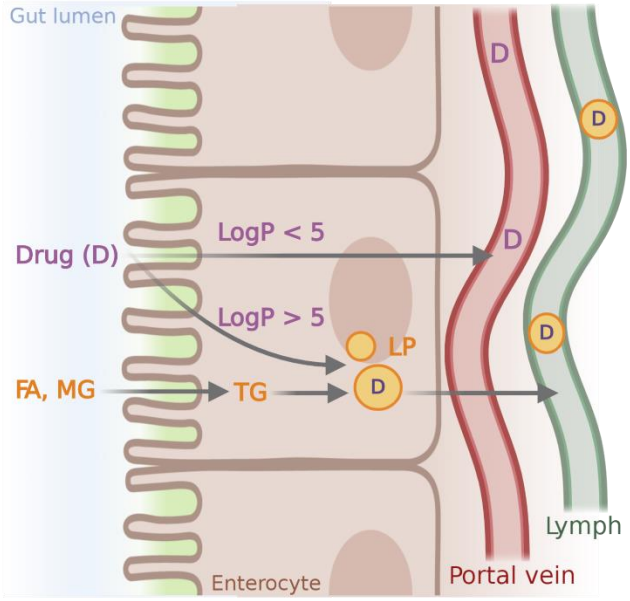

Figure 1.8: Drug absorption *via* the portal vein and the lymph. Lymphatic drug transport is facilitated by FA and MG, which are re-assembled in TG and lipoprotein (LP), and can access the lymphatic circulation.

1.1.4 Oral delivery of PWSDs and related formulation strategies

In the past decade, the amount of newly discovered drugs characterized by high (logP > 5) to moderately high (logP > 3) lipophilicity has steadily increased, accounting for 70 % of the new drug candidates [71]. These compounds are referred to as PWSDs, and they can be affiliated to BCS class II or IV. These drugs are characterized by solubility-limited absorption, as their low solubility in aqueous environments leads to precipitation and thus low bioavailability [72]. Moreover, the dissolution of these compounds in the GI fluids can depend on inter- and intraindividual factors such as the GI physiology, fasted or fasted state and composition of the ingested meal [73]. For BCS class IV compounds, the low membrane permeability that accompanies their low solubility makes them poor

candidates for formulation development, whereas the extent of oral absorption of BCS class II compounds can be altered by loading them into enabling formulations [74].

To answer for the low solubility and variable bioavailability of BCS class II drugs, liposomal formulations and LBFs such as self-nanoemulsifying drug delivery systems (SNEDDSs) have been introduced as two formulation strategies [75, 76], producing a high number of FDA approved drug products for this BCS class [77].

Liposomes are mainly constituted by phospholipids, which are amphiphilic molecules able to arrange upon hydration into a vesicular structure characterized by a phospholipid bilayer surrounding an aqueous core [78]. The lipophilic nature of the phospholipid bilayer allows loading of lipophilic drugs, while the aqueous core can accommodate drugs with a more hydrophilic nature, allowing liposomes to be carriers for drugs with different physicochemical properties [76, 79]. Additionally, the liposomal surface can be modified to confer characteristics such as mucoadhesion and mucopenetration, which can be exploited to improve the oral delivery of drugs by the interaction with or diffusion through the GI mucus layer, respectively [80]. Even though the oral delivery of drugs loaded into liposomes is considered as one of the strategies for the delivery PWSDs, it suffers from the drawback connected to the instability of these drug delivery systems in the presence of gastric acids, bile salts and digestive enzymes [79]. Therefore, these formulations have been either modified to improve their stability in the GI environment, or they have been used for oromucosal drug delivery, which does not cause large instability issues and is able to bypass the first-pass metabolism in the liver [81].

On the other hand, LBFs such as SNEDDSs are composed of oils, surfactants and co-solvents and they are able to spontaneously form nano-emulsions once dispersed in a water phase (*i.e.* oil-in-water emulsions) [82]. The oral delivery of such LBFs has proved to enhance bioavailability of PWSDs by inducing drug solubilization (*i.e.* increase in amount of drug associated with micelles and other colloidal structures), drug supersaturation (*i.e.* increase in free drug compared to the drug equilibrium solubility), precipitation inhibition and by enhancing lymphatic transport [36, 45, 83-86]. Additionally, it has shown to reduce the effect of the prandial state and GI physiology on drug absorption [73, 87]. LBFs can be divided into four groups according to their composition, following the lipid formulation classification system (LFCS) introduced by Pouton and colleagues (Table 1.2) [74].

Table 1.2: Types of LBFs according to the lipid formulation classification system (LFCS) [74].

Excipients	Content of formulation (%)				
	Type I	**Type II**	**Type IIIA**	**Type IIIB**	**Type IV**
Oil	100	40 - 80	40 - 80	< 20	-
Water-insoluble surfactants	-	20 - 60	-	-	0 – 20
Water-soluble surfactants	-	-	20 - 40	20 - 50	30 - 80
Hydrophilic co-solvent	-	-	0 - 40	20 - 50	0 - 50

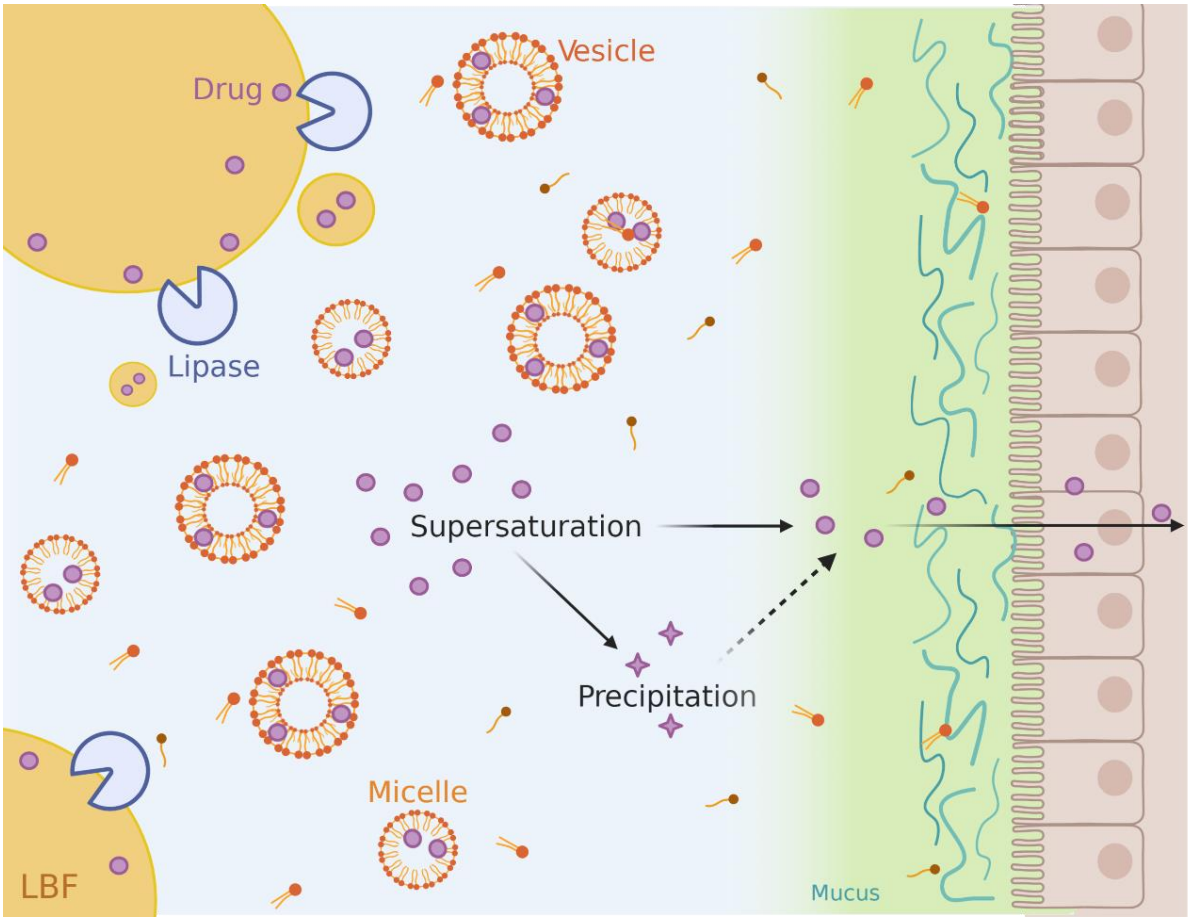

Figure 1.9: PWSD absorption following LBF digestion, drug solubilization, supersaturation and precipitation.

The extent to which the drug is able to be absorbed is therefore closely linked to the interaction between the LBF and the GI physiology. In fact, the colloidal structures formed between the LBF components, their digested portions, endogenous phospholipids, bile

salts and cholesterol are the determining factors affecting the solubilization of the drug and its absorption [70, 75]. For instance, the presence of lipids in the LBF will lead to the secretion of lipases from the gastric mucosa and the pancreas, as well as bile from the gallbladder, leading to lipid digestion (*i.e.* lipolysis) [70, 88, 89]. As a result of this, the drug previously solubilized in the LBF will now be found i) partitioned in the colloidal structures (micelles, vesicles, emulsion droplets) formed upon lipolysis, ii) free in a meta-stable supersaturated solution and iii) precipitated in its crystalline or amorphous form (Figure 1.9) [36, 90, 91]. Because of their impact on drug absorption, the lipolysis-triggered changes affecting drug solubilization and dissolution have to be carefully taken into account for LBFs. As previously mentioned, it is the amount of drug free in solution the portion that is able to be absorbed (Figure 1.6). Therefore, in the case of LBFs the amount of supersaturated drug (*i.e.* free drug present at a concentration higher than its equilibrium solubility) will be the driving force for drug permeation across the intestinal epithelium, while the amount contained in the colloidal structures will represent a reservoir of solubilized drug that will eventually partition in the supersaturated solution (Figure 1.10) [91, 92]. Even though supersaturation induced by LBFs can be beneficial to enhance the bioavailability of PWSDs, its thermodynamic instability can lead to drug precipitation [93]. In fact, drugs tend to precipitate from the supersaturated state until equilibrium solubility is reached, leading to the loss of the enhanced absorption offered by LBF [94]. However, drug precipitation following supersaturation can be inhibited by the presence of the absorptive sink [95, 96]. In fact, the amount of free drug continuously removed by the permeation across the intestinal epithelium can create an alternative to precipitation and change the precipitation kinetics by relieving the thermodynamic instability caused by

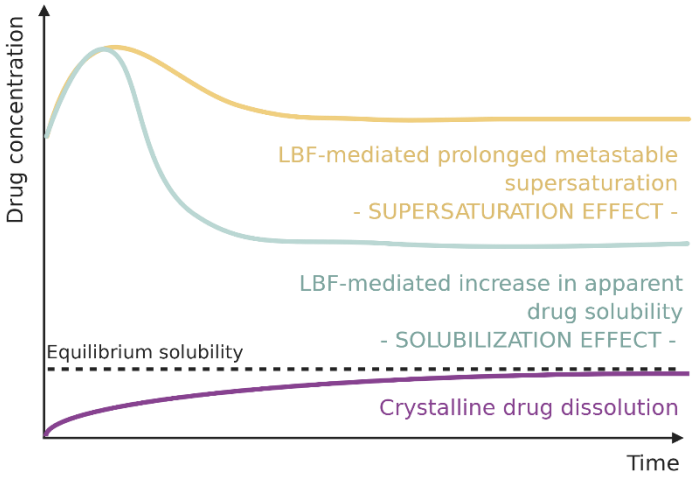

Figure 1.10: LBF-mediated supersaturation and solubilization effect during dispersion and lipolysis.

drug supersaturation [94, 96]. In addition, the intestinal mucus layer has also shown to stabilize the drug in its supersaturated state, thus aiding in promoting an increase in the bioavailability of drugs contained in LBFs [97, 98]. Finally, LBFs have shown to promote lymphatic drug transport of highly lipophilic drugs (log P > 5). In fact, the fatty acids and monoglycerides resulting from the intestinal lipolysis of LBFs can enter the enterocytes, form triglycerides and can be assembled into lipoproteins (Figure 1.8) [83, 99]. The newly synthetized lipoprotein are then able to incorporate lipophilic drugs and access the mesenteric lymphatic system, thus stimulating lymphatic drug transport and avoiding the first-pass metabolism [45, 70, 83].

1.2 *In vitro* assessment of drug absorption and formulation performance

During the early stages of drug discovery and formulation development, the use of *in vitro* models has become increasingly common, due to their cost and time effectiveness and due to the avoidance of the ethical concerns related to animal testing. In fact, *in vitro* models help in the replacement, refinement and reduction of animal research (three Rs concept) [100], and are useful in evaluating the performance of oral drug formulations before preclinical and clinical stages [101, 102]. Moreover, the complexity and physiological relevance of *in vitro* models can be tailored to the specific application, thus enabling both the exclusive simulation of one specific rate-limiting process affecting drug performance (*i.e.* more simplistic models) and also the replication of more complex systems [90]. In general, when assessing oral drug absorption, *in vitro* models can offer the simulation of i) the GI fluids composition and dissolution properties, and/or ii) of the intestinal permeation membrane through which the drug is being absorbed. Moreover, because of the increased number of discovered PWSDs, and because of the relevance of LBFs for the administration of such drugs, the lipolysis-triggered processes affecting drug absorption can also be accounted for in the chosen *in vitro* model. Thus, to unravel the GI absorption-related processes and to predict *in vivo* oral drug absorption, *in vitro* dissolution methods, lipolysis systems and permeation models can be singularly utilized or combined together according to the specific research question.

1.2.1 Simulated intestinal fluids

The evaluation of drug solubility and permeability has been carried out with the use of simple aqueous buffers for several decades; however, in the past years it has become ever so evident that for drugs such as PWSDs the use of such buffers can lead to a false estimation of their *in vivo* performance [61]. Yet, this problem is not shared by drugs having physicochemical characteristics differing from the ones of PWSDs. For this reason, Markopoulos and colleagues proposed the separation of simulated intestinal media in four levels of biorelevance, where level 0 comprises a buffer where only luminal pH is simulated, whereas level 3 simulates luminal pH, osmolarity, buffer capacity, bile, lipids and protein components, together with the digestive processes [103]. The choice of one of the four levels of biorelevance depends on the physicochemical properties of the drug being studied and on the research question being formulated [104]. For example, the solubility of ionizable compounds is strictly connected to the pH of the medium, especially for drugs that change their state of ionization in the selected pH environment. On the other hand, for neutral compounds and molecules that do not change their ionization in the chosen pH interval the presence of bile salts and phospholipids is the main driving factor affecting drug solubilization (Figure 1.11) [60].

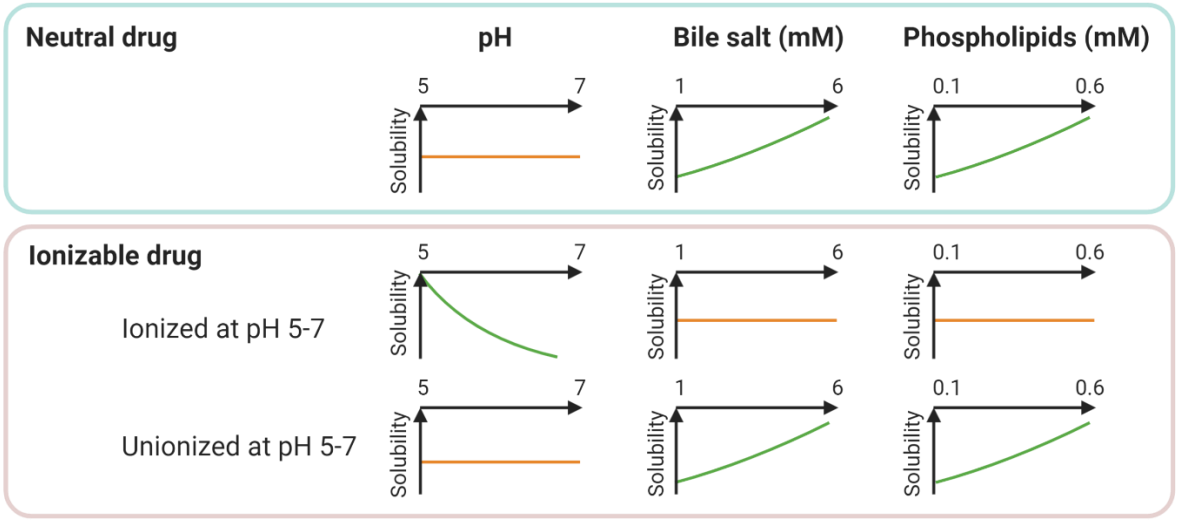

Figure 1.11: Influence of pH, bile salt and phospholipids on the solubility of neutral and ionizable (ionized and unionized in the specific pH interval) drugs.

Additionally, solubilization and permeation of PWSDs can largely vary according to the prandial state of luminal fluids (*i.e*. fasted or fed state). Therefore, the performance of such drugs should be tested in the presence of fasted and fed state intestinal fluids. Furthermore, if these drugs are being loaded into LBFs, the effect of gastric and intestinal digesting enzymes should also be taken into account when evaluating LBFs properties [104].

To answer the need for fluids mimicking human fasted and fed intestinal fluids (HIFs) for *in vitro* studies, different simulated intestinal fluids (SIFs) have been developed and some are now commercially available on the market (biorelevant.com) (Table 1.3) [105-107]. The main difference between fasted and fed state SIFs is the concentration of bile salts and phospholipids, as the fed state SIFs contain a higher amount of these components (Table 1.3). The presence of bile salts and phospholipids in the SIFs can provide the formation of colloidal structures corresponding to those of HIFs, thus enabling the study of drug solubilization, supersaturation and absorption in a biorelevant manner [108]. However, the simulation of fed state HIFs is still regarded as challenging because of the high inter and intraindividual variability of such conditions. Moreover, because of the lack of large lipid droplets and colloidal structures in the currently available FeSSIFs, it has been found that these SIFs are not able to predict *in vivo* drug solubilization to a high extent [34, 59, 107]. On the other hand, fasted state SIFs have shown to better mimic the properties and solubilizing effects of fasted HIFs, probably due to the lower media complexity and variability compared fed state fluids [32].

Table 1.3: Commercially available fasted and fed state simulated intestinal fluids (FaSSIF and FeSSIF, respectively; biorelevant.com) and their characteristics.

	FaSSIF – V1	**FaSSIF – V2**	**FeSSIF – V1**	**FeSSIF – V2**
pH	6.5	6.5	5.0	5.8
Buffer type	Phosphate	Maleic acid	Acetate	Maleic acid
Bile salts (mM)	3	3	15	10
Phospholipids (mM)	0.75	0.20	3.75	2.00
Monoglycerides (mM)	-	-	-	5
Free fatty acids (mM)	-	-	-	0.8

1.2.2 *In vitro* lipolysis models

Dissolution, supersaturation, precipitation and solubilization of orally administered drugs do not only depend on the composition of the GI fluids, but also on the digestion processes occurring in the gastric and intestinal compartment. In particular, lipid digestion (*i.e.* lipolysis) is especially important when evaluating absorption of PWSDs contained in LBFs. To anticipate the effect of lipid digestion on the performance of LBFs, an *in vitro* lipolysis model has been introduced by Zangenberg and colleagues in 2001 [109]. This *in vitro* model consists of a thermostated lipolysis vessel in which SIFs and LBF can be mixed, stirred and kept at a constant physiological temperature (Figure 1.12) [109, 110].

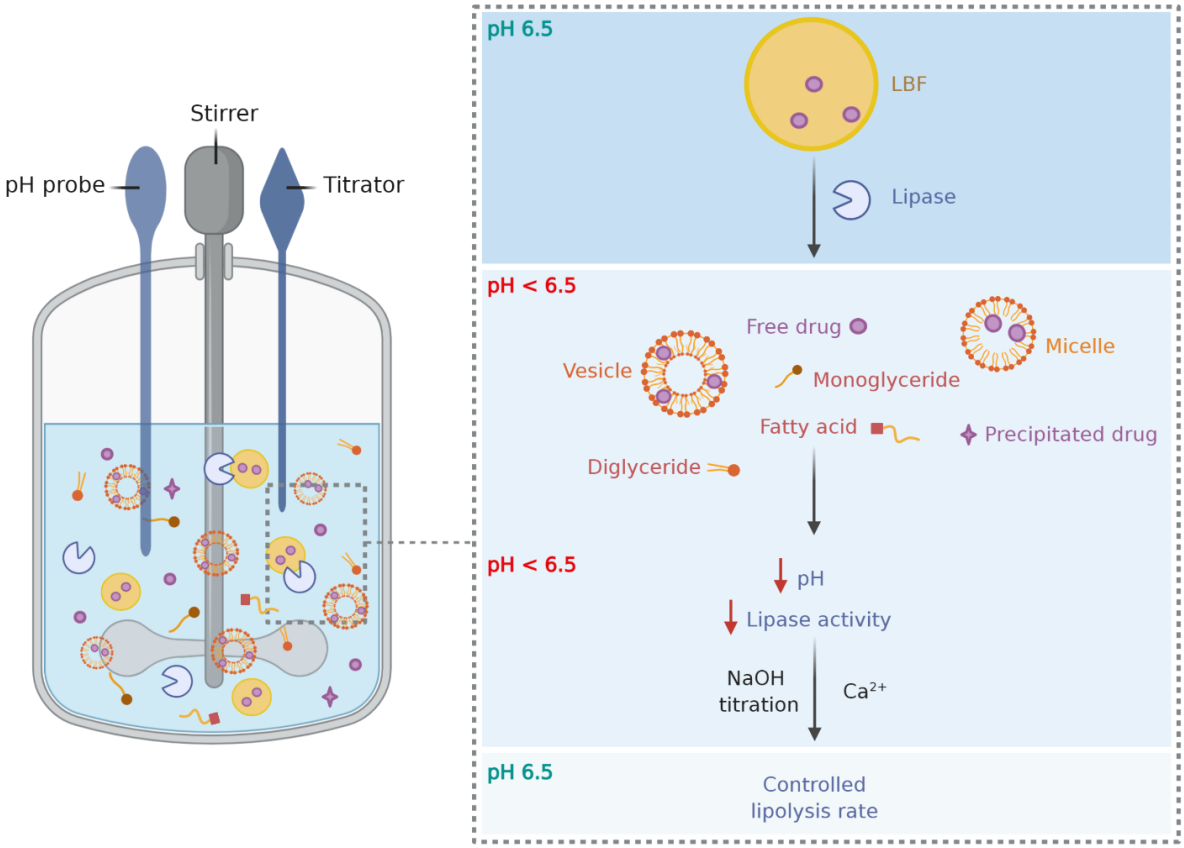

Figure 1.12: *In vitro* lipolysis apparatus, LBF, colloidal structures in the SIF and the effect of lipolysis on SIF pH, lipase activity and drug solubilization.

The lipolysis vessel is connected to a pH-stat apparatus, which is able to keep the pH in the SIFs constant. Upon addition of digesting enzymes (*i.e.* lipases) to the lipolysis medium, the digestible excipients of the LBF will be hydrolyzed, leading to a release of

free fatty acids. In return, the release of free fatty acids in the SIF will cause a drop in pH, which will be neutralized by the pH-stat apparatus by the addition of sodium hydroxide (NaOH) (Figure 1.12). Additionally, the lipolysis inhibition caused by the release of free fatty acids in the lipolysis medium will be prevented by the addition of calcium either continuously through the lipolysis experiment or as an initial bolus (Figure 1.12) [111, 112]. In general, *in vitro* lipolysis models can simulate both the digesting processes occurring in the stomach and in the small intestine, however most of them typically focus on intestinal lipolysis, as most of lipid digestion occurs in the small intestine [113].

For the specific simulation of intestinal lipolysis, porcine pancreatic extract is typically used, as it has proved to reliably substitute human pancreatic enzymes [114, 115], and its activity depends on the pH in the SIF (*e.g.* optimum lipase activity at pH 6.5-8) [116]. In order for the fatty acids resulting from the lipolysis process to be titrated by the addition of NaOH, they need to be ionized. Therefore, since the pKa of the long chain fatty acids in the SIF is approximately 6.5 [117], the targeted pH condition for *in vitro* lipolysis is usually 6.5 (Figure 1.12) [118]. Notably, the buffering capacity of the buffer used for preparation of the SIF needs to be low enough to ensure the pH drop following fatty acid liberation [119]. Therefore, this *in vitro* model allows the determination of the degree of LBF lipolysis thanks to the evaluation of the amount of NaOH used to neutralize the pH decrease. Moreover, the *in vitro* lipolysis model allows the determination of drug distribution upon LBF digestion [88, 90], as the drug can be found distributed in the lipolysis medium into three distinct phases: the oil phase consisting of undigested LBF, the aqueous phase containing colloidal structures formed upon lipolysis and the pellet phase containing precipitated drug, fatty acid calcium soaps and digestive enzymes (Figure 1.13) [118]. The physical separation of the three phases can be obtained by centrifugation, thus allowing the quantification of the drug in each phase. The fraction

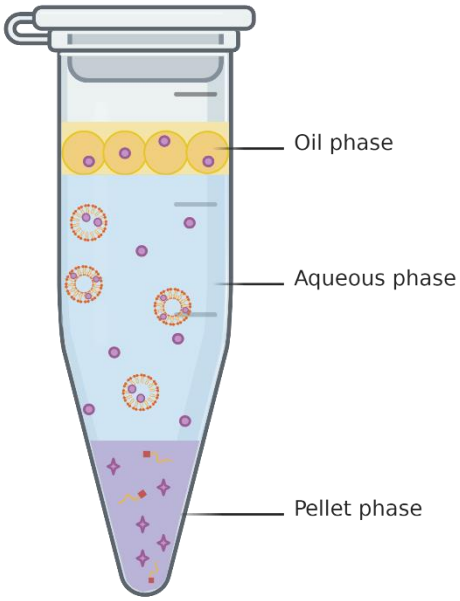

Figure 1.13: Phases formed upon centrifugation after *in vitro* lipolysis, together with drug distribution.

of the free drug found in the aqueous phase represents the amount of drug available for absorption, whereas the amount of drug found in the colloidal structures in the aqueous phase and the amount solubilized in the oil phase can serve as a drug-solubilizing reservoir [91]. One of the shortcomings of the *in vitro* lipolysis model is related to the fact that it is not able to easily separate the amount of drug free for absorption from the one solubilized by the colloidal structures in the aqueous phase, and this can lead to an overestimation of the amount of drug free to be absorbed [120]. Even though very useful for the determination of the degree of LBF lipolysis, the *in vitro* lipolysis model described above is characterized by one limitation: the dependence of the experiment from a costly pH-stat titration apparatus. Therefore, with the aim of developing a pH-stat titration independent *in vitro* lipolysis model, Mosgaard and colleagues introduced the high throughput lipolysis model (*i.e.* the HTP *in vitro* intestinal lipolysis model) [121, 122]. This model relies on the use of a high buffer capacity intestinal medium, able to directly neutralize the pH drop caused by the formation of free fatty acids upon LBF lipolysis. This *in vitro* model proved to be equivalent to the pH-stat lipolysis model, leading to higher time- and cost-effectiveness [122].

1.2.3 Cell free *in vitro* permeation tools

After its dissolution in the GI fluids, the drug will be available for absorption in its free form, and will reach the blood circulation after its permeation through the intestinal epithelium. Consequently, in the prediction of *in vivo* oral drug absorption the assessment of *in vitro* drug permeation is regarded as crucial. For this reason, several *in vitro* cell-free permeation tools have been developed over the past decades. These models can be utilized to evaluate passive drug transport, which is the absorption pathway shared by most of the currently commercially available drugs [123]. Cell-free permeation tools can be divided into two classes: biomimetic barriers (constructed by phospholipids) and non-biomimetic ones (composed of dialysis membranes) (Figure 1.14) [42]. Both classes enable the assessment of apparent drug permeability (P_{app}), which can be calculated after collection of acceptor samples utilizing the equation:

$$P_{app}\left(\frac{cm}{s}\right) = \frac{dQ}{dt} \cdot \frac{1}{A \cdot (C_d - C_a)}$$

where Q represents the cumulative amount of drug found in the acceptor compartment as a function of time t (nmol/s), A is the surface area of the *in vitro* barrier (cm^2), and C_d and C_a are the drug concentrations in the donor and acceptor compartment, respectively (nmol/mL) (see Figure 1.14 for acceptor and donor). Since the *in vitro* permeation experiment is usually carried out under sink conditions (*i.e.* the concentration in the acceptor compartment never exceeds 10% of the drug concentration in the donor compartment), C_a can be considered low enough to be neglected. Thus, the equation can be simplified to:

$$P_{app}\left(\frac{cm}{s}\right) = \frac{dQ}{dt} \cdot \frac{1}{A \cdot C_d}$$

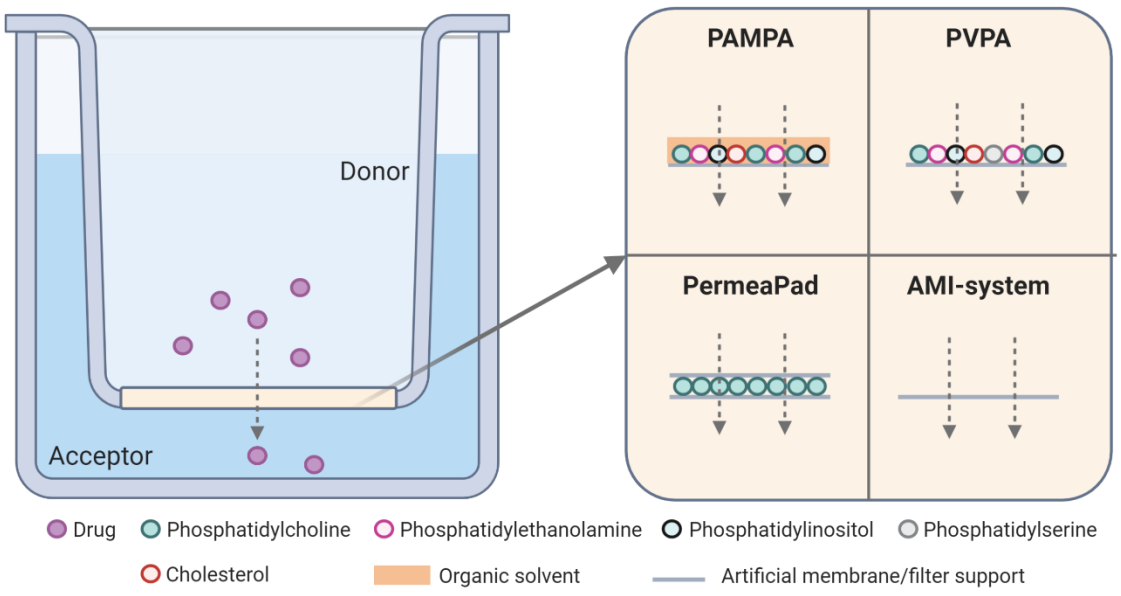

Figure 1.14: *In vitro* permeability setup, composed of a donor and acceptor compartment, separated by a permeation membrane. The main cell-free permeation membranes: PAMPA, PVPA, PermeaPad® and AMI-system.

One of the first *in vitro* permeation barriers developed is the PAMPA (Parallel Artificial Membrane Permeation Assay), which was introduced in 1998 by the Roche team [124]

(Figure 1.14). PAMPA barriers consist of a filter support soaked with an organic solvent in which phospholipids are dissolved, and allow the assessment of passive transcellular diffusion (Figure 1.4). The nature of the filter support, the composition of the phospholipids and the pH in the donor and acceptor compartment has been tailored to simulate different tissues in the human body, leading to different PAMPA barriers [125-132].

The PVPA (Phospholipid Vesicle-based Permeation Assay) was introduced shortly after the PAMPA at the University of Tromsø in 2006 [133]. The PVPA barriers consist of a filter support in which liposomes with different size distributions are immobilized (Figure 1.15). The construction of such biomimetic barriers is based on the fact that liposomes are able to simulate the phospholipid bilayers of cells present in different biological barriers [134-136]; therefore, by immobilizing liposomes in and on top of a membrane filter by centrifugation and freeze-thawing, it is possible to simulate the architecture of several human membranes by changing the composition of the liposomes [137-142]. In particular, liposomes with a diameter below the pore size of the membrane filter are deposited inside the filter, whereas liposomes with higher diameter are placed on top.

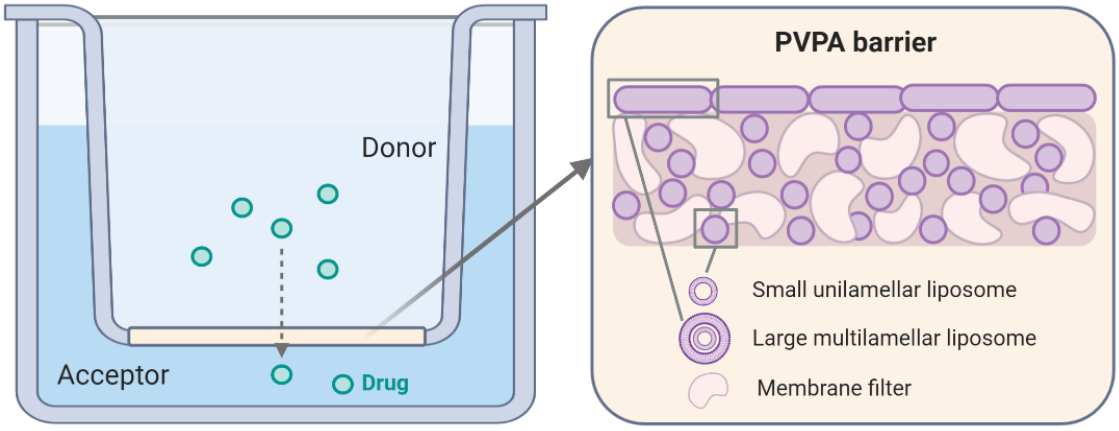

Figure 1.15: Structure of the PVPA barriers, composed of small unilamellar and large multilamellar liposomes immobilized in and on top of a membrane filter.

The first PVPA barriers (original PVPA) mainly consisted of phosphatidylcholine (80 % PC, egg phospholipids), a type of lipid present both in the intestinal epithelium and other

biological membranes [137]. To improve the simulation of the intestinal epithelium, the composition of the PVPA barriers was modified by combining phosphatidylcholine with phosphatidylethanolamine, phosphatidylserine, phosphatidylinositol and cholesterol, leading to the development of the $PVPA_{biomimetic}$. The functionality of the PVPA barriers is assessed by i) studying the permeability of a highly hydrophilic fluorescent marker (*i.e.* calcein) and by ii) measuring the electrical resistance across the barriers. Intact barriers lead on one hand to low calcein permeability, and on the other hand to high electrical resistance [133]. The functionality of the PVPA barriers has been assessed in the presence of different SIFs, GI relevant pH, co-solvents and tensides, highlighting the potential of such *in vitro* model for different applications [136-138, 143].

Another biomimetic barrier is the PermeaPad® developed at the University of Southern Denmark in 2015 [144]. This barrier consists of phospholipids placed between two support sheets, where the phospholipids are able to swell and form a tight phospholipid layer once in contact with water. These barriers have been developed to be mounted on a side-by-side diffusion cell, on a Franz cell diffusion apparatus or to be used in a 96-well plate [145-148].

Finally, the AMI (Artificial Membrane Insert)-system has recently been developed as a non-biomimetic barrier at KU Leuven in 2018 [149]. This system consists of a regenerated cellulose membrane mounted between two support rings, and has proven to be a useful and cost-effective tool for estimation of passive diffusion [149].

All the cell-free permeation membranes described above have been tested in their capability of distinguishing between drugs with different physicochemical properties, and have been used to evaluate the impact of several formulation strategies on drug permeation. Moreover, they proved to be predictive of the fraction of drug absorbed in humans and/or of drug permeation obtained from cell-based permeation membranes, such as the 'golden standard' Caco-2 (human colorectal adenocarcinoma cell line) permeation model [42, 124, 133, 144, 150]. Furthermore, the functionality of most of these models has been tested in the presence of GI relevant pH and SIFs to better simulate the GI physiology. Even though *in vitro* permeation barriers are considerably useful for the evaluation of drug permeation to predict oral drug absorption, they have

often been ignoring the impact that the intestinal mucus layer has on drug absorption. Mucus is in fact the first barrier to drug absorption, and should therefore be carefully considered when drug permeation is being assessed [80].

1.2.4 Mucus models and sources

The *in vivo* assessment of the net influence of mucus on drug transport and absorption is regarded as a complex process to study, since a distinction between the effect of mucus and the one of other physiological factor is problematic. For this reason, several mucus alternatives have been developed to be able to study the impact of mucus on drug absorption. *Ex vivo* mucus samples can be obtained both from animal and humans (Figure 1.16), but the reliability of such samples is relatively limited due to the animal-to-animal, human-to-animal and disease-state variability [22]. On the other hand, different mucus-producing *in vitro* cell models have been developed to study the impact that mucus has on drug permeation. One example of such models is the mucus-secreting Caco-2 HT29-MTX co-culture [151]. Even though very useful for the determination of drug permeation in the presence of mucus, the production of these cell-based mucus-secreting models can be costly both in terms of time and resources [152]. Therefore, because of the limitations connected to *ex vivo* mucus samples and mucus-producing cell cultures, purified mucins from bovine submaxillary gland or from porcine stomach have been largely used for mucus-drug/formulation interaction and permeation studies (Figure 1.16) [80, 153-159]. Mucins dispersions can be added on top of cell-based [62] or artificial barriers [90] to mimic the *in vivo* environment of intestinal mucosa and to assess the impact of the

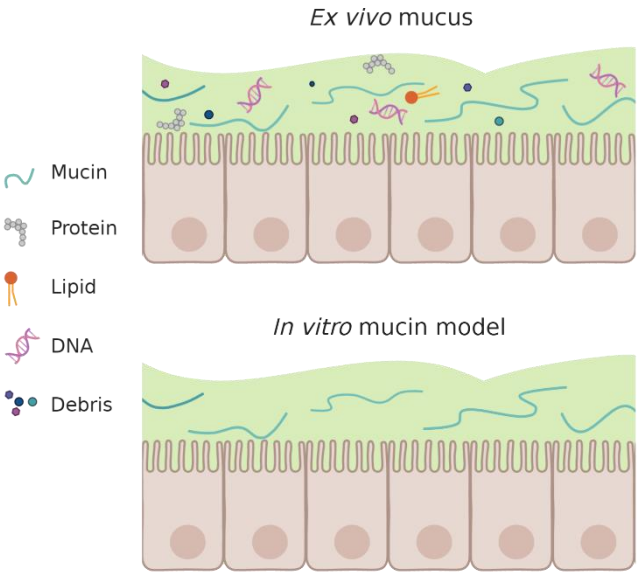

Figure 1.16: Composition of *ex vivo* mucus and *in vitro* mucin model.

presence of the mucus layer on drug permeability. However, the low cross-linking capacity of purified mucins can lead to an under-simulation of the mesh-like structure of mucus, thus not being able to completely encompass the viscoelastic characteristics of GI mucus [27, 160, 161]. Therefore, because of the need for a biosimilar and easily accessible mucus source, the biosimilar mucus model was introduced by Boegh and colleagues [21, 160, 162]. This model was able to closely mimic the composition and rheology of *in vivo* mucus thanks to the combination of mucins with other components such as bovine serum albumin, cholesterol, phospholipids and gel-forming polymers, and was found to be a barrier especially to the permeation of lipophilic molecules [21, 160]. Even though the biosimilar mucus model has been largely utilized in combination with Caco-2 cell lines to study drug permeation [21, 160, 162], its use in combination with cell-free *in vitro* permeation has not been explored in detail, pointing out the lack of a completely artificial GI mucosa-mimicking model.

1.2.5 Combined lipolysis – permeation *in vitro* models

The potential of *in vitro* lipolysis models to predict *in vivo* performance of LBFs has been evaluated by relating the amount of drug found in the aqueous phase *in vitro* with the outputs of *in vivo* pharmacokinetics studies (*e.g.* maximum plasma concentration, area under the curve (AUC)). However, in a large number of cases, a lack of a rank order *in vivo-in vitro* correlation (IVIVC) was observed [163-170], pointing at the inability of the *in vitro* lipolysis model to predict *in vivo* drug absorption. The lack of IVIVC has been linked to the false assumption that high *in vitro* drug solubilization is associated to high drug bioavailability [90]. In fact, the drug found in the aqueous phase during *in vitro* lipolysis exists in an equilibrium between i) its free fraction (*i.e.* amount available for absorption) and ii) the fraction solubilized by the colloidal structures formed upon lipolysis (Figure 1.13), and the *in vitro* lipolysis setup is not able to distinguish between these two. As a result of this, it is not possible to determine the amount of drug freely available for absorption [90]. Additionally, the absence of an absorptive sink can lead to an incorrect estimation of drug solubilization, dissolution and precipitation; in fact, in the *in vitro*

lipolysis model the amount of drug available for absorption is not able to escape the digesting environment *via* a permeation barrier, leading to higher drug supersaturation and precipitation *in vitro* compared to the *in vivo* scenario [171].

To overcome the shortcomings associated with the *in vitro* lipolysis model, this *in vitro* method has been associated both with *ex vivo, in situ* and *in vitro* cell-based and cell-free permeation barriers [73, 90, 120, 146, 171-176]. The first combined *in vitro* lipolysis-permeation models were designed so that, after lipolysis, the digested contents could be transferred to a separate permeation setup, whereas more recent combined models have been able to provide the simultaneous assessment of lipolysis and permeation (Figure 1.17). Overall, the *in vitro* lipolysis-permeation combination led to a better prediction of *in vivo* drug absorption [73, 90, 120, 146, 171, 174, 175]. In particular, the use of cell-free barriers such as the ones described in Section 1.2.3 has been found to be particularly beneficial from a time and cost perspective [73, 90, 146]. The improved IVIVC obtained with the use of such combined models highlighted the importance of the simultaneous evaluation of LBFs digestion, drug dissolution and drug permeation.

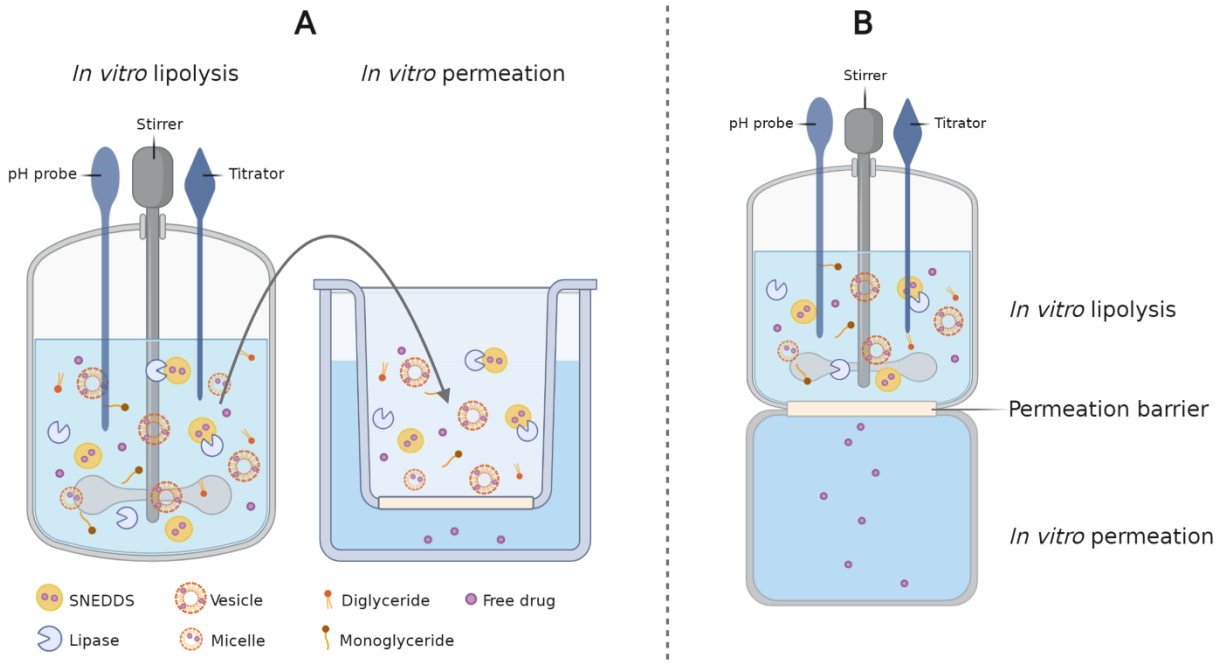

Figure 1.17: A) Combined and B) simultaneous *in vitro* lipolysis-permeation models.

Even though the mentioned combined models provided essential insight into the mechanisms driving drug absorption, for the most part they lacked the presence of a

mucus layer lining the permeation barrier, especially in the case of cell-free barriers. Therefore, because of the impact that mucus has on drug dissolution and permeation, and because of the convenience of cell-free permeation membranes, it would be crucial to include its presence in cell-free combined *in vitro* lipolysis-permeation models.

2 Aims of the thesis

The overall aim of this work was to develop a mucus-comprising *in vitro* permeation model able to mimic the environment of the intestinal mucosa to study drug permeation and predict *in vivo* drug absorption.

To achieve this, the specific aims have been the following:

- Inclusion of an artificial mucus layer on top of the PVPA *in vitro* permeability barriers (Paper I).

- Validation of the mucus-PVPA barriers in terms of their integrity and ability to discriminate between the permeabilities of drugs with different physicochemical properties and between different liposomal formulations (Paper I).

- Evaluation of the impact of intestinally relevant pH on drug permeability using the mucus-PVPA barriers (Paper II).

- Determination of the functionality of the mucus-PVPA barriers in the presence of fasted and fed state simulated intestinal fluids (Paper II).

- Combination of the mucus-PVPA permeation barriers with an *in vitro* lipolysis model to predict *in vivo* drug absorption from lipid-based formulations (Paper III).

- Development of a simultaneous lipolysis-permeation *in vitro* model able to correlate *in vitro* drug permeation with *in vivo* drug absorption from lipid-based formulations (Paper IV).

3 Summary of papers

3.1 Paper I

The aim of Paper I was to include an artificial mucus layer on top of the PVPA *in vitro* permeability barriers to develop a mucus-comprising model mimicking the environment of the intestinal mucosa able to distinguish between drugs with different physicochemical properties and between different liposomal formulations.

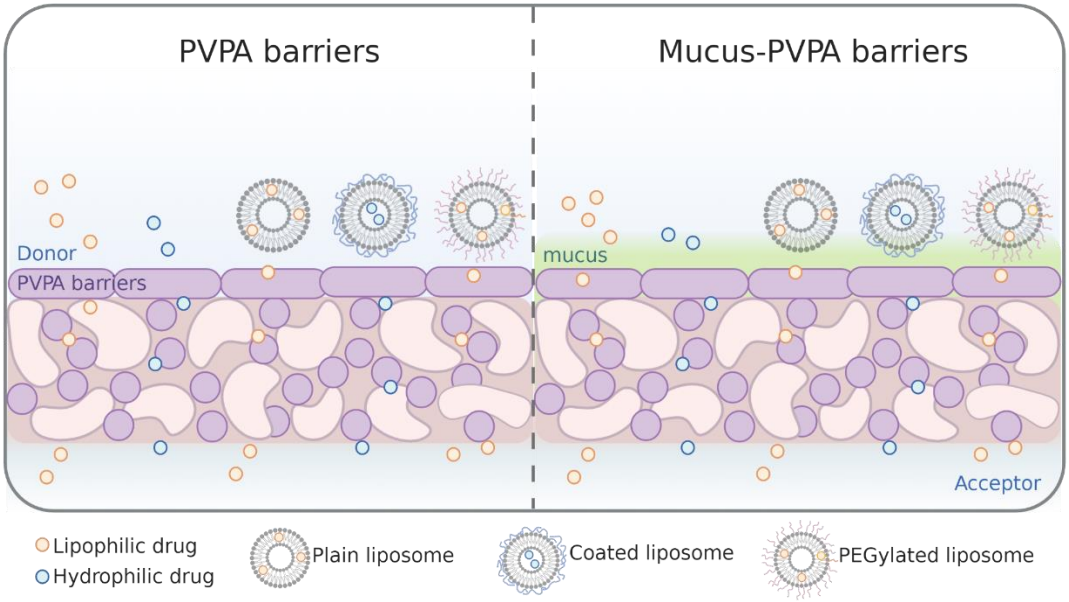

Figure 3.1: Overview of the experimental setup for Paper I

A buffered dispersion of mucin type III from porcine stomach was used to simulate the mucus layer, and the integrity of the PVPA barriers was tested in the presence of mucin dispersions with different concentrations (10, 20 and 40 mg/mL) by evaluating the permeability of a highly hydrophilic fluorescent marker (*i.e.* calcein) and the electrical resistance across the barriers at the end of the permeation experiment. Both calcein P_{app} and electrical resistance did not vary in the presence and absence of the tested mucin dispersions, suggesting that the barriers maintained their integrity in such conditions. The maintained structural functionality of the barriers was also confirmed by confocal laser

scanning microscopy (CLSM) and by the assessment of lipids loss in the presence and absence of mucin dispersions.

The viscosity assessment of the different mucin dispersions revealed that viscosity increased with increasing mucin concentration, pointing out at the Newtonian character of the analyzed dispersions. Because of the similarity in terms of viscosity and impact on barrier integrity for all the prepared mucin dispersions, mucin 10 mg/mL was chosen for further permeation studies. Moreover, the choice of the thickness of the mucin dispersion applied on top of the barriers was made by comparing the permeability of naproxen in the presence of different mucin dispersion volumes (mucin 10 mg/mL). 50 µL of mucin dispersion was chosen as the standard volume to be used in further permeation studies to allow a complete and uniform coverage of the barriers since drug permeation did not vary in the presence of different mucin volumes (20-50 µL).

The permeation of five model compounds was tested in the presence and absence of mucin 10 mg/mL to study the impact of mucin on drug permeation and to evaluate if the barriers were able to discriminate between drugs with different physicochemical properties. The P_{app} of the analyzed drugs confirmed the ability of both the PVPA and the mucus-PVPA barriers to distinguish drugs with different characteristics, and the presence of mucin on top of the barriers led to a decrease in drug permeability.

The permeation of three compounds from solution, plain, chitosan-coated and PEGylated liposomes was studied to evaluate if the mucus-PVPA barriers were able to differentiate between different formulations. The obtained results showed that formulations with positive zeta potential (*i.e.* chitosan-coated liposomes) led to lower drug permeation compared to negatively charged ones, suggesting that the mucus-PVPA model had the potential to discriminate mucopenetrating from mucoadhesive liposomes.

3.2 Paper II

The aim of Paper II was to implement the donor compartment of the mucus-PVPA barriers with intestinally relevant pH conditions and fed/fasted state SIFs to provide a drug permeation tool able to mirror the human intestinal environment.

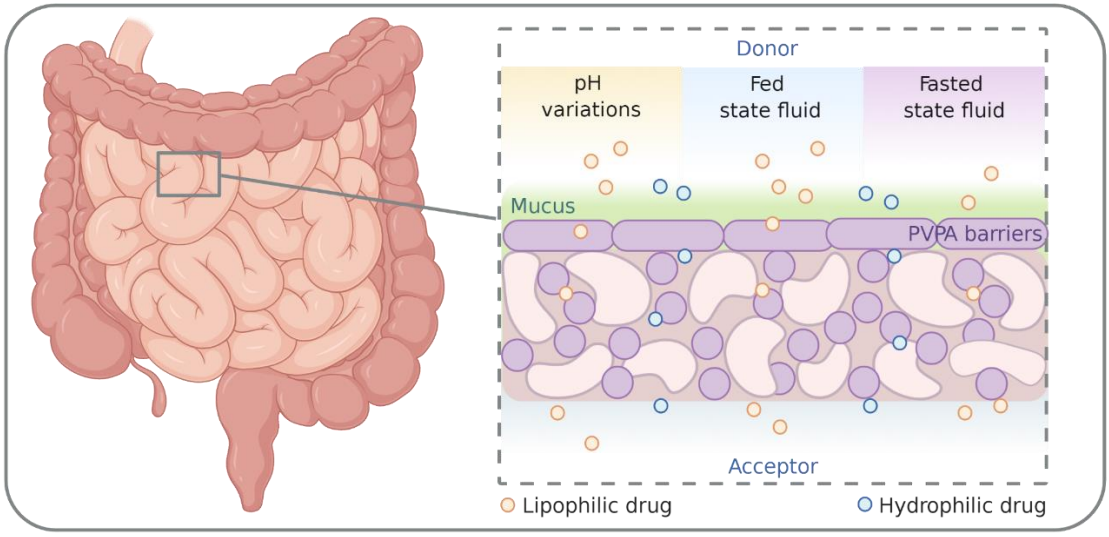

Figure 3.2: Overview of the experimental setup for Paper II

The integrity of the mucus-PVPA barriers was evaluated by the assessment of calcein (highly hydrophilic marker) P_{app} and of the electrical resistance across the barriers in the presence of different pH conditions (*i.e.* pH 5.5, 6.2 and 7.4) and of commercially available fasted and fed state SIFs (namely, FaSSIF and FeSSIF version V1 and V2). The results obtained showed that the barriers were stable in all the tested pH conditions and in the presence of fed state SIFs (FeSSIF V1 and V2), whereas their integrity was impaired in the presence of fasted state SIFs (FaSSIF V1 and V2). These findings were confirmed by the analysis of lipids lost from the PVPA barriers in the presence of the different SIFs. The permeability of a more lipophilic drug in the presence of FaSSIFs and FeSSIFs was also tested. Even though in the presence of the fasted media the electrical resistance suggested barrier impairment, the permeability of the chosen compound did not significantly increase compared to the fed ones. Moreover, for the lipophilic compound,

the presence of the mucin dispersion on top of the PVPA barriers led to a decrease in permeability, which was not observed in the case of calcein.

The rheology of the mucin dispersion used on top of the PVPA barriers (*i.e.* mucin 10 mg/mL) was tested at pH 5.5, 6.2 and 7.4, and the results displayed a non-Newtonian (shear-thinning) behavior for the mucin dispersion at pH 5.5 and a Newtonian character at pH 6.2 and 7.4.

Five model compounds were chosen to cover both acidic and basic features in order to test their pH-dependent solubility and permeability. The solubility of acidic compounds was found to be higher with a pH increase due to a higher degree of ionization at pH higher of their isoelectric point. Conversely, the permeability of these compounds decreased with a pH increase, whereas the P_{app} of a basic compound increased with the pH. The described pH-dependent trend was especially visible in the absence of the mucin dispersion on top of the PVPA barriers.

3.3 Paper III

The aim of Paper III was to couple the mucus-PVPA barriers, used to determine drug permeation, with *in vitro* intestinal lipolysis. This was done to determine whether drug solubilization upon lipolysis of three fenofibrate-containing SNEDDSs would impact drug permeation, and how drug solubilization and permeation would correlate with *in vivo* drug absorption data in rats.

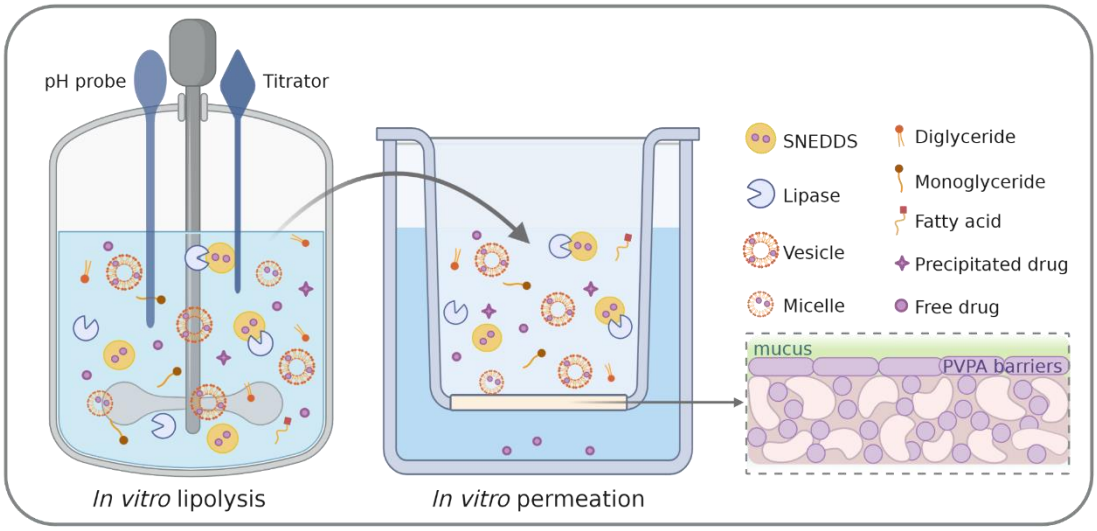

Figure 3.3: Overview of the experimental setup for Paper III

In this study, biosimilar mucus was utilized as the mucus-simulating source instead of mucin 10 mg/mL. This choice was made to account for most of the components found in intestinal mucus, not only mucins. Firstly, the functionality of the PVPA barriers was tested in the presence of biosimilar mucus, SNEDDS, digesting enzymes (*i.e.* pancreatin from porcine pancreas) and combinations of the three. The results obtained showed that the PVPA barriers were particularly stable in the presence of biosimilar mucus when SNEDDSs were placed on top of the barriers, thus this layer was present for all further permeation experiments.

SNEDDSs digestion was carried out using the *in vitro* intestinal lipolysis model, and the ability of three different fenofibrate-loaded SNEDDSs of solubilizing fenofibrate during *in*

vitro lipolysis was evaluated. The data obtained demonstrated that the SNEDDSs wherein the drug was originally present in solubilized form in the formulation (both below and above its equilibrium solubility in the SNEDDS) led to high drug solubilization upon *in vitro* lipolysis, while the SNEDDS where the drug was originally present in suspension caused lower drug solubilization. The drug solubilization results obtained by utilizing *in vitro* lipolysis failed to correlate with *in vivo* absorption data (*i.e.* AUC) published in the literature for the same SNEDDSs.

The permeation of free fenofibrate across the mucus-PVPA barriers before and after *in vitro* lipolysis of the three different SNEDDSs was studied. The concentration of the drug in the donor compartment of the mucus-PVPA barriers was the same for all three formulations to enable the comparison between drug permeation promoted by the three different SNEDDSs. The results obtained highlighted that drug permeation was highest in the case of the SNEDDS where fenofibrate was solubilized in the formulation above its equilibrium solubility. This permeation resulted higher than the one connected to the SNEDDS where the drug was solubilized below its equilibrium solubility. The lowest drug permeation was linked to the SNEDDS where the drug was present both solubilized and also in suspension.

The AUCs resulting from the mass transfer of free fenofibrate across the mucus-PVPA barriers over time for the three SNEDDSs were compared to *in vivo* AUCs obtained from the plasma drug concentration curve in rats found in the literature for the same fenofibrate-loaded SNEDDSs. The Level D correlation between the *in vitro* results obtained in this study and the *in vivo* data was excellent ($R^2 > 0.9$), demonstrating the ability of the combined *in vitro* lipolysis—mucus-PVPA permeation model to predict *in vivo* drug absorption for the chosen formulations.

3.4 Paper IV

The aim of Paper IV was to add the high throughput (HTP) *in vitro* lipolysis model (*i.e.* a pH-stat-independent lipolysis model) on top of the mucus-PVPA barriers to allow the construction of a system where *in vitro* lipolysis of fenofibrate-loaded SNEDDSs and fenofibrate permeation could take place simultaneously.

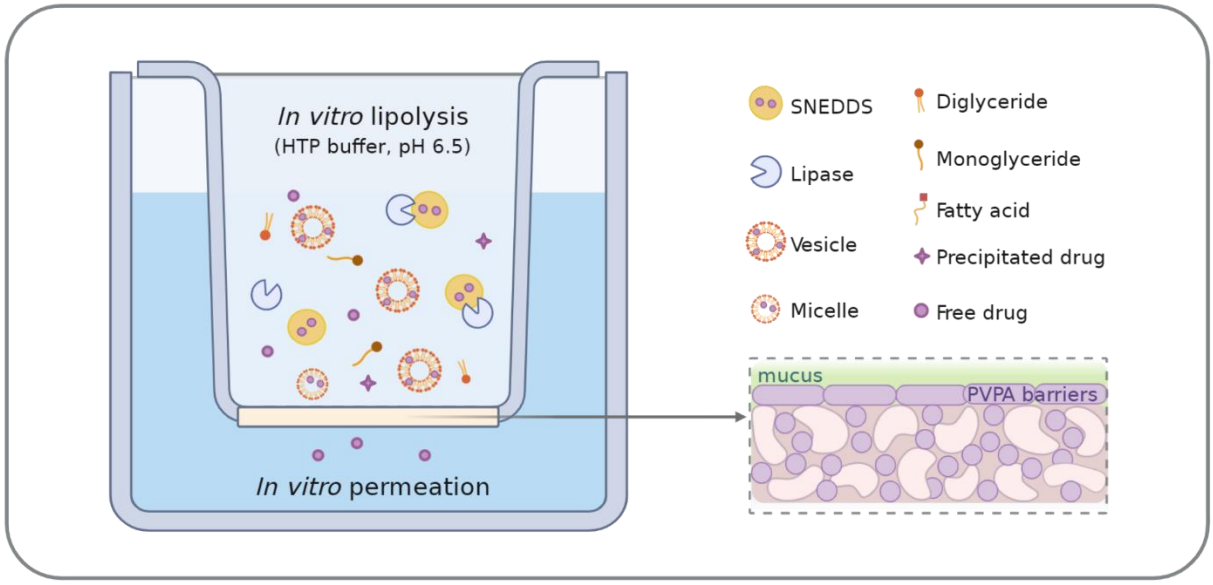

Figure 3.4: Overview of the experimental setup for Paper IV

The same three SNEDDSs evaluated in Paper III were studied to compare the results obtained by the use of the combined *in vitro* lipolysis—mucus-PVPA permeation model with the ones obtained with the developed simultaneous model. The high buffer capacity of the HTP intestinal medium allowed to keep the pH constant during *in vitro* lipolysis of SNEDDSs, ensuring the optimal pH condition for the activity of the lipase used in the study. The distribution of fenofibrate in the aqueous and pellet phase formed upon *in vitro* lipolysis was in accordance with the data presented in Paper III and with already published data regarding the same SNEDDSs. This evidence highlighted the ability of the developed model to produce results in line with the conventional *in vitro* lipolysis model, while being independent from a pH-stat apparatus. As previously shown in Paper III, the

fenofibrate solubilization results collected in this study failed to correlate with *in vivo* absorption data (*i.e.* AUC) published in the literature for the same SNEDDSs.

The permeation of fenofibrate was studied both in the absence and presence of simultaneous *in vitro* lipolysis, and in both cases the SNEDDS that led to the highest drug permeation potential was the one where fenofibrate was solubilized in the formulation above its equilibrium solubility. However, a difference in formulation ranking regarding fenofibrate permeation was found when comparing the remaining two SNEDDSs in the absence and presence of lipolysis. In fact, when lipolysis was not occurring, the SNEDDS where the drug was present suspended at a supersaturated concentration led to higher drug permeation compared to SNEDDS where the drug was solubilized below its equilibrium solubility. On the contrary, upon lipolysis, the mentioned two SNEDDSs led to the same drug permeation. The change in SNEDDSs ranking found in this study was also observed in an *in vivo* study where fenofibrate absorption from the same SNEDDSs was studied both when lipolysis was occurring and when this process was inhibited by the addition of the lipase inhibitor orlistat.

The Level D correlation between the AUCs resulting from the mass transfer of free fenofibrate across the mucus-PVPA barriers over time for the three SNEDDSs and the *in vivo* AUCs obtained from the plasma drug concentration curve in rats found in the literature for the same SNEDDSs resulted to be excellent ($R^2 > 0.98$). Moreover, the *in vitro* results correctly predicted the change in formulations ranking taking place *in vivo* when lipolysis was occurring compared to when it was inhibited by the presence of orlistat.

Overall, this study proves the suitability of the developed model in predicting drug absorption *in vivo* for the chosen fenofibrate-loaded SNEDDSs. Moreover, the model demonstrates to be especially relevant because of its ability to simultaneously assess *in vitro* lipolysis and permeation and because of its independence from a pH-stat apparatus.

4 Results and discussion

The need for an *in vitro* model able to predict oral drug absorption and simulate the intestinal environment has become ever so evident in the past decades [42, 102]. To answer the above-mentioned need, this thesis focused on the development of an *in vitro* model that could be employed to study drug permeation in the presence of an intestinally relevant environment. The construction of the model was stepwise. Firstly, the already established PVPA barriers were implemented with the addition of a mucus layer to simulate the intestinal mucosa, leading to the development of the mucus-PVPA barriers (Paper I). Secondly, intestinally relevant pH conditions and simulated intestinal fluids were added to the mucus-PVPA model to account for their impact on drug absorption (Paper II). Further, the assessment of drug permeation was coupled with *in vitro* lipolysis to produce a combined model capable of mimicking this intestinal process and to unravel the impact of lipid digestion on the permeation of drugs contained in LBFs (Paper III). Finally, the combined model was modified to permit *in vitro* permeation and lipolysis to occur simultaneously (Paper IV).

4.1 From a naked to a mucus-covered *in vitro* permeation barrier – simulation of the intestinal mucosa (Paper I-II)

To simulate the mucus layer covering the intestinal epithelium, Paper I and II focused on the preparation and characterization of a mucin dispersion which was utilized to evaluate the impact of this mucus component on drug permeation.

4.1.1 Simulation of the intestinal mucus

The mucin dispersions employed in Paper I and II to simulate the intestinal mucus were composed of mucin from porcine stomach type III in a buffered solution. The rationale

for the exclusion of the other mucus components (*i.e.* proteins, lipids, DNA and cellular debris) from this mucus model was that the focus of the two studies was to specifically evaluate the impact of mucin on drug permeation. The sole inclusion of mucin is particularly relevant as this component is known to be playing a key role in the barrier function of the mucus layer, contributing to its the gel-like properties [10, 17-19] and preventing the diffusion of exogenous particles thanks to its size and interaction filtering properties [15, 24]. The choice of mucin from porcine stomach type III was made because this commercially available product proved to resemble human mucins [25], and its preparation avoids the degradation that typically occurs in the case of mucin from porcine stomach type II, which can alter the gel-forming properties of this glycoprotein [27]. As both mucin concentration and mucus pH vary along the intestine [102], the viscosity of different mucin dispersions was tested to characterize the mucus model prior to its addition on top of the PVPA barriers. In particular, the viscosity of mucin 10 mg/mL pH 5.5/6.2/7.4, mucin 20 mg/mL pH 7.4 and mucin 40 mg/mL pH 7.4 was studied in Paper I and II, and it is depicted in Figure 4.1.

As can be observed in Figure 4.1, an increase in mucin concentration corresponded to an increase in viscosity, which is to be expected due to the higher gel-forming potential at higher mucin concentration [157, 177]. Moreover, the mucin dispersions at pH 7.4 and 6.2 exhibited a rather Newtonian character (*i.e.* constant viscosity at increasing shear rates), whereas the mucin dispersion at pH 5.5 displayed a non-Newtonian nature (*i.e.* shear-thinning behavior), which better corresponds to the shear-thinning behavior of the mucus found *in vivo* [160, 178]. This pH-dependent shift in mucin rheology and increase in viscosity is thought to be due to a sol-gel transition occurring when the pH goes from a neutral to a more acidic one. In particular, at neutral pH the ionization of the acidic groups in the mucin glycosylated side chains (*e.g.* sialic acid) is able to produce electrostatic interactions, which lead to the formation of a random coil. Instead, when the pH decreases to a more acidic one, mucins exhibit an extended rod-like conformation due to the unfolding and exposure of their protein core (*i.e.* hydrophobic region), which leads to non-covalent crosslinking within the mucin structure and provides stabilization of water molecules and formation of a viscous gel [16, 27].

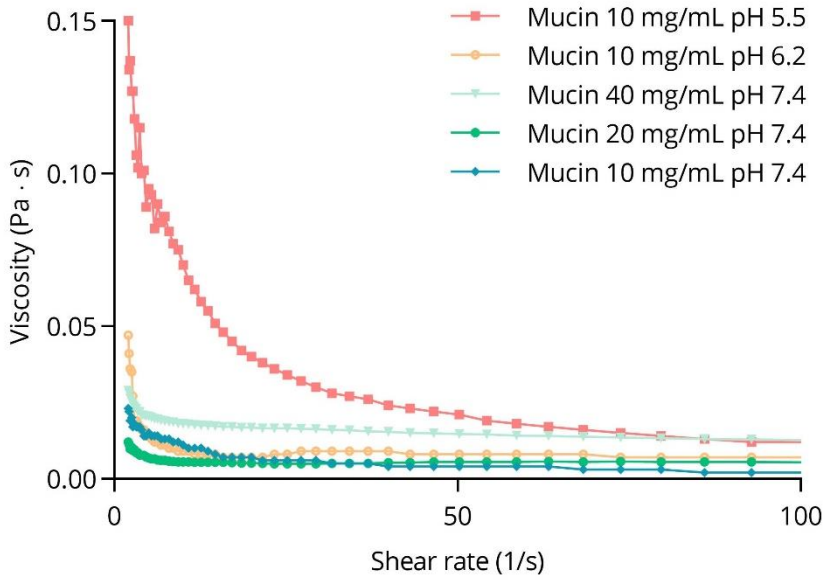

Figure 4.1: Viscosity of mucin dispersions at different mucin concentration (10, 20 and 40 mg/mL) and pH (5.5, 6.2 and 7.4).

Moreover, the resemblance of mucin from porcine stomach type III to human mucus has been confirmed in the study by Teubl and colleagues [69], where it was found that in both cases the gel structure resulted into a network of parallel and crossing mucins. Because of the resemblance between human mucus and the mucin dispersion utilized in Paper I and II, this mucus model was used on top of the PVPA barriers to simulate the environment of the intestinal mucosa.

4.1.2 PVPA barrier integrity in the presence of mucus

Prior to the assessment of drug permeation, the integrity of the PVPA barriers was evaluated in the presence of the mucin dispersions mentioned in Section 4.1.1. The integrity of the PVPA barriers is typically evaluated by studying the permeability (P_{app}) of the highly hydrophilic fluorescent marker calcein (CAL), together with the measurement of the electrical resistance across the barriers at the end of the permeation experiment [133]. Barriers that lead to CAL P_{app} below $0.06 \cdot 10^{-6}$ cm/s and to electrical resistance

above 290 Ω · cm^2 are considered intact (Figure 4.2, dotted lines) [133-136]. An increase in CAL P_{app} above the mentioned limit is thought to be associated to the formation of excess aqueous pores in the PVPA barriers, causing higher permeation for hydrophilic molecules compared to intact barriers.

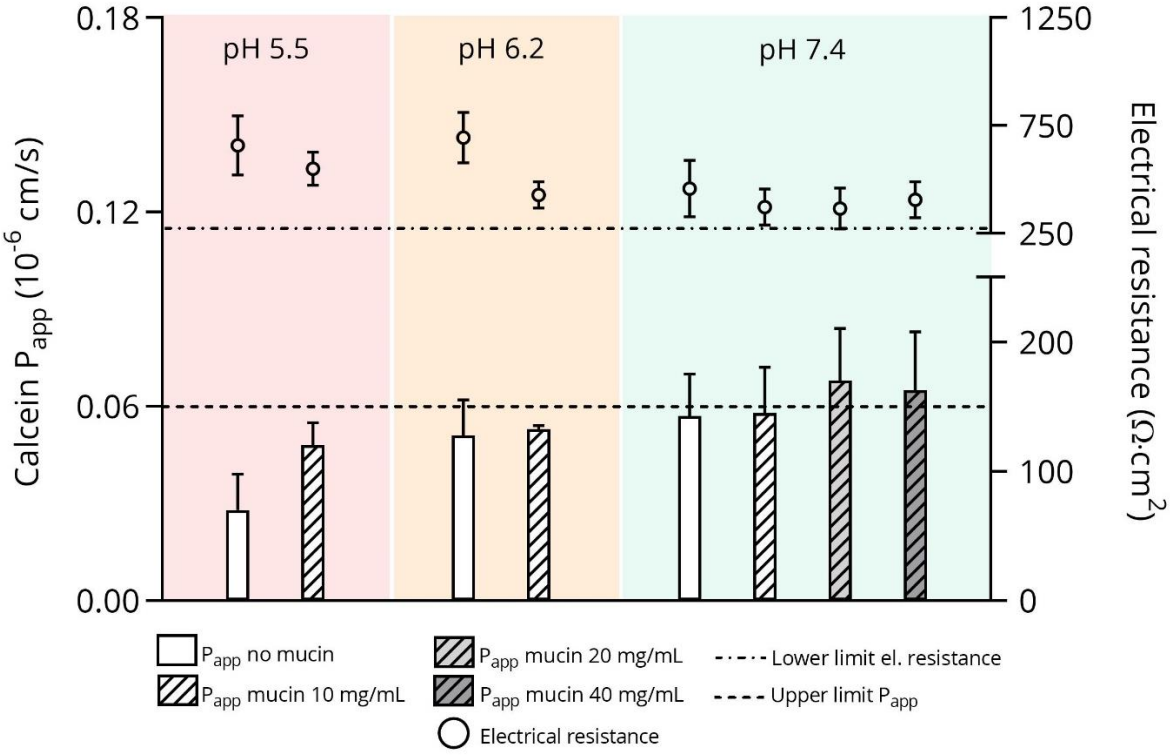

Figure 4.2: Calcein P_{app} and electrical resistance across the PVPA barriers in the presence and absence of mucin (10, 20 and 40 mg/mL) at pH 5.5, 6.2 and 7.4. The results are indicated as mean ± SD (n = 6).

The results collected in Paper I and II regarding CAL P_{app} and electrical resistance across the barriers prove that the PVPA barriers were able to maintain their integrity in the presence of different i) pH conditions (*i.e.* pH 5.5, 6.2 and 7.4) and ii) mucin dispersions (mucin 10, 20, 40 mg/mL) (Figure 4.2). The quantification of phospholipids lost by the PVPA barriers in the presence and absence of the different mucin dispersions also suggested that the barriers were intact in all tested conditions. Moreover, confocal laser scanning microscopy (CLSM) analyses showed that no significant aqueous channels were formed in the presence of the utilized mucin dispersions. These findings are of crucial importance,

as they confirm the possibility of safely utilizing the model for the screening of drug permeability in the mentioned intestinally relevant conditions. Furthermore, the mentioned results suggest that it is possible to compare the results obtained in the presence and absence of the mucus model. On another note, the presence of the mucin dispersions on top of the PVPA barriers did not cause significant changes in CAL P_{app} compared to their absence, suggesting that CAL was able to freely diffuse through this layer (Figure 4.2). These findings could be related to the fact that hydrophilic compounds, such as CAL, usually exhibit low affinity for mucus and they are able to reach the permeation membrane without being highly affected by its presence [160].

4.1.3 Selection of the mucus model used for permeability studies

The permeability of compounds with different physicochemical properties (*i.e.* atenolol ATN, ibuprofen IBP, indomethacin IND and naproxen NPR) was studied in the presence of different mucin dispersions (*i.e.* mucin 10, 20 and 40 mg/mL, pH 7.4) to determine if a difference in drug P_{app} would be observed at varying mucin concentrations, and to define which mucin dispersion would be used in further studies.

As can be observed in Figure 4.3, a consistent trend in drug P_{app} with increasing mucin concentrations could not be observed. In particular, even though a significant decrease in P_{app} could be observed for all the tested drugs in the presence of the mucin dispersions, the permeability decrease was not proportional to the mucin concentration. Therefore, the increase in mucin viscosity with increasing mucin concentration described in Section 4.1.1 did not seem to significantly impact drug permeation. Because of this, and because the aim of the study (Paper I) was to identify a simple mucus model, mucin 10 mg/mL was chosen as the preferred dispersion for further permeation experiments. When designing the preferred mucus model to use on top of permeation barriers, it is important to cautiously consider not only its composition (*e.g.* components and their concentration), but also the volume to utilize. To this regard, it has been reported that the mucus layer in the intestine and colon ranges from 50 to 450 μm [66] and that this can vary according to the prandial state [21]. Therefore, different mucin 10 mg/mL volumes (20, 22, 25 and 50

µL) were placed on top of the PVPA barriers, leading to various thicknesses (580-1450 µm, right Y-axis Figure 4.3), to assess their impact on the permeability of NPR. The chosen volumes had to both permit the complete coverage of the PVPA barriers and the simulation of *in vivo* mucus thickness. As can be observed in Figure 4.3a, NPR P_{app} significantly decreased in the presence of all the different mucus volumes compared to its absence; however, a change in permeability was not observed between the tested volumes. Due to the absence of statistical difference in NPR P_{app} in the presence of different mucin dispersion volumes, 50 µL was chosen as the preferred volume for further studies even though it led to high thickness, as it allows a homogeneous coverage of the permeation barriers.

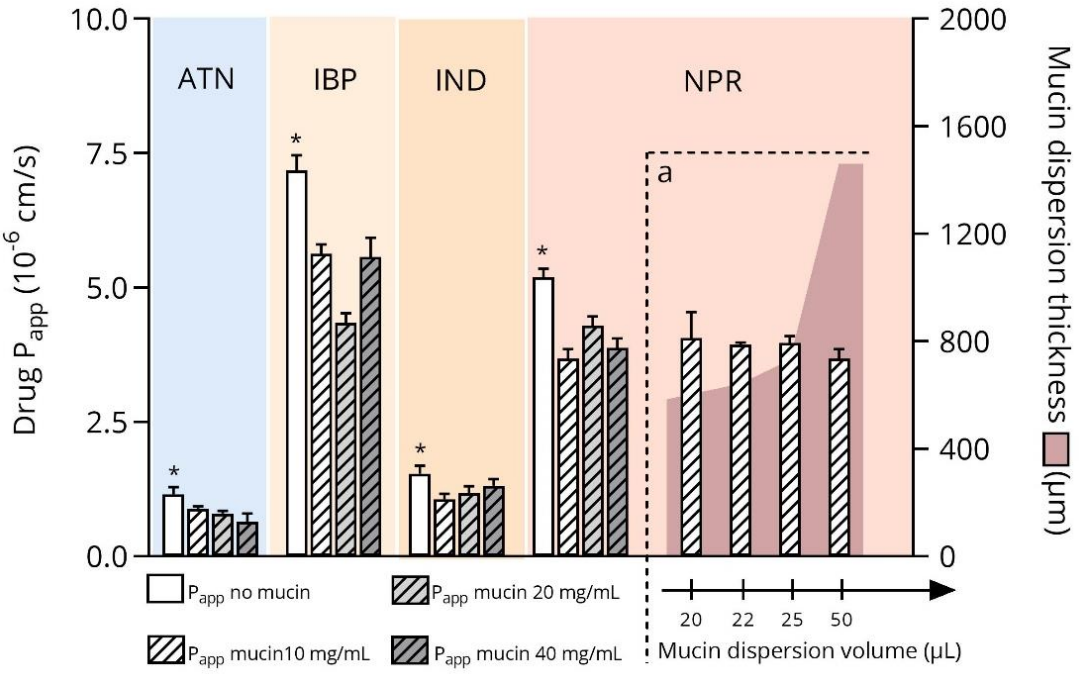

Figure 4.3: P_{app} of ATN, IBP, IND and NPR in the presence and absence of different mucin dispersions (10, 20 and 40 mL), and P_{app} of NPR in the presence of different volumes of mucin 10 mg/mL on top of the PVPA barriers (Figure 4.3a). The results are indicated as mean ± SD (n = 3). * Statistically significant difference ($p < 0.05$) in drug P_{app} between the absence and presence of mucin dispersions.

4.2 Use of the mucus-PVPA barriers to distinguish between different drugs and formulations (Paper I and II)

Once the mucus-PVPA model was established (Section 4.1.1-4.1.3), it was used to determine how the presence of the hydrophilic mucus layer would affect the permeability of drugs with different physicochemical characteristics (Table 4.1) both from solution and from different liposomal formulations.

Table 4.1: Physicochemical characteristics of the compounds studied in Paper I and II.

Compound	MW (g/mol)	pKa	Log P	Log $D_{7.4}$[d]	BCS class
CAL	622.55	1.8/9.2[a]	-1.71[b]	-	-
ATN	266.34	9.54[b]	0.16[d]	-1.03	III
IBP	206.29	4.45[b]	3.97[d]	0.81	II
IND	357.80	4.42[c]	4.27[d]	0.77	II
MTP	267.36	9.56[b]	1.88[d]	0.16	I
MTR	171.16	2.62[e]	-0.02[d]	0.14	I
NPR	230.26	4.15[b]	3.18[d]	1.70	II

[a] [133]; [b] [137]; [c] [138]; [d] [179]

4.2.1 Assessment of drug permeability from solutions (Paper I and II)

As can be observed in Figure 4.4, drug permeability varied both according to the physicochemical characteristics of the drug and to the presence or absence of mucus. In particular, drugs with low Log $D_{7.4}$ (Table 4.1) generally displayed lower permeation potential (*e.g.* ATN) compared to drugs characterized by a more lipophilic nature (*e.g.* NPR). Moreover, when the Log $D_{7.4}$ of two different drugs was comparable (*e.g.* IND-IBP and MTP-MTR), physicochemical properties such as the drug molecular weight (MW) seemed to influence drug permeation. In fact, it was found that smaller molecules led to higher P_{app} compared to larger ones. Furthermore, the P_{app} results were found to be in accordance with the fraction absorbed in humans (F_a %). For instance, the fraction

absorbed in humans for ATN (P_{app} 1.15 · 10^{-6} cm/s; F_a % 55; [137]) resulted to be much lower than the one of NPR (P_{app} 4.53 · 10^{-6} cm/s; F_a % 90; [137]).

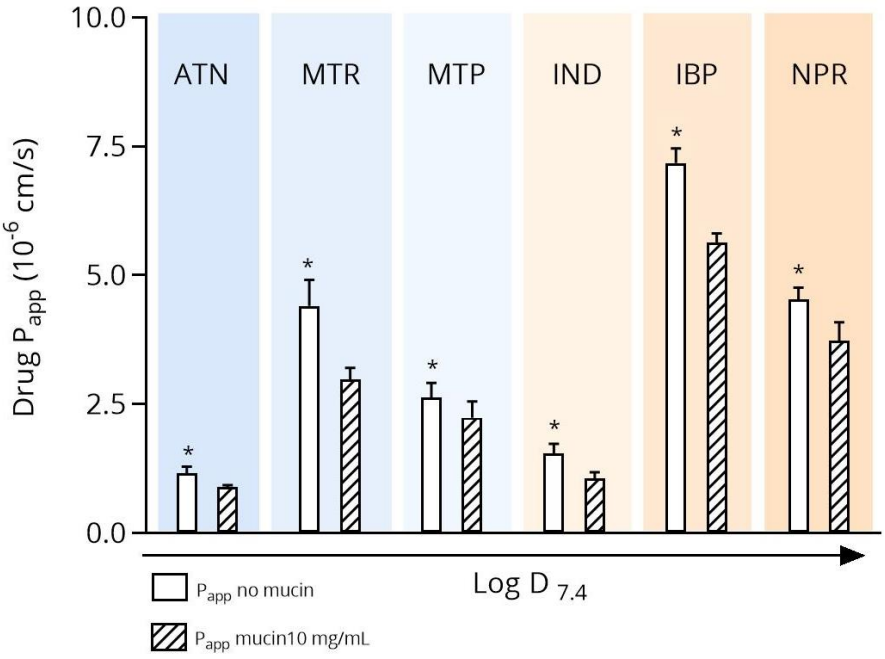

Figure 4.4: P_{app} of ATN, IBP, IND, MTP, MTR and NPR in the presence and absence of mucin 10 mL (pH 7.4). The results are indicated as mean ± SD (n = 3). * Statistically significant difference ($p < 0.05$) in drug P_{app} between the absence and presence of mucin dispersions.

Additionally, the presence of mucin 10 mg/mL led to a decrease in P_{app} for all of the analyzed drugs, and this decrease varied according to the specific drug. To this regard, it has been previously demonstrated that the mucus layer can impair the diffusion and sequential permeation of both hydrophilic and lipophilic drugs thanks to hydrophobic, electrostatic and hydrogen bond mediated interactions, and that this impairment is in fact drug-specific [21, 24, 67, 180].

Thus, the described findings confirm i) the capability of the (mucus-)PVPA barriers to discriminate between different drugs and ii) the fact that drug permeability is compound-specific and depends on the environment to which the drug is presented.

4.2.2 Assessment of drug permeability from liposomal formulations (Paper I)

To successfully deliver drugs through the oral route of administration it is necessary to design an appropriate drug delivery system able to i) incorporate the drug, ii) carry it to the targeted site and iii) release it to allow its absorption. One of the delivery strategies utilized to enable oral drug absorption is the one based on drug loading into mucoadhesive or mucopenetrating formulations. In fact, mucoadhesive systems are able to prolong the resident time of the formulation at the mucosal site, improving the delivery of drugs to the mucosal membrane, whereas mucopenetrating systems easily cross the mucus layer, directly presenting the drug to the epithelial site [80]. Liposomal formulations are a type of drug delivery system that has been investigated for such purposes. The advantages of these delivery systems are mainly related to the fact that they can incorporate both hydrophilic and lipophilic drug (in their aqueous core and phospholipid bilayer, respectively) and to their potential mucoadhesive and mucopenetrating properties obtained through their surface modification [181-185]. Liposomes have been used both for oromucosal drug delivery [81] and for GI delivery of drugs [181], even though in the second case the acidic and digesting environment of the GI tract can be an obstacle for the optimal performance of such delivery systems. Therefore, since *in vitro* permeability models should be used to study the potential of such delivery systems, the mucus-PVPA barriers were utilized to assess the permeability of drugs loaded into different liposomal formulations. The liposomal formulations were chosen as model mucoadhesive/mucopenetrating systems. Specifically, MTR, IND or NPR were loaded into plain, chitosan-coated and PEGylated liposomes to assess the effect of the different formulations on drug permeation. These liposomal formulations were chosen as chitosan-coated liposomes are known for their mucoadhesive properties [21], whereas PEGylated liposomes are known for their mucopenetrating potential [186-188]. Liposomal diameter, polydispersity index (PdI), zeta potential and drug entrapment efficiency (EE %) of the prepared liposomes are summarized in Table 4.2. As can be observed in Table 4.2, the three types of liposomal formulations (*i.e.* plain, chitosan coated and PEGylated) exhibited differences in diameter and zeta potential not only according to their surface modification, but especially to the drug incorporated. For instance, the

chitosan-coating resulted in an increase in zeta potential compared to plain liposomes, but this did not result into a positive zeta potential for all the investigated formulations. Moreover, the drug entrapment efficiency was also found to be drug-dependent (Table 4.2). The dependence of the described liposomal characteristics from the incorporated drug is supposedly related the location of the drug inside the liposome (*i.e.* aqueous core for hydrophilic drugs, phospholipid bilayer for lipophilic drugs) [182-185, 189, 190].

Table 4.2: Size, zeta potential and drug entrapment efficiency of the prepared liposomes. The results are indicated as mean ± SD (n = 3).

Formulation	Diameter nm	PdI	Zeta potential mV	EE %
MTR plain	202.52 ± 2.24	0.52	-2.13 ± 1.34	2.82 ± 0.14
MTR coated	162.27 ± 8.44	0.63	1.91 ± 0.24	2.78 ± 0.01
MTR PEGylated	105.40 ± 5.11	0.20	-4.38 ± 0.519	2.58 ± 0.20
IND plain	140.85 ± 5.87	0.27	-24.75 ± 0.35	83.30 ± 3.88
IND coated	134.15 ± 18.74	0.30	-18.68 ± 1.53	73.87 ± 4.03
IND PEGylated	96.22 ± 5.11	0.23	-10.60 ± 0.34	77.81*
NPR plain	146.30 ± 13.15	0.28	-2.32 ± 1.20	26.15 ± 2.19
NPR coated	138.10 ± 4.38	0.38	0.19 ± 0.50	37.43 ± 5.79
NPR PEGylated	128.00 ± 6.36	0.18	-10.89 ± 2.13	23.58 ± 0.31

*One batch was prepared

The characterization of the prepared liposomes is crucial to understand the impact of these formulations on drug permeation, especially in the presence of the negatively charged and hydrophilic mucus layer. In fact, it has been proved that positively charged particles are able to interact with the mucus layer, highly negatively charged ones are repulsed by it, whereas slightly negative or neutral particles are usually interacting with this layer to a low extent, leading to their free diffusion through it [81]. Thus, only positively and highly negatively charged particles lead to a slowed down diffusion through mucus, possibly causing lower drug permeation [17, 25, 191]. The lower drug permeation caused by the positive zeta potential related to the chitosan coating can be seen for both

MTR and NPR in Figure 4.5. In fact, it can be observed that, in the presence of mucin 10 mg/mL, MTR and NPR permeation was significantly lower in the case of chitosan-coated liposomes compared to plain and/or PEGylated liposomes (Figure 4.5). On the other hand, all liposomes containing IND exhibited a negative zeta potential, thus not causing a difference in drug permeation between the different formulations. However, it should be noted that the extent of drug permeation across a barrier does not depend exclusively on the interaction between the formulation and the mucus layer, but also on factors such as i) the release of the drug from the formulation, ii) the diffusion of the free drug through the mucus layer, iii) the drug permeation potential across the specific barrier, and most importantly iv) on the equilibrium of the drug between the formulation and the medium in which it is found.

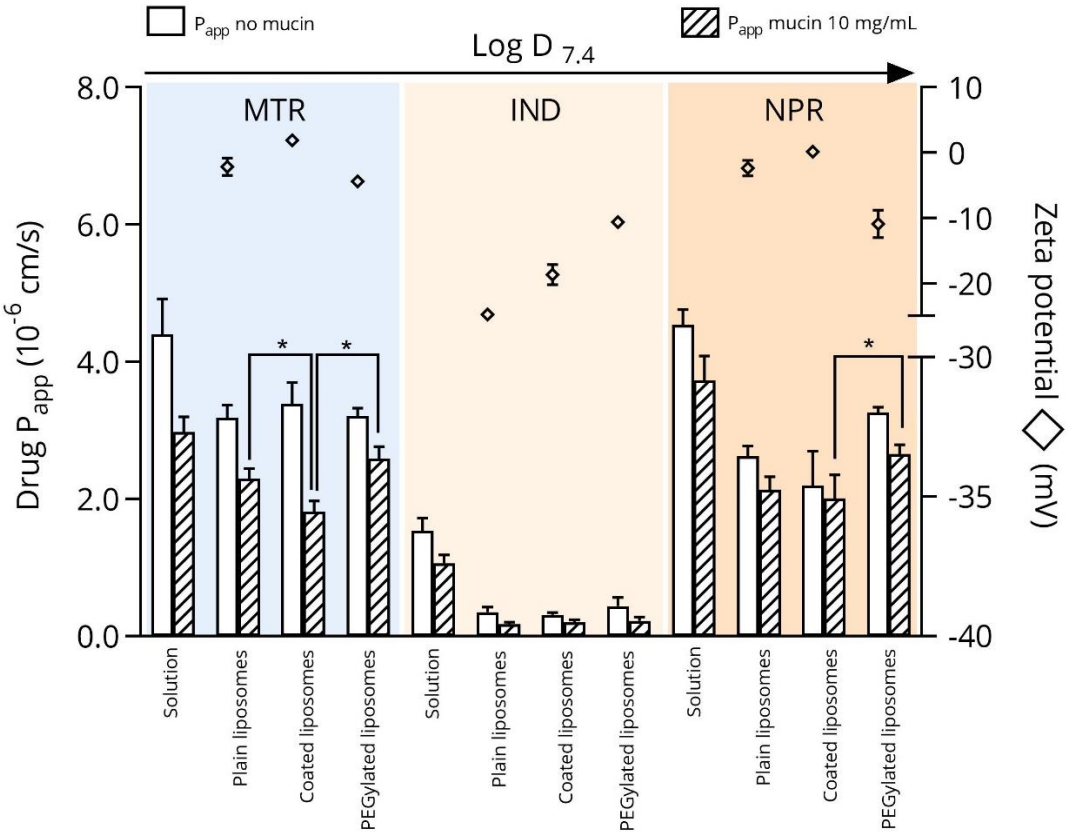

Figure 4.5: P_{app} of MTR, IND, and NPR in the presence and absence of mucin 10 mL (pH 7.4) from solution and different liposomal formulations. The results are indicated as mean ± SD (n = 3). *Statistically significant difference ($p < 0.05$) in drug P_{app} between plain/PEGylated liposomes and chitosan-coated ones.

4.3 Simulation of the intestinal environment on top of the mucus-PVPA barriers (Paper II)

Drug absorption in the intestine can vary according to the environment to which the drug is exposed. For instance, acidic drugs are better absorbed at acidic pH, while the opposite is true for basic drugs [54], and it has also been demonstrated that lipophilic drugs are better absorbed in a fed state compared to a fasted one [8]. Thus, it is crucial that an *in vitro* model designed to predict drug absorption is able to mimic the characteristics of the intestinal environment. For this reason, the mucus-PVPA barriers were used to assess drug permeation at intestinally relevant pH and in the presence of fasted and fed state SIFs.

4.3.1 Solubility-permeability interplay in the presence and absence of mucus

As previously mentioned, drug solubility and permeability directly affect drug absorption in the GI tract. This is especially true in the case of ionizable compounds, as they depend on the pH that the drug is presented to [54]. To this regard, previous findings have emphasized the importance of determining the solubility-permeability trade-off for (novel) drugs [192, 193]. Therefore, in Paper II the use of an intestinal medium which exclusively simulated the intestinal pH made it possible to infer if a pH-dependent trend could be observed in terms of drug solubility and permeability. Five model drugs were chosen to cover different physicochemical characteristics (Table 4.1), and their solubility and permeability (both in the presence and absence of mucin 10 mg/mL) was tested at pH 5.5, 6.2 and 7.4. The medium used corresponded to level 0 in the biorelevance levels proposed by Markopoulos and colleagues [103] (Section 1.2.1).

As can be observed in Figure 4.6, for acidic drugs such as IBP, IND and NPR, characterized by a pKa around 3-4, the solubility increased with an increase in pH, while their permeability had the opposite trend (decreasing P_{app} at increasing pH). The same trend was not visible for MTR (pKa 2.62), since both its solubility and permeability did not

significantly change with the pH. The different pH-dependent trend between MTR and IBP/IND/NPR can be ascribed to the fact that for MTR the pH conditions tested were far from its isoelectric point. In the case of the basic drug MTP, the solubility decreased with the increase in pH, while MTP P_{app} increased within the pH range tested.

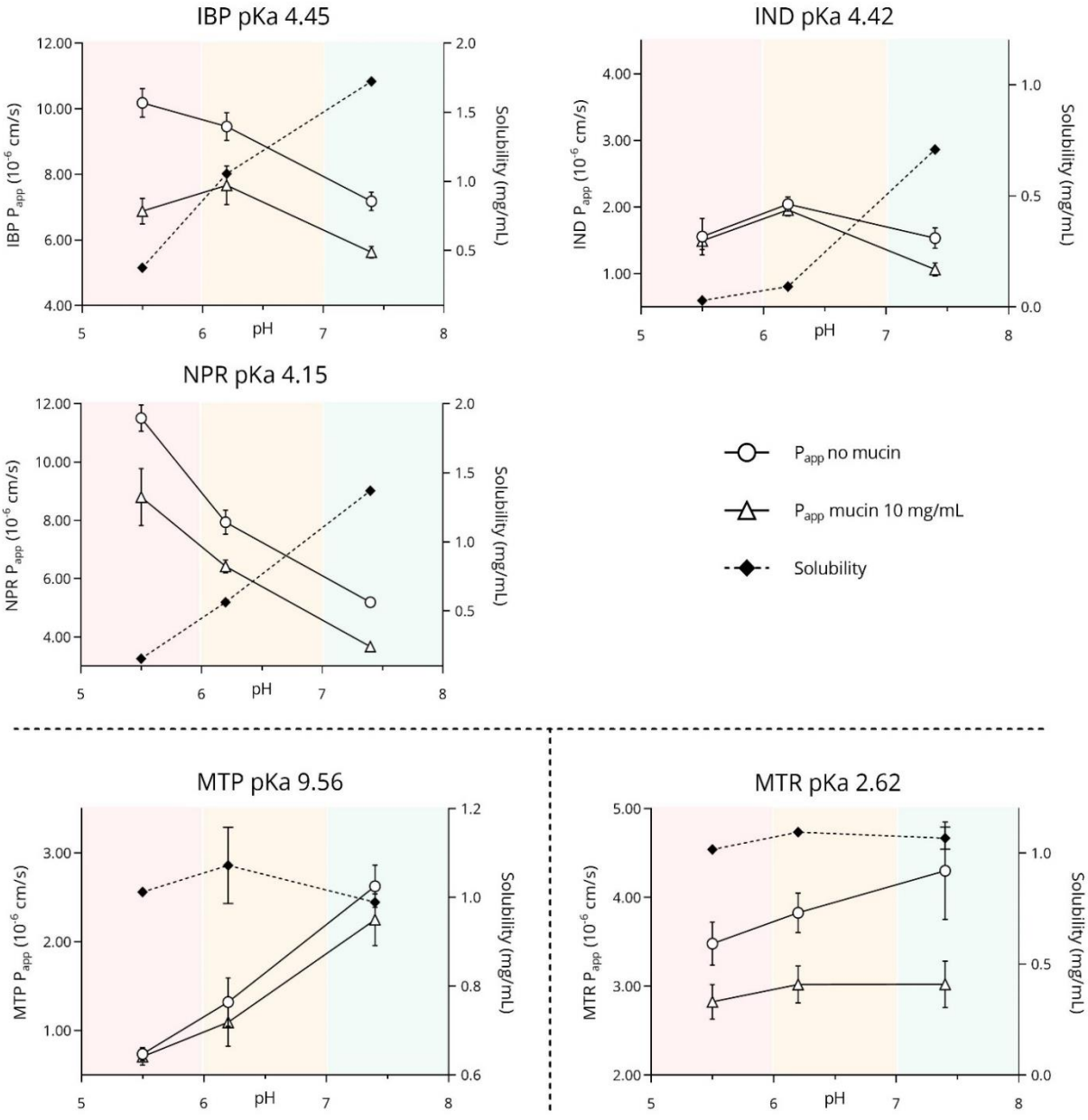

Figure 4.6: pH-dependent solubility (black diamond) and P_{app} in the presence (white triangle) and absence (white circle) of mucin 10 mg/mL for IBP, IND, NPR, MTP and MTR. The results are indicated as mean ± SD (n = 6).

The observed trends are in line with the pH partition hypothesis, which affirms that ionizable compounds display higher solubility when their ionized form is the predominant one, while their permeability is higher when the drugs are in their unionized form [51]. These trends are furthermore in accordance with other *in vitro* and *in silico* studies [48, 55, 194-196]. Additionally, a general decrease in drug P_{app} could be observed in the presence of mucin 10 mg/mL, and the influence of pH was less evident in the presence of this layer on top of the PVPA barriers (Figure 4.6). The decrease in the pH-effect on drug permeability in the presence of the mucus layer could be connected to the fact that mucins themselves exhibit a pH-dependent ionization, especially associated to their abundance in acidic functional groups (*i.e.* sialic acid) [81]. As observed in Figure 4.1, changes in pH can affect the rheological properties of mucin, and this can impact the diffusion and permeation of drugs. Therefore, the collected results suggest that drug permeability in the presence of such layer does not only depend on the drug ionization, but also on the pH-dependent behavior of mucin. Even though the results depicted thus far highlight the importance of simulating the intestinal mucus and the pH condition in this GI compartment, other components present in the intestinal fluids (*e.g.* bile salts, dietary lipids, lipid digestion products etc.) are as essential when studying drug permeation, particularly in the case of PWSDs. Therefore, the impact of fasted and fed state SIFs on drug permeation was assessed with the use of the mucus-PVPA barriers.

4.3.2 Use of fasted and fed state SIFs with the mucus-PVPA barriers

The composition of the intraluminal fluids found in the small intestine can vary according to the prandial state (*i.e.* fasted or fed state), and these differences can affect the absorption of drugs [29]. For this reason, different version of fasted and fed state SIFs (namely, FaSSIF and FeSSIF) have been developed and have proved to be useful for the determination of drug solubility and permeability in several studies [143, 145, 149]. Because of their usefulness, the commercially available FaSSIF and FeSSIF were utilized in the mucus-PVPA setup to evaluate their compatibility with the PVPA barriers and their potential use in drug permeability studies.

4.3.2.1 Mucus-PVPA barriers integrity in the presence of simulated fluids

The compatibility of two versions (V1 and V2) of FaSSIF and FeSSIF with the (mucus-)PVPA barriers was determined by calculating CAL permeability and by measuring the electrical resistance across the barriers in the presence of the chosen SIFs. As can be observed in Figure 4.7, the presence of fasted state SIFs on top of the PVPA barriers led to CAL P_{app} above and electrical resistance below the standard limit both in the presence and absence of mucin 10 mg/mL, suggesting a certain level of barrier impairment. On the other hand, fed state SIFs did not cause an increase in CAL P_{app} nor decrease of electrical resistance compared to the acceptable limit, suggesting correct barrier functionality in such conditions.

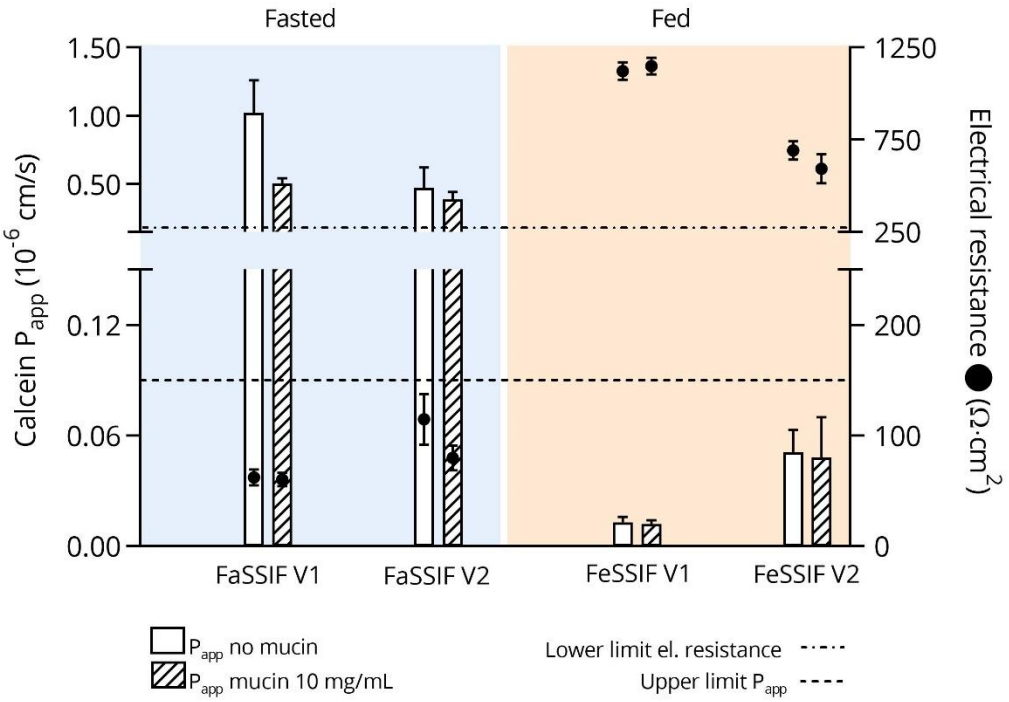

Figure 4.7: Calcein P_{app} and electrical resistance across the PVPA barriers after addition of FaSSIF or FeSSIF (V1 or V2) in the donor compartment of the PVPA barriers in the presence and absence of mucin 10 mg/mL. The results are indicated as mean ± SD (n = 6).

The discussed results were confirmed when the release of barrier phospholipids to the donor compartment of the PVPA barriers was determined in the presence of the different

SIFs. In fact, it was found that fasted state SIFs caused significantly higher phospholipid loss compared to the negative control (*i.e.* phospholipid loss in the presence of PBS pH 7.4 on top of the PVPA barriers) (Figure 4.8). On the other hand, fed state SIFs did not lead to higher phospholipid loss compared to the same control. Even though the fasted state SIFs led to higher barrier impairment compared to fed ones, they did not cause complete barrier disruption as in the case of Triton 0.5% (positive control), confirming the ability of the barriers to withstand their presence to a certain degree.

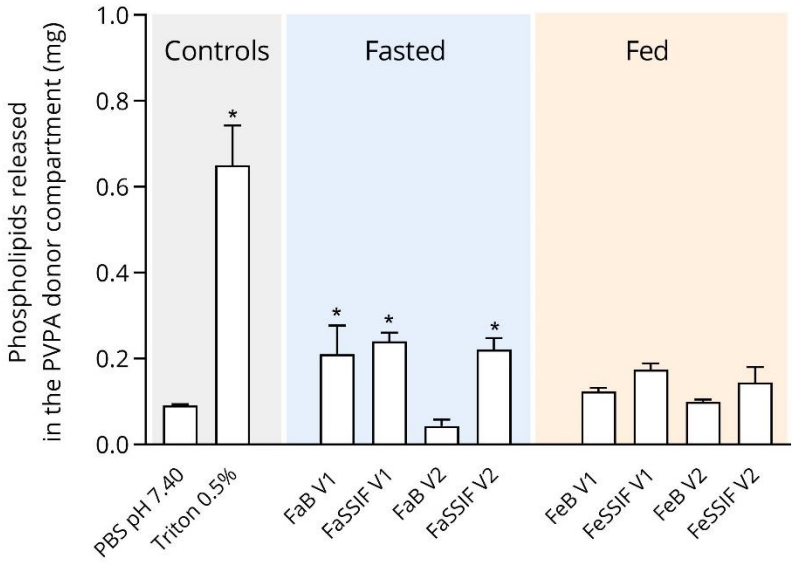

Figure 4.8: Phospholipids lost in the donor compartment of the PVPA barriers in the presence of PBS pH 7.4 (negative control) Triton X-100 0.5% (positive control), fasted and fed state buffers (FaB and FeB respectively) and fasted and fed state SIFs (FaSSIF and FeSSIF, respectively). The results are indicated as mean ± SD (n = 6). *Statistically significant difference ($p < 0.05$) in phospholipids loss compared to PBS pH 7.4.

The different impact on the functionality of the PVPA barriers in the presence of the fasted compared to fed state SIFs could be ascribed to their different composition. In fact, the two types of SIFs differ both in terms of their buffer composition (FaB and FeB) and of the bile salts and lecithin concentrations (Table 4.3). The results depicted in Figure 4.8 show that the fasted buffer V1 alone was able to cause significant increase in phospholipid loss, whereas the same could not be observed for V2. On the other hand, the phospholipid loss caused by V1 and V2 fasted state SIFs could results from the interactions between the micelles formed in such media and the PVPA barriers. The composition of fasted

compared to fed state SIFs can cause the formation of different vesicular structures, which can in turn have a different effect on the integrity of the barriers. To this regard, Riethorst and colleagues have demonstrated how the micellar/vesicular structures formed in fasted and fed state SIFs can differ according to their bile salts/lecithin concentration [33]. Specifically, fasted state SIF showed to be characterized by both small and medium sized micelles (10-50 nm), fed state SIF V1 mainly contained medium micelles (20-50 nm), and fed state SIF V2 showed high abundance of larger structures (50-200 nm) [33]. The mentioned differences in vesicular size could be the reason for the incompatibility of the fasted state SIFs with the PVPA barriers.

Table 4.3: Composition of fasted and fed buffers (FaB/FeB) and SIFs for both version 1 (V1) and version 2 (V2) media.

Name	FaB-V1	FaSSIF-V1	FaB-V2	FaSSIF-V2	FeB-V1	FeSSIF-V1	FeB-V2	FeSSIF-V2
Sodium taurocholate (mM)	-	3.00	-	3.00	-	15.00	-	10.00
Lecithin (mM)	-	0.75	-	0.20	-	3.75	-	2.00
Glycerol monooleate (mM)	-	-	-	-	-	-	-	5.00
Sodium oleate (mM)	-	-	-	-	-	-	-	0.80
Maleic acid (mM)	-	-	19.10	19.10	-	-	55.00	55.00
Monobasic sodium phosphate monohydrate (mM)	28.40	28.40	-	-	-	-	-	-
Sodium chloride (mM)	106	106	68.60	68.60	203	203	126	126
Sodium hydroxide (mM)	8.70	8.70	101	101	101	101	82.00	82.00
Glacial acetic acid (mM)	-	-	-	-	144	144	-	-
pH	6.5	6.5	6.5	6.5	5.0	5.0	5.8	5.8
Osmolarity (mOsm/kg)		270		180		670		390
Buffer capacity (mM/dpH)		12		10		76		25

4.3.2.2 Drug permeability with fasted and fed state SIFs

The permeability of one BCS class II drug (IBP) was tested in the presence of both fasted and fed state SIFs to determine whether the different media would lead to differences in drug permeability.

Firstly, Figure 4.9 displays that the electrical resistance across the barriers in the presence of the fasted state SIFs was below the acceptable limit, in line with the results depicted in Figure 4.7. Even though these results indicated a certain level of barrier impairment, IBP permeability did not seem to drastically change in the presence of fasted state SIFs compared to the control (PBS pH 6.2) as it was observed in the case of CAL P_{app} (Section 4.3.2.1). These findings suggest that the changes in the structure of the barriers in the presence of fasted state SIF could be related to an increase in aqueous pores, which can impact the permeation of hydrophilic compounds (*i.e.* CAL) to a higher extent compared to more lipophilic ones (*i.e.* IBP) [133]. In the case of fed state SIFs, the electrical resistance across the barriers measured at the end of the permeation experiment indicated correct barrier functionality (Figure 4.9). Because of the electrical resistance differences in the fasted compared to the fed conditions, a comparison of IBP permeability could not be carried out. Moreover, minor differences in drug P_{app} could be observed with the fed state SIFs compared to the control (PBS pH 5.5), whereas a significant decrease in IBP permeability was observed in all fed conditions in the presence of mucin 10 mg/mL compared to its absence (Figure 4.9). The same decrease in P_{app} in the presence of mucin 10 mg/mL was not observed in the case of CAL (Figure 4.7), highlighting the fact that this additional layer was able to particularly affect the permeability of a more lipophilic compound. This evidence stresses the importance of the inclusion of a mucus layer on top of permeation membranes especially when evaluating the absorption potential of lipophilic drugs. Moreover, when it comes to lipophilic drugs which exhibit a high affinity for the colloidal structures found in the intestinal fluids, other processes (*e.g.* enzymatic degradation) can affect drug solubilization and permeation [33].

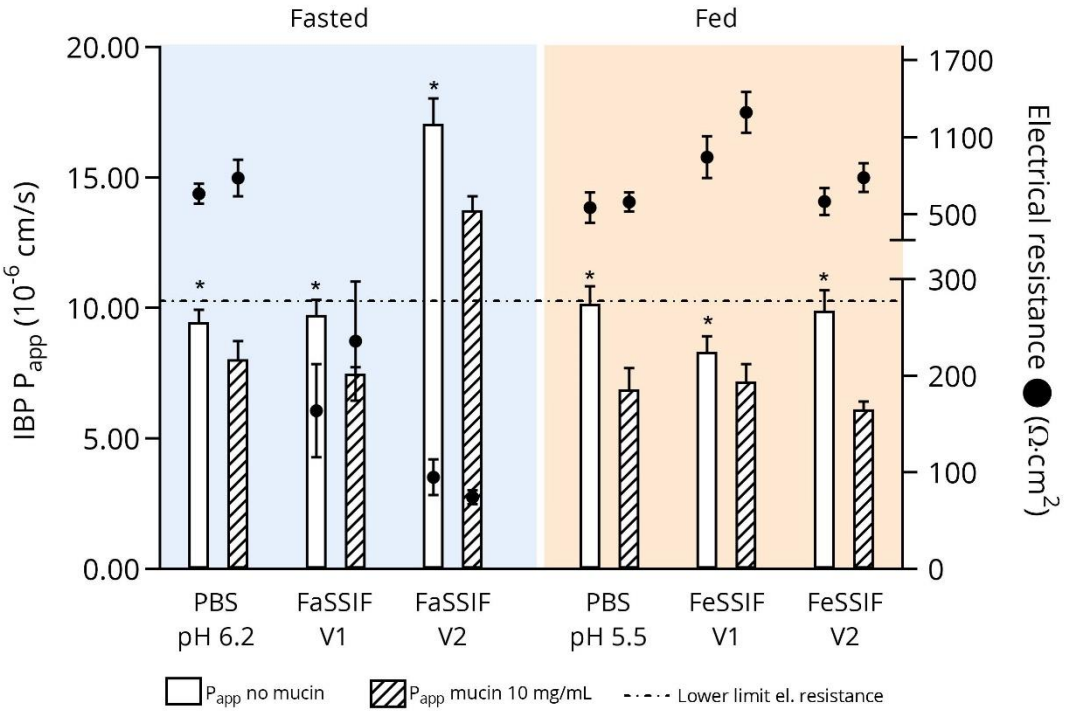

Figure 4.9: IBP permeability from PBS solutions (controls) and from fasted and fed state SIFs (FaSSIF and FeSSIF, respectively). The results are indicated as mean ± SD (n = 6). *Statistically significant difference ($p < 0.05$) in IBP P_{app} between the presence and absence of mucin 10 mg/mL on top of the PVPA barriers.

4.4 Combination of *in vitro* intestinal lipolysis with *in vitro* drug permeation (Paper III)

Loading of drugs into LBFs is one of the commonly used strategies for the oral delivery of PWSDs. LBFs are able to increase drug bioavailability thanks to their drug solubilization and supersaturation effect, their inhibition of drug precipitation and enhancement of lymphatic transport [36, 45, 83, 84, 86]. However, because of their lipid nature, the performance of LBFs can be affected by physiological processes such as the digestion (*i.e.* lipolysis) occurring in the small intestine. This, together with the variability in affinity between PWSDs and the colloidal structures found in the intestinal fluids, can have a substantial impact on drug absorption and should be considered carefully. Therefore, Paper III focused on the combination of the mucus-PVPA permeation model with the *in vitro* intestinal lipolysis model previously developed by Zangenberg [109]. In particular,

three SNEDDSs (namely super-SNEDDS solution, SNEDDS, super-SNEDDS suspension) containing the PWSD fenofibrate were the chosen LBFs in this study. Prior to the *in vitro* permeation study, the compatibility of the PVPA barriers with the digesting environment was studied. Additionally, this study utilized biosimilar mucus as the mucus-simulating source to not only account for mucins (as in Paper I and II), but to also consider the other components present in intestinal mucus.

4.4.1 Mucus-PVPA barrier integrity in the presence of a digesting environment

The compatibility of the PVPA barriers with biosimilar mucus, fasted intestinal medium, SNEDDS and digesting SNEDDS was evaluated in the previously mentioned manner (assessment of CAL P_{app} and measurement of electrical resistance across the barriers). Since the commercially available FaSSIF negatively impacted the PVPA barrier functionality, another fasted state intestinal medium was chosen for this study (composition: bile bovine 2.95 mM; calcium chloride 1.40 mM; maleic acid 2.00 mM; sodium chloride 146.80 mM; S-PC 0.26 mM; Tris 2.00 mM; pH 6.5). The fasted medium was chosen to exclusively assess the impact on drug solubilization and permeation of the lipid digestion products originating from the lipolysis of SNEDDS.

As can be observed in Figure 4.10, the barriers maintained their integrity in all the tested conditions except one, namely the presence of SNEDDS on top of mucus-naked barriers. In fact, in this case, CAL permeability was significantly ($p < 0.05$) above the upper P_{app} limit and below the lower electrical resistance limit. However, the presence of biosimilar mucus on top of the barriers seemed to shield them from the impairing events connected to the presence of SNEDDS (Figure 4.10). Interestingly, the same trend could not be observed when digesting SNEDDS were added on top of the barriers. In fact, digesting SNEDDS did not cause an increase in CAL P_{app}/decrease in electrical resistance in the absence of biosimilar mucus. However, since the presence of biosimilar mucus proved to protect the barriers from SNEDDS, this layer was used in all further permeation experiments. The difference in barrier compatibility between SNEDDS and digesting SNEDDS could be connected to the different structures formed in these two conditions. In fact, SNEDDS

prior to lipolysis usually display a rather homogeneous and distinctive structure (*i.e.* nano-emulsion droplets), while after the addition of lipases they tend to form different colloidal structures which can vary in size and composition (see Section 4.5.1).

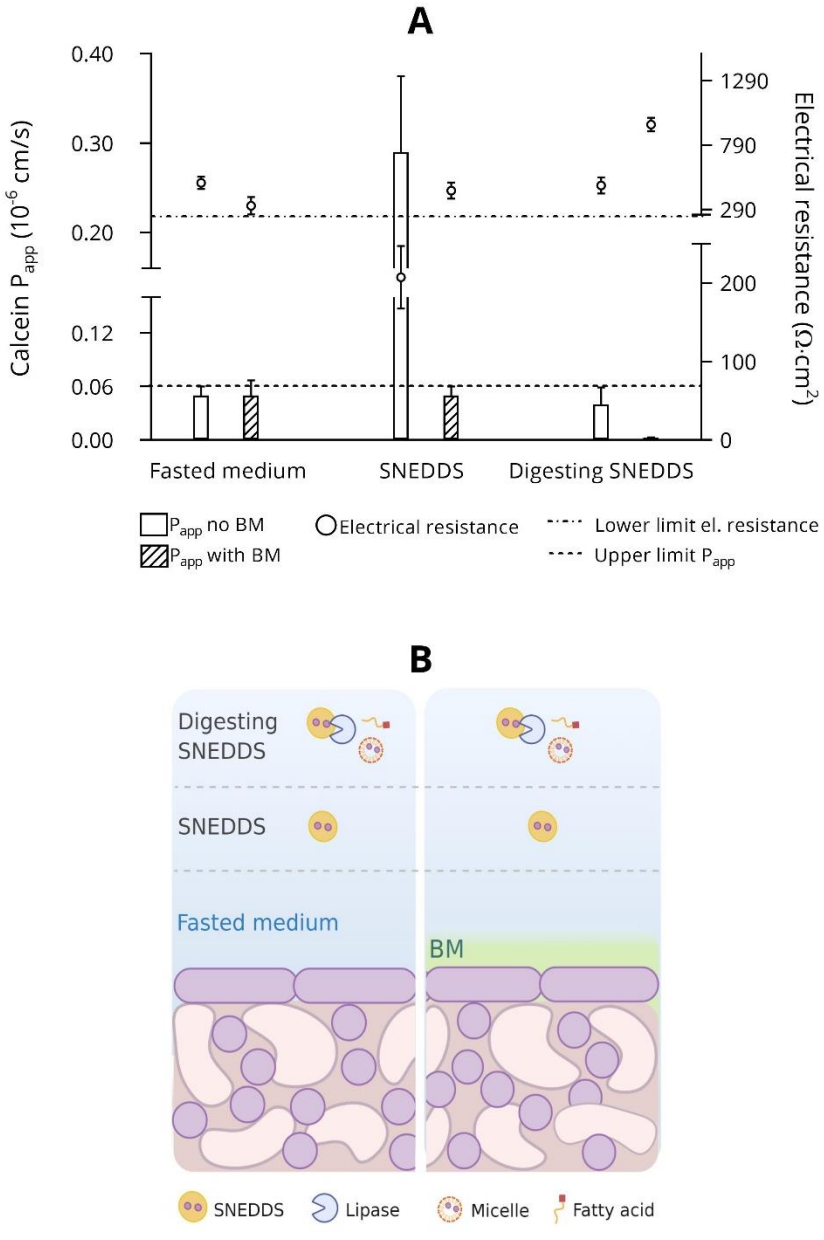

Figure 4.10: A) Calcein P_{app} and electrical resistance across the PVPA barriers in the presence and absence of biosimilar mucus BM, fasted medium, SNEDDS and digesting SNEDDS. The results are indicated as mean ± SD (n = 12). The permeability experiments were performed in the presence of PBS pH in the acceptor side of the PVPA barriers. B) Pictorial representation of the experimental conditions used in the study.

Table 4.4: Equilibrium solubility of fenofibrate in different acceptor media, together with CAL permeability and electrical resistance across the PVPA barriers in the presence of such media. The results are indicated as mean ± SD (n = 3).

Acceptor medium	Equilibrium solubility of fenofibrate (nmol/mL)	CAL P_{app} (10^{-6} cm/s)	Electrical resistance ($\Omega \cdot cm^2$)
Control (PBS pH 7.4)	0.48 ± 0.03	0.059 ± 0.013	727.43 ± 143.51
DMSO 10 mg/mL	0.59 ± 0.08	0.050 ± 0.010	577.00 ± 50.60
DMSO 40 mg/mL	0.82 ± 0.01 [a]	0.030 ± 0.001	702.70 ± 158.70
BSA 1% w/v	14.19 ± 0.13 [a]	0.210 ± 0.030 [b]	60.60 ± 7.30 [c]
BSA 4% w/v	58.02 ± 0.49 [a]	0.450 ± 0.030 [b]	44.90 ± 6.30 [c]
Tween 20 5 mg/mL	116.71 ± 5.73 [a]	0.370 ± 0.030 [b]	116.70 ± 7.30 [c]

[a] Statistically significant difference ($p < 0.05$) in drug equilibrium solubility compared to the control

[b] CAL P_{app} above to the acceptable upper limit ($0.06 \cdot 10^{-6}$ cm/s)

[c] Electrical resistance across the PVPA barriers below the acceptable lower limit ($290\ \Omega \cdot cm^2$)

Due to the poor aqueous solubility of fenofibrate, different PVPA acceptor media were evaluated to promote higher drug transfer across the barriers and thereby allow a better quantification of the permeated drug. Table 4.4 displays the studied media and the connected drug solubility. Moreover, the compatibility of the barriers with the same media was evaluated by calculating CAL P_{app} and measuring the electrical resistance across the PVPA barriers. According to the results obtained, DMSO 40 mg/mL was chosen as the medium to be used in further permeation studies since it was the only one which both provided higher fenofibrate solubility compared to the control (PBS pH 7.4) and did not impair the functionality of the barriers (Table 4.4). The other studied solutions (*i.e.* BSA 1 and 4% w/v, Tween 20 5 mg/mL) were not suitable as acceptor medium due to their barrier impairment effects (Table 4.4). Thus, DMSO 40 mg/mL was used as the acceptor medium when the permeation of fenofibrate from SNEDDS was assessed.

4.4.2 *In vitro* intestinal lipolysis of fenofibrate-loaded SNEDDSs

Three fenofibrate-loaded SNEDDSs were prepared in this study in order to obtain i) SNEDDS where the drug was solubilized in the formulation below its equilibrium solubility (75% of the drug equilibrium solubility in the SNEDDS preconcentrate), ii) super-SNEDDS solution where fenofibrate was solubilized above its equilibrium solubility (150% of the drug equilibrium solubility in the SNEDDS preconcentrate) and iii) super-SNEDDS suspension where the drug was present both solubilized in the formulation and suspended in it (150% of the drug equilibrium solubility in the SNEDDS preconcentrate). The ability of the three SNEDDSs to maintain the drug solubilized upon *in vitro* lipolysis was evaluated. In particular, the distribution of fenofibrate between the aqueous and pellet phase forming after addition of pancreatin from porcine pancreas (*i.e.* lipolysis initiator) was assessed. To allow for comparison, the lipolysis experiments were carried out so that the amount of fenofibrate in the lipolysis vessel would be the same for the three formulations; as a result of this, the amount of SNEDDS preconcentrate (*i.e*. the mixture of oil, surfactant, co-surfactant and co-solvent) in the lipolysis vessel varied according to the tested formulation. For instance, SNEDDS contained fenofibrate corresponding to 75% of the drug equilibrium solubility in the SNEDDS preconcentrate, and it had to be added in a double amount in the lipolysis vessel compared to super-SNEDDS solution and suspension (both containing fenofibrate corresponding to 150% of the drug equilibrium solubility in the SNEDDS preconcentrate).

As shown in Figure 4.11, super-SNEDDS suspension led to the highest degree of drug precipitation, which significantly increased overtime, while super-SNEDDS solution had a lower amount of drug found in the pellet phase and SNEDDS produced little to no precipitation. The ability of SNEDDS to better maintain the drug solubilized in the aqueous phase compared to the super-SNEDDSs is most likely connected to the fact that double the amount of SNEDDS was added to reach the same fenofibrate amount in the lipolysis vessel as the one of the super-SNEDDSs; this led to the presence of double the amount of SNEDDS preconcentrate in the medium and to a higher drug solubilization effect. Moreover, not only the amount of SNEDDS preconcentrate, but also the nature of the loaded drug proved to be important. In fact, in the case where fenofibrate was present

both solubilized and suspended in the formulation (*i.e.* super-SNEDDS suspension) a higher degree of drug precipitation was observed.

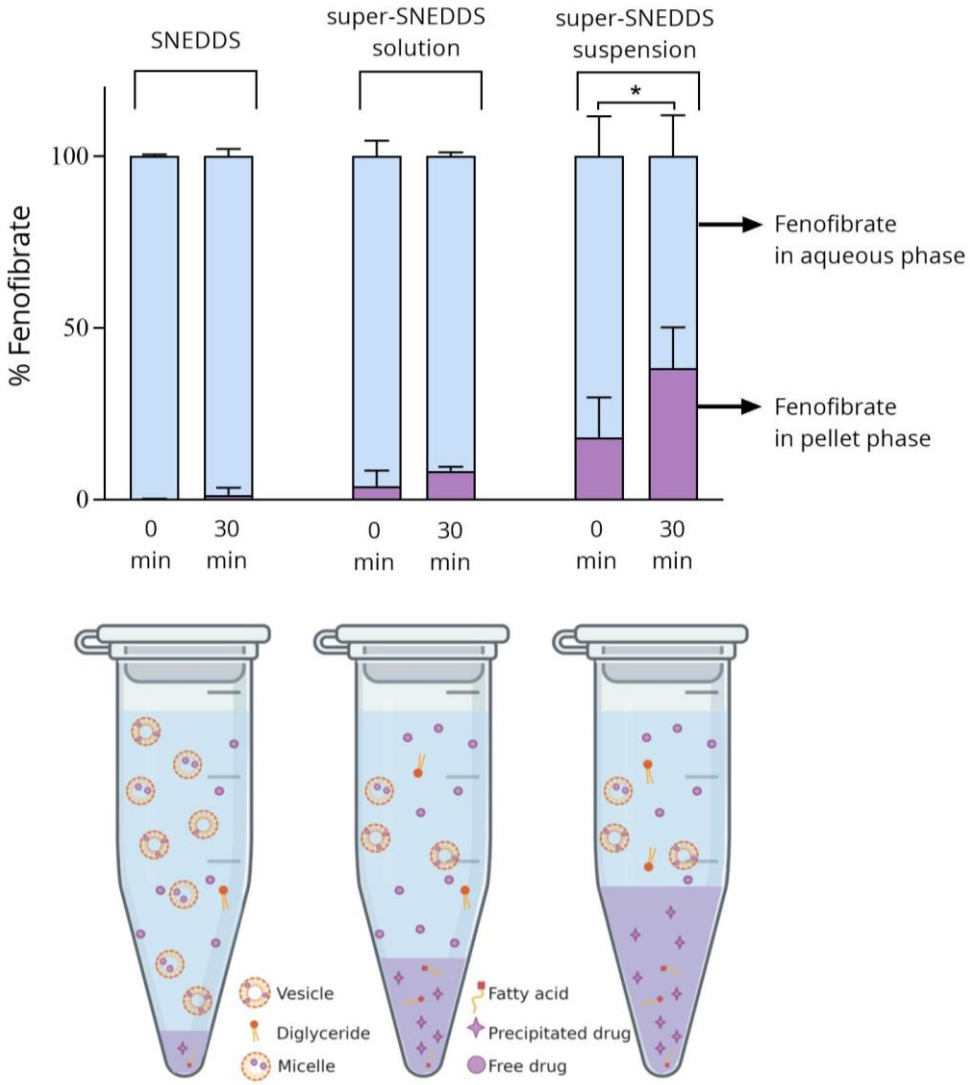

Figure 4.11: Relative amount (%) of fenofibrate found in the aqueous (blue) and pellet (purple) phase before initiation (0 min) and after 30 minutes of *in vitro* lipolysis for SNEDDS, super-SNEDDS solution and super-SNEDDS suspension. The results are indicated as mean ± SD (n = 4). Pictorial representation of the drug distribution in the aqueous and pellet phase (bottom). *Statistically significant ($p < 0.05$) difference between 0 and 30 minutes of *in vitro* lipolysis.

The results discussed thus far are in accordance with previously published data from Michaelsen and colleagues [168], where the ranking of the same three SNEDDSs in terms of drug plasma concentration after *in vitro* intestinal lipolysis was in line with the one presented above. In the mentioned study, the amount of drug in the aqueous phase upon

lipolysis of the three SNEDDSs was compared to the amount absorbed *in vivo* after oral dosing in rats, and a lack of IVIVC was found [168]. These results negated the hypothesis that the amount of drug in the intestinal lumen (represented by the amount of drug in the aqueous phase in the lipolysis vessel) corresponds to the amount able to reach to the blood stream. In fact, as can be observed in the pictorial representation in Figure 4.11, the drug is found in the aqueous phase both free in solution (*i.e.* available for absorption) but also associated to the colloidal structures forming after lipolysis of SNEDDSs and present in the intestinal medium (*i.e.* not available for absorption)[120, 174]. The more the colloidal structures, the more of the PWSD will be likely to be solubilized in them, the higher the chance that data obtained using the *in vitro* lipolysis leads to an overestimation of the drug available for absorption (*e.g.* SNEDDS in Figure 4.11, left side). Regarding this matter, it is known that colloidal structures have a finite capacity to solubilize a specific drug [92]. Thus, in the case of SNEDDS, a higher amount of SNEDDS preconcentrate leads to the formation of more colloidal structures, which have a higher drug solubilization capacity compared to super-SNEDDS solution, since half the amount of colloidal structures are present in the lipolysis medium.

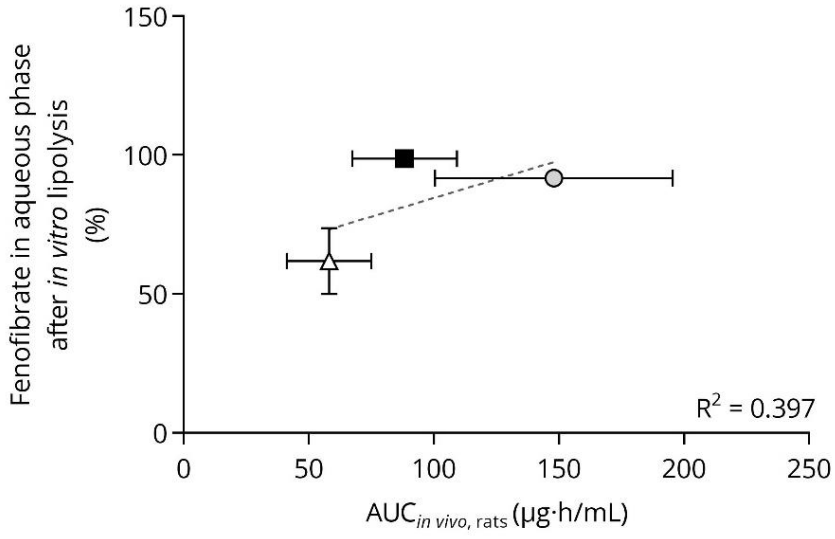

Figure 4.12: Correlation between amount of fenofibrate in the aqueous phase after lipolysis of SNEDDS (black square), super-SNEDDS solution (grey circle) and super-SNEDDS suspension (white triangle) and *in vivo* AUC in rats after oral administration of the same SNEDDSs obtained from Michaelsen and colleagues [168].

Since the analysis of the amount of drug present in the aqueous phase does not specifically give information on the amount of free drug available for absorption, a permeation step is necessary to separate this fraction from the one associated with the above-mentioned colloidal structures. The non-correspondence between the *in vivo* data and the *in vitro* drug solubilization results (*i.e.* fenofibrate found in the aqueous phase) was also observed when the data obtained in the present study was compared to the *in vivo* one collected by Michaelsen and colleagues [168]. In fact, a poor correlation was found between the two (R^2 = 0.397) (Figure 4.12).

4.4.3 Permeation of fenofibrate using the mucus-PVPA barriers

Samples obtained from the *in vitro* lipolysis experiments (*i.e.* after initiation of lipolysis with the addition of pancreatin from porcine pancreas) were transferred on top of the mucus-PVPA barriers to evaluate the permeation of free fenofibrate from the three SNEDDSs in the presence of lipolysis. The PVPA barriers integrity was assessed in parallel to the evaluation of fenofibrate permeation by calculating CAL P_{app} and measuring the electrical resistance across the barriers, as previously described. The results obtained (data not shown) indicated barrier integrity in all fenofibrate permeation experiments.

As shown in Figure 4.13, super-SNEDDS solution provided the highest permeation of fenofibrate, while SNEDDS led to lower drug permeation and super-SNEDDS suspension caused the lowest transfer of the drug across the mucus-PVPA barriers. Thus, the ranking in terms of drug permeation was: super-SNEDDS solution > SNEDDS > super-SNEDDS suspension. The discrepancy between the ranking described here and the one discussed in Section 4.4.2 (*i.e.* SNEDDS > super-SNEDDS solution > super-SNEDDS suspension) highlights how the quantification of drug in the aqueous phase of the lipolysis medium does not give enough information on the amount of drug available for absorption. For example, the drug distribution results for SNEDDS indicated that all of the drug was in the aqueous phase and thus theoretically available for absorption (Figure 4.11). However, this hypothesis was not confirmed by the permeation data obtained for the same formulation, which exhibited lower drug permeation compared to super-SNEDDS solution (Figure 4.13).

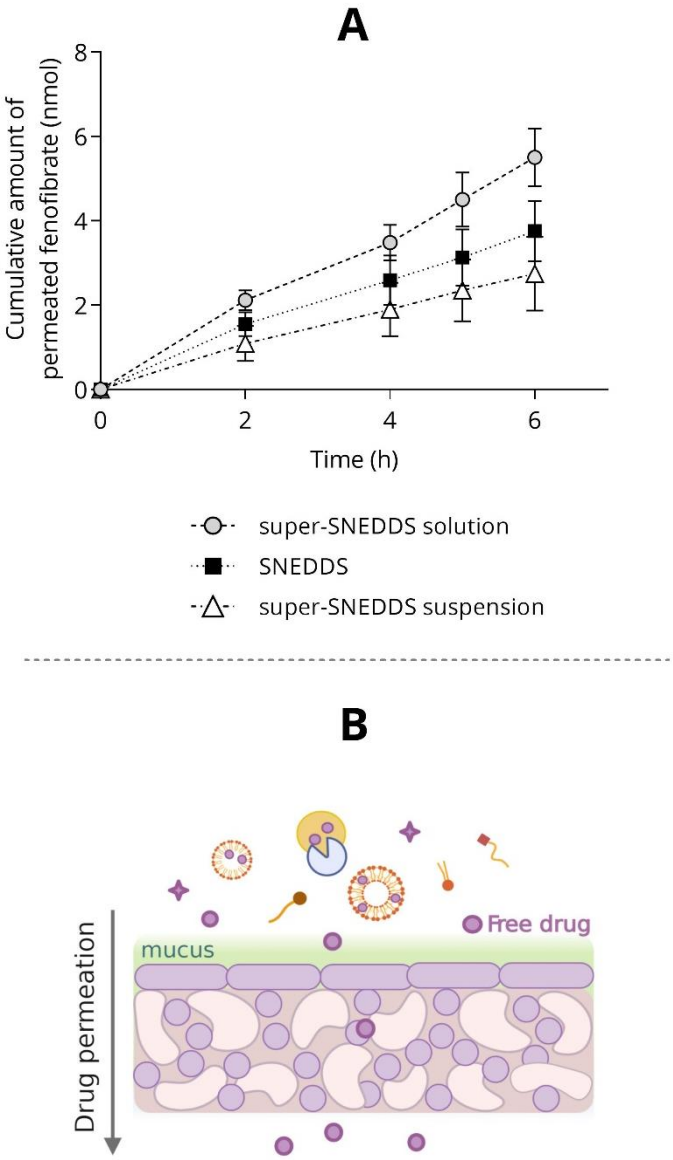

Figure 4.13: A) Cumulative amount of fenofibrate permeated from SNEDDS (black square), super-SNEDDS solution (grey circle) and super-SNEDDS suspension (white triangle) when samples after initiation of lipolysis were transferred on top of the mucus-PVPA barriers. The results are indicated as mean ± SD (n = 6). B) Pictorial representation of the permeation experiment.

As previously discussed, the factor that should be more carefully considered is the amount of SNEDDS preconcentrate present during the lipolysis and permeation experiments, and how this can affect the amount of drug available for permeation. In the case of SNEDDS, it is evident that the double amount of SNEDDS preconcentrate caused high drug solubilization (*in vitro* lipolysis data, Figure 4.11) compared to super-SNEDDS solution, and this led to a lower amount of drug available for permeation since most of

the drug is thought to be associated to the colloidal structures formed in the lipolysis medium, as confirmed by the permeation data (Figure 4.13). On the contrary, super-SNEDDS solution led to higher drug transfer across the mucus-PVPA barriers compared to SNEDDS, probably because this formulation enables more drug to be freely solubilized and available for permeation thanks to the lower content of SNEDDS preconcentrate. In fact, it can be hypothesized that the lower solubilization capacity of the colloidal structures formed from super-SNEDDS solution can provide a better supersaturation potential compared to the more numerous ones formed from SNEDDS. Thus, super-SNEDDS solution has the potential to provide drug supersaturation, which is known to be linked to increased drug absorption [85, 197, 198]. Moreover, not only the amount of SNEDDS preconcentrate, but also the nature of the drug found in the formulation seemed to affect drug permeation. In fact, the presence of fenofibrate both solubilized and suspended in super-SNEDDS suspension led to the highest drug precipitation (Figure 4.11) and, as a result of this, lowest drug permeation. On the other hand, the presence of fenofibrate in a supersaturated and solubilized state (*i.e.* super-SNEDDS solution) caused the highest drug transfer across the mucus-PVPA barriers. Regarding this matter, it is known that the drug solubilized in the colloidal structures and in the formulation can serve as a reservoir, and this amount can replenish the permeated drug and lead to higher drug absorption [199]. Contrarily, the amount of drug precipitated in the case of super-SNEDDS suspension has a lower potential for re-dissolution, leading to lower drug permeation.

4.4.4 Correlation of *in vivo* absorption with *in vitro* permeation data

The *in vitro* AUC obtained from the permeation data described in Section 4.4.3 was plotted against the AUC calculated from the *in vivo* plasma drug concentration curve in rats found by Michaelsen and colleagues [168] for the same fenofibrate-loaded SNEDDSs. As shown in Figure 4.14, the correlation of the *in vitro* ($AUC_{\textit{in vitro}\ \text{permeation}}$) with the *in vivo* data ($AUC_{\textit{in vivo}\ \text{absorption}}$) led to an excellent level D correlation after initiation of *in vitro* lipolysis ($R^2 > 0.99$), proving the ability of the developed combined *in vitro* lipolysis—mucus-PVPA permeation model to predict *in vivo* drug absorption for the chosen SNEDDSs. This

evidence demonstrates that the use of drug permeation data is essential in the prediction of *in vivo* drug absorption.

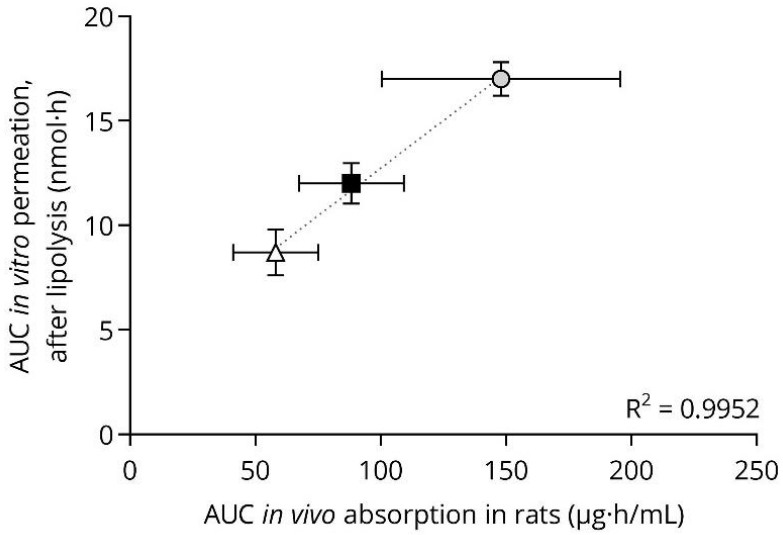

Figure 4.14: Correlation between amount of fenofibrate permeated across the mucus-PVPA barriers after lipolysis initiation for SNEDDS (black square), super-SNEDDS solution (grey circle) and super-SNEDDS suspension (white triangle) and *in vivo* AUC in rats after oral administration of the same SNEDDSs obtained from Michaelsen and colleagues [168].

Overall, Paper III enabled the construction of an *in vitro* model where the physiologically relevant processes affecting drug absorption were taken into account (*i.e*. lipolysis and permeation) and where the physiology of the intestinal environment and membrane were closely mimicked (*i.e.* intestinal fluids, mucus layer, biomimetic barrier). The combination of these factors made it possible to obtain an excellent IVIVC. Nevertheless, even though this model proved to be very useful, it failed to capture the simultaneous occurrence of lipolysis and permeation, as it relied on the combination of two separate tools. Therefore, in Paper IV the focus was put into obtaining a model where lipolysis and permeation could occur simultaneously.

4.5 Simultaneous *in vitro* lipolysis-permeation (Paper IV)

Formulation digestion and drug permeation both contribute to *in vivo* drug bioavailability, and they both influence one-another in a dynamic manner [36, 45, 83, 86]. Therefore, it is of crucial importance to construct *in vitro* models that are not only able to assess both processes, but that also allow them to occur at the same time to account for their dynamic interaction.

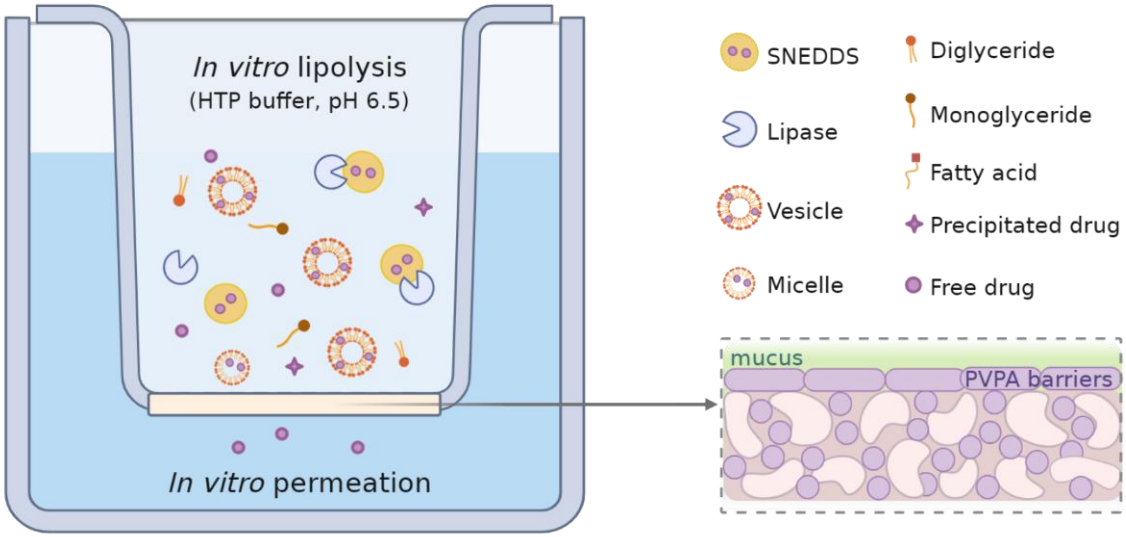

Figure 4.15: Pictorial representation of the experimental setup used for Paper IV, where HTP *in vitro* lipolysis was added on top of the mucus-PVPA barriers to allow SNEDDSs lipolysis and drug permeation to occur simultaneously.

For this reason, Paper IV focused on the addition of a pH-stat-titrator independent *in vitro* lipolysis model (*i.e.* the HTP *in vitro* intestinal lipolysis model) on top of the mucus-PVPA barriers (Figure 4.15), allowing for *in vitro* lipolysis of the three fenofibrate-loaded SNEDDSs utilized in Paper IV and drug permeation to occur simultaneously. To test the predictive potential of the results obtained with such model in terms of *in vivo* drug absorption, *in vitro* data was compared to *in vivo* data in rats for the same SNEDDSs, as already mentioned for Paper III.

4.5.1 Functionality of the HTP *in vitro* intestinal lipolysis model

The ability of the HTP model of being independent from a pH-stat apparatus is based on the fact that the buffer used for the preparation of the intestinal medium in the HTP *in vitro* lipolysis is characterized by a high buffering capacity, which is capable of directly neutralizing the pH drop caused by the formation of free fatty acids upon SNEDDSs lipolysis. This *in vitro* model has previously demonstrated to be equivalent to the pH-stat lipolysis model, leading to higher time and cost-effectiveness [122], and this was also confirmed by the results obtained in Paper IV. In fact, the pH of the intestinal medium in which the SNEDDSs were digested was kept around 6.48 ± 0.03 for the whole duration of the lipolysis-permeation experiment, in accordance with the results from Mosgaard and colleagues [122]. Furthermore, the evaluation of fenofibrate distribution after *in vitro* lipolysis of super-SNEDDS solution, SNEDDS and super-SNEDDS suspension was evaluated for a total of 30 minutes to evaluate which formulation would provide the best drug solubilization potential and whether these results would be in line with previously published data [168] and with the results obtained in Paper III. In addition, fenofibrate distribution was assessed both when lipolysis was absent (*i.e.* sole dispersion of SNEDDS in the HTP intestinal medium) and present (*i.e.* addition of pancreatin from porcine pancreas) to study the impact of this process on drug solubilization. Due to the small volume in the donor compartment and to difficulties in sampling on top of the mucus-PVPA barriers, the *in vitro* lipolysis experiments were carried out in a separate lipolysis vessel. As already mentioned in Section 4.4.2, the concentration of fenofibrate in the lipolysis vessel and on top of the mucus-PVPA barriers was the same for all three SNEDDSs to allow for comparison between the formulations. As shown in Figure 4.16, SNEDDS was able to best maintain the drug solubilized in the aqueous phase, whereas for super-SNEDDS solution and super-SNEDDS suspension drug precipitation was more evident both in the absence (Figure 4.16A) and presence (Figure 4.16B) of lipolysis. Interestingly, drug precipitation overtime (0-30 minutes) was more evident in the presence of lipolysis for super-SNEDDS solution compared to super-SNEDDS suspension (Figure 4.16B), presumably due to the instability of the supersaturated system provided by the super-SNEDDS solution. The described increase in drug precipitation overtime was not visible

when lipolysis was not taking place (*i.e.* sole dispersion of super-SNEDDS solution and suspension in the HTP intestinal medium) (Figure 4.16A).

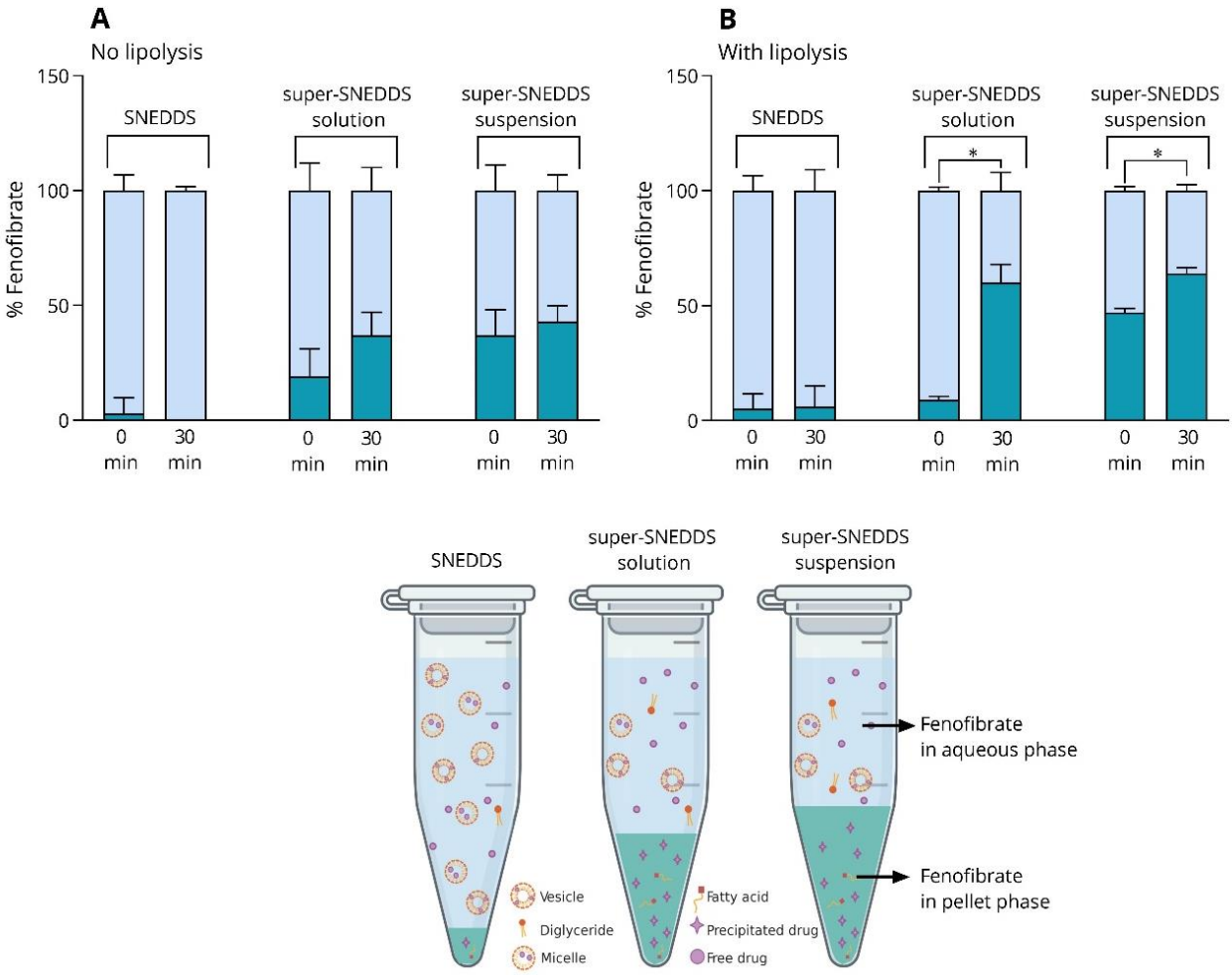

Figure 4.16: Relative amount (%) of fenofibrate found in the aqueous (blue) and pellet (green) phase overtime A) in the absence (*i.e.* sole dispersion) and B) presence of *in vitro* lipolysis for SNEDDS, super-SNEDDS solution and super-SNEDDS suspension. The results are indicated as mean ± SD (n = 3). Pictorial representation of the drug distribution in the aqueous and pellet phase (bottom). *Statistically significant ($p < 0.05$) difference between 0 and 30 minutes of *in vitro* lipolysis.

The fact that drug precipitation significantly increased in the presence of lipolysis compared to its absence can be ascribed to the fact that the addition of pancreatin causes the formation of colloidal structures, such as micelles and vesicles, which solubilize fenofibrate to a different extent compared to the undigested SNEDDSs droplets [121]. To this regard, the diameter of SNEDDSs was measured by dynamic light scattering (DLS) in

Paper IV, and it was found that undigested SNEDDS had a distinct size (50.89 ± 1.09 nm, polydispersity index 0.38), whereas the diameter of digested SNEDDS was not definable due to high polydispersity (polydispersity index > 0.8), giving an indication of the structural differences between the two species. The results described thus-far are in accordance both i) with the data described by Michaelsen and colleagues [168], where fenofibrate distribution for the same SNEDDSs was evaluated both when lipolysis was inhibited by the addition of the pancreatic lipase inhibitor orlistat and in the presence of lipolysis, and ii) with the results described in Paper III. Thus, the data collected in Paper IV confirm the equivalence between the HTP lipolysis model and the pH-stat lipolysis model.

4.5.1.1 Prediction of *in vivo* absorption data with the HTP *in vitro* lipolysis model

According to the results displayed in Figure 4.16, SNEDDS is the formulation able to provide most of the drug solubilized in the aqueous phase both in the presence and absence of lipolysis, possibly leading to higher drug absorption compared to super-SNEDDS solution and suspension. However, when plotting the AUCs resulting from the amount of fenofibrate found in the aqueous phase overtime for the three SNEDDSs against the AUCs resulting from the *in vivo* plasma exposure of the same SNEDDSs in rats (from Michaelsen et al., 2019, [168]) (Figure 4.17), it is evident that drug solubilization data failed to predict *in vivo* drug absorption. The discrepancy between the *in vivo* and *in vitro* data depicted in Figure 4.17 can be attributed both i) to the fact that *in vitro* drug solubilization experiments produce an overestimation of the amount of drug free for absorption and ii) to the absence of an absorptive sink in the *in vitro* lipolysis experimental setup, as already discussed in Section 4.4.2. Specifically, the overestimation of the drug available for absorption is connected to the fact that *in vitro* dispersion/lipolysis experiments are not able to distinguish between the fraction of drug actually available for permeation (*i.e.* free drug) and the portion associated to the colloidal structures formed upon *in vitro* dispersion/lipolysis, concomitantly present in the aqueous phase [168]. Additionally, it has been proven that precipitation kinetics can be different in the presence of an absorption barrier compared to its absence [94, 200]. In fact, in the presence of an

absorptive sink the drug has the chance of being removed from the digesting compartment, preventing the system from reaching a critical degree of supersaturation, and thus providing an alternative to drug precipitation [94].

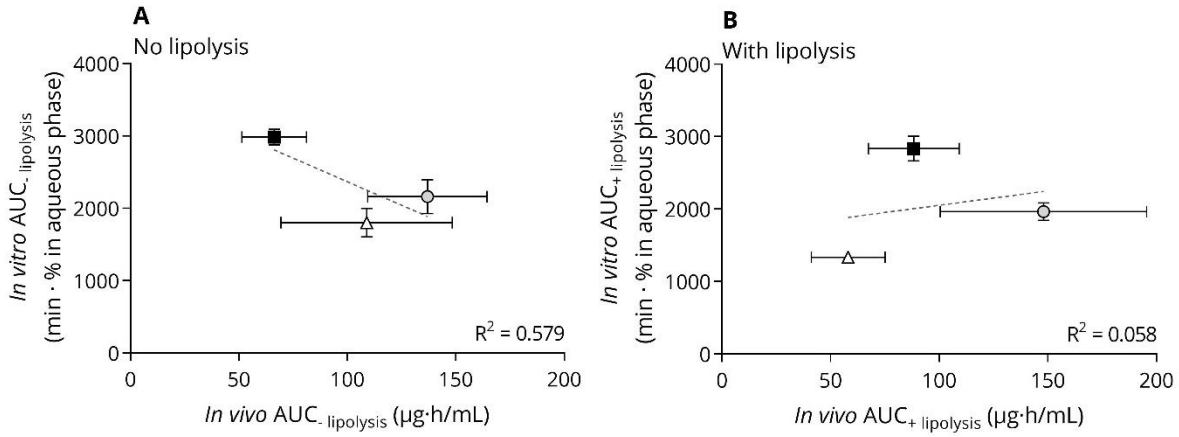

Figure 4.17: Correlation A) in the absence (- lipolysis) and B) presence of lipolysis (+lipolysis) between AUCs resulting from the amount of fenofibrate found *in vitro* in the aqueous phase overtime and AUCs resulting from the *in vivo* plasma curve in rats (from Michaelsen et al., 2019, [168]) for SNEDDS (black square), super-SNEDDS solution (grey circle) and super-SNEDDS suspension (white triangle).

4.5.2 Effect of lipolysis on drug permeation and prediction of *in vivo* drug absorption

To evaluate whether the type of formulation and/or the presence of lipolysis would influence drug permeation, the transfer of fenofibrate from the donor to the acceptor compartment of the mucus-PVPA barriers was determined both in the absence (*i.e.* sole dispersion) and the presence of HTP *in vitro* lipolysis on top of the barriers for SNEDDS, super-SNEDDS solution and super-SNEDDS suspension. To ensure the maintained integrity of the barriers through the permeation experiments, an in-line quantification of CAL permeability was carried out, and at the end of the permeation experiment the electrical resistance across the PVPA barriers was measured. The results obtained in all permeation experiments confirmed the correct functionality of the barriers (*i.e.* CAL permeability < $0.06 \cdot 10^{-6}$ cm/s; electrical resistance > 290 Ohm · cm^2).

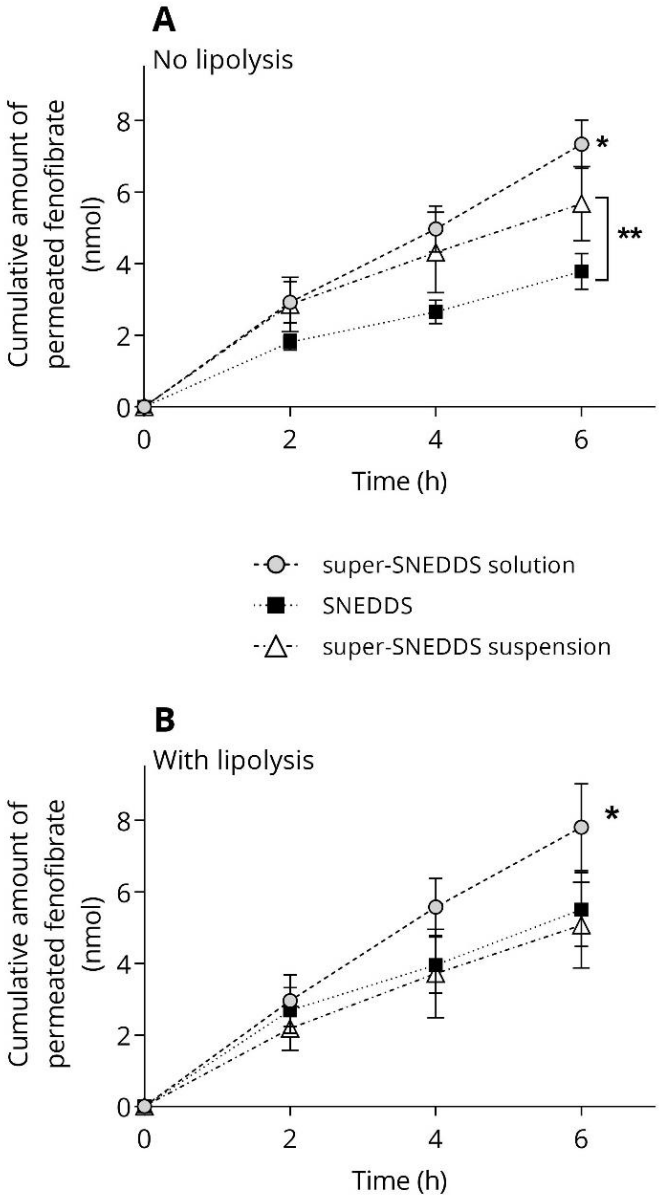

Figure 4.18: Cumulative amount of fenofibrate permeated from SNEDDS (black square), super-SNEDDS solution (grey circle) and super-SNEDDS suspension (white triangle) A) in the absence and B) presence of HTP *in vitro* lipolysis on top of the mucus-PVPA barriers. The results are indicated as mean ± SD (n = 12). * Statistically significant ($p < 0.05$) difference between super-SNEDDS solution and SNEDDS/super-SNEDDS suspension. ** Statistically significant ($p < 0.05$) difference between SNEDDS and super-SNEDDS suspension.

As shown in Figure 4.18, both the type of formulation and the presence of HTP *in vitro* lipolysis on top of the mucus-PVPA barriers had an impact on the permeation of fenofibrate. In particular, super-SNEDDS solution exhibited the highest drug permeation, whereas super-SNEDDS suspension and SNEDDS led to lower fenofibrate transfer across

the barriers in both the absence and presence of lipolysis. Moreover, super-SNEDDS suspension led to significantly higher drug permeation than SNEDDS in the absence of lipolysis (Figure 4.18A), while this difference was not visible in the presence of the digesting process (Figure 4.18B). The change in fenofibrate mass transfer for SNEDDS and super-SNEDDS suspension in the absence compared to the presence of lipolysis can be attributed to the different drug solubilization profiles resulting from these two conditions. Specifically, in the case of SNEDDS, the presence of lipolysis led to higher drug permeation. This was most likely due to the fact that the digesting action of pancreatin provides the liberation of fenofibrate from the SNEDDS droplets, causing an increase in the fraction of drug free and thus available for permeation. This confirms the hypothesis that drug absorption is able to increase only when high drug solubilization is caused by an increase in the fraction of drug free in solution [97]. On the other hand, for super-SNEDDS suspension the presence of lipolysis caused a decrease in drug permeation, which can be ascribed to the increased drug precipitation discussed in Section 4.5.1 and connected to an increase in the thermodynamic instability of the system [95]. The same change in drug permeation observed for SNEDDS and super-SNEDDS suspension was described in the study by Michaelsen and colleagues [168], where the three SNEDDSs were administered to rats both when lipolysis was occurring and when it was inhibited by the use of orlistat (*i.e.* pancreatic lipase inhibitor). As a result of this, the correlation between the *in vitro* permeation data obtained in Paper IV with *in vivo* data from Michaelsen and colleagues in rats was found to be excellent ($R^2 > 0.98$) both in the absence ($R^2 = 0.988$) and presence of lipolysis ($R^2 = 0.991$) (Figure 4.19).

The excellent correlation with *in vivo* data can be due both to the correct simulation of the intestinal lipolysis and permeation processes, and to the reproduction of the physiological structures present in this environment, such as the mucus layer and the permeation membrane. In particular, since it has been suggested that mucus plays an important role in the stabilization of drug supersaturation when SNEDDSs are orally administered, and since this stabilization was found to be drug-specific [98], the inclusion of this layer in an *in vitro* permeation model should be regarded as essential.

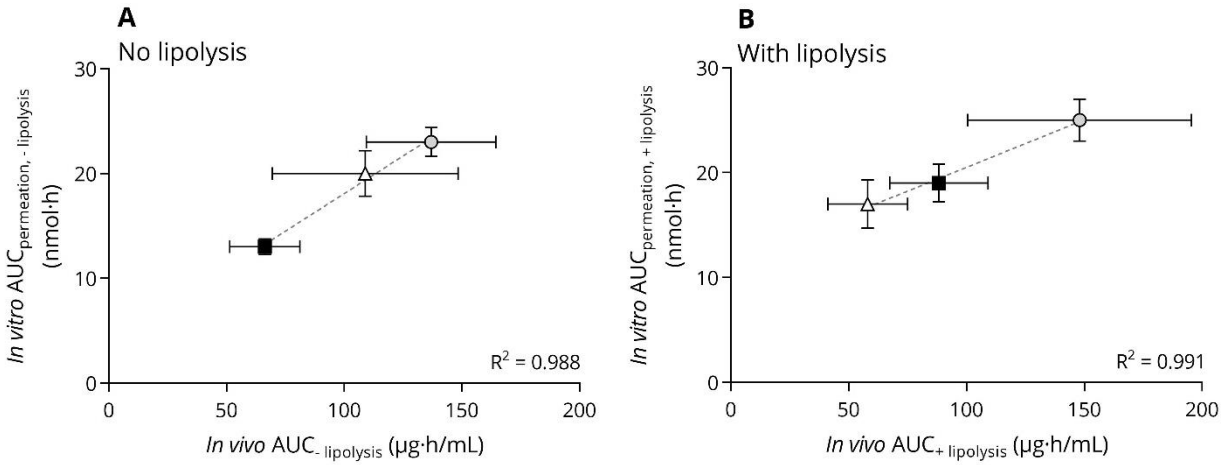

Figure 4.19: Correlation A) in the absence (- lipolysis) and B) presence of lipolysis (+lipolysis) between AUCs resulting from the fenofibrate mass transfer across the mucus-PVPA barriers and AUCs resulting from the *in vivo* plasma curve in rats (from Michaelsen et al., 2019, [168]) for SNEDDS (black square), super-SNEDDS solution (grey circle) and super-SNEDDS suspension (white triangle).

Overall, the *in vitro* model constructed in Paper IV and the results obtained in such study highlight the complexity of the processes affecting the performance of SNEDDSs, emphasizing that the real driving mechanism of drug absorption is the dynamic interaction between drug solubilization, supersaturation and permeation. Even though the experiments were carried out only for one type of formulation and one drug, the model described in Paper IV shows the potential to be used as a valuable tool for the development of new lipid-based formulations.

5 Conclusions

The development of a mucus-comprising *in vitro* permeability model able to mimic the environment of the intestinal mucosa was achieved in the presented work, enabling the prediction of *in vivo* drug absorption.

In particular, the PVPA barriers proved their correct functionality in the presence of both simple (mucin 10 mg/mL) and complex (biosimilar mucus) mucus models, and the developed mucus-PVPA model proved its ability to discriminate between the permeabilities of drugs with different physicochemical properties and between different liposomal formulations. The presence of the mucus layer on top of the PVPA barriers led to changes in drug permeability which were related to its interaction with the specific drug/formulation.

Additionally, the pH environment found in the small intestine was simulated on top of the barriers, and the permeability results obtained exhibited a distinctive pH-dependent trend for ionizable drugs. To increase its biorelevance, the mucus-PVPA model was upgraded with the addition of commercially available fasted and fed state simulated intestinal fluids, and the barriers proved to be particularly stable in the presence of fed state fluids.

Finally, the addition of the digestive environment affecting the oral administration of drug contained in lipid-based formulations was added to the mucus-PVPA model, allowing the assessment of the performance of three fenofibrate-loaded SNEDDSs. Initially, the *in vitro* intestinal lipolysis was combined with the mucus-PVPA barriers, and this combined model proved to predict *in vivo* drug absorption data in rats obtained from the literature for the same formulations. Subsequently, the addition of a pH-stat-titrator independent *in vitro* lipolysis model (*i.e.* the HTP *in vitro* lipolysis model) on top of the mucus-PVPA barriers enabled *in vitro* lipolysis and drug permeation to occur simultaneously. This final lipolysis-permeation model predicted *in vivo* drug absorption for the three fenofibrate-loaded SNEDDSs to the same extent as the combined model, demonstrating the applicability for the use of the simultaneous model for the optimization of novel lipid-based formulations.

6 Perspectives

To validate the prediction potential of the simultaneous *in vitro* lipolysis-permeation model in terms of *in vivo* drug absorption, a plethora of different lipid-based formulations containing drugs with different physicochemical characteristics should be studied with the developed model and compared to *in vivo* data.

Furthermore, an improved quantification of the amount of drug solubilized in the aqueous phase in the donor compartment of the mucus-PVPA barriers should be implemented, with a special focus on the distinction between the portion of free drug and the one associated with colloidal structures.

The use of the previously developed $PVPA_{biomimetic}$ barriers instead of the original PVPA could allow the evaluation of the impact of mucus on the permeation of drug contained in lipid-based formulations, avoiding the barrier impairment events observed when SNEDDSs were applied on top of PVPA barriers in the absence of mucus.

Once a significant number of drug and formulations have been tested with the simultaneous *in vitro* lipolysis-permeation model and the prediction potential of such model has been demonstrated, *in silico* modelling could be implemented by combining the obtained *in vitro* data with *in vivo* data.

References

[1] M. Vertzoni, P. Augustijns, M. Grimm, M. Koziolek, G. Lemmens, N. Parrott, C. Pentafragka, C. Reppas, J. Rubbens, J. Van Den Alphabeele, T. Vanuytsel, W. Weitschies, C.G. Wilson, Impact of regional differences along the gastrointestinal tract of healthy adults on oral drug absorption: An UNGAP review, Eur J Pharm Sci, 134 (2019) 153-175.

[2] C. Stillhart, K. Vucicevic, P. Augustijns, A.W. Basit, H. Batchelor, T.R. Flanagan, I. Gesquiere, R. Greupink, D. Keszthelyi, M. Koskinen, C.M. Madla, C. Matthys, G. Miljus, M.G. Mooij, N. Parrott, A.L. Ungell, S.N. de Wildt, M. Orlu, S. Klein, A. Mullertz, Impact of gastrointestinal physiology on drug absorption in special populations--An UNGAP review, Eur J Pharm Sci, 147 (2020) 105280.

[3] P. Augustijns, M. Vertzoni, C. Reppas, P. Langguth, H. Lennernas, B. Abrahamsson, W.L. Hasler, J.R. Baker, T. Vanuytsel, J. Tack, M. Corsetti, M. Bermejo, P. Paixao, G.L. Amidon, B. Hens, Unraveling the behavior of oral drug products inside the human gastrointestinal tract using the aspiration technique: History, methodology and applications, Eur J Pharm Sci, 155 (2020) 105517.

[4] M. Grimm, M. Koziolek, M. Saleh, F. Schneider, G. Garbacz, J.P. Kuhn, W. Weitschies, Gastric Emptying and Small Bowel Water Content after Administration of Grapefruit Juice Compared to Water and Isocaloric Solutions of Glucose and Fructose: A Four-Way Crossover MRI Pilot Study in Healthy Subjects, Mol Pharm, 15 (2018) 548-559.

[5] M. Koziolek, M. Grimm, F. Schneider, P. Jedamzik, M. Sager, J.P. Kuhn, W. Siegmund, W. Weitschies, Navigating the human gastrointestinal tract for oral drug delivery: Uncharted waters and new frontiers, Adv Drug Deliv Rev, 101 (2016) 75-88.

[6] R. Holm, A. Mullertz, H. Mu, Bile salts and their importance for drug absorption, Int J Pharm, 453 (2013) 44-55.

[7] A. Diakidou, M. Vertzoni, K. Goumas, E. Soderlind, B. Abrahamsson, J. Dressman, C. Reppas, Characterization of the contents of ascending colon to which drugs are exposed after oral administration to healthy adults, Pharm Res, 26 (2009) 2141-2151.

[8] M. Koziolek, S. Alcaro, P. Augustijns, A.W. Basit, M. Grimm, B. Hens, C.L. Hoad, P. Jedamzik, C.M. Madla, M. Maliepaard, L. Marciani, A. Maruca, N. Parrott, P. Pavek, C.J.H. Porter, C. Reppas, D. van Riet-Nales, J. Rubbens, M. Statelova, N.L. Trevaskis, K. Valentova, M. Vertzoni, D.V. Cepo, M. Corsetti, The mechanisms of pharmacokinetic food-drug interactions - A perspective from the UNGAP group, Eur J Pharm Sci, 134 (2019) 31-59.

[9] H. Clevers, The intestinal crypt, a prototype stem cell compartment, Cell, 154 (2013) 274-284.

[10] L. Sardelli, D.P. Pacheco, A. Ziccarelli, M. Tunesi, O. Caspani, A. Fusari, F. Briatico Vangosa, C. Giordano, P. Petrini, Towards bioinspired in vitro models of intestinal mucus, RSC Advances, 9 (2019) 15887-15899.

[11] F. Taherali, F. Varum, A.W. Basit, A slippery slope: On the origin, role and physiology of mucus, Adv Drug Deliv Rev, 124 (2018) 16-33.

[12] R. Bansil, B.S. Turner, The biology of mucus: Composition, synthesis and organization, Adv Drug Deliv Rev, 124 (2018) 3-15.

[13] M.E. Johansson, H. Sjovall, G.C. Hansson, The gastrointestinal mucus system in health and disease, Nat Rev Gastroenterol Hepatol, 10 (2013) 352-361.

[14] L.H. Nielsen, A. Melero, S.S. Keller, J. Jacobsen, T. Garrigues, T. Rades, A. Mullertz, A. Boisen, Polymeric microcontainers improve oral bioavailability of furosemide, Int J Pharm, 504 (2016) 98-109.

[15] J. Leal, H.D.C. Smyth, D. Ghosh, Physicochemical properties of mucus and their impact on transmucosal drug delivery, Int J Pharm, 532 (2017) 555-572.

[16] G. Ruiz-Pulido, D.I. Medina, An overview of gastrointestinal mucus rheology under different pH conditions and introduction to pH-dependent rheological interactions with PLGA and chitosan nanoparticles, Eur J Pharm Biopharm, (2020).

[17] O. Lieleg, I. Vladescu, K. Ribbeck, Characterization of particle translocation through mucin hydrogels, Biophys J, 98 (2010) 1782-1789.

[18] N.A. Peppas, Y. Huang, Nanoscale technology of mucoadhesive interactions, Adv Drug Deliv Rev, 56 (2004) 1675-1687.

[19] K. Khanvilkar, M.D. Donovan, D.R. Flanagan, Drug transfer through mucus, Adv Drug Deliv Rev, 48 (2001) 173-193.

[20] R. Bansil, B.S. Turner, Mucin structure, aggregation, physiological functions and biomedical applications, Current Opinion in Colloid & Interface Science, 11 (2006) 164-170.

[21] M. Boegh, H.M. Nielsen, Mucus as a barrier to drug delivery - understanding and mimicking the barrier properties, Basic Clin Pharmacol Toxicol, 116 (2015) 179-186.

[22] X. Murgia, B. Loretz, O. Hartwig, M. Hittinger, C.M. Lehr, The role of mucus on drug transport and its potential to affect therapeutic outcomes, Adv Drug Deliv Rev, 124 (2018) 82-97.

[23] B.S. Turner, K.R. Bhaskar, M. Hadzopoulou-Cladaras, J.T. LaMont, Cysteine-rich regions of pig gastric mucin contain von Willebrand factor and cystine knot domains at the carboxyl terminal, Biochimica et Biophysica Acta, 1447 (1999) 77-92.

[24] S.S. Olmsted, J.L. Padgett, A.I. Yudin, K.J. Whaley, T.R. Moench, R.A. Cone, Diffusion of Macromolecules and Virus-Like Particles in Human Cervical Mucus, Biophysical Journal, 81 (2001) 1930-1937.

[25] A.C. Groo, F. Lagarce, Mucus models to evaluate nanomedicines for diffusion, Drug Discov Today, 19 (2014) 1097-1108.

[26] X. Cao, R. Bansil, K.R. Bhaskar, B.S. Turner, J.T. LaMont, N. Niu, N.H. Afdhal, pH-Dependent Conformational Change of Gastric Mucin Leads to Sol-Gel Transition, Biophysical Journal, 76 (1999) 1250-1258.

[27] E. Marxen, M.D. Mosgaard, A.M.L. Pedersen, J. Jacobsen, Mucin dispersions as a model for the oromucosal mucus layer in in vitro and ex vivo buccal permeability studies of small molecules, Eur J Pharm Biopharm, 121 (2017) 121-128.

[28] C.A. Bergstrom, R. Holm, S.A. Jorgensen, S.B. Andersson, P. Artursson, S. Beato, A. Borde, K. Box, M. Brewster, J. Dressman, K.I. Feng, G. Halbert, E. Kostewicz, M. McAllister, U. Muenster, J. Thinnes, R. Taylor, A. Mullertz, Early pharmaceutical profiling to predict oral drug absorption: current status and unmet needs, Eur J Pharm Sci, 57 (2014) 173-199.

[29] S. Clarysse, J. Brouwers, J. Tack, P. Annaert, P. Augustijns, Intestinal drug solubility estimation based on simulated intestinal fluids: comparison with solubility in human intestinal fluids, Eur J Pharm Sci, 43 (2011) 260-269.

[30] L. Kalantzi, K. Goumas, V. Kalioras, B. Abrahamsson, J.B. Dressman, C. Reppas, Characterization of the human upper gastrointestinal contents under conditions simulating bioavailability/bioequivalence studies, Pharm Res, 23 (2006) 165-176.

[31] P.B. Pedersen, P. Vilmann, D. Bar-Shalom, A. Mullertz, S. Baldursdottir, Characterization of fasted human gastric fluid for relevant rheological parameters and gastric lipase activities, Eur J Pharm Biopharm, 85 (2013) 958-965.

[32] D. Riethorst, R. Mols, G. Duchateau, J. Tack, J. Brouwers, P. Augustijns, Characterization of Human Duodenal Fluids in Fasted and Fed State Conditions, J Pharm Sci, 105 (2016) 673-681.

[33] D. Riethorst, P. Baatsen, C. Remijn, A. Mitra, J. Tack, J. Brouwers, P. Augustijns, An In-Depth View into Human Intestinal Fluid Colloids: Intersubject Variability in Relation to Composition, Mol Pharm, 13 (2016) 3484-3493.

[34] D. Riethorst, A. Mitra, F. Kesisoglou, W. Xu, J. Tack, J. Brouwers, P. Augustijns, Human intestinal fluid layer separation: The effect on colloidal structures & solubility of lipophilic compounds, Eur J Pharm Biopharm, 129 (2018) 104-110.

[35] C. Litou, D. Psachoulias, M. Vertzoni, J. Dressman, C. Reppas, Measuring pH and Buffer Capacity in Fluids Aspirated from the Fasted Upper Gastrointestinal Tract of Healthy Adults, Pharm Res, 37 (2020) 42.

[36] B.J. Boyd, C.A.S. Bergstrom, Z. Vinarov, M. Kuentz, J. Brouwers, P. Augustijns, M. Brandl, A. Bernkop-Schnurch, N. Shrestha, V. Preat, A. Mullertz, A. Bauer-Brandl, V. Jannin, Successful oral delivery of poorly water-soluble drugs both depends on the intraluminal behavior of drugs and of appropriate advanced drug delivery systems, Eur J Pharm Sci, 137 (2019) 104967.

[37] B. Hens, M. Corsetti, R. Spiller, L. Marciani, T. Vanuytsel, J. Tack, A. Talattof, G.L. Amidon, M. Koziolek, W. Weitschies, C.G. Wilson, R.J. Bennink, J. Brouwers, P. Augustijns, Exploring gastrointestinal variables affecting drug and formulation behavior: Methodologies, challenges and opportunities, Int J Pharm, 519 (2017) 79-97.

[38] D. Dahlgren, H. Lennernas, Intestinal Permeability and Drug Absorption: Predictive Experimental, Computational and In Vivo Approaches, Pharmaceutics, 11 (2019).

[39] K. Sugano, M. Kansy, P. Artursson, A. Avdeef, S. Bendels, L. Di, G.F. Ecker, B. Faller, H. Fischer, G. Gerebtzoff, H. Lennernaes, F. Senner, Coexistence of passive and carrier-mediated processes in drug transport, Nature Reviews, 9 (2010) 597-614.

[40] S.B. Kapitza, B.R. Michel, P. van Hoogevest, M.L. Leigh, G. Imanidis, Absorption of poorly water soluble drugs subject to apical efflux using phospholipids as solubilizers in the Caco-2 cell model, Eur J Pharm Biopharm, 66 (2007) 146-158.

[41] A.T. Florence,N. Hussain, Transcytosis of nanoparticle and dendrimer delivery systems: evolving vistas, Adv Drug Deliv Rev, 50 (2001) S69-S89.

[42] P. Berben, J. Brouwers, P. Augustijns, Assessment of Passive Intestinal Permeability Using an Artificial Membrane Insert System, J Pharm Sci, 107 (2018) 250-256.

[43] P. Artursson, A.L. Ungell, J.E. Lofroth, Selective paracellular permeability in two models of intestinal absorption: cultured monolayers of human intestinal epithelial cells and rat intestinal segments, Pharm. Res., 10(8) (1993) 1123-1129.

[44] P. Berben, A. Bauer-Brandl, M. Brandl, B. Faller, G.E. Flaten, A.C. Jacobsen, J. Brouwers, P. Augustijns, Drug permeability profiling using cell-free permeation tools: Overview and applications, Eur J Pharm Sci, 119 (2018) 219-233.

[45] C.J. Porter, N.L. Trevaskis, W.N. Charman, Lipids and lipid-based formulations: optimizing the oral delivery of lipophilic drugs, Nat Rev Drug Discov, 6 (2007) 231-248.

[46] C.A. Lipinski, Drug-like properties and the causes of poor solubility and poor permeability, J. Pharmacol. Toxicol. Methods, 44 (2000) 235-249.

[47] G.L. Amidon, H. Lennernas, V.P. Shah, J.R. Crison, A theoretical basis for a biopharmaceitoc drug classification: the correlation of in vitro drug product dissolution and in vivo bioavailability, Pharm. Res., 12 (3) (1995) 413-420.

[48] P. Sieger, Y. Cui, S. Scheuerer, pH-dependent solubility and permeability profiles: A useful tool for prediction of oral bioavailability, Eur J Pharm Sci, 105 (2017) 82-90.

[49] A. Teleki, O. Nylander, C.A.S. Bergstrom, Intrinsic Dissolution Rate Profiling of Poorly Water-Soluble Compounds in Biorelevant Dissolution Media, Pharmaceutics, 12 (2020).

[50] A.V. Thomae, H. Wunderli-Allenspach, S.D. Kramer, Permeation of aromatic carboxylic acids across lipid bilayers: the pH-partition hypothesis revisited, Biophys J, 89 (2005) 1802-1811.

[51] P.A. Shore, B.B. Brodie, C.A.M. Hogben, The gastric secretion of drugs: a pH partition hypothesis, J. Pharmacol. Experimental Therapeutics, 119 (3) (1957) 361-369.

[52] A.Y. Abuhelwa, D.J.R. Foster, R.N. Upton, A Quantitative Review and Meta-Models of the Variability and Factors Affecting Oral Drug Absorption-Part I: Gastrointestinal pH, AAPS J, 18 (2016) 1309-1321.

[53] R. Hamed, A. Awadallah, S. Sunoqrot, O. Tarawneh, S. Nazzal, T. AlBaraghthi, J. Al Sayyad, A. Abbas, pH-Dependent Solubility and Dissolution Behavior of Carvedilol--Case Example of a Weakly Basic BCS Class II Drug, AAPS PharmSciTech, 17 (2016) 418-426.

[54] A. Kambayashi, J.B. Dressman, Predicting the Changes in Oral Absorption of Weak Base Drugs Under Elevated Gastric pH Using an In Vitro-In Silico-In Vivo Approach: Case Examples-Dipyridamole, Prasugrel, and Nelfinavir, J Pharm Sci, 108 (2019) 584-591.

[55] C.A. Bergstrom, K. Luthman, P. Artursson, Accuracy of calculated pH-dependent aqueous drug solubility, Eur J Pharm Sci, 22 (2004) 387-398.

[56] J.H. Fagerberg, O. Tsinman, N. Sun, K. Tsinman, A. Avdeef, C.A.S. Bergstrom, Dissolution Rate and Apparent Solubility of Poorly Soluble Drugs in Biorelevant Dissolution Media, Mol. Pharm., 7 (5) (2010) 1419-1430.

[57] C.A.S. Bergstrom, C.M. Wassvik, K. Johansson, I. Hubatsch, Poorly Soluble Marketed Drugs Display Solvation Limited Solubility, J. Med. Chem., 50 (2007) 5858-5862.

[58] L.S. Taylor, G.G.Z. Zhang, Physical chemistry of supersaturated solutions and implications for oral absorption, Adv Drug Deliv Rev, 101 (2016) 122-142.

[59] L. Klumpp, M. Leigh, J. Dressman, Dissolution behavior of various drugs in different FaSSIF versions, Eur J Pharm Sci, 142 (2020) 105138.

[60] C.M. Madsen, K.I. Feng, A. Leithead, N. Canfield, S.A. Jorgensen, A. Mullertz, T. Rades, Effect of composition of simulated intestinal media on the solubility of poorly soluble compounds investigated by design of experiments, Eur J Pharm Sci, 111 (2018) 311-319.

[61] B.N. Singh, A quantitative approach to probe the dependence and correlation of food-effect with aqueous solubility, dose/solubility ratio, and partition coefficient (LogP) for orally active drugs administered as immediate-release formulations, Drug Development Research, 65 (2005) 55-75.

[62] A.E. Riedmaier, K. DeMent, J. Huckle, P. Bransford, C. Stillhart, R. Lloyd, R. Alluri, S. Basu, Y. Chen, V. Dhamankar, S. Dodd, P. Kulkarni, A. Olivares-Morales, C.C. Peng, X. Pepin, X. Ren, T. Tran, C. Tistaert, T. Heimbach, F. Kesisoglou, C. Wagner, N. Parrott, Use of Physiologically Based Pharmacokinetic (PBPK) Modeling for Predicting Drug-Food Interactions: an Industry Perspective, AAPS J, 22 (2020) 123.

[63] M.L. Christiansen, R. Holm, B. Abrahamsson, J. Jacobsen, J. Kristensen, J.R. Andersen, A. Mullertz, Effect of food intake and co-administration of placebo self-nanoemulsifying drug delivery systems on the absorption of cinnarizine in healthy human volunteers, Eur J Pharm Sci, 84 (2016) 77-82.

[64] A.W. Larhed, P. Artursson, E. Bjork, The influence of intestinal mucus components on the diffusion of drugs, Pharm Res, 15 (1998) 66-71.

[65] A.W. Larhed, P. Artursson, J. Gråsjo, E. Bjork, Diffusion of Drugs in Native and Purified Gastrointestinal Mucus, J Pharm Sci, 86 (6) (1997) 660-665.

[66] L.R. Shaw, W.J. Irwin, T.J. Grattan, B.R. Conway, The influence of excipients on the diffusion of ibuprofen and paracetamol in gastric mucus, Int J Pharm, 290 (2005) 145-154.

[67] H.H. Sigurdsson, J. Kirch, C.M. Lehr, Mucus as a barrier to lipophilic drugs, Int J Pharm, 453 (2013) 56-64.

[68] J.P. Gleeson, F. McCartney, Striving Towards the Perfect In Vitro Oral Drug Absorption Model, Trends Pharmacol Sci, 40 (2019) 720-724.

[69] B.J. Teubl, M. Absenger, E. Frohlich, G. Leitinger, A. Zimmer, E. Roblegg, The oral cavity as a biological barrier system: design of an advanced buccal in vitro permeability model, Eur J Pharm Biopharm, 84 (2013) 386-393.

[70] C.J. Porter, C.W. Pouton, J.F. Cuine, W.N. Charman, Enhancing intestinal drug solubilisation using lipid-based delivery systems, Adv Drug Deliv Rev, 60 (2008) 673-691.

[71] U.S. Food and Drug Administration, New drugs at FDA: CDER's new molecular entities and new therapeutic biological products, 2020.

[72] Y. Kawabata, K. Wada, M. Nakatani, S. Yamada, S. Onoue, Formulation design for poorly water-soluble drugs based on biopharmaceutics classification system: basic approaches and practical applications, Int J Pharm, 420 (2011) 1-10.

[73] O.J. Hedge, C.A.S. Bergstrom, Suitability of Artificial Membranes in Lipolysis-Permeation Assays of Oral Lipid-Based Formulations, Pharm Res, 37 (2020) 99.

[74] C.W. Pouton, Formulation of poorly water-soluble drugs for oral administration: physicochemical and physiological issues and the lipid formulation classification system, Eur J Pharm Sci, 29 (2006) 278-287.

[75] A. Mullertz, A. Ogbonna, S. Ren, T. Rades, New perspectives on lipid and surfactant based drug delivery systems for oral delivery of poorly soluble drugs, J Pharm Pharmacol, 62 (2010) 1622-1636.

[76] S. Drescher, P. van Hoogevest, The Phospholipid Research Center: Current Research in Phospholipids and Their Use in Drug Delivery, Pharmaceutics, 12 (2020).

[77] R. Savla, J. Browne, V. Plassat, K.M. Wasan, E.K. Wasan, Review and analysis of FDA approved drugs using lipid-based formulations, Drug Dev Ind Pharm, 43 (2017) 1743-1758.

[78] A.D. Bangham, M.M. Standish, J.C. Watkins, Diffusion of Univalent Ions across the Lamellae of Swollen Phospholipids, J Mol Biol, 13 (1965) 238-252.

[79] Y. Xu, C.B. Michalowski, A. Beloqui, Advances in lipid carriers for drug delivery to the gastrointestinal tract, Current Opinion in Colloid & Interface Science, (2020).

[80] K. Netsomboon, A. Bernkop-Schnurch, Mucoadhesive vs. mucopenetrating particulate drug delivery, Eur J Pharm Biopharm, 98 (2016) 76-89.

[81] T. Klemetsrud, A.L. Kjoniksen, M. Hiorth, J. Jacobsen, G. Smistad, Polymer coated liposomes for use in the oral cavity - a study of the in vitro toxicity, effect on cell permeability and interaction with mucin, J Liposome Res, 28 (2018) 62-73.

[82] A.B. Buya, A. Beloqui, P.B. Memvanga, V. Preat, Self-Nano-Emulsifying Drug-Delivery Systems: From the Development to the Current Applications and Challenges in Oral Drug Delivery, Pharmaceutics, 12 (2020).

[83] N.L. Trevaskis, W.N. Charman, C.J. Porter, Lipid-based delivery systems and intestinal lymphatic drug transport: a mechanistic update, Adv Drug Deliv Rev, 60 (2008) 702-716.

[84] G. Lee, S. Han, Z. Lu, J. Hong, A.R.J. Phillips, J.A. Windsor, C.J.H. Porter, N.L. Trevaskis, Intestinal delivery in a long-chain fatty acid formulation enables lymphatic transport and systemic exposure of orlistat, Int J Pharm, (2021) 120247.

[85] E.J.A. Suys, D.H.S. Brundel, D.K. Chalmers, C.W. Pouton, C.J.H. Porter, Interaction with biliary and pancreatic fluids drives supersaturation and drug absorption from lipid-based formulations of low (saquinavir) and high (fenofibrate) permeability poorly soluble drugs, J Control Release, 331 (2021) 45-61.

[86] T. Tran, P. Bonlokke, C. Rodriguez-Rodriguez, Z. Nosrati, P.L. Esquinas, N. Borkar, J. Plum, S. Strindberg, S. Karagiozov, T. Rades, A. Mullertz, K. Saatchi, U.O. Hafeli, Using in vitro lipolysis and SPECT/CT in vivo imaging to understand oral absorption of fenofibrate from lipid-based drug delivery systems, J Control Release, 317 (2020) 375-384.

[87] S. Kamboj, S. Sethi, V. Rana, Lipid based delivery of Efavirenz: An answer to its erratic absorption and food effect, Eur J Pharm Sci, 123 (2018) 199-216.

[88] D.G. Fatouros, B. Bergenstahl, A. Mullertz, Morphological observations on a lipid-based drug delivery system during in vitro digestion, Eur J Pharm Sci, 31 (2007) 85-94.

[89] G.A. Kossena, W.N. Charman, B.J. Boyd, C.J. Porter, Influence of the intermediate digestion phases of common formulation lipids on the absorption of a poorly water-soluble drug, J Pharm Sci, 94 (2005) 481-492.

[90] R. Berthelsen, M. Klitgaard, T. Rades, A. Mullertz, In vitro digestion models to evaluate lipid based drug delivery systems; present status and current trends, Adv Drug Deliv Rev, 142 (2019) 35-49.

[91] M.U. Anby, H.D. Williams, M. McIntosh, H. Benameur, G.A. Edwards, C.W. Pouton, C.J. Porter, Lipid digestion as a trigger for supersaturation: evaluation of the impact of supersaturation stabilization on the in vitro and in vivo performance of self-emulsifying drug delivery systems, Mol Pharm, 9 (2012) 2063-2079.

[92] A. Elkhabaz, D.E. Moseson, J. Brouwers, P. Augustijns, L.S. Taylor, Interplay of Supersaturation and Solubilization: Lack of Correlation between Concentration-Based Supersaturation Measurements and Membrane Transport Rates in Simulated and Aspirated Human Fluids, Mol Pharm, 16 (2019) 5042-5053.

[93] M. Kataoka, S. Takeyama, K. Minami, H. Higashino, K. Kakimi, Y. Fujii, M. Takahashi, S. Yamashita, In Vitro Assessment of Supersaturation/Precipitation and Biological Membrane Permeation of Poorly Water-Soluble Drugs: A Case Study With Albendazole and Ketoconazole, J Pharm Sci, 108 (2019) 2580-2587.

[94] J. Bevernage, J. Brouwers, P. Annaert, P. Augustijns, Drug precipitation-permeation interplay: supersaturation in an absorptive environment, Eur J Pharm Biopharm, 82 (2012) 424-428.

[95] Y. Tanaka, E. Tay, T.H. Nguyen, C.J.H. Porter, Quantifying In Vivo Luminal Drug Solubilization - Supersaturation-Precipitation Profiles to Explain the Performance of Lipid Based Formulations, Pharm Res, 37 (2020) 47.

[96] N. Thomas, R. Holm, A. Mullertz, T. Rades, In vitro and in vivo performance of novel supersaturated self-nanoemulsifying drug delivery systems (super-SNEDDS), J Control Release, 160 (2012) 25-32.

[97] Y.Y. Yeap, N.L. Trevaskis, C.J. Porter, Lipid absorption triggers drug supersaturation at the intestinal unstirred water layer and promotes drug absorption from mixed micelles, Pharm Res, 30 (2013) 3045-3058.
[98] Y.Y. Yeap, J. Lock, S. Lerkvikarn, T. Semin, N. Nguyen, R.L. Carrier, Intestinal mucus is capable of stabilizing supersaturation of poorly water-soluble drugs, J Control Release, 296 (2019) 107-113.

[99] S.M. Khoo, D.M. Shackleford, C.J.H. Porter, G.A. Edwards, W.N. Charman, Intestinal Lymphatic Transport of Halofantrine Occurs after Oral Administration of a Unit-Dose Lipid-Based Formulation to Fasted Dogs, Pharm Res, 20 (9) (2003) 1460-1465.

[100] N.B. Robinson, K. Krieger, F.M. Khan, W. Huffman, M. Chang, A. Naik, R. Yongle, I. Hameed, K. Krieger, L.N. Girardi, M. Gaudino, The current state of animal models in research: A review, Int J Surg, 72 (2019) 9-13.

[101] M. Schweinlin, A. Rossi, N. Lodes, C. Lotz, S. Hackenberg, M. Steinke, H. Walles, F. Groeber, Human barrier models for the in vitro assessment of drug delivery, Drug Deliv Transl Res, 7 (2017) 217-227.

[102] P.A. Billat, E. Roger, S. Faure, F. Lagarce, Models for drug absorption from the small intestine: where are we and where are we going?, Drug Discov Today, 22 (2017) 761-775.

[103] C. Markopoulos, C.J. Andreas, M. Vertzoni, J. Dressman, C. Reppas, In-vitro simulation of luminal conditions for evaluation of performance of oral drug products: Choosing the appropriate test media, Eur J Pharm Biopharm, 93 (2015) 173-182.

[104] J. Butler, B. Hens, M. Vertzoni, J. Brouwers, P. Berben, J. Dressman, C.J. Andreas, K.J. Schaefer, J. Mann, M. McAllister, M. Jamei, E. Kostewicz, F. Kesisoglou, P. Langguth, M. Minekus, A. Mullertz, R. Schilderink, M. Koziolek, P. Jedamzik, W. Weitschies, C. Reppas, P. Augustijns, In vitro models for the prediction of in vivo performance of oral dosage forms: Recent progress from partnership through the IMI OrBiTo collaboration, Eur J Pharm Biopharm, 136 (2019) 70-83.

[105] E. Galia, E. Nicolaides, D. Horter, R. Lobenberg, C. Reppas, J.B. Dressman, Evaluation of various dissolution media for predicting in vivo performance of class I and II drugs, Pharm Res, 15 (5) (1998) 698-705.

[106] E. Jantratid, N. Janssen, C. Reppas, J.B. Dressman, Dissolution media simulating conditions in the proximal human gastrointestinal tract: an update, Pharm Res, 25 (2008) 1663-1676.

[107] P. Augustijns, B. Wuyts, B. Hens, P. Annaert, J. Butler, J. Brouwers, A review of drug solubility in human intestinal fluids: implications for the prediction of oral absorption, Eur J Pharm Sci, 57 (2014) 322-332.

[108] J.B. Dressman, M. Vertzoni, K. Goumas, C. Reppas, Estimating drug solubility in the gastrointestinal tract, Adv Drug Deliv Rev, 59 (2007) 591-602.

[109] N.H. Zangenberg, A. Mullertz, H.G. Kristensen, L. Hovgaard, A dynamic in vitro lipolysis model I. Controlling the rate of lipolysis by continuous addition of calcium, Eur J Pharm Sci, 14 (2001) 115-122.

[110] A. Dahan, A. Hoffman, Use of a dynamic in vitro lipolysis model to rationalize oral formulation development for poor water soluble drugs: correlation with in vivo data and the relationship to intra-enterocyte processes in rats, Pharm Res, 23 (2006) 2165-2174.

[111] P. Sassene, K. Kleberg, H.D. Williams, J.C. Bakala-N'Goma, F. Carriere, M. Calderone, V. Jannin, A. Igonin, A. Partheil, D. Marchaud, E. Jule, J. Vertommen, M. Maio, R. Blundell, H. Benameur, C.J. Porter, C.W. Pouton, A. Mullertz, Toward the establishment of standardized in vitro tests for lipid-based formulations, part 6: effects of varying pancreatin and calcium levels, AAPS J, 16 (2014) 1344-1357.

[112] P.J. Sassene, M.H. Michaelsen, M.D. Mosgaard, M.K. Jensen, E. Van Den Broek, K.M. Wasan, H. Mu, T. Rades, A. Mullertz, In Vivo Precipitation of Poorly Soluble Drugs from Lipid-Based Drug Delivery Systems, Mol Pharm, 13 (2016) 3417-3426.

[113] F. Carriere, C. Renou, V. Lopez, J. De Caro, F. Ferrato, H. Lengsfeld, A. De Caro, R. Laugier, R. Verger, The specific activities of human digestive lipases measured from the in vivo and in vitro lipolysis of test meals, Gastroenterology, 119 (2000) 949-960.

[114] A. Brodkorb, L. Egger, M. Alminger, P. Alvito, R. Assuncao, S. Ballance, T. Bohn, C. Bourlieu-Lacanal, R. Boutrou, F. Carriere, A. Clemente, M. Corredig, D. Dupont, C. Dufour, C. Edwards, M. Golding, S. Karakaya, B. Kirkhus, S. Le Feunteun, U. Lesmes, A. Macierzanka, A.R. Mackie, C. Martins, S. Marze, D.J. McClements, O. Menard, M. Minekus, R. Portmann, C.N. Santos, I. Souchon, R.P. Singh, G.E. Vegarud, M.S.J. Wickham, W. Weitschies, I. Recio, INFOGEST static in vitro simulation of gastrointestinal food digestion, Nat Protoc, 14 (2019) 991-1014.

[115] P. Capolino, C. Guérin, J. Paume, J. Giallo, J.-M. Ballester, J.-F. Cavalier, F. Carrière, In Vitro Gastrointestinal Lipolysis: Replacement of Human Digestive Lipases by a Combination of Rabbit Gastric and Porcine Pancreatic Extracts, Food Digestion, 2 (2011) 43-51.

[116] M. Armand, P. Borel, P. Ythier, G. Dutot, C. Melin, M. Senft, H. Lafont, D. Lairon, Effects of droplet size, triacylglycerol composition, and calcium on the hydrolysis of complex emulsions by pancreatic lipase: an in vitro study, J Nutr Biochem, 3 (1992) 333-341.

[117] J.E. Staggers, O. Hernell, R.J. Stafford, M.C. Carey, Physical-Chemical Behavior of Dietary and Biliary Lipids during Intestinal Digestion and Absorption. 1. Phase Behavior and Aggregation States of Model Lipid Systems Patterned after Aqueous Duodenal Contents of Healthy Adult Human Beings, Biochemistry, 29 (1990) 2028-2040.

[118] A.T. Larsen, P. Sassene, A. Mullertz, In vitro lipolysis models as a tool for the characterization of oral lipid and surfactant based drug delivery systems, Int J Pharm, 417 (2011) 245-255.

[119] K.J. MacGregor, J.K. Embleton, J.E. Lacy, E.A. Perry, L.J. Solomon, H. Seager, C.W. Pouton, Influence of lipolysis on drug absorption from the gastro-intestinal tract, Adv Drug Deliv Rev, 25 (1997) 33-46.

[120] J. Keemink, E. Martensson, C.A.S. Bergstrom, Lipolysis-Permeation Setup for Simultaneous Study of Digestion and Absorption in Vitro, Mol Pharm, 16 (2019) 921-930.

[121] M.D. Mosgaard, P. Sassene, H. Mu, T. Rades, A. Mullertz, Development of a high-throughput in vitro intestinal lipolysis model for rapid screening of lipid-based drug delivery systems, Eur J Pharm Biopharm, 94 (2015) 493-500.

[122] M.D. Mosgaard, P.J. Sassene, H. Mu, T. Rades, A. Mullertz, High-Throughput Lipolysis in 96-Well Plates for Rapid Screening of Lipid-Based Drug Delivery Systems, J Pharm Sci, 106 (2017) 1183-1186.

[123] A.K. Mandagere, T.N. Thompson, K.K. Hwang, Graphical Model for Estimating Oral Bioavailability of Drugs in Humans and Other Species from Their Caco-2 Permeability and in Vitro Liver Enzyme Metabolic Stability Rates, J Med Chem, 45 (2002) 304-311.

[124] M. Kansy, F. Senner, K. Gubernator, Physicochemical High Throughput Screening: Parallel Artificial Membrane Permeation Assay in the Description of Passive Absorption Processes, J Med Chem, 41 (7) (1998) 1007-1010.

[125] M. Bermejo, A. Avdeef, A. Ruiz, R. Nalda, J.A. Ruell, O. Tsinman, I. Gonzalez, C. Fernandez, G. Sanchez, T.M. Garrigues, V. Merino, PAMPA--a drug absorption in vitro model 7. Comparing rat in situ, Caco-2, and PAMPA permeability of fluoroquinolones, Eur J Pharm Sci, 21 (2004) 429-441.

[126] K. Sugano, H. Hamada, M. Machida, H. Ushio, K. Saitoh, K. Terada, Optimized conditions of bio-mimetic artificial membrane permeation assay, Int J Pharm, 228 (2001) 181-188.

[127] C. Zhu, L. Jiang, T.M. Chen, K.K. Hwang, A comparative study of artificial membrane permeability assay for high throughput profiling of drug absorption potential, Eur J Med Chem, 37 (2002) 399-407.

[128] F. Wohnsland, B. Faller, High-Throughput Permeability pH Profile and High-Throughput Alkane/Water log P with Artificial Membranes, J Med Chem 44 (2001) 923-930.

[129] A. Avdeef, M. Strafford, E. Block, M.P. Balogh, W. Chambliss, I. Khan, Drug absorption in vitro model: filter-immobilized artificial membranes 2. Studies of the permeability properties of lactones in Piper methysticum Forst, Eur J Pharm Sci, 14 (2001), 271-280.

[130] L. Di, E.H. Kerns, K. Fan, O.J. McConnell, G.T. Carter, High throughput artificial membrane permeability assay for blood–brain barrier, European Journal of Medicinal Chemistry, 38 (2003) 223-232.

[131] X. Chen, A. Murawski, K. Patel, C.L. Crespi, P.V. Balimane, A novel design of artificial membrane for improving the PAMPA model, Pharm Res, 25 (2008) 1511-1520.

[132] G. Ottaviani, S. Martel, P.A. Carrupt, Parallel Artificial Membrane Permeability Assay: A New Membrane for the Fast Prediction of Passive Human Skin Permeability, J Med Chem, 49 (2006), 3948-3954.

[133] G.E. Flaten, A.B. Dhanikula, K. Luthman, M. Brandl, Drug permeability across a phospholipid vesicle based barrier: a novel approach for studying passive diffusion, Eur J Pharm Sci, 27 (2006) 80-90.

[134] G.E. Flaten, H. Bunjes, K. Luthman, M. Brandl, Drug permeability across a phospholipid vesicle-based barrier 2. Characterization of barrier structure, storage stability and stability towards pH changes, Eur J Pharm Sci, 28 (2006) 336-343.

[135] G.E. Flaten, M. Skar, K. Luthman, M. Brandl, Drug permeability across a phospholipid vesicle based barrier: 3. Characterization of drug-membrane interactions and the effect of agitation on the barrier integrity and on the permeability, Eur J Pharm Sci, 30 (2007) 324-332.

[136] G.E. Flaten, K. Luthman, T. Vasskog, M. Brandl, Drug permeability across a phospholipid vesicle-based barrier 4. The effect of tensides, co-solvents and pH changes on barrier integrity and on drug permeability, Eur J Pharm Sci, 34 (2008) 173-180.

[137] E. Naderkhani, J. Isaksson, A. Ryzhakov, G.E. Flaten, Development of a biomimetic phospholipid vesicle-based permeation assay for the estimation of intestinal drug permeability, J Pharm Sci, 103 (2014) 1882-1890.

[138] E. Naderkhani, T. Vasskog, G.E. Flaten, Biomimetic PVPA in vitro model for estimation of the intestinal drug permeability using fasted and fed state simulated intestinal fluids, Eur J Pharm Sci, 73 (2015) 64-71.

[139] A. Engesland, M. Skar, T. Hansen, N. Skalko-Basnet, G.E. Flaten, New applications of phospholipid vesicle-based permeation assay: permeation model mimicking skin barrier, J Pharm Sci, 102 (2013) 1588-1600.

[140] A. Engesland, N. Skalko-Basnet, G.E. Flaten, Phospholipid vesicle-based permeation assay and EpiSkin(R) in assessment of drug therapies destined for skin administration, J Pharm Sci, 104 (2015) 1119-1127.

[141] A. Engesland, N. Skalko-Basnet, G.E. Flaten, In vitro models to estimate drug penetration through the compromised stratum corneum barrier, Drug Dev Ind Pharm, 42 (2016) 1742-1751.

[142] S.M. Fischer, G.E. Flaten, E. Hagesaether, G. Fricker, M. Brandl, In-vitro permeability of poorly water soluble drugs in the phospholipid vesicle-based permeation assay: the influence of nonionic surfactants, J Pharm Pharmacol, 63 (2011) 1022-1030.

[143] S.M. Fischer, S.T. Buckley, W. Kirchmeyer, G. Fricker, M. Brandl, Application of simulated intestinal fluid on the phospholipid vesicle-based drug permeation assay, Int J Pharm, 422 (2012) 52-58.

[144] M. di Cagno, H.A. Bibi, A. Bauer-Brandl, New biomimetic barrier Permeapad for efficient investigation of passive permeability of drugs, Eur J Pharm Sci, 73 (2015) 29-34.

[145] H.A. Bibi, M. di Cagno, R. Holm, A. Bauer-Brandl, Permeapad for investigation of passive drug permeability: The effect of surfactants, co-solvents and simulated intestinal fluids (FaSSIF and FeSSIF), Int J Pharm, 493 (2015) 192-197.

[146] H.A. Bibi, R. Holm, A. Bauer-Brandl, Simultaneous lipolysis/permeation in vitro model, for the estimation of bioavailability of lipid based drug delivery systems, Eur J Pharm Biopharm, 117 (2017) 300-307.

[147] A.C. Jacobsen, S. Nielsen, M. Brandl, A. Bauer-Brandl, Drug Permeability Profiling Using the Novel Permeapad(R) 96-Well Plate, Pharm Res, 37 (2020) 93.

[148] A.C. Jacobsen, A. Krupa, M. Brandl, A. Bauer-Brandl, High-Throughput Dissolution/Permeation Screening -A 96-Well Two-Compartment Microplate Approach, Pharmaceutics, 11 (2019).

[149] P. Berben, J. Brouwers, P. Augustijns, The artificial membrane insert system as predictive tool for formulation performance evaluation, Int J Pharm, 537 (2018) 22-29.

[150] P. Artursson, K. Palm, K. Luthman, Caco-2 monolayers in experimental and theoretical predictions of drug transport, Adv Drug Deliv Rev, 46 (2001), 27-43.

[151] Y. Li, E. Arranz, A. Guri, M. Corredig, Mucus interactions with liposomes encapsulating bioactives: Interfacial tensiometry and cellular uptake on Caco-2 and cocultures of Caco-2/HT29-MTX, Food Res Int, 92 (2017) 128-137.

[152] A. Lechanteur, J. das Neves, B. Sarmento, The role of mucus in cell-based models used to screen mucosal drug delivery, Adv Drug Deliv Rev, 124 (2018) 50-63.

[153] A. Fabiano, Y. Zambito, A. Bernkop-Schnurch, About the impact of water movement on the permeation behaviour of nanoparticles in mucus, Int J Pharm, 517 (2017) 279-285.

[154] O. Svensson, K. Thuresson, T. Arnebrant, Interactions between chitosan-modified particles and mucin-coated surfaces, J Colloid Interface Sci, 325 (2008) 346-350.

[155] J.T. Huckaby, S.K. Lai, PEGylation for enhancing nanoparticle diffusion in mucus, Adv Drug Deliv Rev, 124 (2018) 125-139.

[156] A. Sosnik, J. das Neves, B. Sarmento, Mucoadhesive polymers in the design of nano-drug delivery systems for administration by non-parenteral routes: A review, Progress in Polymer Science, 39 (2014) 2030-2075.

[157] J. Griessinger, S. Dunnhaupt, B. Cattoz, P. Griffiths, S. Oh, S. Borros i Gomez, M. Wilcox, J. Pearson, M. Gumbleton, M. Abdulkarim, I. Pereira de Sousa, A. Bernkop-Schnurch, Methods to determine the interactions of micro- and nanoparticles with mucus, Eur J Pharm Biopharm, 96 (2015) 464-476.

[158] M. Dawson, E. Krauland, D. Wirtz, J. Hanes, Transport of Polymeric Nanoparticle Gene Carriers in Gastric Mucus, Biotechnol Prog, 20 (2004) 851-857.

[159] P.C. Griffiths, P. Occhipinti, C. Morris, R.K. Heenan, S.M. King, M. Gumbleton, PGSE-NMR and SANS Studies of the Interaction of Model Polymer Therapeutics with Mucin, Biomacromolecules, 11 (2010) 120-125.

[160] M. Boegh, S.G. Baldursdottir, A. Mullertz, H.M. Nielsen, Property profiling of biosimilar mucus in a novel mucus-containing in vitro model for assessment of intestinal drug absorption, Eur J Pharm Biopharm, 87 (2014) 227-235.

[161] J. Kocevar-Nared, J. Kristl, J. Smid-Korbar, Comparative rheological investigation of crude gastric mucin and natural gastric mucus, Biomaterials, 18 (1997) 677-681.

[162] D. Birch, R.G. Diedrichsen, P.C. Christophersen, H. Mu, H.M. Nielsen, Evaluation of drug permeation under fed state conditions using mucus-covered Caco-2 cell epithelium, Eur J Pharm Sci, 118 (2018) 144-153.

[163] O.M. Feeney, M.F. Crum, C.L. McEvoy, N.L. Trevaskis, H.D. Williams, C.W. Pouton, W.N. Charman, C.A.S. Bergstrom, C.J.H. Porter, 50years of oral lipid-based formulations: Provenance, progress and future perspectives, Adv Drug Deliv Rev, 101 (2016) 167-194.

[164] R. Berthelsen, R. Holm, J. Jacobsen, J. Kristensen, B. Abrahamsson, A. Mullertz, Kolliphor surfactants affect solubilization and bioavailability of fenofibrate. Studies of in vitro digestion and absorption in rats, Mol Pharm, 12 (2015) 1062-1071.

[165] N. Thomas, K. Richter, T.B. Pedersen, R. Holm, A. Mullertz, T. Rades, In vitro lipolysis data does not adequately predict the in vivo performance of lipid-based drug delivery systems containing fenofibrate, AAPS J, 16 (2014) 539-549.

[166] B.T. Griffin, M. Kuentz, M. Vertzoni, E.S. Kostewicz, Y. Fei, W. Faisal, C. Stillhart, C.M. O'Driscoll, C. Reppas, J.B. Dressman, Comparison of in vitro tests at various levels of complexity for the prediction of in vivo performance of lipid-based formulations: case studies with fenofibrate, Eur J Pharm Biopharm, 86 (2014) 427-437.

[167] S.D. Siqueira, A. Mullertz, K. Graeser, G. Kasten, H. Mu, T. Rades, Influence of drug load and physical form of cinnarizine in new SNEDDS dosing regimens: in vivo and in vitro evaluations, AAPS J, 19 (2017) 587-594.

[168] M.H. Michaelsen, S.D. Siqueira Jorgensen, I.M. Abdi, K.M. Wasan, T. Rades, A. Mullertz, Fenofibrate oral absorption from SNEDDS and super-SNEDDS is not significantly affected by lipase inhibition in rats, Eur J Pharm Biopharm, 142 (2019) 258-264.

[169] T. Tran, S. Siqueira, H. Amenitsch, A. Mullertz, T. Rades, In vitro and in vivo performance of monoacyl phospholipid-based self-emulsifying drug delivery systems, J Control Release, 255 (2017) 45-53.

[170] S.D. Siqueira Jorgensen, M. Al Sawaf, K. Graeser, H. Mu, A. Mullertz, T. Rades, The ability of two in vitro lipolysis models reflecting the human and rat gastro-intestinal conditions to predict the in vivo performance of SNEDDS dosing regimens, Eur J Pharm Biopharm, 124 (2018) 116-124.

[171] J. Keemink, C.A.S. Bergstrom, Caco-2 Cell Conditions Enabling Studies of Drug Absorption from Digestible Lipid-Based Formulations, Pharm Res, 35 (2018) 74.

[172] P.J. O'Dwyer, K.J. Box, N.J. Koehl, H. Bennett-Lenane, C. Reppas, R. Holm, M. Kuentz, B.T. Griffin, Novel Biphasic Lipolysis Method To Predict in Vivo Performance of Lipid-Based Formulations, Mol Pharm, 17 (2020) 3342-3352.

[173] A.R. Ilie, B.T. Griffin, M. Brandl, A. Bauer-Brandl, A.C. Jacobsen, M. Vertzoni, M. Kuentz, R. Kolakovic, R. Holm, Exploring impact of supersaturated lipid-based drug delivery systems of celecoxib on in vitro permeation across Permeapad() membrane and in vivo absorption, Eur J Pharm Sci, 152 (2020) 105452.

[174] L.C. Alskar, A. Parrow, J. Keemink, P. Johansson, B. Abrahamsson, C.A.S. Bergstrom, Effect of lipids on absorption of carvedilol in dogs: Is coadministration of lipids as efficient as a lipid-based formulation?, J Control Release, 304 (2019) 90-100.

[175] C. Alvebratt, J. Keemink, K. Edueng, O. Cheung, M. Stromme, C.A.S. Bergstrom, An in vitro dissolution-digestion-permeation assay for the study of advanced drug delivery systems, Eur J Pharm Biopharm, 149 (2020) 21-29.

[176] M.F. Crum, N.L. Trevaskis, H.D. Williams, C.W. Pouton, C.J. Porter, A new in vitro lipid digestion - in vivo absorption model to evaluate the mechanisms of drug absorption from lipid-based formulations, Pharm Res, 33 (2016) 970-982.

[177] M.S. Park, J.W. Chung, Y.K. Kim, S.C. Chung, H.S. Kho, Viscosity and wettability of animal mucin solutions and human saliva, Oral Dis, 13 (2007) 181-186.

[178] S.K. Lai, Y.Y. Wang, D. Wirtz, J. Hanes, Micro- and macrorheology of mucus, Adv Drug Deliv Rev, 61 (2009) 86-100.

[179] L.Z. Benet, F. Broccatelli, T.I. Oprea, BDDCS applied to over 900 drugs, AAPS J, 13 (2011) 519-547.

[180] M. Falavigna, P.C. Stein, G.E. Flaten, M.P. di Cagno, Impact of Mucin on Drug Diffusion: Development of a Straightforward in Vitro Method for the Determination of Drug Diffusivity in the Presence of Mucin, Pharmaceutics, 12 (2020).

[181] K. Tahara, M. Nishio, H. Takeuchi, Evaluation of liposomal behavior in the gastrointestinal tract after oral administration using real-time in vivo imaging, Drug Dev Ind Pharm, 44 (2018) 608-614.

[182] M.W. Joraholmen, Z. Vanic, I. Tho, N. Skalko-Basnet, Chitosan-coated liposomes for topical vaginal therapy: assuring localized drug effect, Int J Pharm, 472 (2014) 94-101.

[183] M.W. Joraholmen, P. Basnet, M.J. Tostrup, S. Moueffaq, N. Skalko-Basnet, Localized Therapy of Vaginal Infections and Inflammation: Liposomes-In-Hydrogel Delivery System for Polyphenols, Pharmaceutics, 11 (2019).

[184] M.W. Joraholmen, P. Basnet, G. Acharya, N. Skalko-Basnet, PEGylated liposomes for topical vaginal therapy improve delivery of interferon alpha, Eur J Pharm Biopharm, 113 (2017) 132-139.

[185] M.W. Joraholmen, N. Skalko-Basnet, G. Acharya, P. Basnet, Resveratrol-loaded liposomes for topical treatment of the vaginal inflammation and infections, Eur J Pharm Sci, 79 (2015) 112-121.

[186] J. das Neves, M. Amiji, B. Sarmento, Mucoadhesive nanosystems for vaginal microbicide development: friend or foe?, Wiley Interdiscip Rev Nanomed Nanobiotechnol, 3 (2011) 389-399.

[187] S.K. Lai, J.S. Suk, A. Pace, Y.Y. Wang, M. Yang, O. Mert, J. Chen, J. Kim, J. Hanes, Drug carrier nanoparticles that penetrate human chronic rhinosinusitis mucus, Biomaterials, 32 (2011) 6285-6290.

[188] A. Mahmood, F. Laffleur, G. Leonaviciute, A. Bernkop-Schnurch, Protease-functionalized mucus penetrating microparticles: In-vivo evidence for their potential, Int J Pharm, 532 (2017) 177-184.

[189] M.W. Joraholmen, A. Bhargava, K. Julin, M. Johannessen, N. Skalko-Basnet, The Antimicrobial Properties of Chitosan Can be Tailored by Formulation, Mar Drugs, 18 (2020).

[190] T. Andersen, Z. Vanic, G.E. Flaten, S. Mattsson, I. Tho, N. Skalko-Basnet, Pectosomes and chitosomes as delivery systems for metronidazole: the one-pot preparation method, Pharmaceutics, 5 (2013) 445-456.

[191] M. Falavigna, M. Pattacini, R. Wibel, F. Sonvico, N. Skalko-Basnet, G.E. Flaten, The Vaginal-PVPA: A Vaginal Mucosa-Mimicking In Vitro Permeation Tool for Evaluation of Mucoadhesive Formulations, Pharmaceutics, 12 (2020).

[192] A. Dahan, J.M. Miller, The solubility-permeability interplay and its implications in formulation design and development for poorly soluble drugs, AAPS J, 14 (2012) 244-251.

[193] D. Porat, A. Dahan, Active intestinal drug absorption and the solubility-permeability interplay, Int J Pharm, 537 (2018) 84-93.

[194] E. Shoghi, E. Fuguet, E. Bosch, C. Rafols, Solubility-pH profiles of some acidic, basic and amphoteric drugs, Eur J Pharm Sci, 48 (2013) 291-300.

[195] G. Volgyi, E. Baka, K.J. Box, J.E. Comer, K. Takacs-Novak, Study of pH-dependent solubility of organic bases. Revisit of Henderson-Hasselbalch relationship, Anal Chim Acta, 673 (2010) 40-46.

[196] M.V. Varma, I. Gardner, S.J. Steyn, P. Nkansah, C.J. Rotter, C. Whitney-Pickett, H. Zhang, L. Di, M. Cram, K.S. Fenner, A.F. El-Kattan, pH-Dependent solubility and permeability criteria for provisional biopharmaceutics classification (BCS and BDDCS) in early drug discovery, Mol Pharm, 9 (2012) 1199-1212.

[197] S.A. Raina, G.G.Z. Zhang, D.E. Alonzo, J. Wu, D. Zhu, N.D. Catron, Y. Gao, L.S. Taylor, Enhancements and limits in drug membrane transport using supersaturated solutions of poorly water soluble drugs, J Pharm Sci, 103 (2014) 2736-2748.

[198] P. Santos, A.C. Watkinson, J. Hadgraft, M.E. Lane, Enhanced permeation of fentanyl from supersaturated solutions in a model membrane, Int J Pharm, 407 (2011) 72-77.

[199] A.S. Indulkar, Y. Gao, S.A. Raina, G.G.Z. Zhang, L.S. Taylor, Crystallization from Supersaturated Solutions: Role of Lecithin and Composite Simulated Intestinal Fluid, Pharm Res, 35 (2018) 158.

[200] C. Stillhart, G. Imanidis, B.T. Griffin, M. Kuentz, Biopharmaceutical modeling of drug supersaturation during lipid-based formulation digestion considering an absorption sink, Pharm Res, 31 (2014) 3426-3444.

Paper I

International Journal of Pharmaceutics 537 (2018) 213–222

Contents lists available at ScienceDirect

International Journal of Pharmaceutics

journal homepage: www.elsevier.com/locate/ijpharm

Mucus-PVPA (mucus Phospholipid Vesicle-based Permeation Assay): An artificial permeability tool for drug screening and formulation development

Margherita Falavigna[a], Mette Klitgaard[a,b], Christina Brase[a], Selenia Ternullo[a], Nataša Škalko-Basnet[a], Gøril Eide Flaten[a,*]

[a] Drug Transport and Delivery Research Group, Department of Pharmacy, University of Tromsø the Arctic University of Norway, Universitetsveien 57, Tromsø, 9037, Norway
[b] Pharmaceutical Design and Drug Delivery, Department of Pharmacy, University of Copenhagen, Copenhagen, Denmark

ARTICLE INFO

Keywords:
In vitro model
Permeability
Mucosal administration
Mucus
Liposomes
Mucoadhesive
Mucopenetrating

ABSTRACT

The mucus layer covering all mucosal surfaces in our body is the first barrier encountered by drugs before their potential absorption through epithelial tissues, and could thus affect the drugs' permeability and their effectiveness. Therefore, it is of key importance to have *in vitro* permeability models that can mimic this specific environment. For this purpose, the novel mucus phospholipid vesicle-based permeation assay (mucus-PVPA) has been developed and used for permeability screening of drugs and formulations. The model proved to be stable under the chosen conditions and demonstrated the ability to discriminate between compounds with different chemical structures and properties. Overall, a decrease in drug permeability was found in the presence of mucus on top of the PVPA barriers, as expected. Moreover, mucoadhesive (chitosan-coated) and mucopenetrating (PEGylated) liposomes were investigated in the newly developed model. The mucus-PVPA was able to distinguish between the different liposomal formulations, confirming the penetration potential of the tested formulations and the related drug permeability. The mucus-PVPA model appears to be a promising *in vitro* tool able to mimic the environment of mucosal tissues, and could therefore be used for further drug permeability screening and formulation development.

1. Introduction

The mucus layer covering mucosal epithelia is the first barrier encountered by many drugs and formulations when entering the body. This layer could thus potentially limit the effectiveness of most drug delivery systems (Groo and Lagarce, 2014). Mucus is found on many epithelial surfaces such as the gastrointestinal tract (GI), the respiratory tract, the eye and the female genital tract; its composition, structure and thickness differ according to the different locations in the body (Friedl et al., 2013; Leal et al., 2017; Sigurdsson et al., 2013). The main components of mucus are water, glycoproteins (i.e. mucins), free proteins, salts and lipids (Groo and Lagarce, 2014). An important role is played by mucins, negatively charged glycoproteins (polypeptide backbone with oligosaccharide side chains), which are secreted by mucosal glands and goblet cells (Leal et al., 2017; Sigurdsson et al., 2013). The structure of the mucin gel can hinder the diffusion of drugs (Boegh and Nielsen, 2015) by two main mechanisms, namely the interaction and size filtering (Olmsted et al., 2001).

Transmucosal drug delivery gained increasing attention in the past two decades. Various strategies have been proposed to improve the mucosal permeability of drugs, including mucoadhesive and mucopenetrating systems, such as liposomes (Leal et al., 2017). Therefore, to properly tackle the screening of new drugs and optimization of novel mucosal formulations, it is of key importance to exploit *in vitro* tools comprising mucus to better understand its impact on drug permeation and absorption and to better predict the fate of a drug *in vivo*. Many models have been developed to study the effect of the sole mucus layer on drug permeability, without the presence of an artificial membrane. Some of them comprise the use of native mucus and some others exploit the use of commercially available mucins in different types of media (Khanvilkar et al., 2001; Legen and Kristl, 2001; Matthes et al., 1992). However, it has to be noted that the removal of mucus from its physiological environment can modify its characteristics (e.g. gel-forming properties) (Kocevar-Nared et al., 1997). Therefore, it becomes challenging to produce a model able to mimic physiological mucus, and the differences between native and reconstituted mucus can lead to variations in the resulting drug permeability. On the other hand, to date, several *in vitro* cell-based (Caco-2 model, Artusson et al., 2001) and

* Corresponding author.
E-mail address: goril.flaten@uit.no (G.E. Flaten).

https://doi.org/10.1016/j.ijpharm.2017.12.038
Received 4 October 2017; Received in revised form 20 December 2017; Accepted 21 December 2017
Available online 26 December 2017
0378-5173/

artificial models (PVPA model, Flaten et al., 2006b; PAMPA model, Kansy et al., 1998; Permeapad™, di Cagno et al., 2015; AMI-system, Berben et al., 2017) have been developed for the screening of new drugs and formulations. Some of those models also include the mucus layer, such as mucus-producing cell systems (i.e. Caco2/HT29-MTX co-culture) and cell-based mucosal models with artificial mucus (Boegh et al., 2014; Lechanteur et al., 2017). Unfortunately, the robustness and reproducibility of these mucus-including models are not yet well defined. Therefore, the lack of a reliable artificial *in vitro* model comprising mucus remains a considerable limitation for permeability studies targeting the mucosal administration route.

Among the non-cell-based models, the phospholipid vesicle-based permeation assay (PVPA) has been developed in our group and established in the past decade as a predictive and reliable artificial model for the screening of drugs and optimization of formulations (Flaten et al., 2006b; Flaten et al., 2011; Kanzer et al., 2010; Naderkhani et al., 2014a,b). So far, this model has not taken into account the crucial influence of mucus on the permeation of drugs. Therefore, in this study, the effect of mucus on drug permeability was assessed and the novel mucus-PVPA developed and validated. The permeability of five model drugs (atenolol, ibuprofen, indomethacin, metronidazole and naproxen) was investigated. The drugs were chosen to cover a range of relevant physicochemical properties to challenge the mucus-PVPA's ability to distinguish between drugs with different physicochemical characteristics. Moreover, since nanoparticulate formulations have demonstrated great efficacy in *in vitro* and *in vivo* experiments (Chen et al., 2013; Netsomboom and Bernkop-Schnürch, 2016), a focus was put on the permeation of three selected drugs (indomethacin, metronidazole and naproxen) from mucoadhesive (chitosan-coated) and mucopenetrating (PEGylated) liposomal formulations, to better understand the influence of the mucus layer on the diffusion of the nanocarriers and permeability of the drugs contained in such delivery systems.

2. Materials and methods

2.1. Materials

Lipoid egg phospholipids E80 (80% phosphatidylcholine), Lipoid soybean lecithin S100 (> 94% phosphatidylcholine) and Lipoid PE 18:0/18:0 (PEG 2000) were obtained from Lipoid GmbH (Ludwigshafen, Germany). Acetic acid (≥99.8%), ammonium molybdate, atenolol, calcein, chitosan (low molecular weight, Brookfield viscosity 20,000 cps, degree of deacetylation 92%), chloroform, ethanol (96%, v/v), Fiske-Subbarow reducer, hydrochloric acid, ibuprofen, indomethacin, methanol CHROMASOLV®, metronidazole, mucin from porcine stomach type III (bound sialic acid 0.5–1.5%, partially purified), naproxen, phosphorus standard solution, potassium phosphate monobasic, sodium chloride, sodium hydroxide and sodium phosphate dibasic dodecahydrate were products of Sigma-Aldrich, Chemie GmbH (Steinheim, Germany). Hydrogen peroxide 30% and titriplex® III were purchased from Merck KGaA (Darmstadt, Germany). Acetonitrile for HPLC (gradient grade) was obtained from VWR chemicals (Fontenay-sous-Bois, France) and sulfuric acid was purchased from May&Baker LTD (Dagenham, England). All chemicals employed were of analytical grade.

Plates and Transwell filter inserts (d = 6.5 mm) were products of Corning Inc. (Corning, New York). The nitrocellulose membrane filters (0.65 µm DAWP) were obtained from Millipore (Billerica, Massachusetts) and the Nucleopore track-etch membrane filters (0.4 and 0.8 µm pore size) were purchased from Whatman (part of GE Healthcare, Oslo, Norway).

2.2. PVPA barriers preparation

The PVPA barriers were prepared by depositing egg-phospholipid liposomes on top of cellulose ester filters by centrifugation followed by a freeze-thaw cycle according to the method previously described (Naderkhani et al., 2014a).

2.3. Mucus barrier

Different concentrations of mucin (10, 20 and 40 mg/mL) were used as a model for the mucus layer. These suspensions were obtained by the hydration of mucin from porcine stomach type III with phosphate buffer saline (PBS) pH 7.40. The viscosity of the mucus was measured at room temperature on HAAKE ViskoTester 7 plus (Thermo, Hafrsfjord, Norway) using spindle TL5. In the *in vitro* permeability studies, the mucin suspension was directly pipetted on top of the PVPA barriers before the addition of the drugs or formulation to be tested. The drug solutions/formulations were carefully added on top of the mucus layer in the donor compartment in order to prevent mixing of the two layers. The division of the two layers was visibly distinct.

2.4. In vitro permeability study using the mucus-PVPA

The permeability of different drugs/marker (calcein, CAL; atenolol, ATN; ibuprofen, IBP; indomethacin, IND; naproxen, NPR; metronidazole, MTR; Table 1) was investigated at room temperature (23–25 °C) in the presence and absence of mucus following the procedure previously described (Naderkhani et al., 2014a). In the experiments performed in the presence of mucus, 50 µL of mucin 10 mg/mL were added, if not stated otherwise, before the careful addition of drug/marker. To maintain sink conditions, the inserts were moved to a new acceptor compartment at certain time intervals for 5 h. After ended experiment, the electrical resistance was measured to confirm the integrity of the barriers and the samples collected as previouslu described (Flaten et al., 2006a,b; Naderkhani et al., 2014a,b)The fluorescent marker calcein was used to monitor the barriers' integrity during the study (Flaten et al., 2006b) and was quantified spectrofluorometrically on POLARstar Galaxy fluorometer (Fluostar, BMG Labtechnologies,

Table 1
Overview of the model drugs/marker included in this study.

Compound	Abbreviation	pKa	Log P	Log $D_{7.4}$[d]	Charge at pH 7.4[b]	Detection method	Wavelength (nm)	St.curve (nmol/mL)
Calcein	CAL	1.8/9.2[a]	−1.71[b]		–	Fluorimeter	Ex.: 485 Em.: 520	0.10 − 2.25
Atenolol.	ATN	9.54[c]	0.16[d]	−1.03	+	UV	274	0.20–80.45
Ibuprofen	IBP	4.45[c]	3.97[d]	0.81	–	UV	220	10–150
Indomethacin	IND	4.42[c]	4.27[d]	0.77	–	HPLC-UV	254	0.016 − 320
Metronidazole	MTR	2.62[e]	−0.02[d]	0.14	0	UV	320	30–200
Naproxen	NPR	4.18[c]	3.18[d]	1.70	–	UV	270	0.8–84

[a] Flaten et al., 2006b.
[b] Naderkhani et al., 2014b.
[c] Avdeef, 2003.
[d] Benet et al., 2011.
[e] Rediguieri et al., 2011.

Offenburg, Germany) at excitation and emission wavelengths of 485 and 520 nm, respectively. The quantification of indomethacin was carried out by HPLC using a Waters X-select™ CSH ™ C18 (2.5 µm, 3.0 × 75 mm) XP column preceded by a Waters X-select™ CSH ™ C18 (3.5 µm, 3.0 × 20 mm) guard cartridge on a Waters e2795 Separation Module connected to a Waters 2489 UV/Visible Detector (Waters, Milford, Massachusetts, USA) at a wavelength of 254 nm. The mobile phase consisted of acetonitrile and MilliQ water (60:40, v/v) with 0.1% glacial acetic acid and the flow rate was set at 0.5 mL/min (retention time 2.8 min). Atenolol, ibuprofen, metronidazole and naproxen were quantified spectrophotometrically on SpectraMax 190 Microplate reader (Molecular Devices Corporation, California, USA) at wavelengths of 274, 220, 320 and 270 nm, respectively.

For each compound the experiment was performed at least in triplicates (6 inserts for each parallel) and the apparent permeability coefficient (P_{app}) was calculated with the equation derived from Fick's law for steady state conditions:

$$P_{app}\left(\frac{cm}{s}\right) = \frac{dQ}{dt} \mathrm{x} \frac{1}{AxCd}$$

where dQ/dt is the slope at the steady-state conditions (nmol/s), A represents the surface area of the PVPA barriers (cm^2) and C_d is the concentration of the compound in the donor compartment (nmol/mL).

As earlier described by our group (Flaten et al., 2006a,b), the concentrations of the drugs investigated in the study were chosen in order to reach a concentration in the acceptor compartment that was below the solubility limits and thus to obtain sink conditions.

2.4.1. The effect of temperature, mucus volume and mucin concentration on the permeability of drugs

The permeability of different drugs/marker (Table 1) was measured in the absence and presence of mucus at 37 °C and compared to the one obtained at room temperature (23–25 °C) to evaluate possible changes in permeability due to elevated temperature. Different concentrations of mucin (10, 20 and 40 mg/mL) were tested to estimate their effect on the permeability of the tested compounds. Moreover, different volumes of mucus (mucin 10 mg/mL; mucus volume range: 20–50 µL) were deposited on top of the PVPA barriers, and the permeability of naproxen was measured to assess if the different mucus' volumes would have any effect on the drug's permeability.

2.5. PVPA barriers – mucus interaction

2.5.1. Phospholipid assay

To determine any changes in the barriers' integrity caused by the addition of mucus on top of the PVPA barriers, the amount of phospholipids released after the addition of the mucus layer was measured by the modified phosphorus assay (Bartlett, 1959) as previously described by us (Naderkhani et al., 2015).

2.5.2. 2.5.2. In vitro mucus binding test

The binding potential of the egg-phospholipid liposomes to mucus was evaluated to determine its interaction with the PVPA barriers. The study was conducted as previously described (Jøraholmen et al., 2017). The experiment was carried out in triplicate and the binding efficiency of mucus to the liposomes was calculated according to Jøraholmen and colleagues (2017).

2.6. Preparation of liposomal formulations

Three different types of liposomal formulations containing either indomethacin (IND), metronidazole (MTR) or naproxen (NPR) were prepared to study the effect of the formulation on drug permeability.

Plain liposomes were obtained using the film hydration technique, according to the method described by Berginc and colleagues (Berginc et al., 2014). The liposome dispersion was sonicated for 1 min using a Sonics high intensity ultrasonic processor (Sonics & Materials Inc., Newtown, Connecticut) (amplitude setting of 500 W/20 kHz processor 40%) to produce a smaller and more homogeneous size distribution. The sonicated liposome dispersion was stored in the refrigerator for at least 2 h prior to further use.

Chitosan-coated liposomes were prepared from plain liposomes in the absence of unentrapped drug as previously described (Jøraholmen et al., 2014; Naderkhani et al., 2014a). After storage in refrigerator (4–8 °C) overnight, the pH was measured and adjusted to 7.40.

PEGylated liposomes were prepared using Lipoid S100 (200 mg), PEG 2000 (36.3 mg) and the drug (IND, MTR or NPR; 20 mg), following the method described by Jøraholmen and colleagues (Jøraholmen et al., 2017).

2.7. Characterization of liposomal formulations

2.7.1. Entrapment efficiency and recovery

The encapsulated drug (IND, MTR or NPR) in the different liposomal formulations was separated from the unentrapped drug by dialysis using a dialysis tubing with a MWCO 12–14,000 Da (Medicell International Ltd., London, UK). The liposomal dispersions (4.2 mL) were dialyzed against a medium (PBS, pH 7.40) for 6 h at room temperature. The volume of PBS was adjusted to assure the solubility of the drugs. Aliquots of the dialyzed liposomes were dissolved in MeOH to free the drug contained in the liposomes and compared with the amount of drug in the medium (unentrapped drug) to calculate the entrapment efficiency for the specific drug. Drugs were quantified as previously described in Section 2.4.

2.7.2. Size analysis and zeta potential measurements

The diameter of the dialyzed liposomes containing different drugs was determined using a Malvern Zetasizer Nano ZS (Malvern, Oxford, UK). Two samples for each batch of liposomes were analysed and the diameters calculated from the mean of three measurements for each sample. The liposome dispersions were diluted 1:50 (v/v) in PBS pH 7.40 for plain and PEGylated liposomes, and PBS pH 7.40 and acetic acid 0.1% (1:1 v/v) for the chitosan-coated ones, in order to dilute the formulations in their own preparation media. The polydispersity index (PI) of each batch was measured to assess the population's homogeneity.

All liposomal formulations (plain, chitosan-coated and PEGylated) were diluted 1:10 (v/v) in freshly filtered water (0.2 µm filters) to determine the zeta potential using a Malvern Zetasizer Nano ZS (Malvern, Oxford, UK). The disposable folded capillary cells (DTS1070) were cleaned before the loading of the sample using ethanol and filtered water. Two samples for each batch of formulations were measured in three parallels at room temperature.

2.8. Statistical analysis

Statistical analysis was done using GraphPad Prism 7.0 software. Student's *t*-test was used to detect significant differences between two sets of data ($p < 0.05$). Comparisons between three or more groups were performed using one-way ANOVA and significance ($p < 0.05$) was found out using the Bonferroni multiple comparison *post hoc* test.

3. Results and discussion

Mucosal tissues, found at various locations in the body, can provide access to both local and systemic drug administration, and are an interesting barrier considering transmucosal delivery (Leal et al., 2017). Moreover, mucosal administration is seen as one of the most convenient, easy and cost-effective routes (Lechanteur et al., 2017). However, the mucus layer covering all mucosal tissues represents a barrier that drugs must overcome to reach deeper epithelia or become absorbed. Therefore, it is of key importance to develop reliable *in vitro*

tools able to evaluate the effect of mucus on drug permeability.

3.1. The effect of mucus on the PVPA barriers

The mucus-PVPA model is expected to provide fast and reliable means to predict/optimize the permeation of drugs once in contact with mucosal surfaces. Unpurified mucin type III from porcine stomach was employed, since this type of mucin has already been exploited in several other studies (Berben et al., 2017; Griffiths et al., 2010; Jøraholmen et al., 2017); the molecular weight and structure of pig mucins resemble human mucins (Groo and Lagarce, 2014). Moreover, its preparation avoids the degradation that occurs with purified mucin type II; the degradation often leads to a different mesh structure and related different rheological properties compared to native mucus (Groo and Lagarce, 2014). To assess whether the mucus-PVPA can provide reliable evidences on drug permeability, the integrity and functionality of the barriers were investigated. The permeability of the hydrophilic marker calcein in the presence of mucus served as a model. Moreover, the effect of different mucus layer thicknesses on the permeability of a model drug as well as characterization of the interaction between mucus and the PVPA barriers were evaluated.

3.1.1. Permeability of a highly hydrophilic marker

The permeability of the hydrophilic marker calcein was investigated in the presence of different mucin concentrations to study their effect on permeability. This fluorescent marker provides information on potential aqueous pathways in the PVPA barrier (Flaten et al., 2006b). Fig. 1 shows that there was no significant change in calcein's P_{app} in the absence or presence of different concentrations of mucin. Considering mucus' overall hydrophilicity and negative charge, more hydrophilic compounds have exhibited lower affinity for mucus compared to hydrophobic ones (Boegh et al., 2014). In our case, considering calcein chemical properties (Table 1), it was not expected that its permeability should be affected to a great extent by the presence of the mucus layer. Therefore, the lack of changes in permeability in the presence of mucus indicates that calcein is free to diffuse through the mucus layer and to permeate through the PVPA barriers without any considerable interaction with this hydrophilic layer. Moreover, as previously stated, no increase in calcein permeability suggests that the barriers are able to maintain their integrity in the presence of mucus. Furthermore, the electrical resistance remained constant in all of the tested conditions (Fig. 1), also indicating no significant changes in the barriers' integrity. These findings are of significant importance especially when compared to the already established cell-based *in vitro* models including the mucus layer such as the Caco-2/HT29-MTX (Hilgendorf et al., 2000). The major drawback of the Caco-2/HT29-MTX model is related to the decrease in transepithelial electrical resistance (TEER) produced by the introduction of the mucus-producing HT29-MTX goblet cells (Schimpel et al., 2014). In fact, the presence of these cells lead to a leakier Caco-2 cell monolayer, thus suggesting an uncertain relevance in comparison of the permeability between the presence and absence of mucus (Lechanteur et al., 2017). On the contrary, in our case, the addition of mucus on top of the barriers did not cause any change in electrical resistance, enabling us to compare values obtained with and without the addition of the mucus layer.

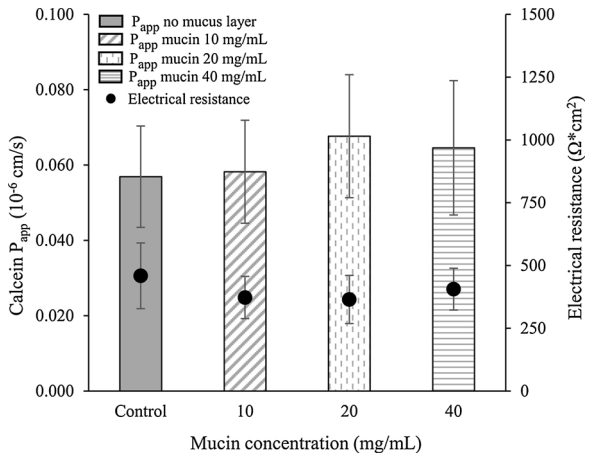

Fig. 1. P_{app} values for calcein and electrical resistance of the PVPA barriers in the presence and absence (control) of different concentrations of mucin (10, 20, 40 mg/mL). The results are indicated as mean ± SD (n = 3).

3.1.2. Characterization of the interaction between mucus and the PVPA barrier

To assess possible disintegration events taking place in the barrier when exposed to mucus, the release of phospholipids from the PVPA barriers into the donor chamber in the presence of mucus (mucin 10 and 40 mg/mL) was quantified and compared to the release in the presence of PBS pH 7.40 on top of the barriers (control). Results showed that the ratios between the PC released in the presence of 10 and 40 mg/mL and the control were 0.95 ± 0.16 and 1.03 ± 0.09 respectively, indicated that no significant difference in phospholipid release was found in the presence and absence of mucus. This evidence is in agreement with previous reports on the robustness of the original PVPA barriers (Flaten et al., 2008) and confirms the maintenance of the barriers' integrity and their low degree of interaction with mucus.

To further test the potential interaction between the liposomes in the PVPA barriers and mucus, a mucin binding test was performed. The results obtained (data not shown) confirmed a lack in binding between the two components, especially evident for liposomes with bigger diameter size, comparable to the liposome size on top of the PVPA barrier. This evidence highlights, once again, the lack of changes produced in the PVPA barriers by the mucus layer.

The lack of structural changes in the barriers was also suggested by studies performed using the confocal laser scanning microscopy (CLSM) (results in Supplementary). The PVPA barriers were investigated to visually examine if the mucus layer would interfere with the barrier's integrity. The micrographs of the cross-sectioned PVPA barriers showed that no aqueous channels were present throughout the barriers, thus confirming the intact integrity of the barriers for all the tested conditions, and that calcein was mainly present in the donor side of the PVPA barrier. These findings are in agreement with previous reports from confocal studies on the PVPA barrier integrity (Flaten et al., 2006a; Fischer et al., 2012).

3.1.3. Viscosity, composition and structure of the mucus layer

Since mucin is the major determinant in mucus rheology (Sigurdsson et al., 2013), the viscosity measurements were performed to study the effect of different mucin concentrations (Fig. 2). The tested suspensions exhibited a Newtonian character, with lower viscosity of mucin in concentration of 10 mg/mL compared to the mucin in higher concentrations. The increase in viscosity with increasing mucin concentrations correlates well with the gel-forming effect of mucin (Grießinger et al., 2015; Dawson et al., 2004). Although the *in vivo* mucus layer has been reported to be of non-Newtonian character (viscoelastic with shear-thinning properties), studies have reported that the hydrated mucin type III from porcine stomach exhibits a Newtonian behaviour (Mackie et al., 2017; Boegh and Nielsen, 2015). Moreover, a comparison between the viscosity of human saliva and porcine gastric mucin was proposed by and Park and colleagues (Park et al., 2007). Both human saliva and animal mucin suspensions exhibited similar viscosities with increasing shear rates. Furthermore, an increase in viscosity was found with increasing mucin concentrations, as also found in our analyses.

As previously stated, the composition and concentration of mucin vary in the body depending on the location and function of the mucosal tissue. However, mucin accounts for generally not more than 5% of the

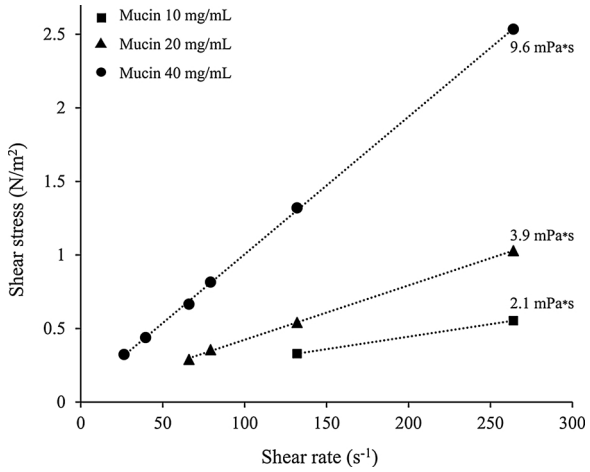

Fig. 2. Mucin viscosity of three mucin concentrations (10, 20 and 40 mg/mL).

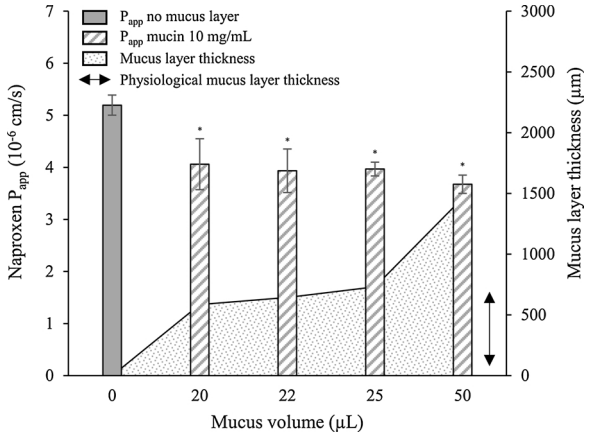

Fig. 3. Naproxen P_{app} (left axis) in the presence of a mucus layer with varying thicknesses (right axis, shaded area), and compared to the physiological mucus layer thickness (), dependent on the volume of mucus (mucin 10 mg/mL) added to the PVPA. The results are indicated as mean ± SD (n = 3). Statistical significance ($p < 0.05$) was investigated with one-way ANOVA using the Bonferroni *post hoc* test.
*Statistically significant difference in drugs' P_{app} in the presence of different mucus volumes compared to its absence.

mucus components (Griffiths et al., 2010). Even though the differences in viscosity have to be taken into account when developing a new model, they are only one of the factors affecting the diffusion of drugs through the mucus (Shaw et al., 2005). For these reasons, mucin in concentration of 10 mg/mL was used as a model for mucus in the permeability experiments in this study.

The mucus-simulating media used in this study was prepared using solely unpurified mucin from porcine stomach type III. Constituents such as lipids, proteins and DNA were not added to keep the mucus-simulating layer as simple as possible and be a general model for mucus, since the content of the other components can vary according to the different site, different species and the specific physiopathological condition (Lieleg et al., 2010). Our aim was to investigate if the presence of sole mucin would affect the permeation of the drugs through the PVPA barriers, and we concluded that it did. However, as reported by Larhed and colleagues (Larhed et al., 1998), other components can significantly hinder the diffusion of drugs through the mucus layer. In particular, the authors found that lipids had a major role in reducing the diffusion of drugs in native pig intestinal mucus. Moreover, it has to be kept in mind that a model mucus system made only out of mucin cannot be considered entirely equivalent to natural mucus, most likely due to the changes in physico-chemical properties caused by the mucin isolation procedures (Kocevar-Nared et al., 1997).

With regards to mucus structure, scanning electron microscopy images of mucin from porcine stomach type III have been obtained by Teubl and colleagues (Teubl et al., 2013). The authors suggested a structural similarity between mucin from porcine stomach and human salivary mucin fibres. The mucus mesh size was also determined for both samples (pore size up to 0.9 µm for porcine gastric and 0.8 µm for human mucin). These results can be compared to the ones by Bajka and colleagues (Bajka et al., 2015), who have investigated *ex vivo* porcine mucus and who have estimated the main pore diameter of the mucin sheets to be around 200 nm. The different results obtained in these two studies could be traced back to the different sample preparation methods and different sample origin (Huckaby and Lai, 2017). These considerations can give us an estimation on how the mucus layer on the PVPA barriers may look like compared to both human and animal mucus and on how particles/formulations could diffuse through this layer, together with the pore size of the mucin mesh. However, it has to be taken into consideration the fact that the structure and composition of the mucus layer differs according to different animal species and different sites of the body (Huckaby and Lai, 2017) and that the mucus-PVPA model so far is aimed to be established as an artificial model for mucosal tissues in general.

3.1.4. Permeability study: the effect of the mucus layer thicknesses

To assess possible changes in drug permeability related to different mucus layer thicknesses on top of the PVPA barriers, the permeability of naproxen was measured in the presence of different volumes of mucus (mucin 10 mg/mL). The thickness of the mucus layer has been reported to be around 600 µm in the human stomach and 50–450 µm in the intestine and colon (Fig. 3, black arrow), although this might vary depending on fasted and fed state (Boegh and Nielsen, 2015; Shaw et al., 2005). Also the thickness in the respiratory tract, in the female reproductive tract and the ocular mucus layer varies according to the specific site (Huckaby and Lai, 2017; Khanvilkar et al., 2001). For the naproxen permeability experiment, 20, 22, 25 and 50 µL of mucus, respectively, were added on top of the barriers and the thickness of the layer (Fig. 3, shaded area) was calculated from the surface area of the filter support. Results showed that there was a significant difference in naproxen's P_{app} when tested in the presence or absence of mucus (addressed in section 3.2), but there was no significant variation between the different mucus volumes/thicknesses. Therefore, even though the calculated mucus layer thickness for 50 µL of mucin suspension exceeded the physiological range, it was considered the best volume to use. This volume assured that the whole surface area of the barriers will be fully covered with mucus and thus reduced any deviations in the application volume.

3.2. Permeability of drugs in solution using the mucus-PVPA

Four different model drugs (naproxen, indomethacin, ibuprofen and atenolol) were used both to evaluate whether the additional mucus layer would affect their permeability and to further highlight whether different mucin concentrations (10, 20 and 40 mg/mL) would have an effect on drug permeability. The drugs were chosen to cover a range of relevant physicochemical properties (Table 1)

Fig. 4 shows that for all drugs there was a significant decrease ($p < 0.05$) in permeation with the addition of the mucus layer. This behaviour was to be expected especially for the more lipophilic drugs (naproxen, indomethacin and ibuprofen), whereas a decrease in permeability was not expected for the more hydrophilic atenolol. However, Boegh and colleagues (2014) have previously reported a significant decrease in permeability of the hydrophilic drug mannitol in the presence of a biosimilar mucus layer on Caco-2 cell monolayer, highlighting the fact that mucus can represent a barrier to both hydrophilic and lipophilic drugs. In fact, it has to be taken into account that there

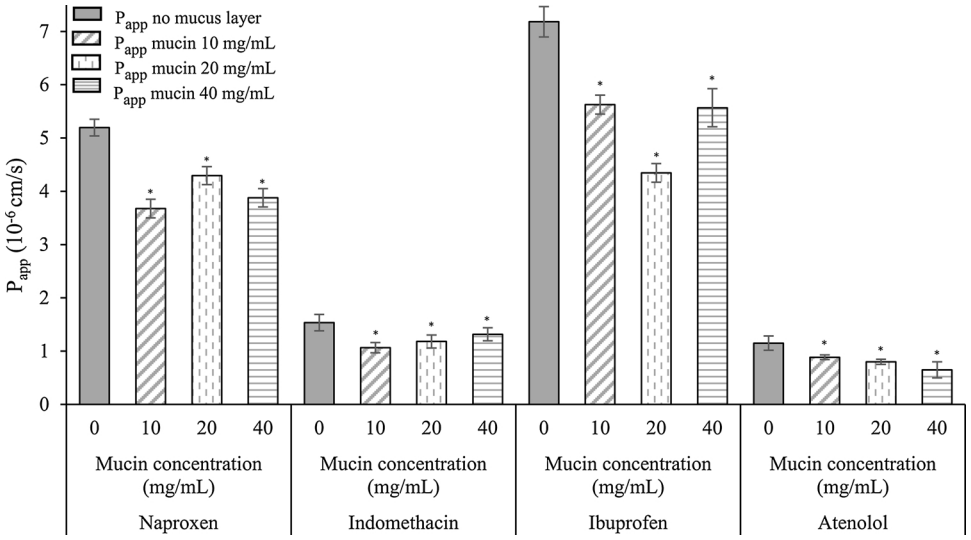

Fig. 4. Drug permeability in the presence and absence of different mucin concentrations (0, 10, 20, 40 mg/mL). The results are indicated as mean ± SD (n = 3). Statistical significance ($p < 0.05$) was investigated with one-way ANOVA using the Bonferroni *post hoc* test.
*Statistically significant difference in drugs' P_{app} in the presence of mucus with different mucin concentrations compared to its absence.

are multiple mechanisms taking place during diffusion of drugs through the mucus layer before the permeation process, and that especially mucins' properties can influence mucus' barrier characteristics. Mucins are formed by a polypeptide backbone to which oligosaccharide side chains are attached, resembling the structure of a bottle-brush. These two different regions provide mucins with both a hydrophobic (protein backbone) and hydrophilic (glycosylated regions) nature, which can affect the diffusion of various types of drugs and formulations (Peppas and Huang, 2004). Moreover, in Olmsted et al. (2001) it is suggested that there are two major mechanisms hindering compounds from diffusing through this layer: i) the interaction filtering, dependant on the electrostatic, hydrophobic forces, hydrogen bonds and specific binding interactions, and ii) the size filtering properties of the mucin mesh. However, the overall hydrophilicity of the mucin gel mostly affects lipophilic compounds, whereas hydrophilic ones tend to be freer to penetrate through (Boegh and Nielsen, 2015). It has been demonstrated how lipophilic drugs are able to interact with the non-glycosylated regions of the mucin macromolecule (naked protein region), which provide an area for a hydrophobic interaction with the drug. Therefore, the interaction between a lipophilic drug and mucin's hydrophobic region can slow down its diffusion through the mucus layer (Khanvilkar et al., 2001). On the other hand, for the hydrophilic compounds, their ionization can be the driving force of the diffusion through the mucus (Shaw et al., 2005).

In conclusion, the use of differently viscous mucus layers (mucin concentration of 10, 20 or 40 mg/mL) did not lead to differences in permeability of all of the tested drugs (Fig. 4), even though an increase in viscosity could suggest a slowed-down diffusion through mucus and a lower permeability through the barrier. Therefore, since no direct correlation was found between the concentration of mucin in the mucus layer and the drugs' permeability, mucin 10 mg/mL was chosen as the preferred suspension since it was the easiest to handle from a practical point of view.

Fig. 5 shows the permeabilities of different compounds in the presence and absence of mucus (no mucin or 10 mg/mL mucin suspension, respectively) at room temperature (23–25 °C) and at the physiological temperature (37 °C). The permeability of the fluorescent marker calcein was measured at both temperatures to assure that the barriers would maintain their integrity in both conditions. In all experiments, the electrical resistance was found to be in the range reported for the barriers with maintained integrity (Flaten et al., 2008). The different P_{apps} of the tested drugs confirmed the ability of the barriers to discriminate between compounds with different chemical structures and properties (Table 1) both for the original PVPA barriers and for the novel mucus-PVPA ones. Although some of the chosen drugs had similar chemical properties, the resulting permeability values were found to be compound-dependent, confirming that multiple forces are responsible for the diffusion and permeation of drugs, and that an *in vitro* screening model should be able to highlight different characteristics, especially in relation to mucus-drug interaction. The permeability of all the tested drugs further increased at 37 °C, most probably due to a more fluid lipid layer of the barriers and potentially a lower viscosity connected to the higher temperature. In general, the addition of mucus on top of the PVPA barriers led to a significant decrease in permeability at both temperatures as earlier discussed and as expected due to the intrinsic characteristic of mucus (Sigurdsson et al., 2013).

However, if all drugs/marker would have behaved identically in presence of the mucus layer compared to its absence, one could conclude that the rate-limiting factor could be the different diffusive pathway length between the original PVPA barriers and the mucus-PVPA model. Nevertheless, what we have found in our study was that the permeabilities were linked to the chemical structure and physiochemical properties of the drug/marker and to the possible interactions with the mucus layer. For this reason, we believe that the interaction with this layer, rather than the longer diffusive pathway, is the important factor influencing the permeability of the compounds analysed in this study.

Permeability experiments were also carried out on filters covered with mucus only (without the phospholipid vesicle barrier), in order to assess the contribution of the sole mucus layer on the permeability of the drugs. However, it was found that the filters were not able to hold the mucus in the donor compartment (58.82 ± 2.57% of the total amount of mucus that was placed on top of the filters was found in the acceptor medium after 5 h). Due to this, it was not possible to assess the contribution of the mucus layer alone and compare it to the PVPA or mucus-PVPA model.

A correlation between permeability coefficients of model drugs obtained with the PVPA model, other well known models (such as Caco-2 and PAMPA) and the fraction absorbed in humans after oral administration was already assessed in previous studies (Flaten et al., 2006b; Naderkhani et al., 2014b). The novel mucus-PVPA model was still able to correctly classify the different model drugs in the same way the original model did (poorly, moderately and excellently absorbed drugs), even though P_{app} values significantly changed with the addition of mucus compared to its absence.

3.3. Permeability of liposome-associated drugs using the mucus-PVPA

Concerning mucosal administration, nanoparticulate mucoadhesive and mucopenetrating formulations have demonstrated great efficacy in

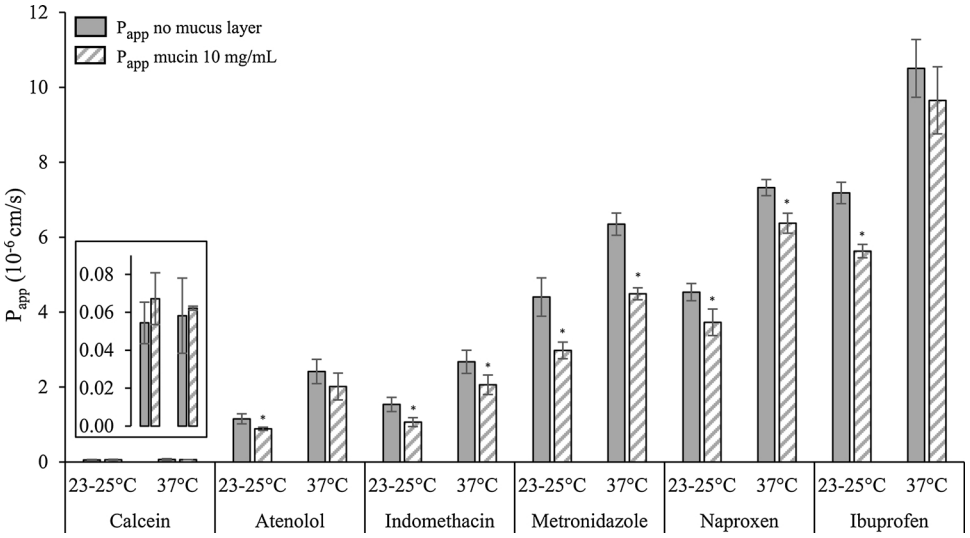

Fig. 5. Permeability of different compounds in the presence and absence of mucin (10 mg/mL) at room temperature (23–25 °C) and at 37 °C. The results are indicated as mean ± SD (n = 3). Statistical significance ($p < 0.05$) was investigated with one-way ANOVA using the Bonferroni *post hoc* test.
*Statistically significant difference in drugs' P_{app} in the presence of mucus compared to its absence.

multiple *in vitro* and *in vivo* studies, for both local and systemic drug delivery, confirming their innovative contribution to the pharmaceutical development (Netsomboom and Bernkop-Schnürch, 2016). In particular, liposomes have been established as promising carriers to improve the absorption of poorly absorbed drugs and several liposomal products are already on the market (Allen and Cullis, 2013). Mucoadhesive formulations (e.g. chitosan-coated liposomes) can actively interact with the mucus layer, extending the resident time in the application site and increasing the local concentration of the drug contained in the delivery systems (Boegh and Nielsen, 2015). On the other hand, mucopenetrating formulations (e.g. PEGylated liposomes) are able to avoid the interaction with the mucus layer, accessing the underlying epithelia in a more effective manner (das Neves et al., 2011; Lai et al., 2011; Mahmood et al., 2017).

The optimal formulation should be able to assure a high drug concentration at the administration site and consequently a concentration gradient, allowing a passive diffusion across the mucus layer. In this study, plain, chitosan-coated and PEGylated liposomes have been chosen as model drug delivery systems to get their diffusive properties be tested on the novel mucus-PVPA model. We have already tested mucoadhesive and plain liposomes on the original PVPA (Naderkhani et al., 2014a). However, we realized the importance of the presence of mucus to optimize the estimation of the penetration potential of nanosystems.

3.3.1. *The effect of the delivery system on drug permeability in the mucus-PVPA*

The degree of interaction with mucus largely depends on the size and surface properties of the delivery system. It has been reported that by increasing the particle size of a delivery system from 124 to 560 nm the amount transported in time through the mucus layer significantly decreases due to a stronger steric impediment (Sanders et al., 2000). Moreover, Takeuchi et al. (2001) have found that 100 nm liposomes are able to diffuse through the mucus layer to a higher extent compared to bigger ones. However, the surface properties of the delivery system could also dictate its interaction with mucus, making the size the secondary diffusion driving force. It has been demonstrated that nanosystems bearing a positive charge are able to actively interact with the negatively charged mucus layer, producing a mucoadhesion effect (e.g. chitosan-coated particles) (Mackie et al., 2017), whereas slightly negatively charged and neutral systems would favour a higher diffusion ability thanks to their lack of interaction with such layer (e.g. PEGylated particles) (Griffiths et al., 2010; Jøraholmen et al., 2017; Lieleg et al., 2010). However, the particles that are strongly attracted to mucus would be completely immobilized, whereas excessively negatively charged particles would be repulsed and unable to diffuse through such a layer (Groo and Lagarce, 2014; Lieleg et al., 2010). Lieleg and colleagues have confirmed that particles' mobility through the mucus layer is particularly influenced by their surface charge. They suggested that charged particles can interact via electrostatic interaction with mucin, slowing down their diffusion through the mucus layer (Lieleg et al., 2010). The authors have compared the diffusion through mucus of differently functionalised particles at different pHs, and found out that at neutral pH the diffusion of charged particles was not majorly hindered compared to that of neutral particles, whereas at pH 3 there was a significant difference in the diffusion of neutral and charged formulations. Moreover, according to the results from Lieleg et al., the zeta potential of the PEGyalted particles changed with the different pH conditions (neutral surface potential at pH 3 and negative at pH 7, Lieleg et al., 2010).

Table 2
Liposomal characteristics. The results are expressed as mean ± SD (n = 3).

Formulation[a]	Vesicle size (nm)	PI	Zeta potential (mV)	Entrapment (%)
Plain liposomes containing NPR	146.30 ± 13.15 (100%)	0.28	−2.32 ± 1.20	26.15 ± 2.19
Coated liposomes containing NPR	138.10 ± 4.38 (95.2%)	0.38	0.19 ± 0.50	37.43 ± 5.79
PEGylated liposomes containing NPR	128.00 ± 6.36 (99.8%)	0.18	−10.89 ± 2.13	23.58 ± 0.31
Plain liposomes containing IND	140.85 ± 5.87 (97.6%)	0.27	−24.75 ± 0.35	83.30 ± 3.88
Coated liposomes containing IND	134.15 ± 18.74 (96.5%)	0.30	−18.68 ± 1.53	73.87 ± 4.03
PEGylated liposomes containing IND	96.22 ± 5.11 (98.3%)	0.23	−10.60 ± 0.34	77.81[b]
Plain liposomes containing MTR	202.52 ± 2.24 (70.1%)	0.52	−2.13 ± 1.34	2.82 ± 0.14
Coated liposomes containing MTR	162.27 ± 8.44 (68.9%)	0.63	1.91 ± 0.24	2.78 ± 0.01
PEGylated liposomes containing MTR	105.40 ± 5.11 (98.6%)	0.20	−4.38 ± 0.519	2.58 ± 0.20

[a] Naproxen (NPR), indomethacin (IND) and metronidazole (MTR).
[b] Only one batch was prepared.

In our study, plain, chitosan-coated and PEGylated liposomes were prepared incorporating three different drugs, respectively (Table 2). The size of the liposomes ranged between 100 and 200 nm and the liposome dispersions exhibited a bimodal size distribution with varying polydispersity indexes (PI), depending on the formulation. The zeta potential varied between the different formulations and was dependant on the incorporated drug. However, the coating process led to an increase in zeta potential for the chitosan-coated formulations, as expected (Berginc et al., 2014). It has to be highlighted that the PEGylated formulations exhibited a negative zeta potential for all the drugs incorporated and this characteristic could be of a key importance regarding the mucus-penetrating properties (Groo and Lagarce, 2014). The fact that negatively charged nanocarriers have the characteristics of being mucopenetrating is also supported by the results from Chen et al. (Chen et al., 2013). Moreover, the surface potential of PEGylated liposomes obtained by Jøraholmen and colleagues, confirms the fact that PEG grafting can produce negatively charged liposomes (Jøraholmen et al., 2017). The entrapment of the three model drugs varied depending on their chemical properties. All formulations were prepared according to the methods reported by Jøraholmen and colleagues (Jøraholmen et al., 2014; Jøraholmen et al., 2015; Jøraholmen et al., 2017). The liposomes prepared in our study exhibited comparable characteristics to the ones described in the above-mentioned papers. In particular, the authors found that PEGylated formulations exhibited a reduced binding efficacy compared to plain and chitosan-coated ones, whereas chitosan-coated liposomes were binding mucin significantly more compared to plain ones (Jøraholmen et al., 2017).

As previously stated, the interaction of liposomal formulations with the mucus layer can be affected by numerous factors, such as the pH of the physiological environment, pH of the specific formulation and pKa and related degree of ionization of the associated drug (Groo and Lagarce, 2014; Jøraholmen et al., 2017; Lieleg et al., 2010; Shaw et al., 2005). In this study, chitosan-coated formulations were prepared at acidic pH and were then adjusted to pH 7.40. This process was carried out to ensure the same pH environment of the liposome-associated drug for all formulations (plain, chitosan-coated, PEGylated liposomes). This pH was selected as a model pH, however the next step would be to adjust it to the targeted mucosal site (e.g. around pH 6 depending on which part of the intestine or 4.5 for the vaginal site).

The permeability of metronidazole, indomethacin and naproxen from different liposome formulations (Fig. 6) indicated decreased permeability for liposomally-associated drugs compared to drugs in solution, confirming that liposomes assured a sustained release of the associated drugs. This is a very important feature considering prolonged release of drugs at the administration site, e.g. vaginal site (Jøraholmen et al., 2014).

For metronidazole-containing liposomes, the drug permeability did not vary between the different formulations in the absence of mucus, suggesting that the chitosan coating and PEGylation processes had a negligible effect on drug release from the liposomes compared to the plain ones, evidence supported by the results obtained by Chen et al. (2013). However, in the presence of the mucus layer, metronidazole's permeability changed according to the type of liposome formulation. In fact, chitosan-coated liposomes displayed a lower permeability of the drug compared to the plain ones, suggesting that the potential interaction between mucus and the chitosan-coating could slow down the permeation process of metronidazole, whereas PEGylated liposomes could easily penetrate through the mucus layer, contributing to a higher permeability. These results can be also explained by the different zeta potentials of the three formulations. Chitosan-coated liposomes, bearing a slightly positive zeta potential, could interact with the negatively charged mucus leading to a mucoadhesive effect, whereas the PEGylated liposomes, having a slightly negative zeta potential, could more freely diffuse through the mucus layer. These results are supported by the findings of Chen and colleagues (2013), who clearly depicted the different mucus penetration potentials of plain phosphatidylcholine, chitosan-coated and Pluronic®-modified liposomes in *ex vivo* penetration studies. Their *in vivo* pharmacokinetic study further demonstrated that the Pluronic®-modified formulation (bearing a zeta potential of −4 mV) could provide the best oral absorption profile for the chosen drug, indicating that the *ex vivo* data correlate well with the *in vivo* data.

The indomethacin- and naproxen-containing liposomes, exhibited a different penetration behaviour; indomethacin-containing plain, chitosan-coated and PEGylated liposomes were all found to be negatively charged (−25, −19 and −10 mV, respectively), a feature that could lead to a lack of significant differences in the diffusion potential of the formulation and permeability of the drug. On the other hand, for the naproxen-containing liposomes, the PEGylation lead to an increase in permeability in the absence of mucus, suggesting an intrinsic penetration behaviour of the formulation. These deviations from the trends described above for the metronidazole-containing liposomes can be ascribed to the complexity of the physicochemical characteristics of the specific liposomal formulation, highlighting the problem/challenge of generalization when studying mucus diffusion properties and permeability potentials of different types of formulations (Fabiano et al., 2017; Netsomboon and Bernkop-Schnürch, 2016). Moreover, we found that the zeta potential of the liposomes prepared varied according to the drug incorporated. Therefore, the mucopenetrating or mucoadhesive behaviour could mainly be linked to the specific zeta potential of the formulation. The permeability of the drugs depends on numerous factors including the penetration potential of the liposome formulation through the mucus layer and the interaction with it, the vesicle surface properties and size, but also the release of the drug from the delivery system, the chemical and structural properties of the specific compound and the drug equilibrium between the different layers. This confirms the high importance and need to have reliable *in vitro* permeability models able to predict the effect of mucus on the permeability of both drugs in solutions and in more complicated formulations.

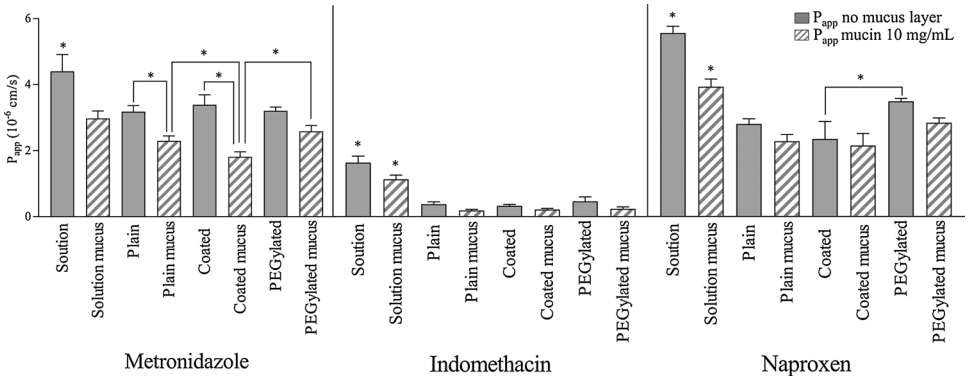

Fig. 6. Permeability of metronidazole, indomethacin and naproxen from different liposomal formulations in the presence and absence of mucin (10 mg/mL). The results are indicated as mean ± SD (n = 3). Statistical significance ($p < 0.05$) was investigated with one-way ANOVA using the Bonferroni *post hoc* test.
*Statistically significant difference in drugs' P_{app} between the highlighted bar and all the others or between 2 different bars.

4. Conclusions

The novel mucus-PVPA model was developed and exploited to better mimic the *in vivo* environment of mucosal tissues by adding a mucus-simulating layer on top of the PVPA barriers. The reliability of this upgraded version of the original PVPA model was proven in terms of the barrier tightness and functionality, and the barriers demonstrated maintained integrity under the chosen conditions. As expected, the mucus layer proved to be an additional barrier to the permeation of the selected drugs. The permeability varied depending on the different chemical structures and properties of the tested drugs. Moreover, the mucus-PVPA barriers showed potential towards being able to discriminate between different types of nanodelivery systems. The mucus-PVPA model was proven as a reliable tool in drug/active compound screening and can serve in the development and optimization of formulations destined for transmucosal delivery.

Conflict of interest

No conflict of interest are declared by the authors.

Acknowledgments

PhD student M. Falavigna is founded by the University of Tromsø The Arctic University of Norway. The generosity of Lipoid GmbH (Ludwigshafen, Germany) for the donation of phospholipids is highly appreciated and acknowledged.

Appendix A. Supplementary data

Supplementary data associated with this article can be found, in the online version, at https://doi.org/10.1016/j.ijpharm.2017.12.038.

References

Allen, T.M., Cullis, P.R., 2013. Liposomal drug delivery systems: from concept to clinical application. Adv. Drug Deliv. Rev. 65, 36–48.
Artusson, P., Palm, K., Luthman, K., 2001. Caco-2 monolayers in experimental and theoretical predictions of drug transport. Adv. Drug Deliv. Rev. 46, 27–43.
Avdeef, A., 2003. Absorption and Drug Development: Solubility, Permeability, and Charge State. John Wiley & Sons, New Jersey.
Bajka, B.H., Rigby, N.M., Cross, K.L., Macierzanka, A., Mackie, A.R., 2015. The influence of small intestinal mucus structure on particle transport *ex vivo*. Colloids Surf. B 135, 73–80.
Bartlett, G.R., 1959. Phosphorus assay in column chromatography. J. Biol. Chem. 234, 466–468.
Benet, L.Z., Broccatelli, F., Oprea, T.I., 2011. BDDCS applied to over 900 drugs. AAPS J. 13 (4), 519–547.
Berben, P., Brouwers, J., Augustijns, P., 2017. Assessment of passive intestinal permeability using an artificial membrane insert system. J. Pharm. Sci. http://dx.doi.org/10.1016/j.xphs.2017.08.002.
Berginc, K., Suljakovic, S., Škalko-Basnet, N., Kristl, A., 2014. Mucoadhesive liposomes as new formulations for vaginal delivery of curcumin. Eur. J. Pharm. Biopharm. 87, 40–46.
Boegh, M., Nielsen, H.M., 2015. Mucus as a barrier to drug delivery – understanding and mimicking the barrier properties. Basic Clin. Pharmacol. Toxicol. 116 (3), 179–186.
Boegh, M., Baldursdóttir, S.G., Müller, A., Nielsen, H.M., 2014. Property profiling of biosimilar mucus in a novel mucus-containing *in vitro* model for assessment of intestinal drug absorption. Eur. J. Pharm. Biopharm. 87, 227–235.
Chen, D., Xia, D., Li, X., Zhu, Q., Yu, H., Zhu, C., Gan, Y., 2013. Comparative study of Pluronic® F127-modified liposomes and chitosan-modified liposomes for mucus penetration and oral absorption of cyclosporine A in rats. Int. J. Pharm. 449, 1–9.
Dawson, M., Krauland, E., Wirtz, D., Hanes, J., 2004. Transport of polymeric nanoparticle gene carriers in gastric mucus. Biotechnol. Prog. 20, 851–857.
Fabiano, A., Zambito, Y., Bernkop-Schnürch, A., 2017. About the impact of water movement on the permeation behaviour of nanoparticles in mucus. Int. J. Pharm. 517, 279–285.
Fischer, S.M., Buckley, S.T., Kirchmeyer, W., Fricker, G., Brandl, M., 2012. Application of simulated intestinal fluid on the phospholipid vesicle-based drug permeation assay. Int. J. Pharm. 422, 52–58.
Flaten, G.E., Bunjes, H., Luthman, K., Brandl, M., 2006a. Drug permeability across a phospholipid vesicle-based barrier 2. Characterization of barrier structure, storage stability and stability towards pH changes. Eur. J. Pharm. Sci. 28, 336–343.
Flaten, G.E., Dhanikula, A.B., Luthman, K., Brandl, M., 2006b. Drug permeability across a phospholipid vesicle barrier: a novel approach for studying passive diffusion. Eur. J. Pharm. Sci. 27, 80–90.
Flaten, G.E., Luthman, K., Vasskog, T., Brandl, M., 2008. Drug permeability across a phospholipid vesicle-based barrier: 4. The effect of tensides, co-solvent and pH changes on barrier integrity and on drug permeability. Eur. J. Pharm. Sci. 34, 173–180.
Flaten, G.E., Kottra, G., Stensen, W., Isaksen, G., Karstad, R., Svendsen, J.S., Daniel, H., Svenson, J., 2011. *In vitro* characterization of human peptide transported hPEPT1 interactions and passive permeation studies of short cationic antimicrobial peptides. J. Med. Chem. 54, 2422–2432.
Friedl, H., Dunnhaupt, S., Hintzen, F., Waldner, C., Parikh, S., Pearson, J.P., Wilcox, M.D., Bernkop-Schnurch, A., 2013. Development and evaluation of a novel mucus diffusion test system approved by self-nanoemulsifying drug delivery system. J. Pharm. Sci. 102, 4406–4413.
Grießinger, J., Dünnhaupt, S., Cattoz, B., Griffiths, P., Oh, S., Borrós i Gómez, S., Wilcox, M., Pearson, J., Gumbleton, M., Abdulkarim, M., Pereira de Sousa, I., Bernkop-Schnürch, A., 2015. Methods to determine the interactions of micro- and nanoparticles with mucus. Eur. J. Pharm. Biopharm. 96, 464–476.
Griffiths, P.C., Occhipinti, P., Morris, C., Heenan, R.K., King, M.S., Gumbleton, M., 2010. PGSE-NMR and SANS studies of the interaction of model polymer therapeutics with mucin. Biomacromolecules 11, 120–125.
Groo, A.C., Lagarce, F., 2014. Mucus models to evaluate nanomedicines for diffusion. Drug Discov. Today 19 (8), 1097–1108.
Hilgendorf, C., Spahn-Langguth, H., Regardh, C.G., Lipka, E., Amidon, G.L., Langguth, P., 2000. Caco-2 versus Caco-2/HT29-MTX co-cultured cell lines: permeabilities via diffusion, inside- and outside-directed carrier-mediated transport. J. Pharm. Sci. 89, 63–75.
Huckaby, J., Lai, S.K., 2017. PEGylation for enhancing nanoparticle diffusion in mucus. Adv. Drug Deliv. Rev. http://dx.doi.org/10.1016/j.addr.2017.08.010.
Jøraholmen, M.W., Vanić, Z., Tho, I., Škalko-Basnet, N., 2014. Chitosan-coated liposomes for topical vaginal therapy: assuring localized drug effect. Int. J. Pharm. 472, 94–101.
Jøraholmen, M.W., Škalko-Basnet, N., Acharya, G., Basnet, P., 2015. Resveratrol-loaded liposomes for topical treatment of the vaginal inflammation and infections. Eur. J. Pharm. Sci. 79, 112–121.
Jøraholmen, M.W., Basnet, P., Acharya, G., Škalko-Basnet, N., 2017. PEGylated liposomes for topical vaginal therapy improve delivery of interferon alpha. Eur. J. Pharm. Biopharm. 113, 132–139.
Kansy, M., Senner, F., Gubernator, K., 1998. Physicochemical high throughput screening: parallel artificial membrane permeation assay in the description of passive absorption processes. J. Med. Chem. 41, 1007–1010.
Kanzer, J., Tho, I., Flaten, G.E., Mägerlein, M., Hölig, P., Fricker, G., Brandl, M., 2010. In-vitro permeability screening of melt extrudate formulations containing poorly water-soluble drug compounds using the phospholipid vesicle-based barrier. J. Pharm. Pharmacol. 62, 1591–1598.
Khanvilkar, K., Donovan, M.D., Flanagan, D.R., 2001. Drug transfer through mucus. Adv. Drug Deliv. Rev. 48, 173–193.
Kocevar-Nared, J., Kristl, J., Smid-Korbar, J., 1997. Comparative rheological investigation of crude gastric mucin and natural gastric mucus. Biomaterials 18, 677–681.
Lai, S.K., Suk, J.S., Pace, A., Wang, Y.Y., Yang, M., Mert, O., Chen, J., Kim, J., Hanes, J., 2011. Drug carrier nanoparticles that penetrate human chronic rhinosinusitis mucus. Biomaterials 32, 6285–6290.
Larhed, A.W., Artursson, P., Björk, E., 1998. The influence of intestinal mucus components on the diffusion of drugs. Pharm. Res. 15 (1), 66–71.
Leal, J., Smyth, H.D.C., Ghosh, D., 2017. Physicochemical properties of mucus and their impact on transmucosal drug delivery. Int. J. Pharm. https://doi.org/10.1016/j.ijpharm.2017.09.018.
Lechanteur, A., das Neves, J., Sarmento, B., 2017. The role of mucus in cell-based models used to screen mucosal drug delivery. Adv. Drug Deliv. Rev. https://doi.org/10.1016/j.addr.2017.07.019.
Legen, I., Kristl, A., 2001. Comparative permeability of some acyclovir derivatives through native mucus and crude mucin dispersions. Drug Dev. Ind. Pharm. 27 (7), 669–674.
Lieleg, O., Vladescu, I., Ribbeck, K., 2010. Characterization of particle translocation through mucin hydrogels. Biophys. J. 98, 1782–1789.
Mackie, A.R., Goycoolea, F.M., Menchicchi, B., Caramella, C.M., Saporito, F., Lee, S., Stephansen, K., Chronakis, I.S., Hiorth, M., Adamczak, M., Waldner, M., Nielsen, H.M., Marcelloni, L., 2017. Innovative methods and applications in mucoadhesion research. Macromol. Biosci. 17, 1600534.
Mahmood, A., Laffleur, F., Leonaviciute, G., Bernkop-Schnürch, A., 2017. Protease-functionalized mucus penetrating microparticles: in-vivo evidence for their potential. Int. J. Pharm. 532, 177–184.
Matthes, I., Nimmerfall, F., Sucker, H., 1992. Pharmazie 47, 505–515.
Naderkhani, E., Erber, A., Škalko-Basnet, N., Flaten, G.E., 2014a. Improved permeability of acyclovir: optimization of mucoadhesive liposomes using the PVPA model. J. Pharm. Sci. 103, 661–668.
Naderkhani, E., Isaksson, J., Ryzakov, A., Flaten, G.E., 2014b. Development of a biomimetic phospholipid vesicle-based permeation assay (PVPA) for the estimation of intestinal drug permeability. J. Pharm. Sci. 103, 1882–1890.
Naderkhani, E., Vasskog, T., Flaten, G.E., 2015. Biomimetic PVPA *in vitro* model for estimation of the intestinal drug permeability using fasted and fed state simulated intestinal fluids. Eur. J. Pharm. Sci. 73, 64–71.
Netsomboon, K., Bernkop-Schnürch, A., 2016. Mucoadhesive vs mucopenetrating particulate drug delivery. Eur. J. Pharm. Biopharm. 98, 76–89.
Olmsted, S.S., Padgett, J.L., Yudin, A.I., Whaley, K.J., Moench, T.R., Cone, R.A., 2001. Diffusion of macromolecules and virus-like particles in human cervical mucus. Biophys. J. 81, 1930–1937.
Park, M.S., Chung, J.W., Kim, Y.K., Chung, S.C., Kho, H.S., 2007. Viscosity and wettability

of animal mucin solutions and human saliva. Oral Dis. 13, 181–186.
Peppas, N.A., Huang, Y., 2004. Nanoscale technology of mucoadhesive interactions. Adv. Drug Deliv. Rev. 56, 1675–1687.
Rediguieri, C.F., Porta, V., Nunes, D.S.G., Nunes, T.M., Junginger, H.E., Kopp, S., Midha, K.K., Shah, V.P., Stavchansky, S., Dressman, J.B., Barends, D.M., 2011. Biowaiver monographs for immediate release solid oral dosage forms: metronidazole. J. Pharm. Sci. 100, 1618–1627.
Sanders, N.N., Smedt, S.C., Van Rompaey, E., Simoens, P., de Baets, F., Demeester, J., 2000. Cystic fibrosis sputum: a barrier to the transport of nanospheres. Am. J. Respir. Crit. Care Med. 162, 1905–1911.
Schimpel, C., Teubl, B., Absenger, M., Meindl, C., Frohlich, E., Leitinger, G., Zimmer, A., Roblegg, E., 2014. Development of an advanced intestinal *in vitro* triple culture permeability model to study transport of nanoparticles. Mol. Pharm. 11, 808–818.
Shaw, L.R., Irwin, W.J., Grattan, T.J., Conway, B.R., 2005. The influence of excipients on the diffusion of ibuprofen and paracetamol in gastric mucus. Int. J. Pharm. 290, 145–154.
Sigurdsson, H.H., Kirch, J., Lehr, C.M., 2013. Mucus as a barrier to lipophilic drugs. Int. J. Pharm. 453 (1), 56–64.
Takeuchi, H., Yamamoto, H., Kawashima, Y., 2001. Mucoadhesive nanoparticulate systems for peptide drug delivery. Adv. Drug Deliv. Rev. 47 (1), 39–54.
Teubl, B.J., Absenger, M., Fröhlich, E., Leitinger, G., Zimmer, A., Roblegg, E., 2013. The oral cavity as a biological barrier system: design of an advanced buccal *in vitro* permeability model. Eur. J. Pharm. Biopharm. 84, 386–393.
das Neves, J., Amiji, M., Sarmento, B., 2011. Mucoadhesive nanosystems for vaginal microbicide development: friend or foe? Wiley Interdiscip. Rev. Nanomed. Nanobiotechnol. 3, 389–399.
di Cagno, M., Bibi, H.A., Bauer-Brandl, A., 2015. New biomimetic Permeapad™ for efficient investigation of passive permeability of drugs. Eur. J. Pharm. Sci. 73, 29–34.

Further reading

Richter, J.F., Schmauder, R., Krug, S.M., Gebert, A., Schumann, M., 2016. A novel method for imaging sites of paracellular passage of macromolecules in epithelial sheets. J. Control. Release 229, 70–79.
Ternullo, S., de Weerd, L., Flaten, G.E., Holsæter, A.M., Škalko-Basnet, N., 2017. The isolated perfused human skin flap model: a missing link in skin penetration studies? Eur. J. Pharm. Sci. 96, 334–341.

Supplementary

Confocal laser scanning microscopy

Methods

Confocal laser scanning microscopy (CLSM) was used to assess possible interactions between the mucin suspensions and the PVPA barriers. The barriers were prepared as described in section 2.2 with the only exception that 0.2 mol% of the Lipoid E80 was replaced by 1,2-dioleoyl-sn-glycero-3-phophoethanolamine-N-(Lissamine rhodamine B sulfonyl) (ammonium salt) rhodamine (purchased from Avanti Polar Lipids, Inc., Alabama, USA) to visualise the lipids composing the barriers. Calcein solution (1.65 mg/mL) was used to produce two suspensions with different mucin concentrations (10 mg/mL and 40 mg/mL). Before the experiment, 50 µL of either calcein solution or mucin suspensions (10 mg/mL and 40 mg/mL) were added to the donor compartment and the system was left to soak for three hours in the acceptor wells containing 600 µL of PBS pH 7.4 to visualise possible aqueous channels throughout the barriers' thickness caused by the mucus layer . After soaking, the donor fluids were removed and the filters carefully detached from the inserts. The CLSM analysis was performed on a Leica TCS SP5 microscope (Leica Microsystems CMS GmbH, Mannheim, Germany) equipped with an Argon laser for calcein and a DPSS 561 laser for rhodamine. Laser lines of 488 and 568 nm were used to excite calcein and rhodamine, respectively. For calcein, fluorescence was detected in the spectral range of 500-550 nm, while rhodamine was detected at 570-610 nm (Ternullo et al., 2017). Images were acquired with a 10x0.4 objective taking z-section micrographs (z-step size of 0.25 µm). To make sure the defects were not present throughout the whole thickness of the barriers, 420 z-sections were analysed for each barrier. The gain, off-set and zoom were kept as constant as possible to maintain the same setup for all the micrographs. The micrographs were superimposed using Volocity® v.6.3 software (PerkinElmer, MA, USA).

Results

In a previous study, Flaten and colleagues have analysed via confocal electron scanning microscopy the filters composing the PVPA barriers without the addition of the liposomes (Flaten et al., 2006a) and used it as a control in order to visualise how aqueous channels look like in the absence of the lipid component. By comparing this control to confocal images of the PVPA barriers, they were able to see that no significant aqueous channels were present throughout the thickness of the PVPA barriers. In our study, we wanted to visualise if the addition of mucus would cause the formation of aqueous channels in the PVPA barriers, especially since the high permeability of molecules (in or case the highly hydrophilic marker calcein) can be traced back to a significant number or defects and aqueous channels in the barriers (Richter et al., 2016).

Confocal images are shown in Fig. S1 (calcein solution in the donor), Fig. S2 (10 mg/mL mucin suspended in calcein solution the donor) and Fig. S3 (40 mg/mL mucin suspended in calcein solution in the donor).

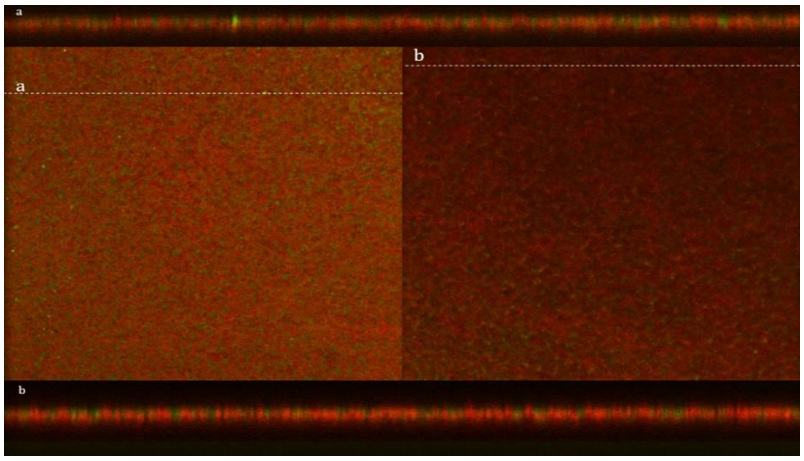

Fig. S1. Confocal laser scanning microscopy of the PVPA barrier labelled with rhodamine (red) after soaking for 3 hours in calcein solution (green). The two micrographs were taken from two different positions in the barrier. The white lines mark the placement of the cross-sections a and b shown at the top and bottom, respectively.

Fig. S1 displays the PVPA barrier after exposure to the calcein solution, showing a dominant red fluorescence representing the rhodamine-associated PVPA barrier and a green fluorescence of the hydrophilic calcein solution. The cross-sections a and b taken in different positions confirm lack of aqueous channels through the barrier, suggesting the maintenance of the barrier's integrity in the given condition. This is in agreement with previous CLSM studies of the original PVPA barriers (Flaten et al. 2006a).

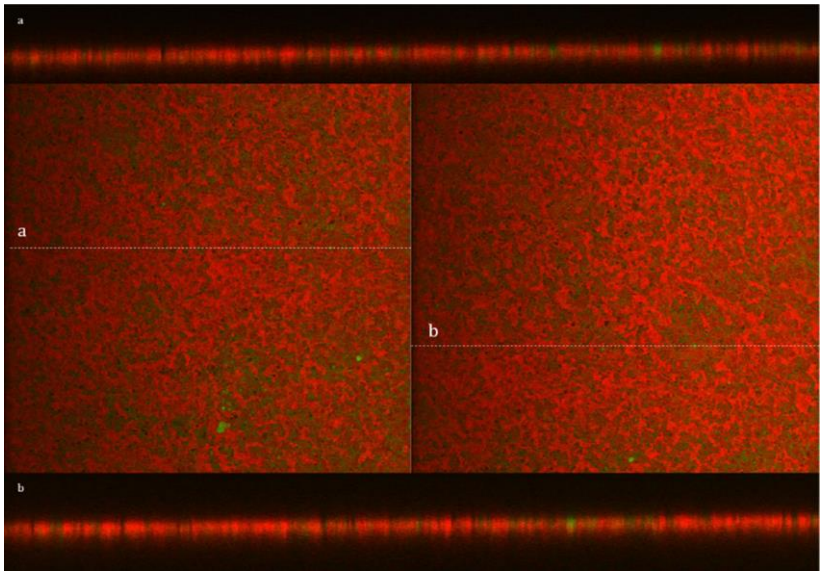

Fig. S2. Confocal laser scanning microscopy of the PVPA barrier labelled with rhodamine (red) after soaking for 3 hours in mucin 10 mg/mL marked with calcein (green). The two micrographs were taken from two different positions in the barrier. The white lines mark the placement of the cross-sections a and b shown at the top and bottom, respectively.

Fig. S2 indicates that no aqueous channels were present after the exposure to the lowest concentration of mucus suspension.

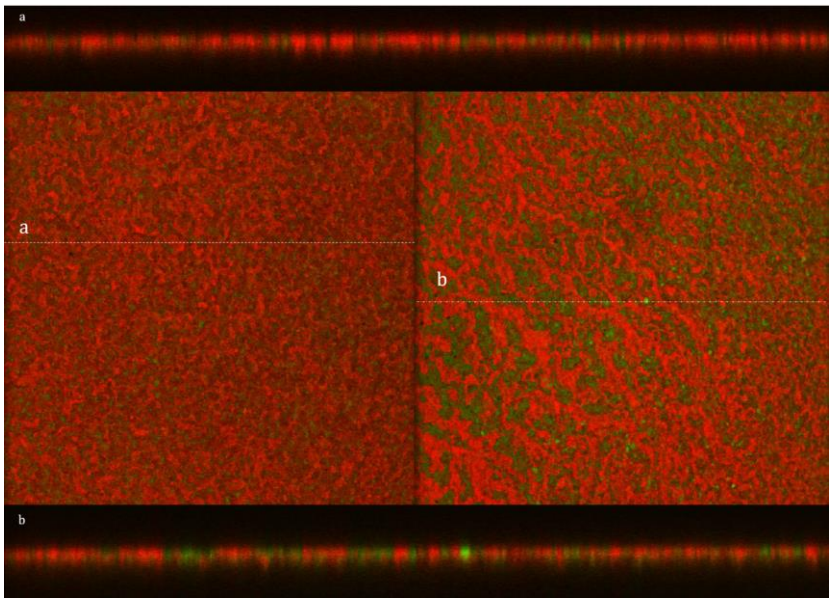

Fig. S3. Confocal laser scanning microscopy of the PVPA barrier labelled with rhodamine (red) after soaking for 3 hours in mucin 40 mg/mL marked with calcein (green). The two micrographs were taken from two different positions in the barrier. The white lines mark the placement of the cross-sections a and b shown at the top and bottom, respectively.

As it can be observed from Fig. S3, calcein was more abundant as compared to previous results (Fig. S1 and S2). The first cross-section (a) indicates a barrier similar to the one when PVPA barrier was exposed to calcein solution (Fig. S1 and S2). In the second micrograph and cross-section (b) calcein was visible in a higher concentration in the donor side of the barrier. However, no significant breaches in the barrier were observed, suggesting that the barrier's integrity was maintained also in the presence of the highest concentration of mucus suspension.

Paper II

European Journal of Pharmaceutical Sciences 132 (2019) 44–54

Contents lists available at ScienceDirect

European Journal of Pharmaceutical Sciences

journal homepage: www.elsevier.com/locate/ejps

Mimicking regional and fasted/fed state conditions in the intestine with the mucus-PVPA *in vitro* model: The impact of pH and simulated intestinal fluids on drug permeability

Margherita Falavigna[a], Mette Klitgaard[a,b], Erik Steene[c], Gøril Eide Flaten[a,*]

[a] Drug Transport and Delivery Research Group, Department of Pharmacy, University of Tromsø The Arctic University of Norway, Universitetsveien 57, 9037 Tromsø, Norway
[b] Physiological Pharmaceutics, Department of Pharmacy, University of Copenhagen, Universitetsparken 2-4, 2100 Copenhagen, Denmark
[c] Biotec Betaglucans AS, Sykehusvegen 23, 9019 Tromsø, Norway

ARTICLE INFO

Keywords:
In vitro model
pH-dependent permeability
pH-dependent solubility
Mucus
FaSSIF/FeSSIF
Simulated intestinal fluids

ABSTRACT

Intestinal drug absorption following oral administration can be influenced by regional conditions (absorbing surface area, bacterial flora, motility, pH, mucus thickness) and food intake, all of which affect drug solubility and permeability. Therefore, it is crucial to assess the impact of these conditions on the drugability of drugs and formulations. In this study, the ability of the liposome-based mucus-PVPA *in vitro* permeability model to handle relevant intestinal pH conditions was evaluated, together with the investigation on the pH-dependent solubility and permeability profiles of five model drugs. This study additionally evaluated the impact of all commercially available versions of the fasted and fed state simulated intestinal fluids (SIFs) on the integrity of the barriers, and the permeabilities of one hydrophilic and one lipophilic compound were examined under these conditions. The model was found to be well-functioning in all tested pH conditions, and a pH-dependent trend was found for both solubility and permeability profiles for acidic and basic compounds, according to their degree of ionization. Moreover, the mucus layer and its pH-dependent viscosity particularly influenced the permeation of more lipophilic compounds. The PVPA barriers primarily maintained their functionality in the presence of the fed state SIFs, and the permeability of the two tested compounds showed to be influenced by their hydrophilicity/lipophilicity, their degree of interaction with mucus and by the bile salts and phospholipids content in the SIFs. Overall, the obtained results highlight the relevance of studying the effect that pH, mucus and SIFs have on intestinal drug absorption, and suggest the suitability of the mucus-PVPA model for such investigations.

1. Introduction

The small intestine forms the largest part of the gastrointestinal (GI) tract promoting the absorption of orally administered drugs (Billat et al., 2017). Its three segments (namely, duodenum, jejunum and ileum) are characterized by differences in length, absorbing surface area, bacterial flora, motility, pH and mucus thickness (Billat et al., 2017). The different regional characteristics can influence the solubility and permeability of drugs, and thereby their absorption after oral administration. For instance, the changes in pH through the length of the GI tract can influence the ionization of the drugs and thus their intestinal absorption, as suggested by the pH partition hypothesis (Shore et al., 1957). Changes in pH can also affect the hydrophilic mucus layer, which lines, lubricates and protects the GI tract. This layer is the first barrier that drugs need to overcome in order to explicate their effect (Johansson et al., 2013), and changes in pH can affect its structure and rheology, consequently impacting the diffusion properties of the drugs through it (Cao et al., 1999; Lieleg et al., 2010).

In addition to the regional physiological changes in the GI tract, the characteristics and composition of the intestinal fluids vary widely according to the pre- or post- prandial state (Clarysse et al., 2009; Riethorst et al., 2016; Riethorst et al., 2018). In this regard, it has been demonstrated that bile salts and phospholipids in the human intestinal fluids can affect drug solubilization, and thus influence permeability through the intestinal walls (Riethorst et al., 2018). These regional and nutritional differences can also have an effect on drug absorption in a different manner according to the intrinsic characteristics of the drug in consideration and to its formulation features (Augustijns et al., 2014). A

* Corresponding author.
E-mail addresses: margherita.falavigna@uit.no (M. Falavigna), mette.jensen@sund.ku.dk (M. Klitgaard), erik.steene@biotec.no (E. Steene), goril.flaten@uit.no (G.E. Flaten).

https://doi.org/10.1016/j.ejps.2019.02.035
Received 28 November 2018; Received in revised form 1 February 2019; Accepted 25 February 2019
Available online 27 February 2019

conspicuous effort has thus been put into simulating the human intestinal fluids, and as a result different versions of fasted and fed state simulated intestinal fluids (FaSSIF and FeSSIF) have been proposed (Galia et al., 1998; Jantratid et al., 2008).

Since all these variables can affect the absorption of drugs and formulations, understanding their impact is crucial, especially as oral drug administration is still regarded as the leading route for drug delivery due to its accessibility, great patient compliance and cost-effectiveness (Berben et al., 2018a). To assess the impact of these variables on drugability (*i.e.* the ability of a drug to be used as a satisfactory candidate for oral administration) while avoiding ethical, time- and cost-consuming issues related to human and animal testing, numerous *in vitro* permeability screening models have been proposed (Caco-2 model, Artusson et al., 2001; PAMPA model, Kansy et al., 1998; PVPA model, Flaten et al., 2006b; Permeapad™, di Cagno et al., 2015; AMI-system, Berben et al., 2018b). Studies combining different *in vitro* permeability models with simulated intestinal fluids (SIFs) have been carried out by several research groups, and a special focus has been put on the impact that SIF-driven drug solubilization and permeation have on drug absorption (Berben et al., 2018b; Bibi et al., 2015; Fischer et al., 2012; Naderkhani et al., 2015). Other studies have focused on the impact that pH variations in the intestine have on drug solubility and permeability, and on the interplay that occurs between the two (Sieger et al., 2017). The effect of the mucus layer on the permeability of drugs and formulations has been investigated both with respect to their diffusion through this layer alone (Fabiano et al., 2017; Shaw et al., 2005), as well as through *in vitro* barriers in the presence of this hydrophilic layer (Falavigna et al., 2018; Keemink and Bergström, 2018; Stappaerts et al., 2018).

In the present study, we aimed to combine all the investigations discussed above. In particular, we utilised our previously developed modification of the PVPA (Phospholipid Vesicle-Based Permeation Assay) barrier comprising mucus (namely, mucus-PVPA, Falavigna et al., 2018) as a model for the intestinal membrane to move one step further toward closer mimicking the *in vivo* environment by studying the impact that pH and fasted/fed state SIFs have on drug permeability, as well as their interplay with mucus. The integrity of these liposome-based barriers was assessed in terms of permeability of a hydrophilic fluorescent marker and of the electrical resistance across the barriers at different pH and in the presence of different fasted and fed state SIFs. Subsequently, the solubility and permeability profiles of five model acidic/basic compounds were evaluated together with the investigation on the rheological behaviour of mucus at different pH conditions. Lastly, the permeability of a hydrophilic marker and a lipophilic BCS class II drug was examined in the presence of all commercially available versions of fasted and fed state SIFs.

Overall, the results collected in this study highlight the importance of assessing the impact that pH, mucus and fasted/fed SIFs have on drug permeability, and suggest the mucus-PVPA to be a promising tool for such purpose.

2. Materials and methods

2.1. Materials

Ammonium molybdate, calcein (CAL), chloroform, ethanol (96%, *v/v*), Fiske-Subbarow reducer, glacial acetic acid (≥ 99.8%), hydrochloric acid, ibuprofen (IBP), indomethacin (IND), maleic acid, methanol CHROMASOLV®, metoprolol (MTP), metronidazole (MTR), mucin from porcine stomach type III (bound sialic acid 0.5–1.5%, partially purified), naproxen (NPR), phosphorus standard solution, potassium phosphate monobasic, sodium chloride, sodium hydroxide, sodium phosphate dibasic dodecahydrate, sodium phosphate monobasic monohydrate and Triton X-100 were products of Sigma-Aldrich Chemie GmbH (Steinheim, Germany). E80 lipoid egg-phospholipids (80% phosphatidylcholine) were obtained from Lipoid GmbH (Ludwigshafen, Germany). Acetonitrile for HPLC (gradient grade) was a product of VWR chemicals (Fontenay-sous-Bois, France) and sulphuric acid was purchased from May&Baker LTD (Dagenham, England). Hydrogen peroxide 30% and Titriplex® III were obtained from Merck KGaA (Darmstadt, Germany). FaSSIF/FeSSIF/FaSSGF, FaSSIF-V2 and FeSSIF-V2 powders were purchased from biorelevant.com (Croydon, UK). All chemicals employed were of analytical grade.

For the preparation of the PVPA barriers, nucleopore track-etch membrane filters (0.4 and 0.8 μm pore size) were purchased from Whatman (part of GE Healthcare, Oslo, Norway) and the nitrocellulose membrane filters (0.65 μm DAWP) were obtained from Millipore (Billerica, Massachusetts, USA). Transwell filter inserts and plates (d = 6.5 mm) were products of Corning Inc. (Corning, New York, USA).

2.2. Drugs pH-dependent solubility studies

The solubility of different drugs (IBP, IND, MTP, MTR, NPR) was investigated at pH 5.5, 6.2 and 7.4 at room temperature (23–25 °C), following the method described by Berthelsen et al. (2014).

Briefly, phosphate buffer saline (PBS) was prepared in order to obtain three buffers with different final pH (5.5, 6.2 and 7.4). 15 mg of drug were dispersed in 15 mL of PBS in a 15 mL tube, and left to rotate on a Labinco test-tube rotor (Breda, The Netherlands) for a total of 24 h. After 1, 4 and 24 h, the tubes were centrifuged for 10 min at 4500 rpm on a Biofuge Stratos thermostated centrifuge (Heraeus Instruments GmbH, Hanau, Germany), where the temperature was kept between 23 and 25 °C to avoid sample heating and further drug solubilization. 1 mL of the supernatant solution was further centrifuged for 10 min at 13000 rpm on a Biofuge pico centrifuge (Heraeus Instruments GmbH, Hanau, Germany), in order to provide an additional separation of the possible undissolved drug, thus making sure that the amount of drug quantified at the end of the experiment would only be the fraction dissolved in the aqueous media. The supernatant was diluted and the amount of drug dissolved was quantified spectrophotometrically on SpectraMax 190 Microplate reader (Molecular Devices Corporation, California, USA). The 15 mL tubes were vortexed and put back on the rotor. For each drug and each pH, 2 samples were prepared and analysed to assess changes in solubility.

IBP, IND, MTP, MTR and NPR were quantified spectrophotometrically on SpectraMax 190 Microplate reader (Molecular Devices Corporation, California, USA) at wavelengths of 220, 254, 274, 320 and 270 nm, respectively.

2.3. PVPA barrier preparation

The PVPA barriers were prepared according to the method previously described by Naderkhani et al. (2014a). Briefly, egg-phospholipids (E80) liposomes were obtained by the film hydration technique and extruded to obtain liposomes with two different size populations by means of 0.8 and 0.4 μm pore size filters. The liposomes were then deposited by centrifugation on top of cellulose ester filters (0.65 μm pore size), followed by a freeze-thaw cycle to immobilize and fuse the liposomes to the filter support.

2.3.1. Mucus-PVPA barrier preparation

To assess the impact of the mucus layer on drug permeability, 50 μL of mucin dispersion were added on top of the PVPA barriers according to the method previously described by us (Falavigna et al., 2018). Briefly, mucin from porcine stomach type III was hydrated with PBS pH 7.4 in order to achieve a final concentration of 10 mg/mL or 40 mg/mL. The dispersion was directly pipetted on top of the PVPA barriers and was left to incubate for 5 min prior to the addition of the drug/marker solution. When the impact of different pH on drug permeability was investigated, the mucin dispersion was adjusted to the investigated pH with the use of HCl or NaOH solutions before its addition on top of the barriers.

2.3.2. Mucus rheology

Rheology measurements of the mucus prepared with different concentrations of mucin (10 and 40 mg/mL) as well as at different pH (5.5, 6.2 and 7.4) were performed on a Discovery HR-2 hybrid rheometer (TA instruments, New Castle, USA) equipped with a Peltier plate environmental system, a cross hatched 40 mm parallel plate geometry, and a cross hatched lower plate. The sample was placed on the lower plate, the geometry was lowered to the measuring gap of 1000 µm, and the system was let equilibrate for 180 s at 25 °C (the same temperature at which the permeability experiments were performed). The viscosity of the different mucus simulating dispersions and the stress applied were measured using a logarithmic flow sweep with steady state sensing, where the shear rate was increased incrementally with 30 points per decade from 2 to 200 1/s. For each mucin concentration and each pH, three samples were prepared and measured.

2.4. Simulated intestinal fluids preparation

To study the effect of simulated intestinal fluids (SIFs) on the integrity of the PVPA barriers and on drug permeability, fasted (Fa-) and fed (Fe-) state SIFs were prepared according to the standardised protocol provided by the supplier (biorelevant.com). In this study, two versions (V1 and V2) of the simulated intestinal powders were used. Briefly, FaSSIF/FeSSIF/FaSSGF (producing FaSSIF-V1 or FeSSIF-V1), FaSSIF-V2 or FeSSIF-V2 powder was dissolved in the corresponding fasted (FaB-V1 or V2) or fed (FeB-V1 or V2) buffer. The compositions of the different media are depicted in Table 1.

2.5. In vitro permeability studies

The (mucus-)PVPA barriers were used to study the permeability of different drugs/marker at room temperature (23–25 °C) following the procedure previously described (Falavigna et al., 2018), in the presence and absence of a mucus layer at different pH conditions and using different dissolution media. When the experiment was carried out in the presence of mucus, 50 µL of mucin dispersion were added on top of the PVPA barriers and let to incubate for 5 min prior to the addition of the drug/marker in solution. After the drug/marker solution (100 µL) was added on top of the PVPA barriers/mucus layer, the inserts were placed in an acceptor compartment containing 600 µL of PBS pH 7.4, simulating the *in vivo* blood circulation. The inserts were moved to fresh acceptor compartments after 1, 2, 3, 3.5, 4, 4.5 and 5 h in order to maintain sink conditions. After 5 h, the samples were collected from the acceptor compartment prior to their quantification, and the electrical resistances of the barriers were measured to examine the integrity of the barriers.

IBP, MTP, MTR and NPR were spectrophotometrically quantified as described in 2.2. IND was quantified by HPLC-UV at a wavelength of 254 nm (retention time 3.05 min; injection volume: 20 µL) using a Waters X-select™ CSH ™ C18 (2.5 µm, 3.0 × 75 mm) XP column (guard cartridge: Waters X-select™ CSH ™ C18 3.5 µm, 3.0 × 20 mm) on a Waters e2795 Separation Module connected to a Waters 2489 UV/Visible Detector (Waters, Milford, Massachusetts, USA). The flow rate was adjusted to 0.5 mL/min and the mobile phase consisted of acetonitrile and MilliQ water with 0.1% glacial acetic acid (60:40, *v*/v). CAL was quantified spectrofluorometrically at excitation and emission wavelengths of 485 and 520 nm, respectively, using a POLARstar Galaxy fluorometer (Fluostar, BMG Labtechnologies, Offenburg, Germany). Validation parameters, LOD and LOQ for the quantification of all compounds can be found in the Supplementary Material.

The apparent permeability coefficient (P_{app}) was calculated with the following equation, derived from Fick's law:

$$P_{app}\left(\frac{cm}{s}\right) = \frac{dQ}{dt} * \frac{1}{A * Cd}$$

where dQ/dt expresses the slope at the steady-state conditions (nmol/s), A is the surface area of the barriers (cm^2) and Cd represents the concentration of the drug/marker in the donor compartment (nmol/mL).

To ensure sink conditions, the drug/marker concentrations added in the donor compartment were selected in order to achieve a value below the solubility limit (< 10% of the donor concentration) in the acceptor compartment (Flaten et al., 2006a, 2006b).

For each drug/marker in each condition, the permeability study was carried out at least in triplicate (6 PVPA barriers tested for each one of the three parallels).

2.5.1. The effect of pH on barrier integrity and drug permeability

To assess changes in P_{app} due to different pH conditions of the solution in the donor compartment, several drugs/marker (*i.e.* CAL, IBP, IND, MTP, MTR and NPR) were dissolved in PBS pH 5.5, 6.2 or 7.4. In the case of the permeability experiment in the presence of mucus, mucin 10 mg/mL was prepared according to the pH of the drug/marker solution.

In particular, as an increase in the permeability of the fluorescent marker CAL would indicate possible disruption of the barriers (Flaten et al., 2006b; Naderkhani et al., 2015), its permeability was quantified to investigate the impact of changes in pH on the integrity of the barriers.

2.5.2. The effect of simulated intestinal media on barrier integrity and drug permeability

To investigate the impact of the SIFs on the integrity of the barrier and on the permeability of drugs, CAL and IBP were dissolved in FaB, FeB, FeSSIF or FaSSIF (V1 and V2), and their P_{app} was evaluated in the presence and absence of mucus (mucin 10 mg/mL). The mucus layer was prepared in accordance with the pH of the media.

As the P_{app} of CAL dissolved in the fasted media was exceeding the standard range (Flaten et al., 2006b), the influence of mucin 40 mg/mL

Table 1
Composition of the fasted (Fa-) and fed (Fe-) state simulated intestinal blank buffers (FaB, FeB) and media (FaSSIF, FeSSIF) for both version 1 and version 2 (V1, V2), as described by the provider (biorelevant.com).

	FaB-V1	FaSSIF-V1	FaB-V2	FaSSIF-V2	FeB-V1	FeSSIF-V1	FeB- V2	FeSSIF- V2
Sodium taurocholate (mM)	–	3.00	–	3.00	–	15.00	–	10.00
Lecithin (mM)	–	0.75	–	0.20	–	3.75	–	2.00
Glycerol monooleate (mM)	–	–	–	–	–	–	–	5.00
Sodium oleate (mM)	–	–	–	–	–	–	–	0.80
Maleic acid (mM)	–	–	19.10	19.10	–	–	55.00	55.00
Monobasic sodium phosphate monohydrate (mM)	28.40	28.40	–	–	–	–	–	–
Sodium chloride (mM)	106	106	68.60	68.60	203	203	126	126
Sodium hydroxide (mM)	8.70	8.70	101	101	101	101	82.00	82.00
Glacial acetic acid (mM)	–	–	–	–	144	144	–	–
pH	6.5	6.5	6.5	6.5	5.0	5.0	5.8	5.8
Osmolarity (mOsm/kg)		270		180		670		390
Buffer capacity (mM/dpH)		12		10		76		25

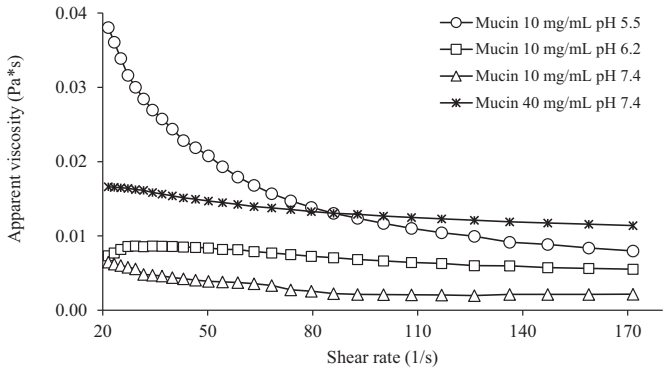

Fig. 1. Viscosity of mucus at different pH conditions (5.5, 6.2 and 7.4) and mucin concentrations (10 mg/mL and 40 mg/mL).

on the permeability of CAL was investigated to examine its potential to act as a further protective layer for the PVPA barriers.

Moreover, the same conditions studied by Fischer et al. (2012) were investigated in this study. Briefly, the PVPA barriers were incubated for 1 h in FaB (V1 or V2) prior to the addition of the CAL solution in the fasted buffers/media (FaB, FaSSIF V1 and V2), and the permeability of CAL was quantified for a total of 4 h following the procedure described in Section 2.5.

2.6. Phospholipid quantification

The amount of phospholipids lost from the PVPA barriers in the presence of fasted and fed state buffers/media was quantified using the modified phosphorus assay (Bartlett, 1959), following the method previously described by Naderkhani and colleagues (2015). Briefly, the PVPA barriers were placed in an acceptor compartment containing 600 µL of PBS pH 7.4 and the donor compartment was loaded with FaB, FeB, FaSSIF or FeSSIF (V1 and V2) (100 µL). The barriers were incubated for 5 h. The incubations in PBS pH 7.4 and 0.5% Triton X-100 were used as negative and positive control, respectively. Samples (50 µL) were withdrawn from the donor compartment after 5 h, diluted with 50 µL of distilled water and treated following the phosphorus assay. Blanks (PBS pH 7.4, 0.5% Triton X-100, FaB, FeB, FaSSIF, FeSSIF, V1 or V2) were treated in the same manner. Three PVPA barriers for each condition were tested.

2.7. Statistical analysis

The statistical evaluation of all results was carried out using GraphPad Prism 7.0 software. When significant difference between two sets of data was to be highlighted, Student *t*-test was employed ($p < 0.05$). One-way ANOVA was used to compare three or more sets of data and the Bonferroni *post hoc* test was employed to detect significant differences ($p < 0.05$).

3. Results and discussion

3.1. The pH environment of the intestinal tract

Drug solubility and permeability in the intestinal tract are regarded as the two major factors affecting oral drug absorption, especially with regards to poorly soluble compounds. As the pH environment of the intestine varies widely through its length (5.6–7.8, Bergström et al., 2014), it is of key importance to investigate its effect on solubility and permeability. In order to infer if a pH-dependent solubility/permeability trend could be observed for drugs with different physicochemical characteristics, we studied the impact that a shift in pH could have on the solubility and permeability of five different drugs. Moreover, as drug permeability was assessed both in the presence and absence of a mucus layer at pH 5.5, 6.2 and 7.4, the investigation on the integrity of the PVPA barriers and the rheological characterization of mucus in such pH conditions were carried out.

3.1.1. Barrier integrity and mucus characterization

To guarantee the optimal functionality of the (mucus-)PVPA barriers, their integrity was investigated at pH 5.5, 6.2 and 7.4. CAL was chosen as a marker to detect changes in barrier integrity at the selected pH conditions both in the presence and absence of the mucus layer. Fig. 3a (shaded area) shows that no significant increase in CAL permeability was found compared to the reference value ($0.06 * 10^{-6}$ cm/s; Flaten et al., 2006b; Flaten et al., 2008), suggesting that the investigated conditions did not cause any barrier impairment. The electrical resistance across the barriers was measured after 5 h, and the results (data not shown) also indicated intact barriers (electrical resistance > 290 Ohm*cm^2, Naderkhani et al., 2015).

Since drug permeability in the intestinal environment could be affected by the rheology of the mucus layer, and as it has been demonstrated that mucus can undergo a conformational change induced by a shift in pH (Lieleg et al., 2010), rheology measurements of the mucus placed on top of the PVPA barriers were carried out at different pH conditions and mucin concentrations.

As it can be observed in Fig. 1, the general Newtonian behaviour of the mucus at pH 6.2 (10 mg/mL) and 7.4 (10 and 40 mg/mL) confirmed previous findings regarding mucus rheology (Falavigna et al., 2018; Mackie et al., 2017). However, when decreasing the pH of the mucin hydration media to 5.5, a non-Newtonian (shear-thinning) behaviour was observed (Fig. 1), correlating with what other research groups have found in the *in vivo* mucus layer (Boegh et al., 2014; Lai et al., 2009). These findings show how the rheology of mucus could be affected by the change in environmental pH. In fact, Cao et al. (1999) have suggested that a sol-gel transition could result from a pH-induced conformational change when decreasing the pH from 6 to 7 to a more acidic one. Lieleg et al. (2010) have also proposed that, at lower pH, the mucus layer tends to generate a stronger barrier toward particle mobility compared to a neutral pH environment. With regards to mucus viscosity, Fig. 1 shows that a decrease in pH or an increase in mucin concentration, causes an increase in apparent viscosity, as previously observed in other studies (Cao et al., 1999; Park et al., 2007).

The results obtained in this study prove that mucus can undergo relevant rheology changes, which should be carefully taken into account when assessing the behaviour of a drug in such environment. These considerations are especially relevant when investigating the diffusion of drugs and formulations through the mucus layer and their subsequent permeation through the intestinal mucosa.

3.1.2. Drugs pH-solubility profiles

The pH-dependent permeability profiles of five model drugs were evaluated using the mucus-PVPA model. The selection of the drugs was carried out to cover both acidic (IBP, IND, MTR and NPR) and basic (MTP) compounds as well as compounds with different degree of lipophilicity (Table 2). Since the pH-dependent solubility of a drug is important when investigating its ability to permeate the GI barrier, solubility studies of the five model drugs were performed at pH conditions simulating different parts of the intestinal tract.

As it can be observed from Fig. 2 and Table 2, the equilibrium solubility of the investigated drugs at the different pH conditions was dependent on their acidity constant (pKa), the pH of the medium in which the drugs were solubilized and their intrinsic hydrophilicity/lipophilicity. In particular, for IBP, IND and NPR (acidic and lipophilic drugs with pKa ≈ 4 and LogP > 3), the solubility significantly increased ($p < 0.05$) from pH 5.5 to 7.4, as their degree of ionization increases at pH higher than their isoelectric point. In the case of the basic drug MTP (pKa 9.56, LogP 1.88), a non-significant decrease in solubility was found when increasing the pH to 7.4. This finding is most

Table 2
Chemical properties and solubility of calcein (CAL), ibuprofen (IBP), indomethacin (IND), metoprolol (MTP), metronidazole (MTR) and naproxen (NPR).

Abbreviation	pKa	Log P	BCS class[f]	MW (g/mol)	Wavelength (nm)	Solubility (mg/mL)
CAL	1.8/9.2[a]	-1.71[b]	–	622.55	Ex.: 485 Em.: 520	- -
IBP	4.45[c]	3.97[d]	II	206.29	220	pH 5.5: 0.37 pH 6.2: 1.06 pH 7.4: 1.72
IND	4.42[c]	4.27[d]	II	357.79	254	pH 5.5: 0.03 pH 6.2: 0.09 pH 7.4: 0.71
MTP	9.56[c]	1.88[d]	I	267.36	274	pH 5.5: 1.01 pH 6.2: 1.07 pH 7.4: 0.99
MTR	2.62[e]	-0.02[d]	I	171.15	320	pH 5.5: 1.02 pH 6.2: 1.09 pH 7.4: 1.07
NPR	4.18[c]	3.18[d]	II	230.26	270	pH 5.5: 0.15 pH 6.2: 0.56 pH 7.4: 1.37

[a] Flaten et al., 2006b.
[b] Naderkhani et al., 2014a.
[c] Avdeef, 2003.
[d] Benet et al., 2011.
[e] Rediguieri et al., 2011.
[f] Amidon et al., 1995.

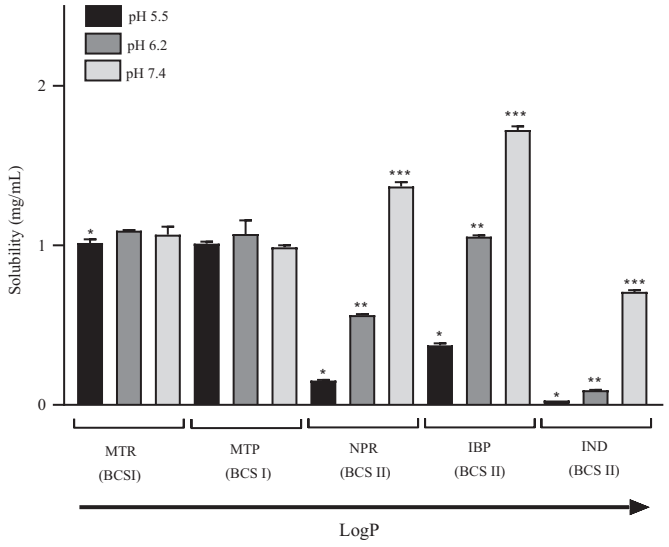

Fig. 2. Solubility of metronidazole (MTR), metoprolol (MTP), naproxen (NPR), ibuprofen (IBP) and indomethacin (IND) at pH 5.5, 6.2 and 7.4. The results are indicated as mean ± SD ($n = 6$). Statistical significance ($p < 0.05$) was investigated with one-way ANOVA using the Bonferroni *post hoc* test.
*statistically significant difference in solubility between pH 5.5 and 6.2/7.4.
**statistically significant difference in solubility between pH 6.2 and 5.5/7.4.
***statistically significant difference in solubility between pH 7.4 and 5.5/6.2.

likely related to the fact that the pH conditions at which the experiments have been performed were far below the isoelectric point of MTP, thus not significantly differentiating the solubilities at pH 5.5, 6.2 and 7.4. For MTR (pKa 2.62, LogP −0.02), a significant increase was only observed when comparing the solubility at pH 5.5 with the other two pH conditions. Again, this is most likely due to the fact that solubility changes are only observable when comparing pH closer to the isoelectric point. Moreover, the hydrophilicity/lipophilicity of the examined drugs highly influenced their solubility. The more hydrophilic compounds such as MTP and MTR were found to be more soluble compared to more lipophilic IBP, IND and NPR, as expected.

These findings are in accordance with previous pH-dependent investigations carried out both *in vitro* and *in silico* (Bergström et al., 2004; Shoghi et al., 2013; Völgyi et al., 2010; Varma et al., 2012).

Nonetheless, it has to be noted that the solubility profiles are substance-specific and that not only the pH, but also the ionic strength and the buffer capacity of the environment simulating the intestinal media should be carefully considered (Bergström et al., 2014; Hamed et al., 2016; Madsen et al., 2018).

3.1.3. Drugs pH-permeability profiles

The P_{app} of the same five model drugs was examined in the presence and absence of mucus layer at different pH conditions (5.5, 6.2 and 7.4) to investigate their possible pH-dependent permeability.

In general, the permeability of the investigated compounds in the absence of the mucus layer was found to be highly affected by their degree of ionization (Fig. 3), in accordance with the pH partition hypothesis (Shore et al., 1957). It has previously been shown that an increase in the fraction of drug in its unionized form directly increases the permeability of the drug (Flaten et al., 2008; Shore et al., 1957). In particular, in our study it was found that, for the BCS class II acidic drugs IBP and NPR, the permeability significantly decreased ($p < 0.05$) with increasing pH of the donor compartment, as the ionized form became the predominant one. Correspondingly, the permeability of the BCS class I basic drug MTP exhibited an increase in P_{app} when the pH was increasing from 5.5 to 7.4. For the BCS class II IND, the decrease in P_{app} with increasing pH was less visible, probably due to the highly lipophilic nature of the compound, which can cause a retention of the drug into the barriers and thereby causing a low recovery at the end of the experiment (Naderkhani et al., 2015). With regards to BCS class I MTR, no change in permeability was found at different pH conditions. This was most likely due to the fact that the pH conditions of the experiments were significantly above the isoelectric point for this acidic compound, in accordance with the solubility results discussed in Section 3.1.2. Furthermore, it has to be noted that more lipophilic compounds such as IBP and NPR (LogP > 3) are able to permeate the lipophilic PVPA barriers to a higher degree compared to more hydrophilic ones such as MTP and MTR due to their intrinsic nature.

The (mucus)-PVPA has previously shown to correlate well with *in vivo* data on the fraction absorbed in humans (Flaten et al., 2006b; Naderkhani et al., 2014b; Falavigna et al., 2018). Furthermore,

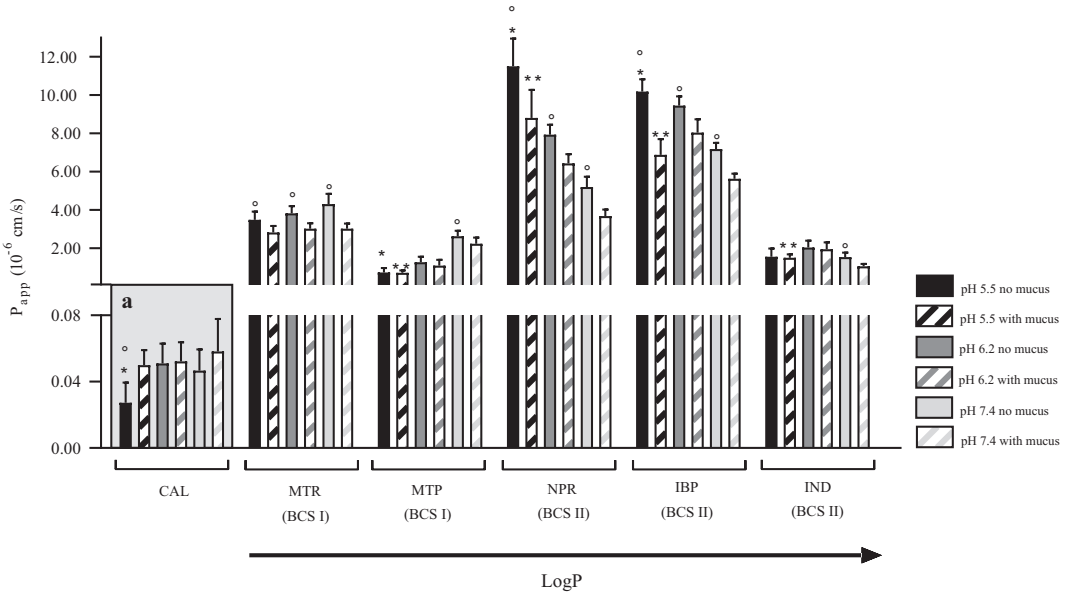

Fig. 3. Apparent permeability (P_{app}) of metronidazole (MTR), metoprolol (MTP), naproxen (NPR), ibuprofen (IBP) and indomethacin (IND) in the presence and absence of mucus at pH 5.5, 6.2 and 7.4. P_{app} of calcein (CAL) (shaded area) was quantified to investigate the integrity of the PVPA barriers at the chosen pH conditions. The results are indicated as mean ± SD (n = 18). Statistical significance ($p < 0.05$) was investigated with one-way ANOVA using the Bonferroni *post hoc* test.

* statistically significant difference in P_{app} between different pH conditions in the absence of mucus.

** statistically significant difference in P_{app} between different pH conditions in the presence of mucus.

° statistically significant difference in P_{app} between the presence and absence mucus.

satisfactory correlations were found between the results obtained in this study at the different pH conditions (7.4, 6.2 and 5.5) and data where drug permeability was assessed at comparable pH (6.83) using a mucus-comprising Caco-2 cell model (Fig. 2S and 3S, Supplementary Material). Especially in the case of the (mucus)-PVPA data at pH 7.4, which was the pH closest to the one used in the Caco-2 cell experiments, R^2 of 0.96 and 0.97 were identified in the presence and absence of mucus respectively.

As the intestinal walls are lined with a mucus layer that differs in pH according to the specific location (Lieleg et al., 2010), the permeability of the same compounds was tested in the presence of mucin 10 mg/mL to assess the impact of this additional layer at different pH conditions. With regards to mucus-drug interaction, it has to be noted that there are multiple mechanisms which could take place when different drugs are in contact with this layer. In particular, Olmsted and colleagues (Olmsted et al., 2001) suggested interaction filtering (depending on specific binding interactions, electrostatic and hydrophobic forces and hydrogen bonds) and size filtering as the two main driving forces for the diffusion of drugs through the hydrophilic mucus layer. This emphasizes the fact that more lipophilic compounds might decrease their rate of diffusion through mucus to a higher extent compared to hydrophilic ones, and that their ionization might further be the driving force according to the pH environment (Khanvilkar et al., 2001; Shaw et al., 2005).

When the hydrophilic mucus layer was added on top of the PVPA barriers, the permeability of the different drugs was generally decreased compared to its absence, and the pH effect was also less evident (Fig. 3). As the isoelectric point of mucin is estimated to be between 2 and 3 (Lee et al., 2005), its ionization would increase with the increase in pH. When the same occurs for ionizable drugs, this could cause an electrostatic repulsion or interaction (according to the nature of the drug) that would translate into a decrease in the P_{app} of the drug (Shaw et al., 2005).

Moreover, the lipophilicity of the drug might also affect its degree of interaction with the mucus layer. In particular, the permeability of the more lipophilic compounds IBP and NPR significantly decreased ($p < 0.05$) in the presence of the mucus layer compared to its absence in all tested pH conditions.

Additionally, changes in the rheological characteristics of mucus, usually occurring with a shift in environmental pH, could affect the diffusion/permeability behaviour of drugs at different pH conditions. In fact, as it can be observed in Fig. 3 for IBP and NPR, the higher viscosity of the mucus at pH 5.5 (Fig. 1) could be a contributing factor to the greater decrease in permeability compared to the results at pH 6.2 and 7.4. The findings obtained in this study highlight how the inclusion of the mucus layer is of key importance when investigating pH-dependent permeability, and emphasize the mucus-PVPA model as a suitable tool to study drug permeation in the intestinal environment.

The permeability-solubility interplay was studied by plotting the permeability and the solubility of the different drugs previously investigated against the pH in the absence of mucus (Fig. 4). A similar trend would be visible by plotting the results in the presence of the mucus layer. As it can be observed, for acidic drugs with pKa around 4 (IBP, NPR and IND; Fig. 4A, B, C) the permeability was higher at more acidic pH, whereas their solubility showed the opposite pH-dependent trend. On the other hand, a pH-driven variation in solubility and permeability was not noticeable for MTR (Fig. 4D), as expected from its physicochemical characteristics (Table 2). For the basic drug MTP (Fig. 4E), the tendency of higher permeability at decreasing degree of ionization was observed, but a significant decrease in solubility was not visible.

The trends observed can be explained by the pH partition hypothesis, which highlights the fact that ionizable drugs tend to permeate lipidic membranes when in their undissociated form (Shore et al., 1957), whereas their solubility is higher when the dissociated form is the predominant one. Moreover, these findings are in agreement with previous investigations on the pH-dependent permeability-solubility interplay for ionizable compounds (Sieger et al., 2017).

Since previous findings have emphasized that the solubility-permeability trade-off should be carefully considered when aiming to design optimal formulations (Dahan and Miller, 2012; Porat and Dahan, 2018), it is essential to combine permeability and solubility *in vitro* tools

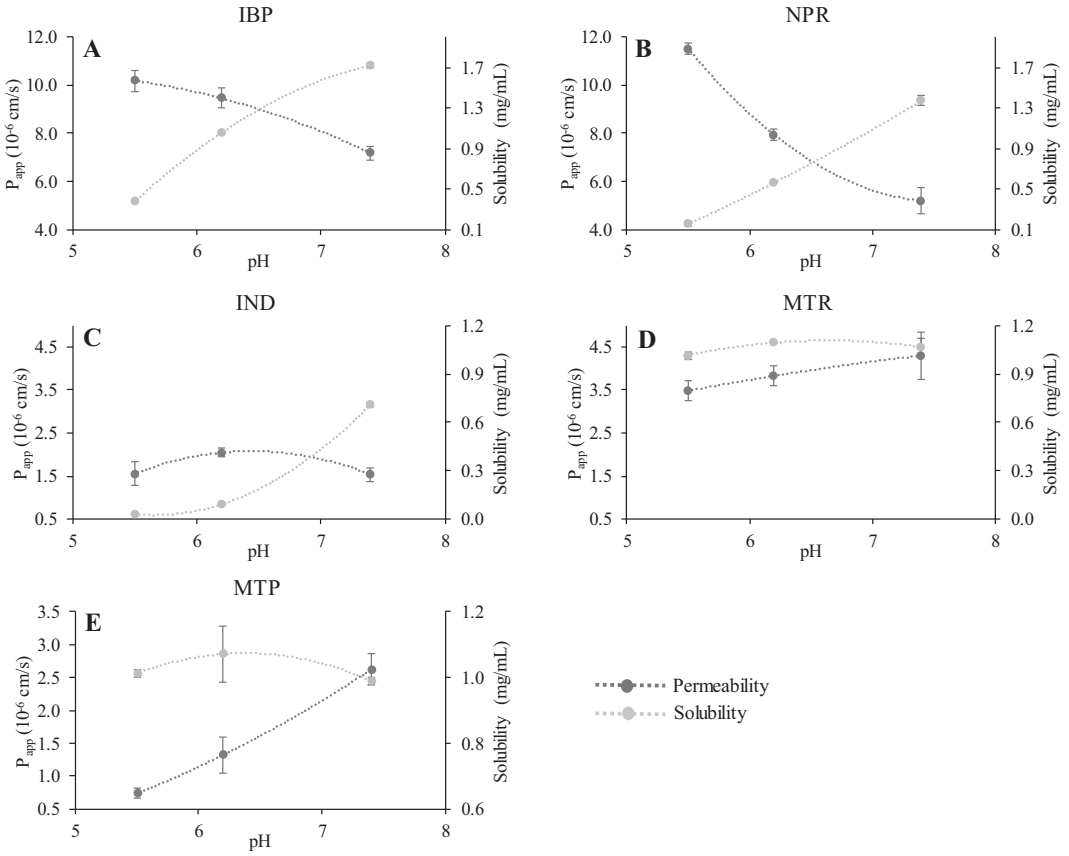

Fig. 4. pH-dependent permeability-solubility interplay in the absence of mucus, depicted as apparent permeability (P_{app}, black dotted line) and solubility (grey dotted line) plots of ibuprofen (4A, IBP), naproxen (4B, NPR), indomethacin (4C, IND), metronidazole (4D, MTR) and metoprolol (4E, MTP).

to elucidate this interplay. The PVPA model used in this study, together with pH-dependent solubility experiments, proved the relevance of this kind of investigation and showed to be appropriate for such purpose.

3.2. The intestinal media environment

Together with the variations in environmental pH, the intestine is also characterized by intraluminal fluids that can vary in composition according to the fasted or fed state (Clarysse et al., 2009).

In particular, bile salts and lecithin have shown to form colloidal structures which can provide the entrapment of drug molecules and their subsequent increased solubilisation, especially with regards to lipophilic drugs (Augustijns et al., 2014; Jantratid et al., 2008; Dahan and Miller, 2012). The fraction of the drug solubilized by these structures is not readily able to permeate the intestinal walls (Miller et al., 2011) and, for this reason, it is important to assess the impact that intestinal fluids have on drug permeation. The commercially available FaSSIF and FeSSIF have previously been proved to mimic the composition of the human intestinal fluids (Jantratid et al., 2008) and have been extensively used in the past decade in numerous solubility and permeability studies using artificial cell-free permeability models (Berben et al., 2018b; Bibi et al., 2015; Fischer et al., 2012; Naderkhani et al., 2015). Therefore, in this study we evaluated the impact that these SIFs have on the PVPA barriers, as well as on the permeability of different compounds.

3.2.1. PVPA barriers in the presence of simulated intestinal media

The PVPA barriers used in this study have previously been shown to be stable in the presence of FaSSIF V1 by another research group (Fischer et al., 2012). However, as the components in the different SIFs could potentially interact with the PVPA lipids and affect the integrity of the barriers, we wanted to investigate this further. For the first time, in this study the PVPA and mucus-PVPA barriers were evaluated in terms of their compatibility with both the fed and fasted state SIFs (namely, FeSSIF and FaSSIF, V1 and 2, composition found in Table 1). To the best of our knowledge, this is the first attempt in studying the impact that all the commercially available media versions (version 1, V1; version 2, V2) have on the functionality of the PVPA barriers; we believe that this investigation is crucial in order to design the best intestinal-resembling *in vitro* permeability model.

The permeability of the fluorescent marker CAL was used to evaluate if the addition of the fed or fasted state SIFs would induce changes in the integrity of the PVPA barriers.

As previously mentioned, an increase in the reference calcein P_{app} value ($0.06 * 10^{-6}$ cm/s) and decrease in barrier electrical resistance (< 290 Ohm*cm^2) would suggest a potential change in barrier integrity (Flaten et al., 2006b; Flaten et al., 2008; Naderkhani et al., 2015).

As it can be observed in Fig. 5, with the fed state buffers/media (Fig. 5A) the permeability of CAL did not increase compared to the control (PBS pH 5.5, Fig. 5A shaded area), suggesting that their presence did not influence the functionality of the barriers, both in the presence and absence of the mucus layer. On the other hand, a general increase in P_{app} and decrease in electrical resistance was observed when experiments with CAL dissolved in the fasted state buffer/media were performed (Fig. 5B). However, permeability of CAL was lower in the presence of buffers compared to the fasted state media, suggesting that the components found in the media (namely sodium taurocholate, lecithin, glycerol monooleate and sodium oleate; Table 1) could be causing changes in the integrity of the barriers.

The presence of mucin 10 mg/mL seemed to shield the barriers from the effect of FaSSIF V1, which was the medium causing the most significant change in CAL permeability. Therefore, to test if mucus with a

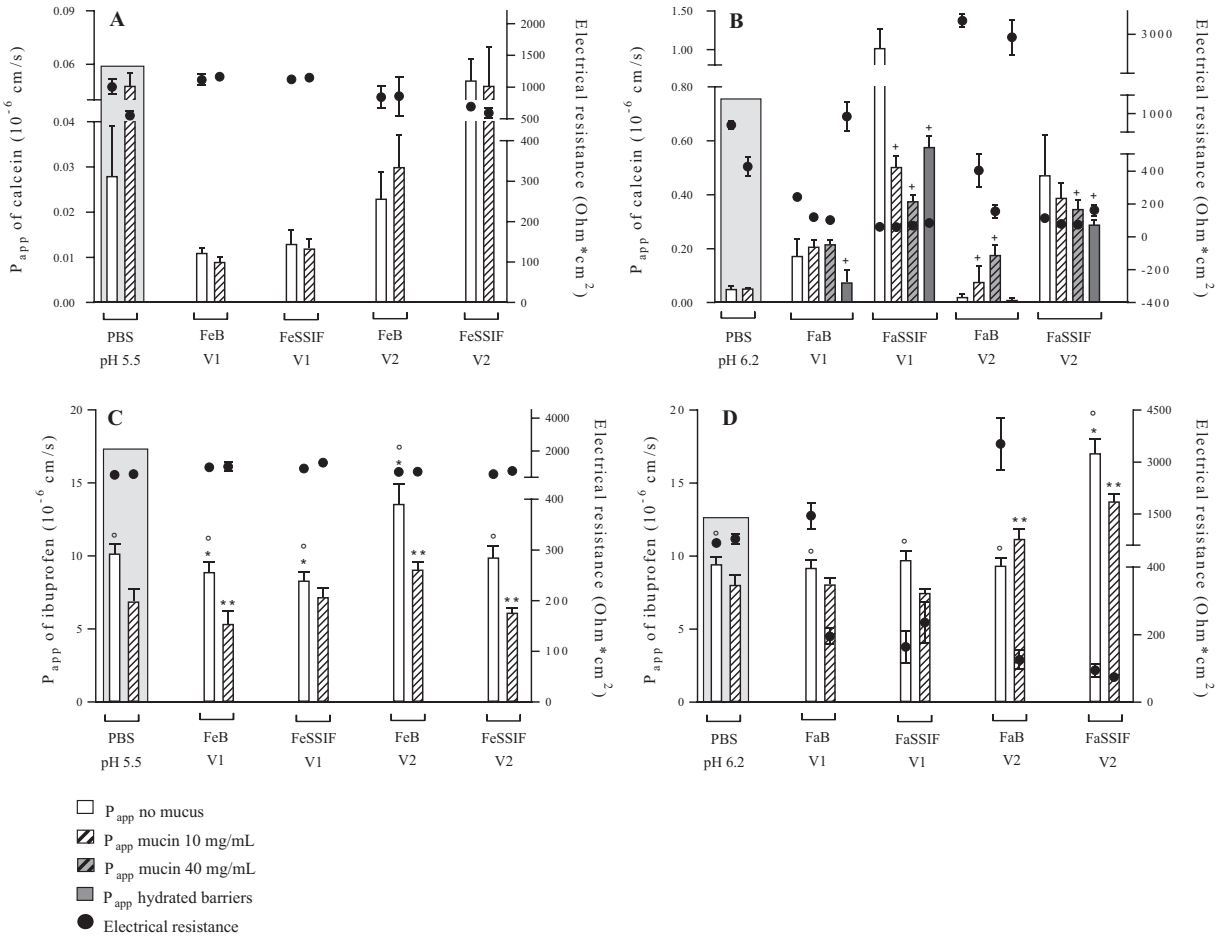

Fig. 5. Apparent permeability (P_{app}) of calcein (CAL; 5A, B) and ibuprofen (IBP; 5C, D), and electrical resistance of the PVPA barriers in the presence of fed (A, C) or fasted (B, D) state media (FeSSIF and FaSSIF, respectively) and corresponding buffers (FeB and FaB, respectively) for both versions 1 and 2 (V1, V2) in the presence and absence of mucus (10 and 40 mg/mL) and with hydrated barriers. P_{app} and electrical resistance in the presence of PBS (pH 5.5 or 6.2) are used as controls (shaded area). The results are indicated as mean ± SD (n = 18). Statistical significance ($p < 0.05$) was investigated with one-way ANOVA using the Bonferroni *post hoc* test.
$^{+}$ statistically significant difference in P_{app} between the absence of mucus and the other 3 conditions (mucus 10 mg/mL, mucus 40 mg/mL and hydrated barriers).
* statistically significant difference in P_{app} between PBS and all other SIFs without mucus.
** statistically significant difference in P_{app} between PBS and all other SIFs with mucus.
° statistically significant difference in P_{app} between the presence and absence of mucus.

higher mucin concentration would provide additional protection of the barriers, mucin 40 mg/mL was also tested. As it can be seen from Fig. 5B, in general this setup led to a decrease in CAL P_{app}, especially in the case of the fasted state media, suggesting a higher degree of protection from the more concentrated mucus layer. However, CAL permeability was still significantly higher compared to the control and the electrical resistance measured in this condition was still below the optimal range (< 290 Ohm*cm^2; Naderkhani et al., 2015).

As mentioned above, Fischer and colleagues (Fischer et al., 2012) concluded that the integrity of the barriers appeared to be maintained in the presence of the fasted state medium (V1) since the results obtained using FaB and FaSSIF (V1) were not statistically different. In this study, PBS pH 7.4 was not included as control. The permeability experiments performed by Fisher and colleagues were carried out in a different manner compared to the present study. In particular, the barriers were hydrated for 1 h in FaB V1 and the following permeability assay was 4 h long. For this reason, we decided to investigate the permeability of CAL in these conditions. As it can be observed in Fig. 5B, a significant decrease in calcein P_{app} was found with the hydrated-barriers setup, especially with the V1 fasted state medium. These findings, together with the differences in surface area and donor volume, as well as lab-to-lab variations, could be the reasons for the differences between the results obtained in the current study and the ones from Fischer and colleagues (Fischer et al., 2012).

Moreover, in previous studies performed in our research group (Naderkhani et al., 2015) a modification of the original PVPA model (namely, $PVPA_{biomimetic}$) was used to assess the impact of the fasted and fed state SIFs (V2). In accordance with our findings (Fig. 5), a higher CAL permeability and lower electrical resistance was observed in the presence of fasted state medium compared to the fed one (Naderkhani et al., 2015). However, with the $PVPA_{biomimetic}$ the fasted medium (V2) was found to be much less aggressive to the barriers and thus more compatible with the model compared to the original PVPA (Naderkhani et al., 2015). The $PVPA_{biomimetic}$ barriers have also shown to be more robust against the presence of co-solvents and tensides compared to the original PVPA (Naderkhani et al., 2014b), and are thus a good alternative when permeability studies with conditions that might affect the original PVPA barriers have to be performed.

However, as the P_{app} of drugs/compounds can be differently affected according to their physicochemical characteristics, we wanted to investigate how the permeability of one more lipophilic compound would be affected in the presence of the SIFs. Therefore, the permeability of the BCS class II drug IBP was evaluated in the presence of fed and fasted state SIFs with and without the presence of the mucus layer, to see if the variation in the permeability of IBP would follow the same trend as the one of the hydrophilic marker CAL.

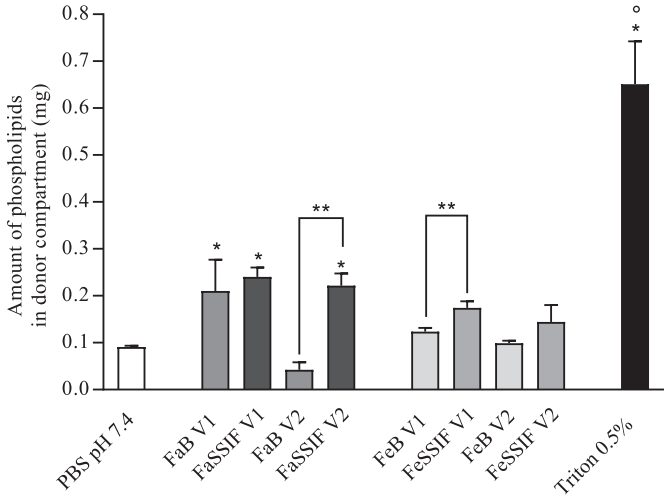

Fig. 6. Amount of phospholipids released to the donor compartment of the PVPA barriers after 5 h of incubation with PBS pH 7.4, fasted (Fa-) and fed (Fe-) state buffers (FaB and FeB) and media (FaSSIF and FeSSIF) (both version V1 and V2) and Triton X-100 0.5%. The results are indicated as mean ± SD (n = 6). Statistical significance ($p < 0.05$) was investigated with one-way ANOVA using the Bonferroni *post hoc* test.

* statistically significant difference in phospholipids loss compared to PBS pH 7.4.

** statistically significant difference in phospholipids loss between the buffer and the media fluids.

° statistically significant difference in phospholipids loss between the presence of Triton 0.5% and all other conditions.

As it can be seen in Fig. 5D, the permeability of IBP dissolved in the fasted state media in the absence of mucus significantly increased ($p < 0.05$) only in the case of FaSSIF V2, when compared to the one where the drug was dissolved in PBS pH 6.2 (Fig. 5D, shaded area). In the presence of the mucus layer, the corresponding buffer (FaB V2) also caused a significant increase in P_{app}. The electrical resistance across the PVPA barriers followed the trend seen in Fig. 5B, suggesting potential barrier impairment in the presence of the fasted state media. However, the permeability of this lipophilic compound was not affected by the presence of this media to the same extent as CAL, suggesting that the changes in the PVPA structure may be related to an increase in aqueous pores through the barriers and not to variations in their lipidic part. In fact, events that affect the structure of the PVPA barriers can cause an increase in aqueous pathways, resulting in a higher permeability especially for hydrophilic compounds (Flaten et al., 2006b).

Fig. 5C shows the apparent permeability of IBP dissolved in the fed state (SIFs). In general, minor changes were found when comparing the P_{app} of the drug dissolved in PBS pH 5.5 (control, shaded area) with the one in the fed state buffers/media in the presence and absence of the mucus layer. These findings could be related to the different solubilization that the drug can exhibit in these different environments, which again can translate into a change in permeability (Dahan and Miller, 2012; Porat and Dahan, 2018). Moreover, in all tested fed conditions, the P_{app} of IBP was found to be lower in the presence of mucus. On the contrary, as it can be seen in Fig. 5A, the permeability of the hydrophilic marker CAL did not significantly change between the presence and absence of mucus. In fact, the presence of the mucus layer can particularly hinder the diffusion of lipophilic drugs because of its hydrophilic nature and of the possible interaction of the drugs with its hydrophobic regions (Khanvilkar et al., 2001). These results were able to prove this concept, and stressed the necessity of a permeability *in vitro* model comprising mucus to properly assess its impact on oral drug absorption.

As previously mentioned, lecithin and bile salts have shown to entrap drug molecules in vesicular structures, thus increasing drug solubilization and lowering the amount of free drug able to permeate through the intestinal walls (Augustijns et al., 2014; Miller et al., 2011). This effect should be particularly evident with the fed state media, where the concentration of the above-mentioned components is higher compared to the fasted state one. As a proof of this concept, Fig. 5C shows a significant decrease ($p < 0.05$) in permeability when comparing the P_{app} of IBP dissolved in FeB V2 with the one in FeSSIF V2, both in the presence and absence of mucus. In fact, the presence of sodium taurocholate, lecithin and other lipolysis products in FeSSIF V2 can provide the formation of micelles, otherwise not present in the fed state buffer (FeB V2), thus influencing drug solubilization and permeability. A similar trend was found with FeB V1 and FeSSIF V1, but not to the same extent. This could be due to the different composition of the two media (Table 1), stressing the significant impact on drug permeation of the presence of FeSSIF V2, which has a higher bile salt-lecithin ratio and additional lipolysis products (sodium oleate and glycerol monooleate). Regarding this matter, it has been previously shown that the complex composition of the fed intestinal fluids could contribute to larger colloidal vesicles (Riethorst et al., 2016) and therefore affect drug absorption to a higher extent. Moreover, according to the bile salt-lecithin ratio, the vesicles could change in dimension and tend either to a bilayered structure or to the one of mixed micelles, as previously discussed (Riethorst et al., 2018). The same trend was not observed for CAL (Fig. 5A), emphasizing that this study was able to highlight the fact that the FeSSIF composition did not affect the permeability of hydrophilic compounds in the same manner as lipophilic ones.

In the presence of mucus, a significant decrease in IBP permeability ($p < 0.05$) was only found between FeB and FeSSIF V2 and not between FeB and FeSSIF V1 (Fig. 5C). This could again be traced back to the different composition of the two media, as well as to the potential interaction of the drug with the mucus. Moreover, the reduction in drug diffusion through native mucus has previously been found to be related to sodium taurocholate, competing with mucins in binding the drug diffusing through this layer (Legen and Kristl, 2001).

All these considerations underline the impact that the different SIFs have on the permeation of different compounds through the PVPA barriers, but also on the diffusion of drugs through the mucus layer. These findings are especially relevant as the need of predictive *in vitro* models simulating the GI tract is further increasing (Berben et al., 2018a; Billat et al., 2017; Riethorst et al., 2018).

3.2.1.1. Loss of lipids from the PVPA barriers in the presence of simulated intestinal media. To further investigate the mechanism behind the possible change in barrier integrity suggested by the increased CAL permeability discussed in Section 3.2.1, the potential loss of lipids from the PVPA barriers in the donor compartment was investigated in the presence of the different SIFs.

Fig. 6 shows how the loss of phospholipids in all tested conditions was significantly lower ($p < 0.05$) than the one caused by the presence of Triton X-100 0.5% (positive control), which is certainly causing barrier disintegration as proved by other authors (Fischer et al., 2011; Naderkhani et al., 2015). However, an increase in amount of phospholipids released from the barrier was observed with some of the SIFs compared to the presence of PBS pH 7.4 (negative control). In particular, a significant increase in phospholipid loss compared to the negative control was observed in the presence of FaB V1, FaSSIF V1 and FaSSIF V2. Moreover, a significant difference in lipid loss was found between the buffer and the medium for the fasted state V2 and the fed state V1.

These trends could explain part of the permeability results shown in Fig. 5B and add more information regarding the effects of the SIFs on the tightness of the PVPA barriers. In particular, a higher loss of lipids is suggested in the presence of the fasted state media, compared to the fed ones, in accordance with the results discussed in Section 3.2.1.

Moreover, the results in Fig. 6 are in the same range as the ones previously observed by Fischer and colleagues (Fischer et al., 2012).

However, they did not compare the loss of phospholipids caused by the fasted state media with the one in the presence of PBS pH 7.4, therefore a negative control as the one discussed in our study was not accessible.

Naderkhani et al. (2015) observed that a lower lipid loss was found with the $PVPA_{biomimetic}$ barriers both in the presence of fasted and fed state media and of Triton X-100 0.5% compared to the original PVPA, highlighting the difference in barrier integrity and further supporting the permeability results discussed in Section 3.2.1.

In the present study, the loss of phospholipids caused by the fed and fasted state buffer/media in the presence of the mucus layer was also investigated. However, the collection process of the samples from the donor compartment led to variations in the amount of mucus present in each sample. As mucus was prepared in phosphorus-containing buffer (PBS), the amount of phosphorus quantified in each sample varied according to the amount of mucus withdrawn from the donor compartment, thus leading to compromised sensitivity of the assay and the results could therefore not be trusted in the presence of this layer.

The different results observed using the FaSSIF and FeSSIF media could be ascribed to their different composition (Table 1), which is not only related to the different amounts of bile salts, lecithin and other lipolysis products, but also to their different buffer composition. In fact, as it can be observed in Figs. 5 and 6, in some cases the buffers themselves seemed to potentially affect the barrier integrity.

Moreover, since it has been reported that the concentration of bile salts and lecithin in fasted state human intestinal fluid is much lower compared to the fed one (Clarysse et al., 2009) and since the SIFs have shown to mimic the human intestinal fluids (Jantratid et al., 2008), the resulting vesicular structures would be different according to FaSSIF or FeSSIF media, thus possibly affecting the PVPA barrier structure in a different manner.

Overall, the results obtained suggest the PVPA barriers to be especially stable in the presence of the fed state media, whereas the ones found with the fasted state media suggest a certain potential of barrier impairment, and precautions should be taken when interpreting results obtained in presence this media. However, as the $PVPA_{biomimetic}$ barriers have shown to be more robust compared to the original ones (Naderkhani et al., 2014b), they could be the best model to use when fasted state SIFs have to be employed to assess drug permeability.

Moreover, the findings discussed in Section 3.2.1 highlight the fact that different media can result in a different impact on the PVPA barrier integrity as well as on the permeability of the model compounds. This emphasizes the relevance of the investigation on both media and both versions carried out in this study.

4. Conclusions

In this study, the impact of regional and nutritional intestinal differences has been successfully investigated using the mucus-PVPA *in vitro* model. The pH-dependent drug permeability and solubility profiles showed trends in agreement with the pH partition hypothesis. An increase in mucus viscosity at lower pH conditions was also observed. Moreover, the impact of bile salts and phospholipids on drug permeation was evident, and the different SIFs showed to influence the permeability to various extents according to the hydrophilicity/lipophilicity of the drugs. Further, the presence of mucus particularly affected the permeability of the more lipophilic compounds. The results obtained in this work thus suggest the suitability of the mucus-PVPA model for investigations on the impact that pH and SIFs, as well as their interplay with mucus, have on intestinal drug absorption.

Acknowledgments

The authors recognize the University of Tromsø The Arctic University of Norway for funding PhD student M. Falavigna. The authors also thank Professor Natasa Skalko-Basnet and Assistant Professor Ragna Berthelsen for the fruitful discussions and inputs. The generosity for the donation of phospholipids from Lipoid GmbH (Ludwigshafen, Germany) is greatly acknowledged. The contribution of COST Action UNGAP (supported by the European Cooperation in Science and Technology; project number: 16205), and Nordic-POP (supported by NordForsk; project number: 85352) is highly appreciated.

Conflict of interest

No conflicts of interest are declared by the authors.

Appendix A. Supplementary data

Supplementary data to this article can be found online at https://doi.org/10.1016/j.ejps.2019.02.035.

References

Amidon, G.L., Lennernäs, H., Shah, V.P., Crison, J.R., 1995. A theoretical basis for a biopharmaceutics drug classification: the correlation of in vitro drug product dissolution and in vivo bioavailability. Pharm. Res. 12, 413–420.
Artusson, P., Palm, K., Luthman, K., 2001. Caco-2 monolayers in experimental and theoretical predictions of drug transport. Adv. Drug Deliv. Rev. 46, 27–43.
Augustijns, P., Wuyts, B., Hens, B., Annaert, P., Butler, J., Brouwers, J., 2014. A review of drug solubility in human intestinal fluids: implications for the prediction of oral absorption. Eur. J. Pharm. Sci. 57, 322–332.
Avdeef, A., 2003. Absorption and Drug Development: Solubility, Permeability, and Charge State. John Wiley & Sons, New Jersey.
Bartlett, G.R., 1959. Phosphorus assay in column chromatography. J. Biol. Chem. 234, 466–468.
Benet, L.Z., Broccatelli, F., Oprea, T.I., 2011. BDDCS applied to over 900 drugs. AAPS J. 13 (4), 519–547.
Berben, P., Bauer-Brandl, A., Brandl, M., Faller, B., Flaten, G.E., Jacobsen, A.C., Brouwers, J., Augustijns, P., 2018a. Drug permeability profiling using cell-free permeation tools: overview and applications. Eur. J. Pharm. Sci. 119, 219–233.
Berben, P., Brouwers, J., Augustijns, P., 2018b. Assessment of passive intestinal permeability using an artificial membrane insert system. J. Pharm. Sci. 107, 250–256.
Bergström, C.A.S., Luthman, K., Artursson, P., 2004. Accuracy of calculated pH-dependent aqueous solubility. Eur. J. Pharm. Sci. 22, 387–398.
Bergström, C.A.S., Holm, R., Jørgensen, S.A., Andersson, S.B.E., Artursson, P., Beato, S., Borde, A., Box, K., Brewster, M., Dressman, J., Feng, K.-I., Halbert, G., Kostewicz, E., McAllister, M., Muenster, U., Thinnes, J., Taylor, R., Mullertz, A., 2014. Early pharmaceutical profiling to predict oral drug absorption: current status and unmet needs. Eur. J. Pharm. Sci. 57, 173–199.
Berthelsen, R., Sjögren, E., Jacobsen, J., Kristensen, J., Holm, R., Abrahamsson, B., Müllerz, A., 2014. Combining in vitro and in silico methods for better prediction of surfactant effects on the absorption of poorly water soluble drugs – a fenofibrate case example. Int. J. Pharm. 473, 356–365.
Bibi, H.A., di Cagno, M., Holm, R., Bauer-Brandl, A., 2015. Permeapad™ for investigation of passive drug permeability: the effect of surfactants, co-solvents and simulated intestinal fluids (FaSSIF and FeSSIF). Int. J. Pharm. 493, 192–197.
Billat, P.A., Roger, E., Faure, S., Lagarce, F., 2017. Models for drug absorption from the small intestine: where are we and where are we going? Drug Discov. Today. 22, 761–775.
Boegh, M., Baldursdóttir, S.G., Müller, A., Nielsen, H.M., 2014. Property profiling of biosimilar mucus in a novel mucus-containing in vitro model for assessment of intestinal drug absorption. Eur. J. Pharm. Biopharm. 87, 227–235.
di Cagno, M., Bibi, H.A., Bauer-Brandl, A., 2015. New biomimetic Permeapad™ for efficient investigation of passive permeability of drugs. Eur. J. Pharm. Sci. 73, 29–34.
Cao, X., Bansil, R., Bhaskar, K.R., Turner, B.S., LaMont, J.T., Niu, N., Afdhal, N.H., 1999. pH-dependent conformational change of gastric mucin leads to sol-gel transition. Biophys. J. 76, 1250–1258.
Clarysse, S., Tack, J., Lammert, F., Duchateau, G., Reppas, C., Augustijns, P., 2009. Postprandial evolution in composition and characteristics of human duodenal fluids in different nutritional states. J. Pharm. Sci. 98, 1177–1192.
Dahan, A., Miller, J.M., 2012. The solubility-permeability interplay and its implications in formulation design and development of poorly soluble drugs. AAPS J. 14 (2), 244–250.
Fabiano, A., Zambito, Y., Bernkop-Schnurch, A., 2017. About the impact of water movement on the permeation behaviour of nanoparticles in mucus. Int. J. Pham. 517, 279–285.
Falavigna, M., Klitgaard, M., Brase, C., Ternullo, S., Skalko-Basnet, N., Flaten, G.E., 2018. Mucus-PVPA (mucus phospholipid vesicle-based permeation assay): an artificial permeability tool for drug screening and formulation development. Int. J. Pharm. 537, 213–222.
Fischer, S.M., Flaten, G.E., Hagesæther, E., Fricker, G., Brandl, M., 2011. In-vitro permeability of poorly water soluble drugs in the phospholipid vesicle-based permeation assay: the influence of nonionic surfactants. J. Pharm. Pharmacol. 63, 1022–1030.
Fischer, S.M., Buckley, S.T., Kirchmeyer, W., Fricker, G., Brandl, M., 2012. Application of simulated intestinal fluid on the phospholipid vesicle-based drug permeation assay. Int. J. Pharm. 422, 52–58.

Flaten, G.E., Bunjes, H., Luthman, K., Brandl, M., 2006a. Drug permeability across a phospholipid vesicle-based barrier 2. Characterization of barrier structure, storage stability and stability towards pH changes. Eur. J. Pharm. Sci. 28, 336–343.
Flaten, G.E., Dhanikula, A.B., Luthman, K., Brandl, M., 2006b. Drug permeability across a phospholipid vesicle barrier: a novel approach for studying passive diffusion. Eur. J. Pharm. Sci. 27, 80–90.
Flaten, G.E., Luthman, K., Vasskog, T., Brandl, M., 2008. Drug permeability across a phospholipid vesicle-based barrier: 4. The effect of tensides, co-solvent and pH changes on barrier integrity and on drug permeability. Eur. J. Pharm. Sci. 34, 173–180.
Galia, E., Nicolaides, E., Hörter, D., Löbenberg, R., Reppas, C., Dressman, J.B., 1998. Evaluation of various dissolution media for predicting in vivo performance of class I and II drugs. Pharm. Res. 15, 698–705.
Hamed, R., Awadallah, A., Sunoqrot, S., Tarawneh, O., Nazzal, S., AlBaraghthi, T., Al Sayyad, J., Abbas, A., 2016. pH-dependent solubility and dissolution behaviour of carvedilol – case xample of a weakly basic BCS class II drug. AAPS PharmSciTech 17 (2), 418–426.
Jantratid, E., Janssen, N., Reppas, C., Dressman, J.B., 2008. Dissolution media simulating conditions in the proximal human gastrointestinal tract: an update. Pharm. Res. 25, 1663–1676.
Johansson, M.E.V., Sjövall, H., Hansson, G.C., 2013. The gastrointestinal mucus system in health and disease. Nat. Rev. Gastroenterol. Hepatol. 10, 352–361.
Kansy, M., Senner, F., Gubernator, K., 1998. Physicochemical high throughput screening: parallel artificial membrane permeation assay in the description of passive absorption processes. J. Med. Chem. 41, 1007–1010.
Keemink, J., Bergström, C.A.S., 2018. Caco-2 cell conditions enabling studies of drug absorption from digestible lipid-based formulations. Pharm. Res. 35 (74), 1–11.
Khanvilkar, K., Donovan, M.D., Flanagan, D.R., 2001. Drug transfer through mucus. Adv. Drug Deliv. Rev. 48, 173–193.
Lai, S.K., Wang, Y.Y., Wirtz, D., Hanes, J., 2009. Micro- and macrorheology of mucus. Adv. Drug Deliv. Rev. 61, 86–100.
Lee, S., Muller, M., Rezwan, K., Spencer, N.D., 2005. Porcine gastric mucin (PGM) at the water/poly(dimethylsiloxane) (PDMS) interface: influence of pH and ionic strength on its conformation, adsorption, and aqueous lubrication properties. Langmuir 21 (18), 8344–8353.
Legen, I., Kristl, A., 2001. Comparative permeability study of some acyclovir derivatives through native mucus and crude mucin dispersions. Drug Dev. Ind. Pharm. 27 (7), 669–674.
Lieleg, O., Vladescu, I., Ribbeck, K., 2010. Characterization of particle translocation through mucin hydrogels. Biophys. J. 98, 1782–1789.
Mackie, A.R., Goycoolea, F.M., Menchicchi, B., Caramella, C.M., Saporito, F., Lee, S., Stephansen, K., Chronakis, I.S., Hiorth, M., Adamczak, M., Waldner, M., Nielsen, H.M., Marcelloni, L., 2017. Innovative methods and applications in mucoadhesion research. Macromol. Biosci. 17, 1600534.
Madsen, C.M., Feng, K.I., Leithead, A., Canfield, N., Jørgensen, S.A., Müllertz, A., Rades, T., 2018. Effect of composition of simulated intestinal media on the solubility of poorly soluble compounds investigated by design of experiments. Eur. J. Pharm. Sci. 111, 311–319.
Miller, J.M., Beig, A., Krieg, B.J., Carr, R.A., Borchardt, T.B., Amidon, G.E., Amidon, G.L., Dahan, A., 2011. The solubility-permeability interplay: mechanistic modeling and predictive application of the impact of micellar solubilization on intestinal permeation. Mol. Pharm. 8, 1848–1856.
Naderkhani, E., Erber, A., Škalko-Basnet, N., Flaten, G.E., 2014a. Improved permeability of acyclovir: optimization of mucoadhesive liposomes using the PVPA model. J. Pharm. Sci. 103, 661–668.
Naderkhani, E., Isaksson, J., Ryzhakov, A., Flaten, G.E., 2014b. Development of a biomimetic phospholipid vesicle-based permeation assay for the estimation of intestinal drug permeability. J. Pharm. Sci. 103, 1882–1890.
Naderkhani, E., Vasskog, T., Flaten, G.E., 2015. Biomimetic PVPA in vitro model for estimation of the intestinal drug permeability using fasted and fed state simulated intestinal fluids. Eur. J. Pharm. Sci. 73, 64–71.
Olmsted, S.S., Padgett, J.L., Yudin, A.I., Whaley, K.J., Moench, T.R., Cone, R.A., 2001. Diffusion of macromolecules and virus-like particles in human cervical mucus. Biophys. J. 81, 1930–1937.
Park, M.S., Chung, J.W., Kim, Y.K., Chung, S.C., Kho, H.S., 2007. Viscosity and wettability of animal mucin solutions and human saliva. Oral Dis. 13, 181–186.
Porat, D., Dahan, A., 2018. Active intestinal drug absorption and the solubility-permeability interplay. Int. J. Pharm. 537, 84–93.
Rediguieri, C.F., Porta, V., Nunes, D.S.G., Nunes, T.M., Junginger, H.E., Kopp, S., Midha, K.K., Shah, V.P., Stavchansky, S., Dressman, J.B., Barends, D.M., 2011. Biowaiver monographs for immediate release solid oral dosage forms: metronidazole. J. Pharm. Sci. 100, 1618–1627.
Riethorst, D., Mols, R., Duchateau, G., Tack, J., Brouwers, J., Augustijns, P., 2016. Characterization of human duodenal fluids in fasted and fed state conditions. J. Pharm. Sci. 105, 673–681.
Riethorst, D., Brouwers, J., Motmans, J., Augustijns, P., 2018. Human intestinal fluid factors affecting intestinal drug permeation in vitro. Eur. J. Pharm. Sci. 121, 338–346.
Shaw, L.R., Irwin, W.J., Grattan, T.J., Conway, B.R., 2005. The influence of excipients on the diffusion of ibuprofen and paracetamol in gastric mucus. Int. J. Pharm. 290, 145–154.
Shoghi, E., Fuguet, E., Bosch, E., Rafols, C., 2013. Solubility-pH profiles of some acidic, basic and amphoteric drugs. Eur. J. Pharm. Sci. 48, 291–300.
Shore, P.A., Brodie, B., Hogben, C.A.M., 1957. The gastric secretion of drugs: a pH partition hypothesis. J. Pharmacol. Exp. Ther. 119, 361–369.
Sieger, P., Cui, Y., Scheuerer, S., 2017. pH-dependent solubility and permeability profiles: a useful tool for prediction of oral bioavailability. Eur. J. Pharm. Sci. 105, 82–90.
Stappaerts, J., Berben, P., Cevik, I., Augustijns, P., 2018. The effect of 2-hydroxypropyl-β-cyclodextrin on the intestinal permeation through mucus. Eur. J. Pharm. Sci. 114, 238–244.
Varma, M.V., Gardner, I., Steyn, S.J., Nkanash, P., Rotter, C.J., Whitney-Pickett, C., Zhang, H., Di, L., Cram, M., Fenner, K.S., El-Kattan, A.F., 2012. pH-dependent solubility and permeability criteria for provisional biopharmaceutics classification (BCS and BDDCS) in early drug discovery. Mol. Pharm. 9, 1199–1212.
Völgyi, G., Baka, E., Box, K.J., Comer, J.E.A., Takacs-Novak, K., 2010. Study of pH-dependent solubility of organic bases. Revisit of Henderson-Hasselbalch relationship. Anal. Chim. Acta 673, 40–46.

Supplementary material

Mimicking regional and fasted/fed state conditions in the intestine with the mucus-PVPA *in vitro* model: the impact of pH and simulated intestinal fluids on drug permeability

Margherita Falavigna[a], Mette Klitgaard[a, b], Erik Steene[c], Gøril Eide Flaten[a, *]

[a] Drug Transport and Delivery Research Group, Department of Pharmacy, University of Tromsø The Arctic University of Norway, Universitetsveien 57, 9037 Tromsø, Norway. margherita.falavigna@uit.no; goril.flaten@uit.no.
[b] Physiological Pharmaceutics, Department of Pharmacy, University of Copenhagen, Universitetsparken 2-4, 2100, Copenhagen, Denmark. mette.jensen@sund.ku.dk.
[c] Biotec Betaglucans AS, Sykehusvegen 23, 9019 Tromsø, Norway. erik.steene@biotec.no.

*Corresponding author: Gøril Eide Flaten, Drug Transport and Delivery Research Group, Department of Pharmacy, University of Tromsø The Arctic University of Norway, Universitetsveien 57, 9037 Tromsø, Norway; Tel: +47-776-46169; Fax: +47-776-46151; Email: goril.flaten@uit.no

1. Quantification methods: drug permeated in the acceptor compartment

The quantification of the amount of drug found in the acceptor compartment at the end of the permeability study was carried out with different quantification methods according to the specific compound. Previous studies by us have assessed the possibility of interference of lipids from the PVPA barrier in the quantification process, and have concluded that no lipids were found in the acceptor compartment (Flaten et al., 2007). UV-Vis spectrophotometry was sensitive enough for the quantification of IBP, MTP, MTR and NPR in the permeation studies, as the absorbance of each specific drug found in the acceptor compartment was inside the specific standard curve range and above the LOD and LOQ values (Table 1S). However, for the quantification on IND, HPLC-UV was needed since the absorbance in the acceptor compartment was not appreciable enough by the UV-Vis spectrophotometry quantification method.

Table 1S: Parameters for the quantification of CAL, IBP, IND, MTP, MTR and NPR.

	pH	Cal. Curve range (nmol/mL)	R^2	LOD (nmol/mL)	LOQ (nmol/mL)
CAL	5.5	0.10-2.20	0.9999	0.05	0.16
	6.2	0.10-2.20	0.9998	0.07	0.22
	7.4	0.02-2.20	0.9995	0.09	0.27
IBP	5.5	8.00-150.00	0.9994	6.70	20.29
	6.2	8.00-150.00	0.9994	6.70	20.29
	7.4	8.00-150.00	0.9999	2.99	9.06
IND UV	5.5	12.00-120.00	1	1.16	3.53
	6.2	12.00-120.00	1	0.82	2.49
	7.4	12.00-120.00	0.9992	7.86	23.82
IND HPLC	7.4	0.015-30.00	0.9998	0.56	1.70
MTP	5.5	1.00-30.00	0.9991	1.86	5.65
	6.2	1.00-30.00	0.9997	1.09	3.31
	7.4	1.00-30.00	0.9992	2.08	6.32
MTR	5.5	18.00-366.00	0.9997	14.00	42.42
	6.2	18.00-366.00	0.9999	8.75	26.50
	7.4	18.00-366.00	0.9998	6.50	19.70
NPR	5.5	50.00-250.00	0.9989	20.07	60.82
	6.2	50.00-250.00	0.9993	16.72	50.67
	7.4	50.00-250.00	0.9991	18.77	56.89

For the validation of the HPLC-UV quantification method of IND, different parameters have been assessed. First, the evaluation of the right column type, mobile phase, time run and flow was carried out by injecting a standard IND solution (in PBS pH 7.4) and by monitoring the separation profile at 254 nm. The retention time of IND obtained with a Waters X-select™ CSH ™ C18 (2.5 μm, 3.0 × 75 mm) XP column, a flow rate of 0.5 mL/min and a mobile phase of acetonitrile and MilliQ water with 0.1% glacial acetic acid (60:40, v/v) was found to be 3.05 during a total run time of 5.5 minutes, while the retention time of the solvent front was found to be 1.07 minutes (Fig. 1S). The IND standard was injected at increasing concentrations (9 dilutions; 3 replicates for each dilution; 0.015-30 nmol/mL) in order to obtain a satisfactory calibration curve (R^2 = 0.9998; LOD = 0.56 nmol/mL; LOQ = 1.70 nmol/mL). The retention

capacity factor k was also evaluated and found to be acceptable (k = 1.87), together with the peak asymmetry factor (A_s = 1.22) and efficiency (N = 674). As both the standard IND solution and the samples obtained from the permeability study were only containing IND, the assessment of the selectivity and resolution was not possible.

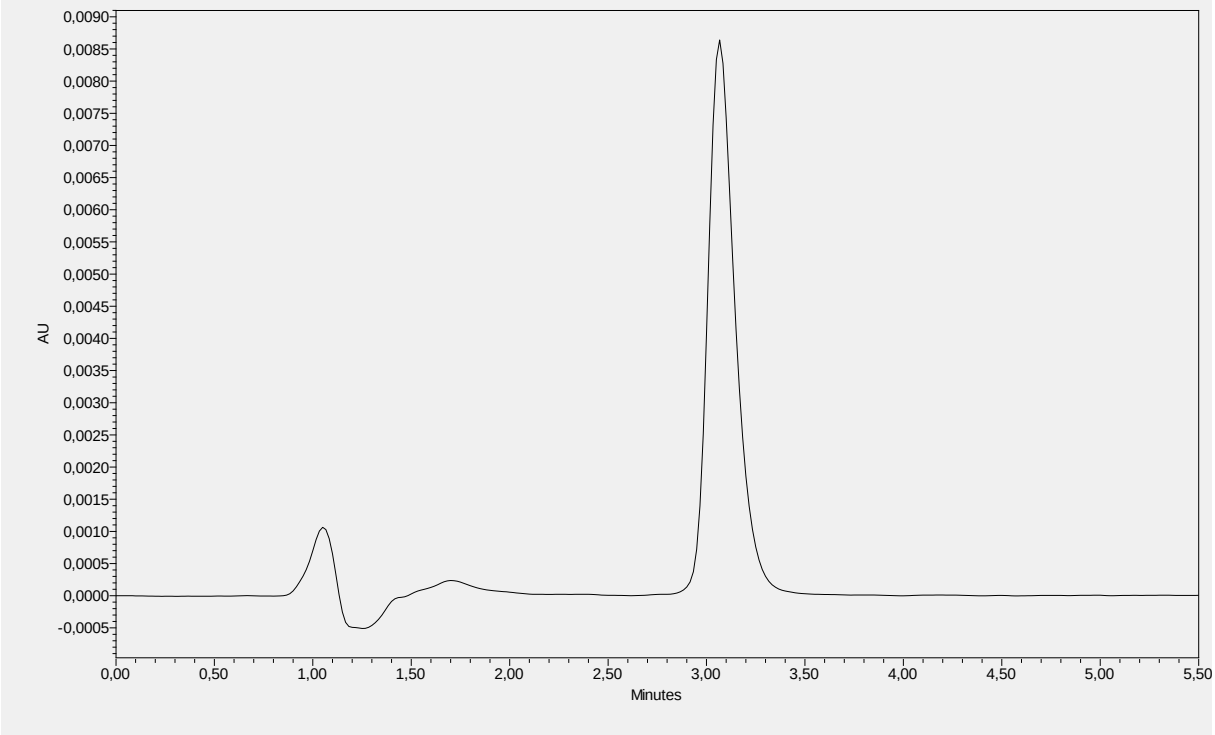

Fig. 1S: Chromatogram of IND standard.

The spectrofluorometric determination of CAL was carried out following the method described by Flaten and colleagues (2006b). The excitation and emission wavelengths (485 and 520 nm, respectively) were chosen to accurately quantify the compound and to avoid a crosstalk between excitation and emission curves. A CAL standard solution (in PBS pH 7.4) was prepared at increasing concentrations (9 dilutions; 3 replicates for each dilution; 0.02-2.2 nmol/mL) in order to obtain a suitable calibration curve (R^2 = 0.9995; LOD = 0.09 nmol/mL; LOQ = 0.27 nmol/mL).

2. Correlation between the (mucus)-PVPA and the Caco-2 model

A correlation between permeabilities obtained using a mucus-comprising Caco-2 model (Berben et al., 2018b) with the permeability of four different drugs (IBP, IND, NPR, MTP) obtained using the PVPA barriers both in the absence and presence of mucus was carried out. The Caco-2 data used for these correlations was obtained from a study where mucus was added on top of Caco-2 cells prior to the addition of the drug in solution, which was dissolved in FaHIF (fasted state human intestinal fluids) at pH 6.83 (Berben et al., 2018b). The correlations are the following:

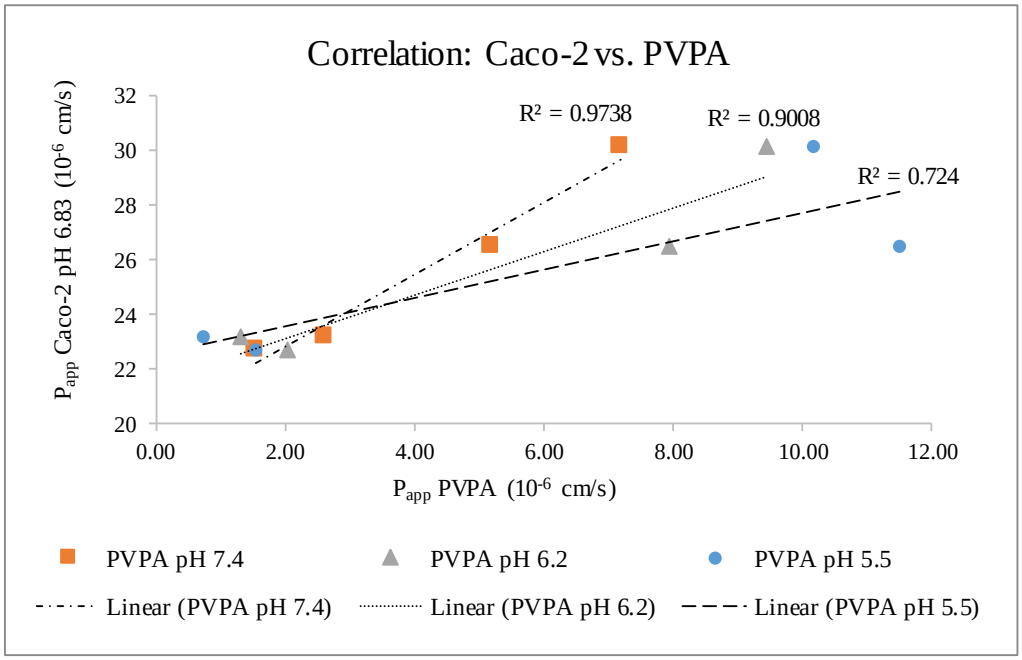

Fig. 2S: Correlation between the P_{app} obtained using the Caco-2 model (data from: Berben et al., 2018b) and the PVPA model.

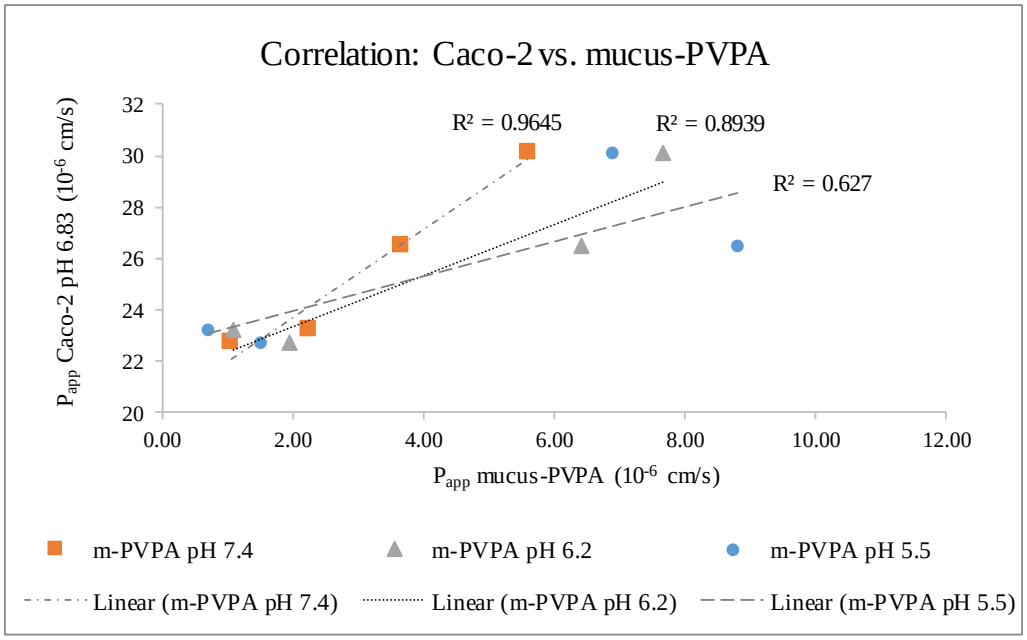

Fig. 3S: Correlation between the P_{app} obtained using the Caco-2 model (data from: Berben et al., 2018b) and the mucus-PVPA model.

As it can be observed in Fig. 2S and 3S, a satisfactory correlation for all pH conditions between the permeability data obtained using the Caco-2 model and the (mucus)-PVPA model has been obtained. This was especially evident in the case of (mucus)-PVPA data at pH 7.4, most likely due to the fact that the Caco-2 data was exclusively collected at pH 6.83. These correlations suggest the suitability of the model used in the current study for the investigation on drug permeation.

Paper III

Journal of Pharmaceutical Sciences 110 (2021) 208-216

Contents lists available at ScienceDirect

Journal of Pharmaceutical Sciences

journal homepage: www.jpharmsci.org

Pharmaceutics, Drug Delivery and Pharmaceutical Technology

Predicting Oral Absorption of fenofibrate in Lipid-Based Drug Delivery Systems by Combining *In Vitro* Lipolysis with the Mucus-PVPA Permeability Model

Margherita Falavigna [a], Mette Klitgaard [b], Ragna Berthelsen [b], Anette Müllertz [b], Gøril Eide Flaten [a, *]

[a] Drug Transport and Delivery Research Group, Department of Pharmacy, UiT The Arctic University of Norway, Universitetsveien 57, 9037 Tromsø, Norway
[b] Physiological Pharmaceutics, Department of Pharmacy, University of Copenhagen, Universitetsparken 2-4, 2100 Copenhagen, Denmark

ARTICLE INFO

Article history:
Received 1 July 2020
Revised 19 August 2020
Accepted 24 August 2020
Available online 8 September 2020

Keywords:
Gastrointestinal tract
In vitro/in vivo (IVIVC) correlation
In vitro model
Lipid-based formulation
Oral drug delivery
Permeability
Poorly water-soluble drug
Precipitation
Self-emulsifying

ABSTRACT

The aim of this work was to develop a new *in vitro* lipolysis-permeation model to predict the *in vivo* absorption of fenofibrate in self-nanoemulsifying drug delivery systems (SNEDDSs). More specifically, the *in vitro* intestinal lipolysis model was combined with the mucus-PVPA (Phospholipid Vesicle-based Permeation Assay) *in vitro* permeability model. Biosimilar mucus (BM) was added to the surface of the PVPA barriers to closer simulate the intestinal mucosa. SNEDDSs for which pharmacokinetic data after oral dosing to rats was available in the literature were prepared, and the ability of the SNEDDSs to maintain fenofibrate solubilized during *in vitro* lipolysis was determined, followed by the assessment of drug permeation across the mucus-PVPA barriers. The amount of drug solubilized over time during *in vitro* lipolysis did not correlate with the AUC (area under the curve) of the plasma drug concentration curve. However, the AUC of the drug permeated after *in vitro* lipolysis displayed a good correlation with the *in vivo* AUC ($R^2 > 0.9$). Thus, it was concluded that the *in vitro* lipolysis–mucus-PVPA permeation model, simulating the physiological digestion and absorption processes, was able to predict *in vivo* absorption data, exhibiting great potential for further prediction of *in vivo* performance of SNEDDSs.

Introduction

In the past decades, lipid-based drug delivery systems (LbDDSs) have attracted increasing attention due to their ability to improve the bioavailability of poorly water-soluble drugs[1] *via* solubilization enhancement, supersaturation,[2,3] permeation enhancement and lymphatic transport.[4] Among LbDDSs, self-nanoemulsifying drug delivery systems (SNEDDSs; mixture of oil, surfactant, co-surfactant and co-solvent) have especially been studied because of their ability to spontaneously form nanoemulsions after dispersion in an aqueous environment. Once entered into the gastrointestinal (GI) tract, these formulations are dispersed in the gastric and intestinal fluids and are concomitantly affected by digestive enzymes. These physiological processes result in the formation of a wide range of colloidal structures able to affect the solubilization of the administered drug, and thus impacting its absorption.[5]

Although several studies have been carried out regarding the potential of LbDDSs as oral drug delivery systems[3,6–8] and several LbDDSs have reached the market,[9] the development of an optimal LbDDS is still regarded as a challenging process.[1] The main reason for this is that numerous excipients can be used for LbDDSs, and the selection of the appropriate excipients is a demanding procedure due to *e.g.* insufficient methods currently able to estimate the *in vivo* absorption profile.[5,8] In this regard, the UNGAP (Understanding Gastrointestinal Absorption-related Processes) European COST Action Network has recently stressed the problems related to a poor comprehension of GI drug absorption, and has highlighted the current approaches and further developments needed in this field.[10] For instance, the *in vitro* intestinal lipolysis model has been developed to investigate the performance of LbDDSs prior to *in vivo* testing.[11] Even though the model provides valuable information on the lipolysis rate of a LbDDS, as well as drug solubilization during lipolysis of a LbDDS, recent studies have shown that the *in vitro* model does to not always predict the *in vivo* performance of LbDDSs in terms of drug absorption.[3,8,12] For instance, in the study by Michaelsen et al.[12] the amount of fenofibrate found in the aqueous

* Corresponding author.
E-mail address: goril.flaten@uit.no (G.E. Flaten).

https://doi.org/10.1016/j.xphs.2020.08.026
0022-3549/

phase after *in vitro* lipolysis of three different SNEDDSs (*i.e.* $SNEDDS_{75}$, super-$SNEDDS\ solution_{150}$ and super-$SNEDDS\ suspension_{150}$) failed to correlate with *in vivo* drug absorption in rats, and it has been proposed that the lack of an absorption step in the *in vitro* lipolysis model could be the reason for the low correlation with *in vivo* data.[13] In parallel, numerous *in vitro* permeability models have been validated to mimic the intestinal mucosa and to assess drug absorption from different drug delivery systems (*e.g.* the Caco-2 model[14]; the PAMPA model[15]; the PVPA model[16]; the Permeapad™[17]; and the AMI system[18]). The PVPA (Phospholipid Vesicle-based Permeation Assay) *in vitro* barriers, composed of liposomes immobilized in and on top of nitrocellulose filters, have been established in the past decade and have proved to simulate the intestinal mucosa.[16] However, all the above-mentioned permeation models were developed without considering the GI digestion affecting LbDDSs. Since neither the *in vitro* lipolysis models nor the *in vitro* permeation models alone are able to provide a full picture of the physiological processes driving GI drug absorption from LbDDSs, they have recently been combined to allow the concomitant study of lipolysis and permeation. For instance, a cell-free artificial membrane, the Permeapad™, has been combined with the *in vitro* intestinal lipolysis model using porcine pancreatin as source of digestive enzymes.[6,13] Moreover, a cell-based system, the Caco-2 cell model, has been combined with the *in vitro* intestinal lipolysis utilizing immobilized microbial lipase as the digestive enzyme.[7,19,20] Several of these combined studies led to improved prediction of *in vivo* absorption data compared to the *in vitro* lipolysis models or *in vitro* permeation models alone.[13] Besides Keemink and Bergstrom,[19] where mucin from porcine stomach type III was used as a mean to protect the Caco-2 cell layer, all other models were designed without simulating the mucus layer covering the intestinal wall, thus not fully mimicking the physiological environment of the intestinal mucosa.[21] In fact, the mucus layer is the first barrier that a drug gets in contact with after entering the lumen, and the drug partition between the intestinal luminal fluids, the mucus layer and the intestinal epithelium can affect the extent of drug permeation.[21] Moreover, mucus has shown to affect the absorption of drugs, lipids and nutrients, and lipid digestion products can conversely modulate the properties of this barrier.[22–24] Therefore, it is of key importance to include the mucus layer in such *in vitro* models, in order to be able to consider its impact on drug absorption. Thus, efforts have been made to simulate the mucus layer covering the GI tract and, as a result of this, an artificial biosimilar mucus (BM) has been developed,[25] and proved to resemble both the composition and the rheological properties of porcine intestinal mucus.[25,26]

In light of the importance of including mucus in combined *in vitro* lipolysis-permeation models, as described above, the present study aimed at evaluating if the PVPA *in vitro* permeability model covered with biosimilar mucus would be compatible with a digesting environment. Moreover, the model was tested in terms of its ability to predict the *in vivo* plasma exposure of fenofibrate (poorly water-soluble drug; LogP 5.8[27]) from $SNEDDS_{75}$, super-$SNEDDS\ solution_{150}$ and super-$SNEDDS\ suspension_{150}$ previously found by Michaelsen et al.,[12] and thus lead to *in vivo-in vitro* correlation (IVIVC).

Materials and Methods

Materials

Bovine bile, bovine serum albumin (BSA), 4-bromophenylboronic acid (BBBA), calcein, cholesterol, fenofibrate, maleic acid, MES hydrate, magnesium sulphate, mucin from porcine stomach type II, pancreatin from porcine pancreas, soybean oil (long-chain (LC) glycerides), tris-(hydroxymethyl)aminomethane (Tris) were products of Sigma Aldrich (St. Luis, MO, USA). Acetonitrile (High-Performance Liquid Chromatography, HPLC, grade), dimethyl sulfoxide (DMSO), ethanol (EtOH; Ph. Eur. Grade), methanol (MeOH; HPLC grade) sodium chloride (NaCl) were purchased from VWR (Herlev, Denmark). Calcium chloride dihydrate, sodium hydroxide were obtained from Merck (Darmstadt, Germany), whereas polysorbate 80 (Tween 80) and polysorbate 20 (Tween 20) were obtained from Fluka Chemie AG (Buchs, Switzerland). Maisine 35–1 was kindly donated by Gattefossé (St. Priest, France) and Kolliphor RH-40 was kindly received from BASF (Ludwigshafen, Germany). Polyacrylic acid (Carbopol® 974P NF) was purchased from Lubrizol (Brussels, Belgium). E80 lipoid egg-phospholipids (80% phosphatidylcholine) and soy phospholipids (S-PC) were obtained from Lipoid (Ludwigshafen, Germany). All chemicals employed were of analytical grade.

Methods

Biosimilar Mucus Preparation

Biosimilar mucus (BM) was prepared following the method described by Boegh et al.[25] Briefly, Carbopol® was dissolved in a hypo-tonic buffer (10 mM MES buffer with 1.0 mM $MgSO_4$ and 1.3 mM $CaCl_2$; pH 6.5) and mucin type II from porcine stomach was added. A lipid mixture was separately prepared in an isotonic buffer (10 mM MES buffer with 1.0 mM $MgSO_4$, 1.3 mM $CaCl_2$ and 137 mM NaCl; pH 6.5) by mixing SPC, cholesterol and polysorbate 80. Finally, BSA and the lipid mixture were added to the Carbopol®-mucin mixture, in order to obtain the final concentrations: Carbopol® (0.9% w/v), mucin type II from porcine stomach (5% w/v), *S*-PC (0.18% w/v), cholesterol (0.36% w/v), polysorbate 80 (0.16% w/v) and BSA (3.1% w/v). The pH was carefully adjusted to 6.5 and the BM was stored at 4 °C overnight before its use.

PVPA Barrier Preparation

The PVPA barriers were prepared as previously described by Falavigna et al.[28,29] Briefly, liposomes with two different size distributions (0.4 and 0.8 μm) were obtained using the thin-film hydration technique followed by extrusion. In order to provide immobilization and fusion of the liposomes, they were centrifuged and freeze-thawed on top of nitrocellulose membrane filters fused to Transwell inserts (surface area 0.33 cm^2) (Corning Inc., New York, USA).

Preparation of SNEDDSs

SNEDDS composed of soybean oil (27.5% w/w), Maisine 35–1 (27.5% w/w), Kolliphor RH-40 (35% w/w) and absolute ethanol (10% w/w) were prepared following the method previously described by Michaelsen et al.[12] Firstly, soybean oil, Maisine 35–1 and Kolliphor RH-40 were heated at 50 °C, and subsequently Maisine 35–1 and soybean oil were mixed in a 1:1 (w/w) ratio; Kolliphor RH-40 was then added to the mixture, which was left to stir until cooled down to room temperature. Lastly, absolute ethanol was added, and the SNEDDS pre-concentrate was stirred until homogeneity was reached.

Three fenofibrate-loaded SNEDDSs were prepared by adding different amounts of the drug to the pre-concentrate. The equilibrium solubility (S_{eq}) of fenofibrate in the pre-concentrate was previously reported to be 88.5 mg/g[8]. $SNEDDS_{75}$ was prepared by adding drug corresponding to 75% of the fenofibrate S_{eq} to the pre-concentrate (Table 1) and leaving it to stir at room temperature (23–25 °C) to aid the dissolution process until use. The super-$SNEDDS\ suspension_{150}$ was prepared in the same way as the $SNEDDS_{75}$, but 150% of the S_{eq} was added to the pre-concentrate. The super-$SNEDDS\ solution_{150}$ was prepared by adding drug

Table 1
Fenofibrate Loading and form in the Prepared SNEDDSs.

Name	Drug Concentration (% of Drug S_{eq} in the Pre-Concentrate)	Drug State
$SNEDDS_{75}$	75	In solution
Super-$SNEDDS\ solution_{150}$	150	In solution
Super-$SNEDDS\ suspension_{150}$	150	In suspension

corresponding to 150% of the fenofibrate S_{eq} to the pre-concentrate (Table 1), which was then bath-sonicated for 30 min, heated for 3 h at 60 °C, and finally left to cool to 37 °C overnight.

Solubility Studies to Select Acceptor Medium for Permeation Experiment

The solubility of fenofibrate in different aqueous media was tested in order to select a good acceptor medium for the permeation experiments. The method employed followed the procedure described by Berthelsen et al.[30] Briefly, 10 mg of fenofibrate were suspended in 15 mL of either PBS pH 7.4; Tween 20 5 mg/mL; DMSO 10 mg/mL; DMSO 40 mg/mL; BSA 4% (w/v) or BSA 1% (w/v) (all media were prepared in PBS pH 7.4) and the suspensions were left to rotate at 37 °C for a total of 48 h. The tubes containing the suspensions were centrifuged after 1, 4, 24 and 48 h of incubation for 10 min at 6500×*g*, and samples (1 mL) from the supernatant were withdrawn and centrifuged for 10 min at 19,000×*g*. The supernatant was finally diluted with MeOH prior to the quantification of fenofibrate solubilized in the chosen medium. Difference in fenofibrate solubility in one specific medium below 5% between two consequent time points was considered enough to state that the solubility was reached. The quantification of fenofibrate was carried out by HPLC (Dionex UltiMate 3000 pump, ASI 100 automated sample injector, Dionex Ultimate 3000 detector; all from Thermo Fischer, Waltham, MA, USA), using a Phenomenex Kinetix 5u XB-C18 100A column (100 × 4.6 mm; Phenomenex, Torrance, CA, USA). Fenofibrate was detected at a wavelength of 288 nm, with a retention time of approximately 2.5 min. The mobile phase was composed of 20% purified water and 80% of MeOH and the flow was set to 1 mL/min. In the case of BSA (1 and 4% w/v) as acceptor medium, acetonitrile was added to the samples in order to precipitate the BSA prior to the quantification *via* HPLC. The solubility in each medium was tested in triplicate (n = 3).

Compatibility of the PVPA Barriers with Donor and Acceptor Media

Before the assessment of fenofibrate permeation from SNEDDSs, the permeation of calcein (5.5 mM) was tested to assess the compatibility of the PVPA barriers with the different donor media (Fig. 1B) using PBS pH 7.4 as the acceptor medium. Once the donor media had been evaluated, the compatibility of the PVPA barriers with different acceptor media (see Section Solubility Studies to Select Acceptor Medium for Permeation Experiment) was studied. All experiments were performed at 37 °C. For the experiment being performed in the presence of BM, the mucus layer (50 µL) was carefully pipetted on top of the PVPA barriers and left to incubate for 10 min prior to the addition of the donor medium (Fig. 1B). The donor samples (100 µL; Fig. 1B) were directly pipetted on top of the barriers (with or without BM). The

a

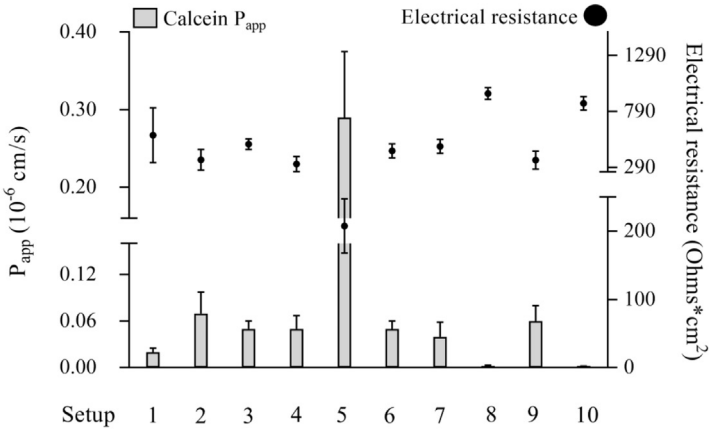

b

Setup	Donor medium	BM	Sample added to donor medium
1	PBS Control	X	Calcein
2	PBS Control	✓	Calcein
3	Intestinal medium	X	Calcein
4	Intestinal medium	✓	Calcein
5	Intestinal medium	X	Calcein + $SNEDDS_{75}$
6	Intestinal medium	✓	Calcein + $SNEDDS_{75}$
7	Intestinal medium	X	Calcein + digesting $SNEDDS_{75}$
8	Intestinal medium	✓	Calcein + digesting $SNEDDS_{75}$
9	Intestinal medium	X	Calcein + digested $SNEDDS_{75}$+ BBBA
10	Intestinal medium	✓	Calcein + digested $SNEDDS_{75}$+ BBBA

Fig. 1. A) PVPA barrier integrity expressed as apparent permeability (P_{app}) of calcein (5.5 mM) and electrical resistance across the PVPA barriers with different setups (Mean ± SD; n = 12). B) Setups tested in terms of PVPA barrier compatibility with and without BM. PBS pH 7.4 was used as the acceptor medium.

barriers were then placed into an acceptor Transwell well containing the acceptor medium (600 μL) and were moved into new wells with the same medium after 2, 4, 5 and 6 h to uphold sink conditions. At the end of the permeation experiment, calcein P_{app} was calculated and the electrical resistance across the PVPA barriers was measured using a Millicell-ERS volt-ohmmeter (Millicell-ERS, Millipore, USA). The measured electrical resistance was then subtracted with the electrical resistance of the nitrocellulose filter (119 Ohm), and the resulting value was normalized with the surface area of the PVPA barriers (0.33 cm^2). The quantification of calcein was carried out using a Tecan Infinite M200 fluorimeter/spectrophotometer (Salzburg, Austria; Software: Magellan) at excitation wavelength of 485 nm and emission of 520 nm (gain: 70). For each condition tested, 12 PVPA barriers were used (n = 12). Values of calcein P_{app} below $0.06 \cdot 10^{-6}$ cm/s and electrical resistance above 290 Ohm · cm^2 indicate that the integrity of the barriers was maintained.[29]

In Vitro Lipolysis of Fenofibrate-Loaded SNEDDSs

The lipolysis of the SNEDDSs under fasted state conditions using the *in vitro* intestinal lipolysis model was carried out following the method described by Michaelsen et al.[12] with minor adjustments. In particular, the SNEDDSs were weighed into a thermostated vessel (37 °C), and subsequently 26 mL of fasted state intestinal medium was added (bile bovine 2.95 mM, calcium chloride 1.40 mM, calcein 5.50 mM, maleic acid 2.00 mM, sodium chloride 146.80 mM, *S*-PC 0.26 mM, tris 2.00 mM; pH 6.50).

The amount of SNEDDS added into the vessel was adjusted to obtain a final fenofibrate concentration of 480 μg/mL in all experiments, following the procedure described by Michaelsen et al.[12] The pancreatic lipase solution was prepared by mixing the crude lipase extract with 5 mL of intestinal medium in the absence of calcein, centrifuging the mixture for 7 min at 6500×*g*, and collecting the supernatant. Lipolysis was initiated by adding 4 mL of pancreatic lipase solution to the thermostated reaction vessel (final activity of 550 USP/mL). The decrease in pH due to the release of free fatty acids from the digested SNEDDS was countered by the use of an automated pH-stat (Metrohm Titrino 744, Tiamo version 1.3, Herisau, Switzerland) with automated addition of NaOH (0.4 M) in order to keep the pH constant at 6.5. The calcium chloride present in the intestinal medium allowed for a continued lipolysis by removing the free fatty acids by precipitation, and thereby avoiding inhibition of the lipase activity.

Samples (1 mL) were taken from the vessel after dispersion (*i.e.* before lipase addition; 0 min) and after 30 min of lipolysis, both to be used for the analysis of fenofibrate distribution between the aqueous and pellet phase, and for permeability experiments. Lipolysis in the samples used for the investigation of the fenofibrate distribution was inhibited by the addition of 5 μL BBBA (1 M in MeOH). The inhibited samples (time point 0 and 30 min) were centrifuged for phase separation (19,000×*g* for 10 min), and the concentration of fenofibrate in the aqueous phase was quantified by HPLC after appropriate dilution in MeOH following the method described in Section Solubility Studies to Select Acceptor Medium for Permeation Experiment. To quantify the total amount and determine the recovery of fenofibrate in the lipolysis vessel, samples were taken before centrifugation and analysed by HPLC. The lipolysis was carried out four times for each SNEDDS (n = 4). The permeability samples were directly pipetted (100 μL) on top of the mucus-PVPA barriers to study the permeation of fenofibrate (see Section Fenofibrate Permeation Using the Mucus-PVPA Model). The lipolysis of the SNEDDSs was not inhibited for the permeation samples after 30 min of lipolysis.

Fenofibrate Permeation Using the Mucus-PVPA Model

Once the preferred donor and acceptor media for the permeation experiment had been selected (Section Compatibility of the PVPA Barriers with Donor and Acceptor Media), the permeation of fenofibrate from SNEDDS (*i.e.* $SNEDDS_{75}$, super-SNEDDS $solution_{150}$, super-SNEDDS $suspension_{150}$) was tested using the mucus-PVPA barriers. Calcein was added to all donor media, in order to enable an in-line assessment of the mucus-PVPA barrier integrity (data not shown). As described above (Section Compatibility of the PVPA Barriers with Donor and Acceptor Media), BM was pipetted (50 μL) on top of the PVPA barriers 10 min prior to the addition of the donor sample (100 μL). The donor sample was either obtained after dispersion of SNEDDSs in the intestinal medium (*i.e.* sample before lipolysis; time point 0 min), or after 30 min of lipolysis (*i.e.* digesting SNEDDSs in intestinal medium; no lipolysis inhibition). The barriers were then placed into an acceptor Transwell well containing the acceptor medium (600 μL) and were moved into new wells with the same medium after 2, 4, 5 and 6 h to uphold sink conditions. The electrical resistance across the PVPA barriers was measured after 6 h to test if the integrity of the barriers was maintained, as discussed above (Section Compatibility of the PVPA Barriers with Donor and Acceptor Media). The quantification of calcein and fenofibrate in the acceptor compartment was carried out using a Tecan Infinite M200 fluorimeter/spectrophotometer (Salzburg, Austria; Software: Magellan) at excitation wavelength of 485 nm and emission of 520 nm (gain: 70) for calcein and 288 nm for fenofibrate. For each condition tested, six PVPA barriers were used (n = 6).

Calculations

The apparent permeability (P_{app}) of calcein was calculated using the following equation:

$$P_{app}\left(\frac{cm}{s}\right) = \frac{dQ}{dt} * \frac{1}{A * Cd}$$

Where *dQ/dt* expresses the flux at the steady state (nmol/s), *A* is the surface area of the PVPA barriers (0.33 cm^2) and C_d the initial fenofibrate/calcein concentration in the donor compartment (nmol/mL).

The area under the curve (AUC) was calculated using GraphPad Prism 7.03 (GraphPad Software, San Diego, CA, USA), which employed a linear trapezoidal model from t = 0 to t = 6 h.

Statistical Analysis

GraphPad Prism 7.03 was employed for the statistical analysis of the presented results (GraphPad Software, San Diego, CA, USA). The data was analysed using one-way ANOVA followed by Šidák *post hoc* test to detect significant differences ($p < 0.05$) when comparing three or more sets of data. If a comparison between two sets of data was made, student t-test was employed ($p < 0.05$).

Results and Discussion

In this study, the development and validation of the *in vitro* lipolysis − mucus-PVPA permeation model was carried out. Biosimilar mucus (BM) was added on top of the PVPA barriers, leading to a better simulation of the intestinal mucosa, which also contains a mucus layer.

The integrity of the PVPA barriers was evaluated in the presence of BM, simulated intestinal medium, undigested and digesting SNEDDSs. The lipolysis of fenofibrate-loaded SNEDDSs was studied using the *in vitro* intestinal lipolysis model, followed by the drug permeation assessment using the mucus-PVPA barriers. Finally, the correlation of *in vitro* lipolysis and lipolysis-permeation data with

in vivo plasma data of fenofibrate in rats was determined. The type of IVIVC assessed in this study can be referred to as a Level D correlation, and it is considered a qualitative correlation which can be used in the development of new formulations.[31]

Lipolysis-Permeation Model Setup

Donor Medium Selection

The compatibility of the PVPA barriers, with and without mucus, with the donor medium compositions in Fig. 1B, using PBS pH 7.4 as acceptor medium, was evaluated by assessing the permeation of the hydrophilic marker calcein, and the electrical resistance across the barriers at the end of the permeation assay (see Section Compatibility of the PVPA Barriers with Donor and Acceptor Media).

As it can be observed in Fig. 1, the PVPA barriers were able to maintain their functionality in all the tested donor media in the presence of BM. In the absence of BM, the medium with undigested $SNEDDS_{75}$ (Fig. 1, Setup 5) led to barrier impairment; calcein P_{app} was $0.29 \cdot 10^{-6}$ cm/s and the electrical resistance was 208 Ohm $\cdot$ cm^2, which were both values outside the limits set for intact barriers (*i.e.* calcein P_{app} above $0.06 \cdot 10^{-6}$ cm/s and electrical resistance below 290 Ohm $\cdot$ cm^2 indicate loss of barrier integrity[28]). However, the digested $SNEDDS_{75}$ in the donor compartment showed to be compatible with the barrier also in the absence of mucus (Fig. 1, Setup 7). The difference in barrier compatibility between the undigested and digested $SNEDDS_{75}$ might be due to the colloidal structures that are generated during the lipolysis of SNEDDSs. $SNEDDS_{75}$ before lipolysis display a very distinct structure characterized by nano-emulsion droplets, while during lipolysis their lipid fractions result in the formation of different colloidal structures, such as vesicles and micelles, composed of both lipolysis products and components present in the simulated intestinal medium.[12]

BM, fasted state simulated intestinal medium, undigested $SNEDDS_{75}$ (in the presence of BM) and digested $SNEDDS_{75}$ (both with uninhibited and inhibited pancreatin) were compatible with the barriers (Fig. 1). As the presence of BM maintained barrier integrity with undigested $SNEDDS_{75}$ (Fig. 1, Setup 6), BM was applied on top of the barriers during the assessment of the permeation of fenofibrate from SNEDDSs before and after *in vitro* lipolysis.

Acceptor Medium Selection

The solubility of fenofibrate was determined in the acceptor medium for the permeation study described in Section Solubility Studies to Select Acceptor Medium for Permeation Experiment. Higher solubility of the lipophilic drug in the acceptor compartment of the PVPA model would enable a larger amount of drug to permeate, thereby easing the quantification of the amount of permeated drug. As can be observed in Table 2, the highest solubility of fenofibrate was in Tween 20 5 mg/mL and BSA 4% w/v. Moreover, DMSO significantly increased the solubility of fenofibrate at a concentration of 40 mg/mL, but not at 10 mg/mL, when compared to PBS pH 7.4 (Table 2).

Table 2
Equilibrium Solubility of Fenofibrate in Different Aqueous Media Prepared in PBS pH 7.4 (Mean ± SD; n = 3).

Acceptor Medium	Equilibrium Solubility (nmol/mL)
PBS pH 7.4	0.48 ± 0.03
DMSO 10 mg/mL	0.59 ± 0.08
DMSO 40 mg/mL	0.82 ± 0.01[a]
BSA 1% w/v	14.19 ± 0.13[a]
BSA 4% w/v	58.02 ± 0.49[a]
Tween 20 5 mg/mL	116.71 ± 5.73[a]

[a] Statistically significant difference in fenofibrate equilibrium solubility compared to PBS pH 7.4 ($p < 0.05$).

Only DMSO (1–40 mg/mL) has previously been investigated regarding its compatibility with the PVPA barriers,[32] and showed not to impair the integrity of the barriers up to a concentration of 40 mg/mL. Thus, to select the best acceptor medium, the functionality of the barriers in the presence of each acceptor medium was investigated before performing permeation experiments, while using calcein solution (in PBS pH 6.5; 5.5 mM) on the donor side. As can be seen in Fig. 2 the barriers maintained their integrity in the presence of PBS pH 7.4 and DMSO (10 and 40 mg/mL). In contrast, BSA (1 and 4% w/v) and Tween 20 5 mg/mL caused barrier impairment, as demonstrated by an increased calcein P_{app} and decreased electrical resistance. Based on the effect on PVPA barrier integrity and the solubility of fenofibrate, DMSO 40 mg/mL was chosen as the acceptor medium in the fenofibrate permeation studies.

In Vitro Lipolysis *of Fenofibrate-Loaded SNEDDSs*

Three SNEDDSs ($SNEDDS_{75}$, super-$SNEDDS\ solution_{150}$ and super-$SNEDDS\ suspension_{150}$) were analysed in terms of their capability of solubilizing fenofibrate after 30 min of *in vitro* lipolysis. Fig. 3 depicts the distribution of fenofibrate in the aqueous and the pellet phase before (0 min) and after (30 min) lipolysis. For $SNEDDS_{75}$, little to no precipitation was observed both before (0 min) and after (30 min) lipolysis, while for the super-$SNEDDS\ solution_{150}$, precipitation of fenofibrate was observed at the start of lipolysis and after 30 min. In the case of the super-$SNEDDS\ suspension_{150}$, the presence of drug precipite was pronounced both after dispersion (0 min) and after lipolysis (30 min), and a significant increase over time ($p < 0.05$) was observed when comparing the amount of precipitate before and after lipolysis (Fig. 3). The differences between the SNEDDSs can be due to that twice as much $SNEDDS_{75}$ was added, compared to the super-$SNEDDS\ solution_{150}$ and the super-$SNEDDS\ suspension_{150}$, in order to keep the fenofibrate concentration constant in the lipolysis vessel. This lower amount of lipid caused a decrease in drug solubilization and an increase in drug precipitation.

When comparing the two super-SNEDDSs, containing the same amount of lipid vehicle, the presence of precipitated fenofibrate

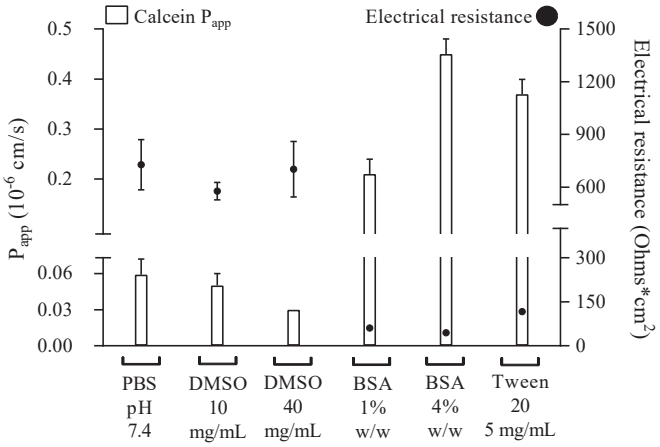

Fig. 2. PVPA barrier integrity expressed as apparent permeability (P_{app}) of calcein (5.5 mM) and electrical resistance across the barriers with different media in the acceptor compartment, and calcein 5.5 mM in the donor compartment (in PBS pH 6.5). (Mean ± SD; n = 12).

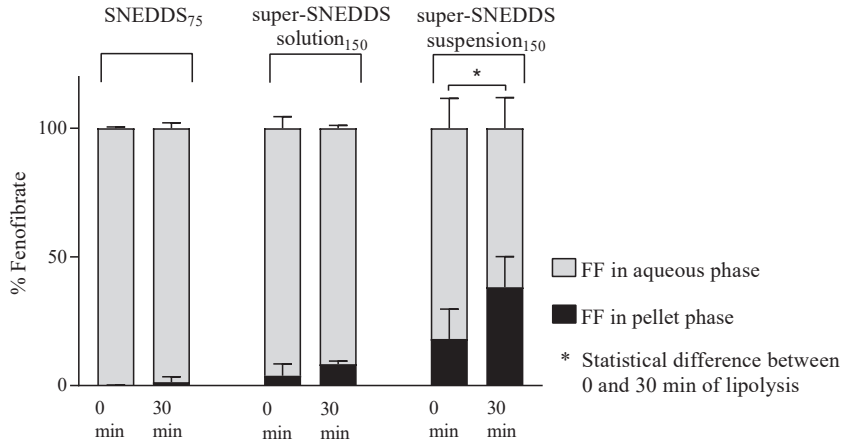

Fig. 3. Relative amount of fenofibrate present in the aqueous phase (*grey*) and pellet phase (*black*) during *in vitro* intestinal lipolysis of $SNEDDS_{75}$, super-SNEDDS $solution_{150}$ and super-SNEDDS $suspension_{150}$. (Mean ± SD; n = 4). * Statistical difference between the percentages of fenofibrate in solution after 0 min compared to 30 min of lipolysis.

was more pronounced for the super-SNEDDS $suspension_{150}$ (Fig. 3). This is due to the nature of the super-SNEDDS $suspension_{150}$ where the drug is only partially dissolved, whereas the drug is completely dissolved in the super-SNEDDS $solution_{150}$.

Michaelsen et al.,[12] studied the same fenofibrate-containing SNEDDSs, and the impact of fenofibrate load and SNEDDSs lipolysis on drug solubilization and absorption was evaluated *via* an *in vivo* pharmacokinetic study in rats and *in vitro* lipolysis. The results depicted in Fig. 3 are in accordance with the *in vitro* lipolysis data obtained by Michaelsen et al.[12] Even though the ranking in terms of drug precipitation of the three SNEDDSs was the same as the findings in the present study, the percentage of drug precipitated during lipolysis was higher in the results presented by Michaelsen et al.[12] The difference in drug precipitation between the two studies can be explained by the different experimental setups of the *in vitro* lipolysis applied in the two studies: in the present study, calcium was added to the simulated intestinal medium prior to lipolysis (initial/bolus addition of calcium) to simplify the experimental setup, whereas in the study by Michaelsen et al.[12] calcium was continuously added during lipolysis to control the rate of lipolysis (dynamic addition of calcium). It has previously been demonstrated that initial and continuous addition of calcium can lead to differences in terms of drug precipitation during lipolysis of LbDDSs, and that the calcium concentration can also have an effect on the extent of lipolysis.[33]

In Vivo Absorption-*In Vitro* Lipolysis Correlation

In the study by Michaelsen et al.,[12] the super-SNEDDS $solution_{150}$ had a superior *in vivo* performance after oral dosing to rats (*i.e.* higher $AUC_{0-30h,\ in\ vivo}$ and C_{max}) compared to $SNEDDS_{75}$ and super-SNEDDS $suspension_{150}$ (Table 3). This was not correlating with the observed drug solubilization during *in vitro* lipolysis, where $SNEDDS_{75}$ led to a higher drug solubilization. Thus, Michaelsen et al.[12] were not able to find a correlation between the *in vivo* absorption and the drug solubilization during *in vitro* lipolysis.

In accordance with the findings from Michaelsen et al.,[12] the present study did not find a correlation between the drug solubilized during *in vitro* lipolysis (Section In vitro *lipolysis* of fenofibrate-loaded SNEDDSs) and the *in vivo* plasma data ($R^2 = 0.397$; Fig. 4, Table 3), highlighting the fact that *in vitro* solubilization alone cannot predict the *in vivo* absorption of fenofibrate from the SNEDDS analysed in this study. Even though it is generally assumed that the SNEDDS able to maintain the most drug in solution during lipolysis leads to the highest bioavailability,[34] it should be noted that the amount of fenofibrate in the aqueous phase during *in vitro* lipolysis is in a dynamic equilibrium between free drug and drug solubilized in vesicles and other colloidal structures resulting from the lipolysis products (*e.g.* free fatty acids and monoglycerides) and their interaction with bile salts and phospholipid in the medium.[13] Only the free drug is available for absorption, and therefore it is of interest to quantify this, by adding a permeation step to the *in vitro* lipolysis.

In Vitro Permeation

The permeation of fenofibrate across the mucus-PVPA barriers following administration of three different SNEDDSs was evaluated before (0 min) and after (30 min) *in vitro* lipolysis. This allowed the

Table 3
Area Under the Curve (AUC) Resulting From Fenofibrate Absorption During *In Vivo* Studies in Rats (*[12], $AUC_{0-30h,\ in\ vivo}$), % of Fenofibrate Found in the Aqueous Phase After 30 min of *In Vitro* Lipolysis, and AUC Resulting from the Mass Transfer of Fenofibrate Permeated Across the Mucus-PVPA Barriers ($AUC_{0-6h,\ perm}$) Before (0 min) and After (30 min) *In Vitro* Lipolysis From Super-SNEDDS $Solution_{150}$, $SNEDDS_{75}$ and Super-SNEDDS $Suspension_{150}$.

	Super-SNEDDS $Solution_{150}$	$SNEDDS_{75}$	Super-SNEDDS $Suspension_{150}$
$AUC_{0-30h,\ in\ vivo}$ (μg·h/mL) *in vivo* rats*	148.0 ± 47.5[a,b]	88.3 ± 20.9[a]	58.1 ± 16.9[b]
Fenofibrate (%) in the aqueous phase after 30 min of *in vitro* lipolysis	91.7 ± 1.11	98.6 ± 2.1	61.8 ± 11.9
$AUC_{0-6h,\ perm}$ (nmol·h) *in vitro* mucus-PVPA: f enofibrate permeation before lipolysis	17.0 ± 1.6[c]	14.0 ± 1.2	9.9 ± 2.2[c]
$AUC_{0-6h,\ perm}$ (nmol·h) *in vitro* mucus-PVPA: fenofibrate permeation after 30 min *in vitro* lipolysis	17.0 ± 0.8[d,e]	12.0 ± 1.0[d]	8.7 ± 1.1[e]

Values labelled with the same letter are significantly different. (Mean ± SEM; n = 6).

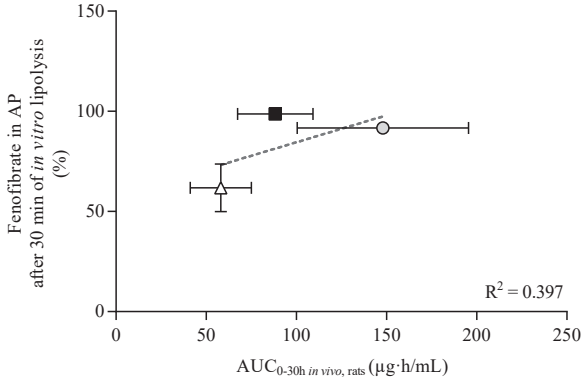

Fig. 4. Fenofibrate (%) found in the aqueous phase (AP) after 30 min of *in vitro* lipolysis as a function of the AUC $_{0-30h,\ in\ vivo}$ from the plasma curve after oral dosing in rats (Michaelsen et al., 2019[12]) of super-SNEDDS solution$_{150}$ (*grey circle*), SNEDDS$_{75}$ (*black square*) and super-SNEDDS suspension$_{150}$ (*white triangle*).

investigation of whether fenofibrate permeation was influenced by i) SNEDDSs composition and ii) lipolysis of the SNEDDSs. The in-line assessment of the mucus-PVPA barrier integrity carried out by measuring the permeation of calcein confirmed the correct functionality of the mucus-PVPA barriers (data not shown), and confirmed that the componenets present in the donor compartment of the permeation barriers did not affect the mucus-PVPA barriers integrity.

As can be observed from Fig. 5, both before and after lipolysis, the super-SNEDDS solution$_{150}$ allowed the highest permeation of fenofibrate, followed by the SNEDDS$_{75}$ and the super-SNEDDS suspension$_{150}$. Even though the ranking of the three SNEDDSs was the same before (Fig. 5A) and after lipolysis (Fig. 5B), differences in the permeation profiles in the two conditions led to differences in AUC$_{0-6h,\ perm}$ (Table 3). The AUC$_{0-6h,\ perm}$ for the undigested super-SNEDDS solution$_{150}$ was significantly higher than for the super-SNEDDS suspension$_{150,}$ but not the SNEDDS$_{75}$. After 30 min of *in vitro* lipolysis, the AUC$_{0-6h,\ perm}$ for the super-SNEDDS solution$_{150}$ was significantly higher than the AUC$_{0-6h,\ perm}$ for both the super-SNEDDS suspension$_{150}$ and the SNEDDS$_{75}$ (Table 3). This is in accordance with the *in vivo* data presented by Michaelsen et al.[12] where the ranking of the *in vivo* AUC$_{0-30h,\ in\ vivo}$ was: super-SNEDDS solution$_{150}$ > SNEDDS$_{75}$ > super-SNEDDS suspension$_{150}$ (Table 3). The difference between the AUC$_{0-6h,\ perm}$ before and after lipolysis can be explained by a change in drug concentration in the aqueous phase upon lipolysis. The nanoemulsion droplets of SNEDDS formed after dispersion in the intestinal medium (*i.e.* before *in vitro* lipolysis) can have a different impact on drug solubilization compared to the colloidal structures formed during lipolysis. This will especially impact the equilibrium between the amount of drug free in solution and the one associated with colloidal structures, and thus the amount of drug available for permeation across the PVPA barriers.

The results discussed thus far demonstrate that, even though the total drug concentration in the donor compartment was the same (480 µg/mL) for all the analysed SNEDDSs, the amount of fenofibrate permeating through the barriers was affected by the SNEDDS in the donor compartment. Moreover, even though the *in vitro* lipolysis showed that the SNEDDS$_{75}$ resulted in the highest amount of drug solubilized in the aqueous phase (Fig. 3), the super-SNEDDS solution$_{150}$ exhibited the highest permeation (Fig. 5). Thomas et al.[35] have demonstrated that drug precipitation following lipolysis of super-SNEDDS solutions does not necessarily translate to lower *in vivo* drug absorption. The difference in drug permeation between the super-SNEDDS solution$_{150}$ and SNEDDS$_{75}$ can be due to the partitioning of the drug between being free in solution and in the colloidal structures, formed upon dispersion/lipolysis of the SNEDDS on top of the permeation barriers. For SNEDDS$_{75}$, the lipid content is higher, and more drug can be associated to the colloidal structures, thus not being able to permeate. In contrast, for super-SNEDDS solution$_{150,}$ the lower lipid content can lead to a higher amount of drug being free in solution, and thus able to permeate through the mucus-PVPA barriers, as demonstrated in Fig. 5.

In Vivo Absorption-*In Vitro* Permeation Correlation

To assess the correlation between *in vitro* and *in vivo* data, the *in vitro* AUC$_{0-6h,\ perm}$ from the fenofibrate permeation was depicted as a function of the *in vivo* AUC$_{0-30h,\ in\ vivo}$ (Table 3[12]) in Fig. 6. The correlation of the permeation data after 30 min of *in vitro* lipolysis was better (Fig. 6B, R^2 = 0.9952) compared to the permeation of fenofibrate from undigested SNEDDSs (Fig. 6A, R^2 = 0.9255), highlighting the positive impact of the presence of lipolysis on the IVIVC. Comparing these findings to Fig. 4, it is clear that for the investigated SNEDDSs, the amount of drug solubilized during *in vitro* lipolysis studies alone cannot predict the *in vivo* absorption of fenofibrate, while an additional permeation step can enable a prediction of the performance of SNEDDS *in vivo*.

In the present study, the presence of the BM layer on top of the absorptive PVPA barriers permitted the development of a permeation model able to withstand a digesting environment (Fig. 1). Moreover, the addition of BM on top of the PVPA barriers allowed for a better simulation of the intestinal mucosa, and possibly contributed to the estimation of the *in vivo* performance of the

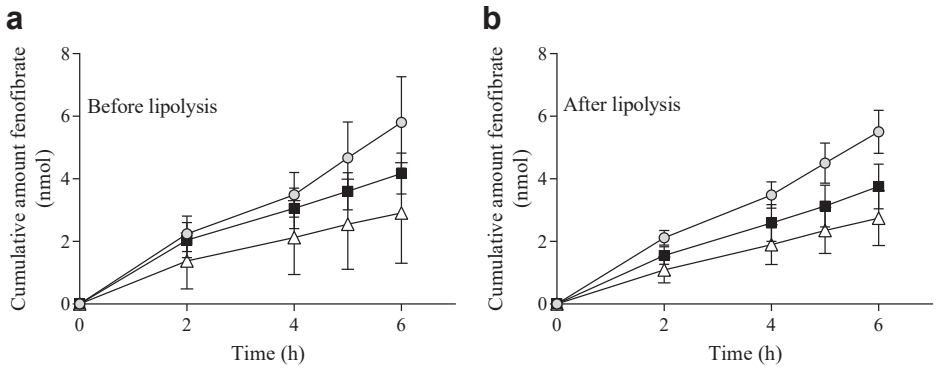

Fig. 5. Cumulative amount of fenofibrate permeated across the mucus-PVPA barriers from super-SNEDDS solution$_{150}$ (*grey circle*), SNEDDS$_{75}$ (*black square*) and super-SNEDDS suspension$_{150}$ (*white triangle*) A) before (0 min) and B) after (30 min) lipolysis. (Mean ± SD; n = 6).

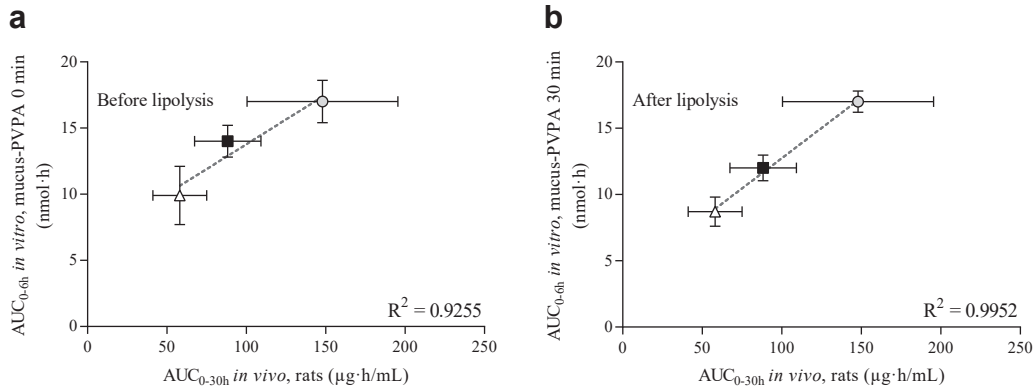

Fig. 6. *In-vivo-in-vitro* correlation (IVIVC) of *in vivo* plasma exposure (Michaelsen et al., 2019[12]) and *in vitro* fenofibrate permeation across the mucus-PVPA barriers A) before (0 min) and B) after (30 min) lipolysis from super-SNEDDS solution$_{150}$ (*grey circle*), SNEDDS$_{75}$ (*black square*) and super-SNEDDS suspension$_{150}$ (*white triangle*).

SNEDDSs tested by Michaelsen et al.[12] As all the *in vitro* fenofibrate permeation experiments were performed in the presence of mucus, the comparison in terms of drug permeation between the presence and absence of the mucus layer could not be assessed. The hydrophilic mucus barrier in the mucus-PVPA model has previously shown to affect drug permeation depending on the physicochemical properties of the investigated drug, drug formulation and the simulated physiological conditions,[28,29,36] and it is thus regarded as an essential part of the artificial absorption barrier. The presence of mucus is also important as it has been shown that SNEDDSs can rapidly permeate across this layer thanks to the low interaction of their hydrophobic surface with the hydrophilic regions of mucus and thanks to their low droplet size, consequently enabling higher drug absorption.[37,38] Thus, the inclusion of mucus on top of an *in vitro* permeation membrane is crucial to simulate the environment that SNEDDSs would be presented to *in vivo*, and allows these drug delivery systems to explicate the positive effect on drug absorption related to their high mucus permeation.

Conclusion

In the present study, the *in vitro* lipolysis – mucus-PVPA permeation model was developed. The model allowed the combination of the assessment of drug distribution during lipolysis for fenofibrate-loaded SNEDDSs typical of the *in vitro* intestinal lipolysis model with the quantification of the fenofibrate permeation through an artificial membrane mimicking the intestinal epithelium (*i.e.* mucus-PVPA barrier). The barriers used in this work were more stable when lined with a mucus layer, thus being able to closely mimic the physiology of the intestinal mucosa and to improve the relevance of the model for oral absorption studies. The investigated SNEDDSs had different abilities to keep fenofibrate solubilized in the aqueous phase during *in vitro* lipolysis, and led to different drug permeation profiles. No correlation was found between already published *in vivo* absorption and drug solubilization during *in vitro* lipolysis ($R^2 < 0.4$), whereas a satisfactory correlation was found between the same *in vivo* data with *in vitro* permeation data both before and after *in vitro* lipolysis ($R^2 > 0.9$), highlighting the importance of the permeation step following lipolysis in the prediction of *in vivo* drug absorption. The combination of *in vitro* lipolysis with *in vitro* permeation led to a better correlation ($R^2 = 0.9952$) compared to absence of lipolysis ($R^2 = 0.9255$). However, the satisfactory correlation in the absence of lipolysis suggests that this step might not be necessary. In order to validate this statement, further studies with other types of SNEDDSs need to be carried out.

By applying the *in vitro* lipolysis – mucus-PVPA permeation model, it was possible to mimic physiological processes (*i.e.* lipolysis and permeation) and to correlate the amount of fenofibrate permeated *in vitro* with the AUC after oral dosing of the applied SNEDDSs in rats.

Conflicts of Interest

The authors confirm no conflicts of interest.

Acknowledgments

The authors acknowledge UiT The Arctic University of Norway for funding PhD student Margherita Falavigna. The authors thank Lipoid GmbH (Ludwigshafen, Germany) for the donation of phospholipids. The contributions from NordicPOP (supported by NordForsk for the Nordic University Hub project number: 85352), and COST Action UNGAP (supported by the European Cooperation in Science and Technology; project number: 16205) are greatly appreciated.

References

1. Porter CJH, Trevaskis NL, Charman WN. Lipids and lipid-based formulations: optimizing the oral delivery of lipophilic drugs. *Nat Rev Drug Discov*. 2007;6(3):231-248.
2. Gao P, Morozowich W. Development of supersaturatable self-emulsifying drug delivery system formulations for improving the oral absorption of poorly soluble drugs. *Expet Opin Drug Deliv*. 2006;3(1):97-110.
3. Siqueira SDVS, Müllertz A, Gräeser K, Kasten G, Mu H, Rades T. Influence of drug load and physical form of cinnarizine in new SNEDDS dosing regimens: in vivo and in vitro evaluations. *AAPS J*. 2017;19(2):587-594.
4. Trevaskis NL, Charman WN, Porter CJH. Lipid-based delivery systems and intestinal lymphatic drug transport: a mechanistic update. *Adv Drug Deliv Rev*. 2008;60(6):702-716.
5. Feeney OM, Crum MF, McEvoy CL, et al. 50 years of oral lipid-based formulations: provenance, progress and future perspectives. *Adv Drug Deliv Rev*. 2016;101:167-194.
6. Bibi HA, Holm R, Bauer-Brandl A. Simultaneous lipolysis/permeation in vitro model, for the estimation of bioavailability of lipid based drug delivery systems. *Eur J Pharm Biopharm*. 2017;117:300-307.
7. Keemink J, Mårtensson E, Bergström CAS. Lipolysis-permeation setup for simultaneous study of digestion and absorption in vitro. *Mol Pharm*. 2019;16:921-930.
8. Thomas N, Richter K, Pedersen TB, Holm R, Müllertz A, Rades T. In vitro lipolysis data does not adequately predict the in vivo performance of lipid-based drug delivery systems containing fenofibrate. *AAPS J*. 2014;16(3):539-549.
9. Savla R, Browne J, Plassat V, Wasan KM, Wasan EK. Review and analysis of FDA approved drugs using lipid-based formulations. *Drug Dev Ind Pharm*. 2017;43:1743-1758.
10. Boyd BJ, Bergström CAS, Vinarov Z, et al. Successful oral delivery of poorly water-soluble drugs both depends on the intraluminal behaviour of drugs and of appropriate advanced drug delivery systems. *Eur J Pharm Sci*. 2019;137:104967.

11. Zangenberg NH, Müllertz A, Kristensen HG, Hovgaard L. A dynamic in vitro lipolysis model I. Controlling the rate of lipolysis by continuous addition of calcium. *Eur J Pharm Sci*. 2001;14:115-122.
12. Michaelsen MH, Siqueira Jørgensen SD, Abdi IM, Wasan KM, Rades T, Müllertz A. Fenofibrate oral absorption from SNEDDS and super-SNEDDS is not significantly affected by lipase inhibition in rats. *Eur J Pharm Biopharm*. 2019;142:258-264.
13. Berthelsen R, Klitgaard M, Rades T, Müllertz A. In vitro digestion models to evaluate lipid based drug delivery systems; present status and current trends. *Adv Drug Deliv Rev*. 2019;142:35-49.
14. Artursson P, Palm K, Luthman K. Caco-2 monolayers in experimental and theoretical predictions of drug transport. *Adv Drug Deliv Rev*. 2001;46:27-43.
15. Kansy M, Senner F, Gubernator K. Physicochemical high throughput screening: parallel artificial membrane permeation assay in the description of passive absorption processes. *J Med Chem*. 1998;41:1007-1010.
16. Flaten GE, Dhanikula AB, Luthman K, Brandl M. Drug permeability across a phospholipid vesicle barrier: a novel approach for studying passive diffusion. *Eur J Pharm Sci*. 2006;27:80-90.
17. di Cagno M, Bibi HA, Bauer-Brandl A. New biomimetic Permeapad™ for efficient investigation of passive permeability of drugs. *Eur J Pharm Sci*. 2015;73:29-34.
18. Berben P, Brouwers J, Augustijns P. Assessment of passive intestinal permeability using an artificial membrane insert system. *J Pharm Sci*. 2018;107:250-256.
19. Keemink J, Bergstrom CAS. Caco-2 cell conditions enabling studies of drug absorption from digestible lipid-based formulations. *Pharm Res (N Y)*. 2018;35:74.
20. Alskär LC, Parrow A, Keemink J, Johansson P, Abrahamsson B, Bergström CAS. Effect of lipids on absorption of carvedilol in dogs: is coadministration of lipids as efficient as a lipid-based formulation? *J Control Release*. 2019;304:90-100.
21. Lechanteur A, das Neves J, Sarmento B. The role of mucus in cell-based models used to screen mucosal drug delivery. *Adv Drug Deliv Rev*. 2018;124:50-63.
22. Miyazaki K, Kishimoto H, Muratani M, Kobayashi H, Shirasaka Y, Inoue K. Mucins are involved in the intestinal permeation of lipophilic drugs in the proximal region of rat small intestine. *Pharm Res (N Y)*. 2019;36(162):1-11.
23. Rezhdo O, Speciner L, Carrier R. Lipid-associated oral delivery: mechanisms and analysis of oral absorption enhancement. *J Control Release*. 2016;240:544-560.
24. Yildiz HM, Speciner L, Ozdemir C, Cohen DE, Carrier RL. Food-associated stimuli enhance barrier properties of gastrointestinal mucus. *Biomaterials*. 2015;54:1-8.
25. Boegh M, Baldursdóttir SG, Müllertz A, Nielsen HM. Property profiling of biosimilar mucus in a novel mucus-containing in vitro model for assessment of intestinal drug absorption. *Eur J Pharm Biopharm*. 2014;87:227-235.
26. Boegh M, Garcia-Diaz M, Müllertz A, Nielsen HM. Steric and interactive barrier properties of intestinal mucus elucidated by particle diffusion and peptide permeation. *Eur J Pharm Biopharm*. 2015;95:136-143.
27. Roese E, Bunjes H. Drug release studies from lipid nanoparticles in physiological media by a new DSC method. *J Control Release*. 2017;256:92-100.
28. Falavigna M, Klitgaard M, Brase C, Ternullo S, Skalko-Basnet N, Flaten GE. Mucus-PVPA (mucus phospholipid vesicle-based permeation assay): an artificial permeability tool for drug screening and formulation development. *Int J Pharm*. 2018;537:213-222.
29. Falavigna M, Klitgaard M, Steene E, Flaten GE. Mimicking regional and fasted/fed state conditions in the intestine with the mucus-PVPA in vitro model: the impact of pH and simulated intestinal fluids on drug permeability. *Eur J Pharm Sci*. 2019;132:44-54.
30. Berthelsen R, Sjögren E, Jacobsen J, et al. Combining in vitro and in silico methods for better prediction of surfactant effects on the absorption of poorly water soluble drugs – a fenofibrate case example. *Int J Pharm*. 2014;473:356-365.
31. Schen JS, Burgess DJ. In vitro-in vivo correlation for complex non-oral drug products: where do we stand? *J Control Release*. 2015;219:644-651.
32. Flaten GE, Luthman K, Vasskog T, Brandl M. Drug permeability across a phospholipid vesicle-based barrier: 4. The effect of tensides, co-solvent and pH changes on barrier integrity and on drug permeability. *Eur J Pharm Sci*. 2008;34:173-180.
33. Sassene P, Kleberg K, Williams HD, et al. Toward the establishment of standardized in vitro tests for lipid-based formulations, Part 6: effects of varying pancreatin and calcium levels. *AAPS J*. 2014;16(6):1344-1356.
34. Dahan A, Hoffman A. Use of a dynamic in vitro lipolysis model to rationalize oral formulation development for poor water soluble drugs: correlation with in vivo data and the relationship to intra-enterocyte processes in rats. *Pharm Res (N Y)*. 2006;23(9):2165-2174.
35. Thomas N, Holm R, Müllertz A, Rades T. In vitro and in vivo performance of novel supersaturated self-nanoemulsifying drug delivery systems (super-SNEDDS). *J Control Release*. 2012;160:25-32.
36. Falavigna M, Stein PC, Flaten GE, Pio di Cagno M. Impact of mucin on drug diffusion: development of a straightforward in vitro method for the determination of drug diffusivity in the presence of mucin. *Pharmaceutics*. 2020;12(168):1-13.
37. Abdulkarim M, Sharma PK, Gumbleton M. Self-emulsifying drug delivery system: mucus permeation and innovative quantification technologies. *Adv Drug Deliv Rev*. 2019;142:62-74.
38. Leal J, Smyth HDC, Ghosh D. Physicochemical properties of mucus and their impact on transmucosal drug delivery. *Int J Pharm*. 2017;532:555-572.

Paper IV

International Journal of Pharmaceutics 596 (2021) 120258

Contents lists available at ScienceDirect

International Journal of Pharmaceutics

journal homepage: www.elsevier.com/locate/ijpharm

Simultaneous assessment of *in vitro* lipolysis and permeation in the mucus-PVPA model to predict oral absorption of a poorly water soluble drug in SNEDDSs

Margherita Falavigna [a], Sunniva Brurok [a], Mette Klitgaard [b], Gøril Eide Flaten [a,*]

[a] Drug Transport and Delivery Research Group, Department of Pharmacy, UiT The Arctic University of Norway, Universitetsveien 57, 9037 Tromsø, Norway
[b] Physiological Pharmaceutics, Department of Pharmacy, University of Copenhagen, Universitetsparken 2-4, 2100 Copenhagen, Denmark

ARTICLE INFO

Keywords:
In vivo-in vitro correlation (IVIVC)
In vitro permeation
In vitro lipolysis
Lipid-based formulation
Oral drug delivery
Poorly water-soluble drugs

ABSTRACT

The prediction of the *in vivo* performance of self-nanoemulsifying drug delivery systems (SNEDDSs) is currently gaining increasing attention. Therefore, the need for reliable *in vitro* models able to assess the drug solubilization capacity of such formulations upon *in vitro* lipolysis, as well as to concomitantly evaluate *in vitro* drug permeation, has become ever so evident. In the current study, the high-throughput *in vitro* intestinal lipolysis model was combined with the mucus-PVPA *in vitro* permeation model to study the solubilization capacity of SNEDDSs for the poorly water-soluble drug fenofibrate and to study the consequent drug permeation. Moreover, drug solubilization and permeation were evaluated both in the presence and absence of lipolysis. The results obtained demonstrated that the presence of *in vitro* lipolysis significantly impacted the solubilization and permeation profiles of fenofibrate compared to its absence. The results were in accordance with already published *in vivo* data regarding the same fenofibrate-loaded SNEDDSs. Additionally, the correlation between the *in vitro* permeation data and *in vivo* plasma concentration in rats was found to be excellent both in the presence and absence of lipolysis ($R^2 > 0.98$), highlighting the ability of the developed combined *in vitro* model to predict *in vivo* drug absorption.

1. Introduction

The complexity of the physiological processes and characteristics of the gastrointestinal (GI) tract have shown to greatly affect the therapeutic outcome of oral drug-delivery systems (Lin and Wong, 2017). For instance, drug absorption can be largely influenced by the pH condition of the specific GI compartment, the presence and activity of metabolic enzymes and by the presence and composition of the food components possibly present along the GI tract (Vertzoni et al., 2019). These factors can have different effects on drug absorption according to the specific administered drug and its physicochemical characteristics. In particular, as up to 70% of new drug entities have been shown to be poorly water-soluble, increasing focus has been put on developing formulations able to overcome the low bioavailability connected to this type of drugs, and to understand the physiological processes affecting the performance of such formulations (Berben et al., 2018). In particular, lipid-based formulations such as self-nanoemulsifying drug delivery systems (SNEDDSs) have shown to improve the bioavailability of poorly water-soluble drugs (PWSD) thanks to enhancement of solubilization and permeation, lymphatic transport and stimulation of supersaturation (Gao and Morozowich, 2006; Porter et al., 2007; Siqueira et al., 2017; Trevaskis et al., 2008). The dispersion of these formulations into the gastric and intestinal fluids and the digestion processes initiated by digestive enzymes are two of the key factors affecting the performance of SNEDDSs and the related drug absorption (Feeney et al., 2016). Even though several SNEDDSs have already reached the market, their optimization is still regarded as challenging due to the complex array of processes (*i.e.* equilibrium between SNEDDSs digestion, drug supersaturation, precipitation and absorption) that can affect their performance (Savla et al., 2017). Due to the challenges related to predicting the behavior of these lipid-based formulations, the need for *in vitro* models able to evaluate the *in vivo* performance of SNEDDSs has become ever so evident. Consequently, several research efforts initially focused on producing *in vitro* models able to either study the effect of digestive

* Corresponding author.
E-mail addresses: margherita.falavigna@gmail.com (M. Falavigna), sunnivabrurok@gmail.com (S. Brurok), mette.klitgaard@sund.ku.dk (M. Klitgaard), goril.flaten@uit.no (G.E. Flaten).

https://doi.org/10.1016/j.ijpharm.2021.120258
Received 30 November 2020; Received in revised form 7 January 2021; Accepted 10 January 2021
Available online 21 January 2021

enzymes on the *in vitro* drug solubilization capacity of SNEDDSs (*i.e.* the *in vitro* intestinal lipolysis model (Zangenberg et al., 2001)), or on evaluating the *in vitro* permeation of PWSDs with the use of permeation barriers (*i.e.* the Caco-2 model (Artursson et al., 2001); the PAMPA model (Kansy et al., 1998); the PVPA model (Flaten et al., 2006); the Permeapad™ (di Cagno et al., 2015); and the AMI system (Berben et al., 2018)). However, the separate evaluation of *in vitro* lipolysis and *in vitro* drug permeation did not lead to a complete overview of the physiological processes affecting oral drug absorption. In fact, it has been shown that the evaluation of drug solubilization upon *in vitro* lipolysis of lipid-based formulations in the absence of an absorptive sink overestimates drug supersaturation and precipitation and underestimates drug absorption, while the addition of a permeation step leads to a more representative prediction of oral drug absorption *in vivo* (Bevernage et al., 2012; Stillhart et al., 2014). As a result of this, these two processes have been pooled together to produce combined *in vitro* lipolysis-permeation models (Alskär et al., 2019; Berthelsen et al., 2019; Bibi et al., 2017; Hedge and Bergström, 2020; Ille et al., 2020; Keemink et al., 2019; Keemink and Bergström, 2018; O'Dwyer et al., 2020). These combined models proved to predict the *in vivo* drug absorption from SNEDDSs to a higher extent compared to *in vitro* lipolysis or *in vitro* permeation alone. However, all of the mentioned models except one (Keemink and Bergström, 2018) lack the presence of a mucus layer on top of the permeation barriers, thus not being able to closely mimic the physiology of the GI mucosa (Falavigna et al., 2020a; Lechanteur et al., 2018). Notably, it has been shown that the presence of the mucus layer can stabilize supersaturation of PWSDs after *in vitro* lipolysis of lipid-based formulations, and it has been proposed that this could be one of the intrinsic mechanisms of action of these formulations (Yeap et al., 2013, 2019). Further, several studies have pointed at the influence that mucus has on the diffusion and permeation of PWSDs, thus further emphasizing the importance of taking this additional barrier into account (Falavigna et al., 2020b; Miyazaki et al., 2019). To account for the need of mucus in a combined *in vitro* lipolysis-permeation model, a biosimilar mucus layer was added on top of the PVPA (Phospholipid Vesicle-based Permeation Assay) barriers (*i.e.* mucus-PVPA barriers) (Falavigna et al., 2020a). The mucus-PVPA barriers were used in combination with the *in vitro* intestinal lipolysis model equipped with a pH-stat-titration apparatus (Falavigna et al., 2020a), and it was found that the combined *in vitro* lipolysis-permeation model was able to predict the *in vivo* oral absorption of fenofibrate from SNEDDSs for which *in vivo* data was available in the literature (Falavigna et al., 2020a; Michaelsen et al., 2019). However, while the above-mentioned combined models provided insightful information in the prediction of *in vivo* absorption data, for the most part they share the dependence from a pH-stat-titration apparatus to conduct the *in vitro* lipolysis step, thus limiting them to the availability of such laboratory equipment.

In light of the limitations connected to the already available combined *in vitro* models, the current study utilized the pH-stat-titration independent *in vitro* lipolysis model (*i.e.* the high-throughput (HTP) intestinal lipolysis model) developed by Mosgaard et al. (2015), in combination with the mucus-PVPA *in vitro* permeation model to study the performance of three fenofibrate-loaded SNEDDSs. Specifically, the HTP *in vitro* intestinal lipolysis model has previously shown to predict drug distribution between aqueous, oil and pellet phase during lipolysis of SNEDDSs in the same manner as the *in vitro* intestinal lipolysis model, while not being tied to a pH-stat-titration apparatus (Mosgaard et al., 2015, 2017). In fact, the high buffer capacity of the HTP intestinal medium is able to prevent the pH drop usually occurring after the release of free fatty acids from the digested SNEDDSs (Mosgaard et al., 2015), thus leading to a constant pH and eliminating the need for the pH-stat titrator. The mucus-PVPA barriers were chosen as the *in vitro* permeation model because of their ability to provide the combination of a biosimilar mucus layer with a permeation barrier, and as these barriers have previously proven to mimic the intestinal mucosa physiology (Falavigna et al., 2018, 2019). More specifically, the mucus-PVPA barriers allow the assessment of passive drug diffusion from their donor to the acceptor compartment similarly to other cell-free *in vitro* permeation tools used to assess intestinal drug permeation (*i.e.* PAMPA model (Kansy et al., 1998); Permeapad™ (di Cagno et al., 2015); AMI system (Berben et al., 2018)). The mentioned cell-free tools are not able to take into account the active and carrier-mediated transport occurring when a drug is being absorbed *in vivo*. However, even though an underestimation of active and carrier-mediated transport is a consequence of the mentioned tools, they provide a good estimation of *in vivo* passive drug diffusion, which is thought to be the predominant transport mechanism especially for lipophilic drugs (Dahlgren and Lennernäs, 2019).

The results obtained were compared to *in vivo* absorption data obtained by Michaelsen et al. (2019), where the same fenofibrate-loaded SNEDDSs were administered to rats, and for which no *in vivo-in vitro* correlation (IVIVC) was found when comparing the *in vivo* absorption data with *in vitro* lipolysis data. To evaluate if the model developed in the present study would predict the *in vivo* data collected by Michaelsen et al. (2019), the correlation between these *in vivo* data and the *in vitro* data obtained in the present study was evaluated.

2. Materials and methods

2.1. Materials

Acetonitrile CHROMANORM® (High-Performance Liquid Chromatography, HPLC, grade), ethanol NORMAPUR® 96%, v/v (HPLC grade), methanol CHROMANORM® (HPLC grade) were purchased from VWR (Radnor, PA, USA). Bile bovine, Bis-Tris, bovine serum albumin (BSA), 4-bromophenylboronic acid (BBBA), calcein, calcium chloride dihydrate ($CaCl_2 \cdot 2H_2O$), chloroform, cholesterol, dimethyl sulfoxide (DMSO), fenofibrate, hydrochloric acid (HCl), magnesium sulfate ($MgSO_4$), maleic acid, MES hydrate, mucin from porcine stomach type II, pancreatin from porcine pancreas, potassium phosphate monobasic, sodium chloride (NaCl), sodium hydroxide (NaOH), sodium phosphate dibasic dodecahydrate, soybean oil, Tween® 80, Trizma® base were products of Sigma-Aldrich (St. Louis, MO, USA). Ethanol 99.9% (v/v) was purchased from Arcus AS (Oslo, Norway). Kolliphor RH-40 was purchased from BASF (Ludwigshafen, Germany). Lipoid egg phospholipids E80 (80% phosphatidylcholine, PC) and Lipoid soybean lecithin S100 (>94% PC S100) were kindly gifted from Lipoid GmbH (Ludwigshafen, Germany), while Maisine CC was kindly donated from Gattefossé (St. Priest, France). Polyacrylic acid (Carbopol® 974 PNF, PAA) was obtained from Lubrizol (Brussels, Belgium). All chemicals employed were of analytical grade.

2.2. Methods

In this study, the mucus-PVPA barriers were used to assess the *in vitro* permeation of fenofibrate from three different SNEDDSs (*i.e.* super-SNEDDS solution$_{150}$, SNEDDS$_{75}$ and super-SNEDDS suspension$_{150}$) in the absence or presence of *in vitro* lipolysis utilizing the HTP *in vitro* intestinal lipolysis model. The results obtained from the *in vitro* lipolysis and permeation experiments were compared to *in vivo* plasma concentration of fenofibrate in rats after administration of the same SNEDDSs to assess the IVIVC between these sets of data.

2.2.1. Preparation of the mucus-PVPA barriers

2.2.1.1. Biosimilar mucus. Biosimilar mucus (BM) was prepared according to the method described by Boegh et al. (2014) and as described in Table 1. Specifically, PAA was dissolved in non-isotonic buffer (10 mM MES, 1.3 mM $CaCl_2$, 1.0 mM $MgSO_4$) and mucin was added and stirred until homogeneously dispersed. In parallel, a lipid mixture was prepared by mixing PC S100 lipids, cholesterol and Tween® 80 in

Table 1
Composition of biosimilar mucus (BM).

Components	Ratio (w/v) %
PAA	0.90
Mucin	5.00
Cholesterol	0.36
PC S100	0.18
Tween® 80	0.16
BSA	3.10

isotonic buffer (10 mM MES, 1.3 mM $CaCl_2$, 1.0 mM $MgSO_4$, 137 mM NaCl). Finally, the lipid mixture and BSA were added to the PAA mixture, and stirred until homogeneity was reached. The pH of the final mixture (BM) was adjusted to 6.5.

2.2.1.2. Mucus-PVPA barriers. The PVPA barriers were prepared following the method previously described (Falavigna et al., 2018, 2019). Briefly, liposomes with two different size distributions (0.4 and 0.8 μm) were immobilized by series of centrifugation and freeze-thawing on top of membrane filters (nitrocellulose, pore size 0.65 μm) fused on Transwell inserts (Corning Inc., New York, USA).

To produce the mucus-PVPA barriers, BM (50 μL) was deposited on top of the PVPA barriers 10 min prior to the start of the permeation experiment.

2.2.2. Preparation of high-throughput intestinal medium

The HTP intestinal medium was prepared according to the method described by Mosgaard et al. (2015), as illustrated in Table 2. Briefly, the HTP intestinal medium was prepared by weighing the components listed in Table 2 and dissolving them in MilliQ water. Finally, the pH of the HTP intestinal medium was adjusted to 6.5. Calcein (5 mM) was added to the HTP intestinal medium to determine its permeability across the mucus-PVPA barriers, and thus to assess their integrity (see Section 2.2.4.2).

2.2.3. Preparation of fenofibrate-loaded SNEDDSs

The fenofibrate-loaded SNEDDSs were prepared starting from a SNEDDS pre-concentrate according to the method described by Michaelsen et al. (2019). Briefly, the SNEDDS pre-concentrate was obtained by heating soybean oil, Maisine CC and Kolliphor RH-40 at 50 °C, and by mixing them in the following ratio: soybean oil-Maisine CC (1:1 w/w) 55% (w/w), Kolliphor RH-40 35% (w/w). Ethanol 99.9% (v/v) was added (10% (w/w)) once the mixture reached room temperature. The pre-concentrate was stirred until homogeneous at room temperature (23–25 °C).

Fenofibrate was added to the pre-concentrate to yield three different fenofibrate-loaded SNEDDSs, namely super-SNEDDS solution$_{150}$, SNEDDS$_{75}$ and super-SNEDDS suspension$_{150}$. SNEDDS$_{75}$ and super-SNEDDS suspension$_{150}$ were obtained by adding to the SNEDDS pre-concentrate an amount of fenofibrate corresponding to 75% and 150% of its equilibrium solubility, respectively (fenofibrate equilibrium solubility in the SNEDDS pre-concentrate: 88.5 mg/g (Thomas et al., 2014)). SNEDDS$_{75}$ and super-SNEDDS suspension$_{150}$ were left to stir at room temperature (23–25 °C) until homogeneity was reached. Fenofibrate was completely dissolved in the SNEDDS$_{75}$ (concentration lower than the equilibrium solubility), whereas for super-SNEDDS suspension$_{150}$ the drug was found both solubilized and in suspension (concentration higher than the equilibrium solubility). The super-SNEDDS solution$_{150}$ was obtained by dissolving an amount of fenofibrate corresponding to 150% of its equilibrium solubility to the SNEDDS pre-concentrate. To aid the complete solubilization of the drug in the pre-concentrate (*i.e.* avoid the formation of a suspension above the equilibrium solubility), the super-SNEDDS solution$_{150}$ was bath-sonicated for 30 min, heated at 60 °C for 3 h and then let cool down at 37 °C overnight.

Table 2
Composition HTP intestinal medium.

Components	Concentration (mM)
Bile bovine	2.96
PC S100	0.26
$CaCl_2 \cdot 2\ H_2O$	4.50
Bis-Tris	200

2.2.4. In vitro lipolysis-permeation experiment

This study focused on the development of a model where *in vitro* lipolysis and permeation could occur in parallel. The concomitant evaluation of drug distribution between aqueous and pellet phase during *in vitro* lipolysis and the assessment of drug permeation using the mucus-PVPA barriers was enabled by the use of HTP intestinal medium, which allowed the study to be independent from the pH-stat-titration apparatus typically used in the *in vitro* intestinal lipolysis model (Zangenberg et al., 2001). To account for the impact that lipolysis has on *in vitro* drug distribution and on *in vitro* drug permeation, fenofibrate distribution between the aqueous and pellet phase in the HTP intestinal medium and permeation across the mucus-PVPA barriers were evaluated both after dispersion of SNEDDSs in the HTP intestinal medium (*i.e.* absence of lipolysis) and after commencement of *in vitro* lipolysis. This evaluation allowed the comparison of the data obtained in the present study with the data obtained by Michaelsen et al. (2019), where *in vivo* absorption of fenofibrate was studied both while lipolysis had been inhibited by the co-administration of the pancreatic lipase inhibitor orlistat, and in the presence of lipolysis.

2.2.4.1. In vitro lipolysis. The three fenofibrate-loaded SNEDDSs (*i.e.* super-SNEDDS solution$_{150}$, SNEDDS$_{75}$ and super-SNEDDS suspension$_{150}$) were separately weighed in a beaker and dispersed in 26 mL of HTP intestinal medium (Table 2). The amount of SNEDDS (*i.e.* either super-SNEDDS solution$_{150}$, SNEDDS$_{75}$ or super-SNEDDS suspension$_{150}$) added to the beaker was chosen in order to obtain a final fenofibrate concentration of 480 μg/mL for all SNEDDSs and to have the same drug concentration as the one utilized in the *in vitro* lipolysis experiments performed by Michaelsen et al. (2019). The mixture was stirred at 37 °C for 20 min prior to the addition of the pancreatic lipase solution (4 mL) in the case of the presence of lipolysis, or of HTP intestinal medium (4 mL) in the case of sole dispersion (*i.e.* absence of lipolysis). To obtain the pancreatic lipase solution, the crude lipase extract was mixed with 5 mL of HTP intestinal medium in the absence of calcein, and the mixture was centrifuged for 7 min at 6500 × g. The supernatant (4 mL) was added to the beaker to initiate the lipolysis (final activity of 550 USP/mL). To simulate physiological temperature, the experiment was performed at 37 °C. Samples (1 mL), either utilized for the assessment of fenofibrate distribution in the aqueous phase or used for the permeation study, were taken out of the beaker after initial dispersion, after 30 min of additional dispersion or after 30 min from the initiation of lipolysis. This allowed to study both how the presence or absence of lipolysis affects the distribution of fenofibrate in the HTP intestinal medium on top of the mucus-PVPA barriers, and to evaluate the resulting drug permeation.

To study the distribution of fenofibrate between the aqueous and pellet phase before the start of lipolysis (*i.e.* 0 min) and after 30 min of dispersion/lipolysis, 5 μL of BBBA (1 M in MeOH) were added to the 1 mL sample to inhibit lipolysis. The inhibited samples (0 and 30 min) were exposed to centrifugation for 10 min at 19,000 × g to allow phase separation. The concentration of fenofibrate in the aqueous phase was quantified via HPLC after dilution in MeOH, and compared to the total amount of drug in the beaker. The quantification of fenofibrate was carried out via HPLC using a Waters 2690 Separation Module HPLC system, equipped with Waters 996 Photodiode Array Detector (Waters Corporation, Milford, MA, USA) and utilizing a Phenomenex Kinetix 5u XB-C18 100A column (100 × 4.6 mm; Phenomenex, Torrance, CA, USA). The drug was detected at a wavelength of 288 nm (retention time

~ 2.5 min) using a mobile phase composed of 20% MilliQ water and 80% of MeOH (flow 1 mL/min). The study of fenofibrate distribution in the different phases upon lipolysis was carried out in triplicate for each SNEDDS.

To confirm that the pH conditions were kept constant during dispersion/lipolysis by the buffering capacity of the HTP intestinal medium, the pH was monitored using a SensION^{TM} pH 31 pH meter (HACH, Dusseldorf, Germany). Moreover, the size of the SNEDDSs droplets after dispersion and after initiation of lipolysis was determined using a Malvern Zetasizer Nano ZS (Malvern, Oxford, UK). Samples were prepared by dispersing the SNEDDS pre-concentrate in HTP intestinal medium (concentration 1.45 mg/mL), and for the investigation on the effect of lipolysis on the droplet size, pancreatic lipase extract was added to the dispersion in order to obtain a final activity of 550 USP/mL. The operating conditions used for the size determination were the following: viscosity of the sample dispersant 0.8872 cP, temperature 25.0 °C, measurement angle 173 ° backscatter, cell type disposable cuvettes (DTS0012), number of measurements 3.

2.2.4.2. In vitro permeation. To study the permeation of fenofibrate from the different SNEDDSs, samples (1 mL) were taken out of the beaker before the start of lipolysis (*i.e.* sole dispersion, absence of lipolysis) and right after initiation of lipolysis (*i.e.* after the addition of the pancreatic extract), and were transferred (100 μL) on top of the mucus-PVPA barriers. The samples where lipolysis was initiated (100 μL) were transferred on top of the mucus-PVPA barriers without inhibiting lipolysis, thus allowing this process to continue on top of the barriers. The mucus-PVPA barriers were then placed in acceptor Transwell wells containing 600 μL of acceptor medium and the permeation experiment was carried out at 37 °C for a total of 6 h. DMSO 40 mg/mL in phosphate buffered saline (PBS) pH 7.4 was chosen as the acceptor medium to both simulate the pH conditions of the systemic blood circulation and to enable higher fenofibrate solubility compared to PBS pH 7.4 (Falavigna et al., 2020a). Higher fenofibrate solubility in the acceptor medium resulting from the presence of DMSO allows a higher amount of drug to permeate and this aids in the quantification of the permeated drug (Falavigna et al., 2020a). The barriers were moved to wells containing fresh acceptor medium after 2, 4 and 6 h to maintain sink conditions. At the end of the permeation experiment, samples (200 μL) from the acceptor compartments were taken out to quantify the amount of fenofibrate permeated over time.

As the previous assessment of the compatibility of the PVPA barriers with the components in the donor compartment showed that the presence of BM was essential for the correct functionality of the barriers (Falavigna et al., 2020a), BM was placed on top of the PVPA barriers in all of the permeation experiments. Moreover, in the present study, to assure the correct functionality of the mucus-PVPA barriers during the permeation experiment, an in-line assessment of barrier integrity was carried out in parallel to the fenofibrate permeation study. This evaluation was done by measuring the permeability of calcein contained in the HTP intestinal medium and the electrical resistance across the barriers at the end of the permeation study. To this regard, it has been demonstrated that high calcein permeability (>0.06 * 10^{-6} cm/s) and low electrical resistance (<290 Ohm * cm^2) indicate barrier impairment (Falavigna et al., 2018, 2019).

The quantification of fenofibrate was carried out at 288 nm using the spectrophotometer module of the Spark Multimode Microplate Reader (Tecan, Männendorf, Switzerland), while calcein was quantified using the spectrofluorometer module of the same apparatus at excitation wavelength of 485 nm and emission of 520 nm.

Calcein apparent permeability (*i.e.* P_{app}) was calculated following the equation:

$$P_{app}\left(\frac{cm}{s}\right) = \frac{dQ}{dt} * \frac{1}{A * Cd}$$

where dQ/dt is the flux at the steady state (nmol/s), A expresses the surface area of the PVPA barriers (0.33 cm^2) and C_d is the calcein concentration in the donor compartment at time zero (nmol/mL).

All permeability experiments were conducted using a total of 12 PVPA barriers.

2.2.5. In vivo-in vitro correlation

The areas under the curve (AUCs) resulting from the *in vivo* plasma concentration of fenofibrate in rats obtained by Michaelsen et al. (2019) for the three SNEDDSs (*i.e.* super-SNEDDS solution$_{150}$, SNEDDS$_{75}$ and super-SNEDDS suspension$_{150}$) were compared to the AUC resulting from either i) the *in vitro* dispersion/lipolysis described in Section 2.2.4.1, or ii) the *in vitro* permeation data described in Section 2.2.4.2. The *in vitro* dispersion/lipolysis/permeation AUC was calculated using GraphPad Prism 8.4.1 (GraphPad Software, San Diego, CA, USA) by utilizing a linear trapezoidal model from t = 0 to t = 30 min/6h. For the calculation of the AUC resulting from *in vitro* dispersion/lipolysis, the amount of fenofibrate found in the aqueous phase upon lipolysis over time was utilized. The AUCs of the *in vitro* permeation study was obtained from the mass transfer of fenofibrate permeated across the mucus-PVPA barriers over time. This comparison allowed to determine the IVIVC between the above-mentioned sets of data, and to study if the *in vitro* dispersion/lipolysis or combined dispersion/lipolysis/permeation data could predict *in vivo* drug absorption for the investigated SNEDDSs.

2.2.6. Statistical analysis

GraphPad Prism 8.4.1 (GraphPad Software, San Diego, CA, USA) was used for the statistical analysis of the results obtained in this study. One-way ANOVA was used to compare three or more sets of data, followed by Šidák *post hoc* test to determine significant difference between results ($p < 0.05$).

3. Results and discussion

In the present study, the need for a combined *in vitro* lipolysis-permeation model able to predict *in vivo* drug absorption from SNEDDSs was met by the combination of the HTP *in vitro* lipolysis model with the mucus-PVPA *in vitro* permeation model. In particular, the HTP *in vitro* lipolysis model allowed a simple and pH-stat-titration-independent evaluation of fenofibrate distribution in the aqueous and pellet phase after dispersion or lipolysis of three SNEDDSs, whereas the mucus-PVPA model allowed the evaluation of fenofibrate permeation. Finally, *in vitro* drug solubilization and drug permeation data were separately compared to *in vivo* absorption data present in the literature (Michaelsen et al., 2019) to assess the prediction potential of the experimental setups utilized in this study. The Level D correlation between *in vivo* and *in vitro* data was therefore determined since it is considered as a useful qualitative correlation that can be utilized during formulation development (Schen and Burgess, 2015).

3.1. Effect of in vitro lipolysis of SNEDDSs on fenofibrate distribution

The distribution of fenofibrate between the aqueous and pellet phase was studied after addition of the three SNEDDSs to the HTP intestinal medium both in the absence (*i.e.* sole dispersion) and presence of *in vitro* lipolysis for a total of 30 min. This investigation was carried out to estimate i) how much of the drug would be found in the aqueous phase over time (*i.e.* amount of drug potentially available for absorption) ii) which SNEDDS would result in a better drug solubilization upon dispersion/lipolysis and iii) how the presence of lipolysis affects the drug distribution between the aqueous and pellet phase compared to the absence of lipolysis. Moreover, the pH in the presence of *in vitro* lipolysis was measured to assure that the optimal pH condition for the activity of the pancreatic lipase would be maintained (*i.e.* pH ~ 6.5). In fact, the activity of the pancreatic enzyme has shown to induce the release of fatty acids upon digestion of SNEDDS, resulting in a decrease in pH and

thus inhibition of the lipolysis process (Zangenberg et al., 2001). To this regard, the HTP intestinal medium proved to be able to keep the pH around 6.48 ± 0.03 thanks to its high buffer capacity throughout all *in vitro* lipolysis experiments, in accordance with the results from Mosgaard et al. (2015). This pH condition was also kept in the absence of lipolysis, thus enabling the comparison between the drug distribution in the presence and absence of lipolysis.

As can be observed in Fig. 1, both in the absence (Fig. 1A) and presence (Fig. 1B) of lipolysis, $SNEDDS_{75}$ was able to maintain most of the drug solubilized in the aqueous phase during 30 min of dispersion/lipolysis. However, for both super-$SNEDDS\ solution_{150}$ and super-$SNEDDS\ suspension_{150}$ the absence and presence of lipolysis both caused precipitation of the drug, thus increasing the amount found in the pellet phase. The same trend has previously been observed, where super-$SNEDDS\ solution_{150}$ caused higher fenofibrate precipitation over time than $SNEDDS_{75}$ and lower precipitation than super-$SNEDDS\ suspension_{150}$ (Falavigna et al., 2020a). Notably, in the presence of lipolysis drug precipitation occurred to a greater extent from 0 to 30 min in the case of super-$SNEDDS\ solution_{150}$ compared to super-$SNEDDS\ suspension_{150}$ (Fig. 1B). In fact, a modest change in precipitation was observed for super-$SNEDDS\ suspension_{150}$, while for super-$SNEDDS\ solution_{150}$ this change was more drastic, most likely due to the instability of the supersaturated system resulting from this formulation.

While drug precipitation in the pellet phase significantly increased over time ($p < 0.05$) in the presence of lipolysis (Fig. 1B) for super-$SNEDDS\ solution_{150}$ and super-$SNEDDS\ suspension_{150}$, after 30 min of dispersion (*i.e.* absence of lipolysis) the amount of drug found in the pellet phase was the same as at the start of the experiment (Fig. 1A). This trend was also found in the study by Michaelsen et al. (2019), where fenofibrate distribution between the aqueous and pellet phase of the same SNEDDSs was evaluated in two conditions, i) inhibition of dynamic *in vitro* lipolysis by the use of the pancreatic lipase inhibitor orlistat and ii) the presence of dynamic *in vitro* intestinal lipolysis. Further, the precipitation of fenofibrate remained constant in the presence of the pancreatic lipase inhibitor, whereas in its absence (*i.e.* active lipolysis) drug precipitation increased over time for super-$SNEDDS\ solution_{150}$ and super-$SNEDDS\ suspension_{150}$ (Michaelsen et al., 2019). The increase in drug precipitation upon *in vitro* lipolysis is to be expected as the addition of the pancreatic lipase can induce the formation of different colloidal structures (*i.e.* micelles and vesicles) which are able to solubilize the incorporated drug to a different extent compared to the nanoemulsion droplets of the SNEDDSs obtained after dispersion in the HTP intestinal medium (Mosgaard et al., 2015). To this regard, the size of the SNEDDSs droplets was determined after dispersion and after initiation of lipolysis. The results showed that the SNEDDSs diameter after dispersion was around 50.89 ± 1.09 nm with a polydispersity index of 0.38, suggesting a rather monodispersed size distribution, whereas after initiation of lipolysis it was not possible to determine the size of the SNEDDSs due to a highly polydispersed size population (polydispersity index > 0.8), suggesting the formation of structures with various sizes upon the initiation of lipolysis. The structural changes in the colloidal species formed after dispersion compared to after lipolysis could have an effect on drug precipitation, and could be the underlying cause for the differences in drug solubilization shown in Fig. 1.

The results discussed thus far confirm the correct functionality of the HTP intestinal medium in maintaining the desired pH condition for the *in vitro* lipolysis process, and highlight the similarity of the obtained results with already published data. The use of the HTP intestinal medium eliminates the need for the pH-stat-titration typically used in the *in vitro* intestinal lipolysis method, resulting in a simpler and less apparatus-dependent model.

3.2. *In vitro permeation of fenofibrate*

The permeation of fenofibrate across the mucus-PVPA barriers was determined both in the absence (*i.e.* sole dispersion) and presence of lipolysis to determine i) which SNEDDS would enable the highest drug mass transfer across the barriers and ii) whether the presence of lipolysis would cause a change in mass transfer compared to its absence. In parallel to the estimation of fenofibrate mass transfer, an in-line assessment of barrier integrity was carried out by measuring the permeability of the highly hydrophilic marker calcein and by determining the electrical resistance across the mucus-PVPA barriers at the end of the permeation experiment. As can be observed in Table 3, the barriers maintained their integrity in all of the tested conditions, as values of calcein P_{app} and electrical resistance were within the limits previously associated to barrier integrity (*i.e.* calcein $P_{app} < 0.06 \cdot 10^{-6}$ cm/s and electrical resistance >290 Ohm · cm^2 (Falavigna et al., 2018))

In terms of fenofibrate mass transfer across the mucus-PVPA barrier, both in the absence (Fig. 2A) and presence (Fig. 2B) of lipolysis, super-$SNEDDS\ solution_{150}$ exhibited the highest fenofibrate mass transfer, suggesting that this formulation would lead to the highest bioavailability in both cases. Instead, for $SNEDDS_{75}$ and super-$SNEDDS\ suspension_{150}$ the ranking was different according to the absence or

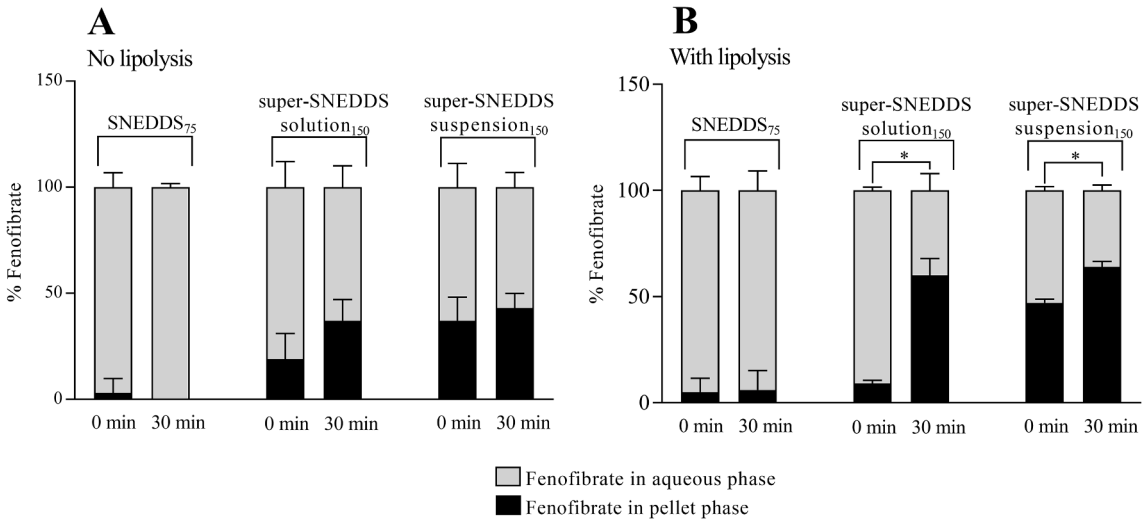

Fig. 1. Fenofibrate (%) present in the pellet (black) and aqueous phase (grey) over time A) in the absence of lipolysis (*i.e.* sole dispersion) and B) with lipolysis for $SNEDDS_{75}$, super-$SNEDDS\ solution_{150}$ and super-$SNEDDS\ suspension_{150}$. (Mean ± SD; n = 3). * Statistically significant ($p < 0.05$) difference between the percentages of fenofibrate in the aqueous phase after 0 min compared to 30 min.

Table 3
Calcein P_{app} and the electrical resistance across the mucus-PVPA barriers during dispersion/lipolysis-permeation experiments. (Mean ± SD; n = 12).

	SNEDDS	Calcein P_{app} (10^{-6} cm/s)	Electrical resistance (Ω cm^2)
No lipolysis (dispersion)	Super-SNEDDS solution$_{150}$	0.050 ± 0.017	422 ± 22
	SNEDDS$_{75}$	0.055 ± 0.002	373 ± 8
	Super-SNEDDS suspension$_{150}$	0.057 ± 0.011	450 ± 3
With lipolysis	Super-SNEDDS solution$_{150}$	0.023 ± 0.005	562 ± 37
	SNEDDS$_{75}$	0.027 ± 0.001	541 ± 5
	Super-SNEDDS suspension$_{150}$	0.018 ± 0.004	818 ± 112

presence of lipolysis; in fact, super-SNEDDS suspension$_{150}$ promoted a significantly higher mass transfer of fenofibrate in the absence of lipolysis compared to SNEDDS$_{75}$, whereas in its presence SNEDDS$_{75}$ and super-SNEDDS suspension$_{150}$ led to a similar drug permeation across the mucus-PVPA barriers (Fig. 2).

The change in ranking in terms of fenofibrate plasma concentration was also observed by Michaelsen et al. (2019), where the same SNEDDSs were administered to rats both in the presence of lipolysis and after this process was inhibited by the co-administration of the pancreatic lipase inhibitor orlistat. The authors found that the absorption of fenofibrate from super-SNEDDS suspension$_{150}$ significantly increased when orlistat was present. Regarding this, it was suggested that when lipolysis is inhibited, the SNEDDS nano-emulsion droplets remain present in the GI tract, providing constant solubilization of the drug and aid in the drug absorption process while avoiding further precipitation (Michaelsen et al., 2019). The positive effect of the absence of lipolysis on drug solubilization can also be observed in Fig. 1A, where fenofibrate precipitation did not increase over time in the absence of lipolysis, whereas when this process was initiated, drug precipitation increased (Fig. 1B). Therefore, in the case of the super-SNEDDS suspension$_{150}$ for both this study and the one from Michaelsen et al. (2019) the inhibition of lipolysis maintained fenofibrate solubilized for a longer time. However, it has to be noted that the drug found in the aqueous phase is present as both solubilized in the SNEDDS nano-emulsion droplets/in the colloidal structures formed upon lipolysis and free in solution. The ability to keep the drug free in solution promotes drug permeation, as only this fraction is able to cross the permeation barrier (Keemink and Bergström, 2018). In the current study, a difference in drug transfer between the absence and presence of lipolysis was also observed for SNEDDS$_{75}$, where drug permeation was found to be higher in the presence of lipolysis. In contrast to the super-SNEDDS suspension$_{150}$, where fenofibrate is present both as a precipitate and solubilized in the SNEDDS, the SNEDDS$_{75}$ has all the drug completely solubilized in the nano-emulsion droplets. Thus, when SNEDDS$_{75}$ is dispersed in the HTP intestinal medium most of the drug is possibly solubilized in the SNEDDS, rather than free in solution. The formation of different colloidal structures upon *in vitro* lipolysis can shift the equilibrium of the drug towards the fraction free in solution, translating to higher fenofibrate permeation in the presence of lipolysis. The increase in fenofibrate permeation in the presence of lipolysis for SNEDDS$_{75}$ was not observed in the previous study (Falavigna et al., 2020a), as it was found that SNEDDS$_{75}$ had similar fenofibrate permeation both in the absence and presence of lipolysis. Differences in fenofibrate permeation between published data and the results collected in the present study could be due to the different compositions of the utilized simulated intestinal fluids. In fact, in the case of HTP intestinal medium, the high concentration of Bis-Tris might affect i) the droplet size of the SNEDDSs and of the colloidal structures forming upon lipolysis, ii) the drug equilibrium between the fraction free in solution and the one solubilized by the SNEDDS and iii) the extent and nature of drug precipitate, thus possibly leading to a change in drug permeation. Moreover, it has to be noted that drug solubilization in SNEDDSs in the absence of drug supersaturation or precipitation can reduce the drug thermodynamic activity (Yeap et al., 2013), and it has been demonstrated that drug solubilization in SNEDDSs does not lead to higher drug absorption if the free drug concentration does not increase, despite the rise in total solubilized drug (Yeap et al., 2013). On the other hand, drug supersaturation can result in an increase in thermodynamic activity and instability, possibly resulting in drug precipitation (Tanaka et al., 2020), as suggested by the results described in Section 3.1 with regards to super-SNEDDS solution$_{150}$ and super-SNEDDS suspension$_{150}$ (Fig. 1). However, drug precipitation caused by the thermodynamic instability of a supersaturated state does not necessarily translate to lower drug absorption, as the solid state of the precipitate could re-dissolve and thus lead to high absorption (Tanaka et al., 2020). However, to confirm the hypothesis that fenofibrate could re-dissolve from its precipitated state and to identify the mechanisms behind this process, further characterization of the drug and SNEDDSs would be needed.

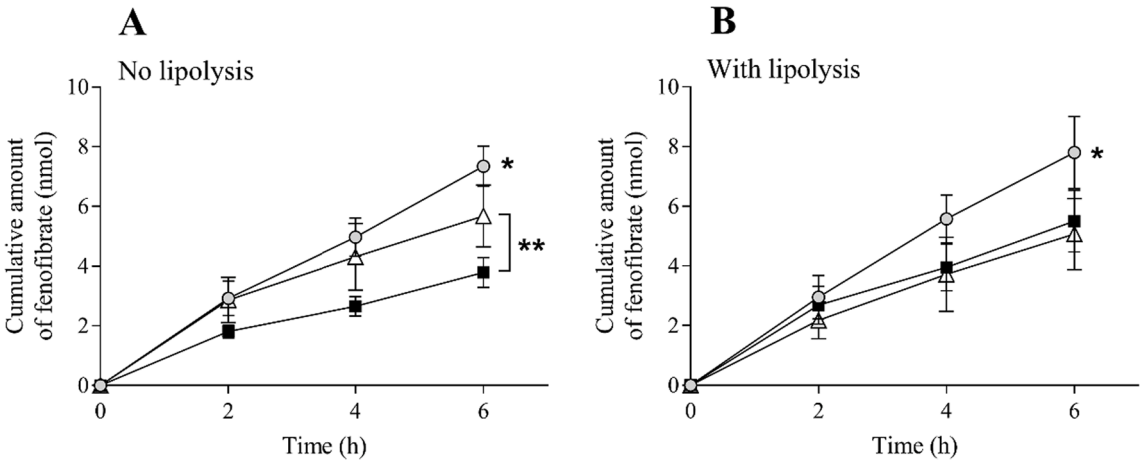

Fig. 2. Fenofibrate permeated across the mucus-PVPA barriers (cumulative amount) from super-SNEDDS solution$_{150}$ (grey circle), SNEDDS$_{75}$ (black square) and super-SNEDDS suspension$_{150}$ (white triangle) A) in the absence of lipolysis and B) with lipolysis. (Mean ± SD; n = 12). *Statistically significant ($p < 0.05$) difference between the amount of fenofibrate permeated from super-SNEDDS solution$_{150}$ and from super-SNEDDS suspension$_{150}$ and SNEDDS$_{75}$. **Statistically significant ($p < 0.05$) difference between the amount of fenofibrate permeated from super-SNEDDS suspension$_{150}$ and SNEDDS$_{75}$.

3.3. In vivo-in vitro correlation

The results obtained in this study and described in Section 3.1 and 3.2 were compared to the ones obtained by Michaelsen et al. (2019), where the same SNEDDSs were utilized to study fenofibrate absorption in rats. In particular, the AUCs resulting from the *in vivo* study, where lipolysis was either inhibited (−) by presence of orlistat or taking place (+) (AUC $_{in\ vivo,\ -/+\ lipolysis}$), were compared to the AUCs resulting from the amount of drug found in the aqueous phase after *in vitro* dispersion (−) or lipolysis (+) over time (AUC $_{in\ vitro,\ -/+\ lipolysis}$). The same *in vivo* data was also compared to the AUCs calculated from the fenofibrate mass transfer after *in vitro* permeation in the absence (−) or presence (+) of lipolysis using the mucus-PVPA barriers (AUC $_{in\ vitro\ permeation,\ -/+\ lipolysis}$) (Table 4). Moreover, the statistical difference in AUC between absence and presence of lipolysis for both *in vivo* and *in vitro* results was evaluated (Table 4), and the IVIVC between these sets of data were determined (Fig. 3 and Fig. 4).

3.3.1. Correlation with in vitro drug solubilization upon dispersion/lipolysis

As can be observed in Fig. 3 and Table 4, the *in vitro* solubilization data (AUC $_{0–0.5h,\ -/+\ lipolysis}$) failed to correlate with *in vivo* plasma concentration in rats both in the absence and presence of lipolysis. In fact, the prediction of drug absorption *via* the evaluation of drug found in the aqueous phase during dispersion/lipolysis does not take into account that the fenofibrate present in the aqueous phase is in a dynamic equilibrium between its fraction freely dissolved in the luminal contents and the fraction solubilized by the SNEDDS colloidal structures formed upon lipolysis. Therefore, the drug in the aqueous phase is an overestimation of the amount of drug freely solubilized and thus available for permeation (Michaelsen et al., 2019). This was clearly evident when $SNEDDS_{75}$ was evaluated. In fact, according to the drug distribution in the aqueous and pellet phase after dispersion/lipolysis (AUC $_{0–0.5h,\ -/+\ lipolysis}$), $SNEDDS_{75}$ is the one where most of the drug is found in the aqueous phase (Fig. 1, Table 4), whereas *in vivo* the corresponding AUC is lower than for the super-SNEDDS $solution_{150}$. The difference in the ranking between the *in vitro* dispersion/lipolysis and *in vivo* plasma concentration data can be ascribed to the above-mentioned lack of distinction between the freely solubilized drug and the drug in the colloidal structures, and also to the lack of an absorption step. In fact, Bevernage et al. (2012) have evaluated the influence of an absorption step on supersaturation and precipitation of a poorly water-soluble drug, and found that precipitation from a supersaturated system can be suppressed by the escape of the drug *via* the absorption sink, thus averting the system from reaching a critical degree of supersaturation and the start of precipitation. Thus, the results described in the study by Bevernage et al. (2012) suggest that precipitation kinetics change when supersaturated drugs have the chance of permeating instead of precipitating, and that the shift towards drug permeation instead of precipitation increases with increasing degrees of supersaturation.

Table 4
Area under the curve (AUC) resulting from fenofibrate absorption from *in vivo* studies in rats in the absence (−) or presence (+) of lipolysis [26] (*in vivo* $AUC_{0–30h,\ -/+\ lipolysis}$), AUC from drug solubilization without (−) and with (+) *in vitro* lipolysis (*i.e.* amount of drug found in the aqueous phase; *in vitro* AUC $_{0–0.5h,\ -/+\ lipolysis}$) and mass transfer of fenofibrate permeated across the mucus-PVPA barriers without (−) or with (+) lipolysis (*in vitro* $AUC_{0–6h\ permeation,\ -/+\ lipolysis}$) from super-SNEDDS $solution_{150}$, $SNEDDS_{75}$ and super-SNEDDS $suspension_{150}$. (Mean ± SEM; n = 6).

	Super-SNEDDS $solution_{150}$	$SNEDDS_{75}$	Super-SNEDDS $suspension_{150}$
In vivo $AUC_{0–30h,\ -\ lipolysis}$ (μg·h/mL)	136.9 ± 27.5	66.3 ± 14.9	108.9 ± 39.5
In vivo $AUC_{0–30h,\ +\ lipolysis}$ (μg·h/mL)	148.0 ± 47.5	88.3 ± 20.9	58.1 ± 16.9
In vitro AUC $_{0–0.5h,\ -\ lipolysis}$ (min·%)	2160.0 ± 235.8	2985.0 ± 105.4	1800.0 ± 197.1
In vitro AUC $_{0–0.5h,\ +\ lipolysis}$ (min·%)	1965.0 ± 121.5	2835.0 ± 168.5	1335.0 ± 46.1
In vitro $AUC_{0–6h\ permeation,\ -\ lipolysis}$ (nmol·h)	23.0 ± 1.4	13.0 ± 0.8	20.0 ± 2.2
In vitro $AUC_{0–6h\ permeation,\ +\ lipolysis}$ (nmol·h)	25.0 ± 2.0	19.0 ± 1.8	17.0 ± 2.3

3.3.2. Correlation with in vitro drug permeation

The results depicted in Fig. 4, where the AUCs resulting from the *in vitro* permeation of fenofibrate ($AUC_{0–6h\ permeation,\ -/+\ lipolysis}$) were plotted against the *in vivo* drug absorption data ($AUC_{0–30h,\ -/+\ lipolysis}$), are proof of the importance of the absorption step in *in vitro* models evaluating lipid-based formulations, (Fig. 4). In fact, an excellent IVIVC ($R^2 > 0.98$) was found when comparing the *in vitro* drug permeation in the absence or presence of lipolysis with *in vivo* data where lipolysis was either inhibited (*i.e.* use of orlistat) or taking place. The lack of IVIVC using *in vitro* drug distribution data from the dispersion/lipolysis experiments alone (AUC $_{0–0.5h,\ -/+\ lipolysis}$) (Fig. 3) compared to the good correlation obtained using the *in vitro* permeation data following dispersion/permeation (Fig. 4) suggests that the intrinsic solubilization of SNEDDSs does not dictate the degree of drug absorption, whereas the propensity of SNEDDSs to promote supersaturation seems to be more important (Yeap et al., 2013).

Moreover, the presence of the mucus layer on top of the mucosa of the small intestine has been suggested to play an important role in stabilizing drug supersaturation. In fact, it has been found that mucin and pig intestinal mucus were both able to delay precipitation during supersaturation-permeation experiments for two PWSD (Yeap et al., 2019). It has been proposed that the mechanisms enabling the stabilization of supersaturation exerted by the mucus layer were drug-specific. In particular, it has been shown that the presence of mucin and pig intestinal mucus delayed carvedilol and piroxicam precipitation, and that the absorption of carvedilol from a supersaturated solution was higher across mucus-producing co-culture of Caco-2 cell-layers compared to non-mucus-producing ones (Yeap et al., 2019). Therefore, the absence of biosimilar mucus in the HTP dispersion/lipolysis setup (Section 3.1) could be another reason why the *in vitro* lipolysis evaluation did not correlate with *in vivo* data, as the stabilization of drug supersaturation could not be carried out by the mucus layer. During the *in vitro* permeation experiments, on the other hand, the biosimilar mucus layer lining the PVPA barriers possibly enabled the maintenance of fenofibrate supersaturation by delaying drug precipitation, and thus leading to higher mass transfer for those formulations providing a supersaturated fenofibrate concentration (*i.e.* super-SNEDDS $solution_{150}$ and super-SNEDDS $suspension_{150}$). The good IVIVC obtained using the mucus-PVPA model (Fig. 4) together with the results described by Yeap et al. (2019) highlight the importance of having a mucus layer lining the permeation barrier when studying the permeation of supersaturated PWSD. This is especially relevant as the supersaturation stabilization process could be seen as an intrinsic mechanism of action for lipid-based formulations, and it should thus be taken into consideration in the development of novel drug delivery systems.

Overall, the results presented in this study underline the complexity of the processes affecting the performance of SNEDDSs *in vivo,* and emphasize that drug solubilization, supersaturation, precipitation and permeation all coexist in a dynamic equilibrium that drives drug absorption. This could be simulated with the use of an appropriate *in vitro* model as the one presented in this work. Further studies assessing a broader selection of drugs and formulations need to be performed to investigate the full potential of the combined *in vitro* model developed in this study. At this stage, this appears to be a very promising approach to estimate *in vivo* performance of lipid-based formulations, and as such a highly valuable tool in the development and optimization of this type of formulations.

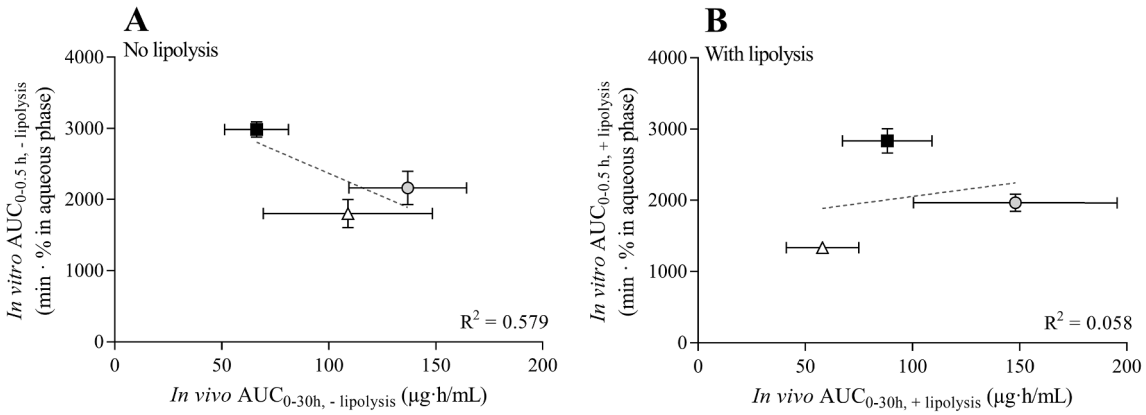

Fig. 3. IVIVC between *in vivo* plasma exposure (Michaelsen et al., 2019) and *in vitro* fenofibrate solubilization (*i.e.* amount of drug in the aqueous phase) of super-SNEDDS solution$_{150}$ (grey circle), SNEDDS$_{75}$ (black square) and super-SNEDDS suspension$_{150}$ (white triangle) A) in the absence (−) of lipolysis and B) with (+) lipolysis.

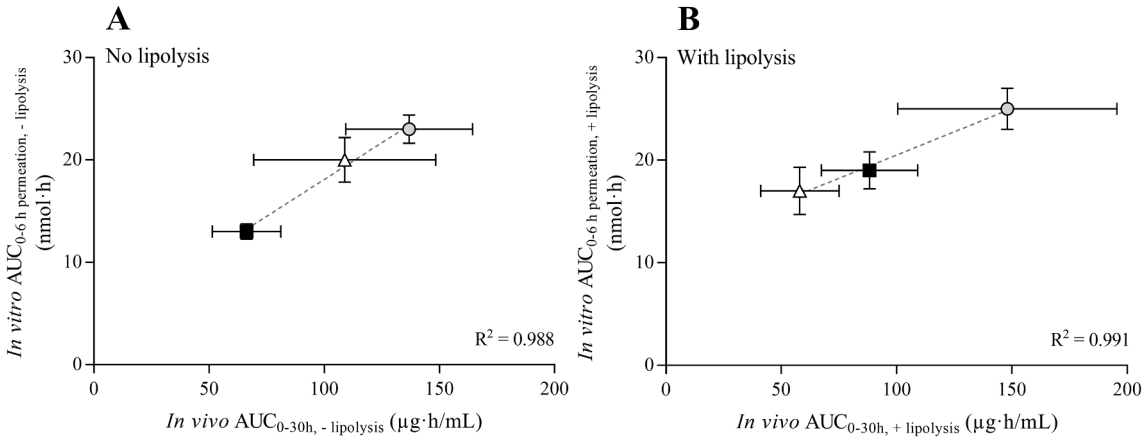

Fig. 4. IVIVC between *in vivo* plasma exposure (Michaelsen et al., 2019) and *in vitro* fenofibrate permeation across the mucus-PVPA barriers A) in the absence (−) of lipolysis and B) with (+) lipolysis from super-SNEDDS solution$_{150}$ (grey circle), SNEDDS$_{75}$ (black square) and super-SNEDDS suspension$_{150}$ (white triangle).

4. Conclusion

The obtained results demonstrate that the present study succeeded in the development of a combined *in vitro* lipolysis-permeation model able to predict *in vivo* drug absorption from the investigated SNEDDSs. The typical *in vitro* intestinal lipolysis model was substituted with the HTP *in vitro* lipolysis model to allow the use of a pH-stat-titration-independent system and permit the simultaneous investigation of *in vitro* lipolysis and permeation. While no correlation was found when comparing the amount of drug solubilized in the aqueous phase upon *in vitro* dispersion/lipolysis with the *in vivo* literature data (Michaelsen et al., 2019) ($R^2 < 0.58$), the addition of an *in vitro* permeation step using the mucus-PVPA barriers led to excellent IVIVCs ($R^2 > 0.98$). Also, the difference in fenofibrate *in vivo* absorption between the presence and absence of lipolysis could be accurately predicted by the combined *in vitro* model. Herewith, the evidence gathered in this study suggests that the evaluation of *in vitro* drug distribution alone cannot predict drug plasma concentration *in vivo*, while the combination with *in vitro* drug permeation assessed with the use of the mucus-PVPA model is able to do so to a higher extent. The combined *in vitro* model presented in this study could thus be a highly valuable tool in the development and optimization of novel lipid-based formulations.

CRediT authorship contribution statement

Margherita Falavigna: Conceptualization, Methodology, Data curation, Formal analysis, Validation, Writing - original draft, Visualization, Supervision, Writing - review & editing, Project administration. **Sunniva Brurok:** Methodology, Data curation, Formal analysis, Validation, Investigation, Writing - review & editing. **Mette Klitgaard:** Conceptualization. **Gøril Eide Flaten:** Conceptualization, Supervision.

Declaration of Competing Interest

The authors declare that they have no known competing financial interests or personal relationships that could have appeared to influence the work reported in this paper.

Acknowledgements

The authors thank UiT The Arctic University of Norway for funding PhD student Margherita Falavigna and Lipoid GmbH (Ludwigshafen, Germany) for the donation of phospholipids. NordicPOP (supported by NordForsk for the Nordic University Hub project number: 85352), and COST Action UNGAP (supported by the European Cooperation in Science and Technology; project number: 16205) are highly acknowledged for enabling fruitful collaboration.

Funding

This research did not receive any specific grant from funding agencies in the public, commercial, or not-for-profit sectors.

References

Alskär, L.C., Parrow, A., Keemink, J., Johansson, P., Abrahamsson, B., Bergström, C.A.S., 2019. Effect of lipids on absorption of carvedilol in dogs: is coadministration of lipids as efficient as a lipid-based formulation? J. Control. Release 304, 90–100. https://doi.org/10.1016/j.jconrel.2019.04.038.

Artursson, P., Palm, K., Luthman, K., 2001. Caco-2 monolayers in experimental and theoretical predictions of drug transport. Adv. Drug Deliv. Rev. 46, 27–43. https://doi.org/10.1016/s0169-409x(00)00128-9.

Berben, P., Brouwers, J., Augustijns, P., 2018. Assessment of passive intestinal permeability using an artificial membrane insert system. J. Pharm. Sci. 107, 250–256. https://doi.org/10.1016/j.xphs.2017.08.002.

Berthelsen, R., Klitgaard, M., Rades, T., Müllertz, A., 2019. In vitro digestion models to evaluate lipid based drug delivery systems; present status and current trends. Adv. Drug Deliv. Rev. 142, 35–49. https://doi.org/10.1016/j.addr.2019.06.010.

Bevernage, J., Brouwers, J., Annaert, P., Augustijns, P., 2012. Drug precipitation–permeation interplay: Supersaturation in an absorptive environment. Eur. J. Pharm. Biopharm. 82, 424–428. https://doi.org/10.1016/j.ejpb.2012.07.009.

Bibi, H.A., Holm, R., Bauer-Brandl, A., 2017. Simultaneous lipolysis/permeation in vitro model, for the estimation of bioavailability of lipid based drug delivery systems. Eur. J. Pharm. Biopharm. 117, 300–307. https://doi.org/10.1016/j.ejpb.2017.05.001.

Boegh, M., Baldursdóttir, S.G., Müllertz, A., Nielsen, H.M., 2014. Property profiling of biosimilar mucus in a novel mucus-containing in vitro model for assessment of intestinal drug absorption. Eur. J. Pharm. Biopharm. 87, 227–235. https://doi.org/10.1016/j.ejpb.2014.01.001.

Dahlgren, D., Lennernäs, H., 2019. Intestinal permeability and drug absorption: predictive experimental, computational and in vivo approaches. Pharmaceutics 11 (8), 411. https://doi.org/10.3390/pharmaceutics11080411.

di Cagno, M., Bibi, H.A., Bauer-Brandl, A., 2015. New biomimetic Permeapad™ for efficient investigation of passive permeability of drugs. Eur. J. Pharm. Sci. 73, 29–34. https://doi.org/10.1016/j.ejps.2015.03.019.

Falavigna, M., Klitgaard, M., Berthelsen, R., Müllertz, A., Flaten, G.E., 2020a. Predicting oral absorption of fenofibrate in lipid-based drug delivery systems by combining in vitro lipolysis with the mucus-PVPA permeability model. J. Pharm. Sci. https://doi.org/10.1016/j.xphs.2020.08.026.

Falavigna, M., Klitgaard, M., Brase, C., Ternullo, S., Skalko-Basnet, N., Flaten, G.E., 2018. Mucus-PVPA (mucus phospholipid vesicle-based permeation assay): an artificial permeability tool for drug screening and formulation development. Int. J. Pharm. 537, 213–222. https://doi.org/10.1016/j.ijpharm.2017.12.038.

Falavigna, M., Klitgaard, M., Steene, E., Flaten, G.E., 2019. Mimicking regional and fasted/fed state conditions in the intestine with the mucus-PVPA in vitro model: the impact of pH and simulated intestinal fluids on drug permeability. Eur. J. Pharm. Sci. 132, 44–54. https://doi.org/10.1016/j.ejps.2019.02.035.

Falavigna, M., Stein, P.C., Flaten, G.E., Pio di Cagno, M., 2020b. Impact of mucin on drug diffusion: development of a straightforward in vitro method for the determination of drug diffusivity in the presence of mucin. Pharmaceutics 12 (168), 1–13. https://doi.org/10.3390/pharmaceutics12020168.

Feeney, O.M., Crum, M.F., McEvoy, C.L., Trevaskis, N.L., Williams, H.D., Pouton, C.W., Charman, W.N., Bergström, C.A.S., Porter, C.J.H., 2016. 50 years of oral lipid-based formulations: provenance, progress and future perspectives. Adv. Drug Deliv. Rev. 101, 167–194. https://doi.org/10.1016/j.addr.2016.04.007.

Flaten, G.E., Dhanikula, A.B., Luthman, K., Brandl, M., 2006. Drug permeability across a phospholipid vesicle barrier: a novel approach for studying passive diffusion. Eur. J. Pharm. Sci. 27, 80–90. https://doi.org/10.1016/j.ejps.2005.08.007.

Gao, P., Morozowich, W., 2006. Development of supersaturatable self-emulsifying drug delivery system formulations for improving the oral absorption of poorly soluble drugs. Exp. Opin. Drug Deliv. 3 (1), 97–110. https://doi.org/10.1517/17425247.3.1.97.

Hedge, O.J., Bergström, C.A.S., 2020. Suitability of ArtificialMembranes in lipolysis-permeation assays of oral lipid-based formulations. Pharm. Res. 37, 99. https://doi.org/10.1007/s11095-020-02833-9.

Ille, A.R., Griffin, B.T., Brandl, M., Bauer-Brandl, A., Jacobsen, A.C., Vertzoni, M., Kuentz, M., Kolakovic, R., Holm, R., 2020. Exploring impact of supersaturated lipid-based drug delivery systems of celecoxib on in vitro permeation across Permeapad® membrane and in vivo absorption. Eur. J. Pharm. Sci. 152, 105452. https://doi.org/10.1016/j.ejps.2020.105452.

Kansy, M., Senner, F., Gubernator, K., 1998. Physicochemical high throughput screening: parallel artificial membrane permeation assay in the description of passive absorption processes. J. Med. Chem. 41, 1007–1010. https://doi.org/10.1021/jm970530e.

Keemink, J., Bergström, C.A.S., 2018. Caco-2 cell conditions enabling studies of drug absorption from digestible lipid-based formulations. Pharm. Res. 35, 74. https://doi.org/10.1007/s11095-017-2327-8.

Keemink, J., Mårtensson, E., Bergström, C.A.S., 2019. Lipolysis-Permeation setup for simultaneous study of digestion and absorption in vitro. Mol. Pharm. 16, 921–930. https://doi.org/10.1021/acs.molpharmaceut.8b00811.

Lechanteur, A., das Neves J, Sarmento B., 2018. The role of mucus in cell-based models used to screen mucosal drug delivery. Adv. Drug Deliv. Rev. 124, 50–63. https://doi.org/10.1016/j.addr.2017.07.019.

Lin, L., Wong, H., 2017. Predicting oral drug absorption: mini review on physiologically-based pharmacokinetic models. Pharmaceutics 9 (41), 1–14. https://doi.org/10.3390/pharmaceutics9040041.

Michaelsen, M.H., Siqueira Jørgensen, S.D., Abdi, I.M., Wasan, K.M., Rades, T., Müllertz, A., 2019. Fenofibrate oral absorption from SNEDDS and super-SNEDDS is not significantly affected by lipase inhibition in rats. Eur. J. Pharm. Biopharm. 142, 258–264. https://doi.org/10.1016/j.ejpb.2019.07.002.

Miyazaki, K., Kishimoto, H., Muratani, M., Kobayashi, H., Shirasaka, Y., Inoue, K., 2019. Mucins are involved in the intestinal permeation of lipophilic drugs in the proximal region of rat small intestine. Pharm. Res. 36 (162), 1–11. https://doi.org/10.1007/s11095-019-2701-9.

Mosgaard, M.D., Sassene, P., Mu, H., Rades, T., Müllertz, A., 2015. Development of a high-throughput in vitro intestinal lipolysis model for rapid screening of lipid-based drug delivery systems. Eur. J. Pharm. Biopharm. 94, 493–500. https://doi.org/10.1016/j.ejpb.2015.06.028.

Mosgaard, M.D., Sassene, P.J., Mu, H., Rades, T., Müllertz, A., 2017. High-throughput lipolysis in 96-well plates for rapid screening of lipid-based drug delivery systems. J. Pharm. Sci. 106, 1183–1186. https://doi.org/10.1016/j.xphs.2016.12.026.

O'Dwyer, P.J., Box, K.J., Koehl, N.J., Bennett-Lenane, H., Reppas, C., Holm, R., Kuentz, M., Griffin, B.T., 2020. Novel biphasic lipolysis method to predict in vivo performance of lipid-based formulations. Mol. Pharm. 17, 3342–3352. https://doi.org/10.1021/acs.molpharmaceut.0c00427.

Porter, C.J.H., Trevaskis, N.L., Charman, W.N., 2007. Lipids and lipid-based formulations: optimizing the oral delivery of lipophilic drugs. Nat. Rev. Drug Discov. 6 (3), 231–248. https://doi.org/10.1038/nrd2197.

Savla, R., Browne, J., Plassat, V., Wasan, K.M., Wasan, E.K., 2017. Review and analysis of FDA approved drugs using lipid-based formulations. Drug Develop. Ind. Pharm. 43, 1743–1758. https://doi.org/10.1080/03639045.2017.1342654.

Schen, J.S., Burgess, D.J., 2015. In vitro-in vivo correlation for complex non-oral drug products: where do we stand? J. Control. Release 219, 644–651. https://doi.org/10.1016/j.jconrel.2015.09.052.

Siqueira, S.D.V.S., Müllertz, A., Gräeser, K., Kasten, G., Mu, H., Rades, T., 2017. Influence of drug load and physical form of cinnarizine in new SNEDDS dosing regimens: in vivo and in vitro evaluations. AAPS J. 19 (2), 587–594. https://doi.org/10.1208/s12248-016-0038-4.

Stillhart, C., Imanidis, G., Griffin, B.T., Kuentz, M., 2014. Biopharmaceutical modeling of drug supersaturation during lipid-based formulation digestion considering an absorption sink. Pharm. Res. 31, 3426–3444. https://doi.org/10.1007/s11095-014-1432-1.

Tanaka, Y., Tay, E., Nguyen, T.H., Porter, C.J.H., 2020. Quantifying in vivo luminal drug solubilization-supersaturation-precipitation profiles to explain the performance of lipid based formulations. Pharm. Res. 37 (47), 1–17. https://doi.org/10.1007/s11095-020-2762-9.

Thomas, N., Richter, K., Pedersen, T.B., Holm, R., Müllertz, A., Rades, T., 2014. In vitro lipolysis data does not adequately predict the in vivo performance of lipid-based drug delivery systems containing fenofibrate. AAPS J. 16 (3), 539–549. https://doi.org/10.1208/s12248-014-9589-4.

Trevaskis, N.L., Charman, W.N., Porter, C.J.H., 2008. Lipid-based delivery systems and intestinal lymphatic drug transport: a mechanistic update. Adv. Drug Deliv. Rev. 60 (6), 702–716. https://doi.org/10.1016/j.addr.2007.09.007.

Vertzoni, M., Augustijns, P., Grimm, M., Koziolek, M., Lemmens, G., Parrott, N., Pentafragka, C., Reppas, C., Rubbens, J., Van Den Abeele, J., Vanuytsel, T., Weitschies, W., Wilson, C.G., 2019. Impact of regional differences along the gastrointestinal tract of healthy adults on oral drug absorption: an UNGAP review. Eur. J. Pharm. Sci. 134, 153–175. https://doi.org/10.1016/j.ejps.2019.04.013.

Yeap, Y.Y., Lock, J., Lerkvikarn, S., Semin, T., Nguyen, N., Carrier, R.L., 2019. Intestinal mucus is capable of stabilizing supersaturation of poorly water-soluble drugs. J. Control. Release 296, 107–113. https://doi.org/10.1016/j.jconrel.2018.11.023.

Yeap, Y.Y., Trevaskis, N., Porter, C.J.H., 2013. Lipid absorption triggers drug supersaturation at the intestinal unstirred water layer and promotes drug absorption from mixed micelles. Pharm. Res. 30, 3045–3058. https://doi.org/10.1007/s11095-013-1104-6.

Zangenberg, N.H., Müllertz, A., Kristensen, H.G., Hovgaard, L., 2001. A dynamic in vitro lipolysis model I. Controlling the rate of lipolysis by continuous addition of calcium. Eur. J. Pharm. Sci. 14, 115–122. https://doi.org/10.1016/s0928-0987(01)00169-5.